

A STUDY OF HIGH PRECISION GRAVIMETRY

David Lyness

Thesis presented for the degree of Doctor of  
Philosophy of the University of Edinburgh  
in the Faculty of Science  
July 1984



### **DECLARATION**

I hereby declare that the work presented in this thesis is my own unless otherwise stated in the text, and that the thesis has been composed by myself.

## ACKNOWLEDGEMENTS

My supervisor, Roger Hipkin has been a constant source of help and encouragement. I should like to express my considerable gratitude for his academic assistance and guidance. It has been a great pleasure for me to work with him. His sense of the aesthetic, sound logic and good humour has been greatly appreciated.

I should like to thank everyone in the Geophysics Department at Edinburgh for putting up with me this long. I should also like to thank those people from other bodies who I came in contact with through this work, namely T. Longmore, G. Archibald, A. Weir, R. Sillitto and R. Edge. Fieldwork in Greece was carried out with Vagelis Lagios. Vagelis, Eli, and their friends made me most welcome in their country.

The author acknowledges the financial support of the Northern Ireland Department of Education.

## ABSTRACT

A study of high precision gravimetry was undertaken to assess the limits of accuracy of modern portable gravity meters. Recent interest has centred on the use of precise gravity observations preferably in conjunction with geodetic measurements (e.g. levelling, Very Long Baseline Interferometry) to determine temporal height variations associated with tectonical activity. When special procedures are followed, modern portable gravity meters can measure relative gravity differences with a standard deviation of less than 0.1 gravity units (1 g.u. =  $10^{-6}$  m.s.<sup>-2</sup>). These procedures are, firstly, the accurate determination of the Earth tide at the site, secondly, the elimination of intrinsic instrumental drift, thirdly, a correction for environmental influences on the gravity meter, and lastly, determination of the instrument's calibration factor.

Several computer programs for the prediction of the tidal potential using dissimilar methods are discussed and compared. Observations at the only known modern Scottish Earth tide station, an I.D.A. (International Deployment of Accelerometers) instrument at Eskdalemuir, are analysed. The ocean load vector is calculated for 13 main frequency groups (the magnitude, local phase and gravimetric factors for  $M_2$  and  $O_1$  are 0.016g.u.,  $128^\circ$ , 1.139 and 0.023 g.u.,  $111^\circ$ , 1.083 respectively. Published  $O_1$  gravimetric factors for

Europe and Britain are significantly greater than this observed value suggesting an instrument error greater than the stated maximum.

Extensive instrumental tests on the Edinburgh gravity meter (La Coste and Romberg , G-275) to study environmental effects and drift were necessary before data were collected. The method of fitting cubic spline functions by least squares was developed to eliminate instrumental drift. The instrument scale factor was evaluated on the National Calibration Line and in the laboratory using specially designed tilting apparatus. The National Calibration line results obtained using G-275 are analysed and compared with the results from several other model G meters. An ancillary platform, on to which the meter may be bolted, was constructed. The platform accommodates more sensitive levelling vials and screw feet of a finer pitch enabling the observer to level the instrument more accurately. The platform may be used in the laboratory or in the field. The platform was used as a tilt table, the angle being obtained by electronically counting laser interference fringes.

To assess the practical application of high precision gravimetry, annual measurements were made in Scotland, a tectonically quiet area and in East Central Greece, an active area. The Scottish network consists of six Ordnance Survey fundamental bench marks with gravity differences less than 10 g.u.. A unique observation procedure was followed in which the meter was allowed to attain

equilibrium by observing over a long time section of the drift curve. Gravity differences are found by spline adjustment of the drift curve rather than a point value. Some of these stations were measured during a pilot study in the years 1976, 1977, and 1978, and all six stations were measured using the ancillary platform (described above) in 1980 and 1981. The average observed difference between consecutive years is 0.081 g.u. with a standard deviation of 0.073 g.u.. The Greek network consists of sixty eight stations in an area of seismic risk near Atalanti ( $38^{\circ}38'N$ ,  $23^{\circ}06'E$ ). The network was established using two gravimeters in ladder sequences during 1981 yielding individual standard deviations less than 0.08g.u.. Subsequent re-measurement has revealed no gravity change at the 0.11g.u. level, and tectonic activity was undetected within this limit. It is concluded that the equilibrium observation procedure does not offer a significant increase in measurement precision.

A local engineering study to detect mining subsidence gravimetrically was also completed at Solsgirth Colliery, Fife, Scotland. Gravity observations combined with precise levelling yielded an excellent correlation between height and gravity change with a gradient of  $2.17g.u.m^{-1}$  ( $\sigma = 0.097 g.u.m^{-1}$ ), demonstrating that gravity can be a commercial alternative to precise levelling.

## CONTENTS

|   |     |
|---|-----|
| Title   | i   |
| Acknowledgements                                | iii |
| Abstract  | iv  |
| Contents  | vii |
| List of Figures                                 | xi  |
| <br>  |     |
| <u>Chapter I</u> Introduction                   |     |
| 1.0 Background                                  | 1   |
| 1.1 The Problems                                | 2   |
| 1.2 Fieldwork                                   | 3   |
| <br>  |     |
| <u>Chapter II</u> High Precision Gravimetry     | 5   |
| 2.1 The Meaning of High Precision               | 5   |
| 2.2 Recent Studies                              | 9   |
| 2.3 Measurements in Tectonically Active Regions | 11  |
| 2.4 Engineering Applications                    | 19  |
| 2.5 Underground Gravity Measurements            | 21  |
| <br>  |     |
| <u>Chapter III</u> The Measuring Instrument     |     |
| 3.1 The La Coste and Romberg Gravity Meter      | 22  |
| 3.2 Instrumental Modifications                  | 26  |
| 3.3 Instrumental Investigations                 | 31  |
| 3.4 Conclusions                                 | 47  |

## Chapter IV The Earth Tides

|     |  |    |
|-----|--|----|
| 4.1 | Calculation of the Tidal Potential and Tidal Force | 51 |
| 4.2 | Earth Deformation                                  | 59 |
| 4.3 | Ocean Loading                                      | 65 |
| 4.4 | Tidal Prediction using Computer Programs.          | 66 |

## Chapter V Spline Fitting and Data Adjustment

|     |                                   |    |
|-----|-----------------------------------|----|
| 5.1 | Introduction                      | 70 |
| 5.2 | Drift Adjustment with Splines     | 73 |
| 5.3 | Adjustment of Some Collected Data | 77 |
| 5.4 | Multilinear                       | 84 |

## Chapter VI Instrument Calibration

|      |  |     |
|------|--|-----|
| Pt.1 | Field Tests                                  | 86  |
| 6.1  | Introduction                                 | 86  |
| 6.2  | Periodic Errors                              | 90  |
| 6.3  | UK Calibration Lines                         | 90  |
| 6.4  | University Measurements                      | 91  |
| Pt.2 | Calibration by Tilting                       | 98  |
| 6.5  | The Method                                   | 98  |
| 6.6  | Experimental Procedure                       | 102 |
| 6.7  | Interferometric Measurement of Tilting Angle | 102 |
| 6.8  | Data Reduction and Results                   | 110 |
| 6.9  | Conclusions                                  | 119 |



## Chapter VII Determination of Ocean Loading at Eskdalemuir

|     |                            |     |
|-----|----------------------------|-----|
| 7.1 | Introduction               | 120 |
| 7.2 | The I.D.A. Network         | 122 |
| 7.3 | I.D.A. Instrument Response | 124 |
| 7.4 | Data Analysis              | 128 |
| 7.5 | Tidal Analysis             | 132 |
| 7.6 | The Observed Load          | 137 |

## Chapter VIII Secular Gravity Studies in Scotland

|     |                            |     |
|-----|----------------------------|-----|
| 8.1 | Introduction               | 147 |
| 8.2 | Scotland as a Test Bed     | 149 |
| 8.3 | The Observations           | 154 |
| 8.4 | Data Reduction and Results | 157 |
| 8.5 | Conclusions                | 169 |

## Chapter IX Gravity Measurements in East Central Greece

|     |                      |     |
|-----|----------------------|-----|
| 9.1 | Introduction         | 172 |
| 9.2 | Greek Tectonics      | 173 |
| 9.3 | The Atalanti Network | 180 |
| 9.4 | Data Analysis        | 184 |
| 9.5 | Data Results         | 188 |

## Chapter X Subsidence Measurements

|      |               |     |
|------|---------------|-----|
| 10.1 | Introduction  | 197 |
| 10.2 | Field Area    | 202 |
| 10.3 | Measurements  | 203 |
| 10.4 | Field Results | 206 |
| 10.5 | Model Studies | 211 |

## Chapter XI Conclusions

|      |             |     |
|------|-------------|-----|
| 11.1 | Summary     | 219 |
| 11.2 | Future Work | 222 |

|                   |     |
|-------------------|-----|
| <u>References</u> | 224 |
|-------------------|-----|

## Appendices

1. Computer Program: NSPL
2. Computer Program: WFIT
3. Computer Program: MULTILINEAR
4. Computer Program: PBAS
5. Computer Program: LSQTILT
6. Computer Program: NEWSM9
7. Published Paper: Geophys. J. Rastr. Soc. (1984) 77, 875-882  
A microgrametric network in East Central Greece - an area of potential seismic hazard.

LIST OF FIGURES

|      |   |    |
|------|---|----|
| 2.1  | The frequency spectrum of temporal gravity variations                     | 7  |
| 2.2  | High precision gravity profiles in Scandanavia                            | 10 |
| 2.3  | The gravitational effect of a thrust fault and<br>a dilating sphere       | 14 |
| 2.4  | Namafjall gravity profile   | 16 |
| 2.5  | Gravity change following the San Fernando<br>earthquake                   | 17 |
| 2.6  | Gravity change after the Haicheng earthquake                              | 18 |
| 3.1  | The spring arrangement of a typical gravity meter                         | 23 |
| 3.2  | Spring extension curve  | 23 |
| 3.3  | Extract from the 1945 La Coste and Romberg Patent                         | 25 |
| 3.4  | Instrumental Modifications  | 29 |
| 3.5  | Plan and elevation of tripod  | 30 |
| 3.6  | Representative drift curves for La Coste and<br>Romberg gravimeter G-275  | 33 |
| 3.7  | Drift curve from Sanderson (1982)   | 34 |
| 3.8  | The Effect of temperature variation on G-275                              | 36 |
| 3.9  | Typical Nickel Cadnium all discharge curves                               | 34 |
| 3.10 | Effect of varying voltage on G-275 reading                                | 41 |
| 3.11 | Schematic representation of Helmholtz coils and applied<br>magnetic field | 44 |
| 3.12 | (a) Effect of varying magnetic field                                      | 45 |
|      | - (d)   | 46 |

|      |   |     |
|------|---|-----|
| 4.1  | Earth Moon system   | 53  |
| 4.2  | Spherical triangle  | 53  |
| 4.3  | Zonal harmonics   | 56  |
| 4.   | Deformation of the earth's surface  | 60  |
| 5.1  | Cubic spline  | 71  |
| 5.2  | Arbitrary function $f(t)$   | 71  |
| 5.3  | Schematic flow diagrams of program NSPL   | 75  |
| 5.4  | Four separate reading sequences   | 79  |
| 5.5  | 10 node solution  | 80  |
| 5.6  | 18 " "  | 80  |
| 5.7  | Superposition of data sets PARTS = 4  | 81  |
| 5.8  | Eleven node solution for test data set  | 83  |
| 5.9  | " " " for field example   | 83  |
| 5.10 | Schematic flow diagram of general data reduction procedure                              | 85  |
| 6.1  | Graphical representation of manufacturer's calibration curve                            | 87  |
| 6.2  | The Cloudcroft Junior method  | 88  |
| 6.3  | Schematic representation of model 'G' gearbox   | 88  |
| 6.4  | U.K. airport net  | 94  |
| 6.5  | Stations measured with G-275 on long calibration run                                    | 94  |
| 6.6  | Results of university observations on UK short calibration lines                        | 96  |
| 6.7  | Simplified diagram of gravimeter tilting  | 96  |
| 6.8  | Boedecker's experimental arrangement  | 99  |
| 6.9  | Fine structure of the calibration function as observed by Boedecker                     | 101 |
| 6.10 | Examples of observed drift (preliminary experiments, angle estimated from screw thread) | 103 |

|      |   |         |
|------|---|---------|
| 6.11 | Observed tilt parabolas (preliminary experiments                                | 104     |
| 6.12 | Experimental arrangement for the interferometric estimation<br>of tilting angle | 105     |
| 6.13 | Circuit diagram of comparator   | 108     |
| 6.14 | Oscilloscope trace illustrating comparator input and output                     | 109     |
| 6.15 | Observed tilt parabolas (long level)  | 113     |
| 6.16 | Quadratic fit residuals   | 117     |
| 6.17 | Misfit amplitude as a function of observed dial turns                           | 118     |
|      |   |         |
| 7.1  | Theoretical $M_2$ tidal gravity loading in Britain                              | 121     |
| 7.2  | Block diagram of I.D.A. meter system  | 123     |
| 7.3  | Eskdalemuir response curves   | 127     |
| 7.4  | Schematic flow chart for I.D.A. magnetic tape handling and data<br>retrieval    | 131     |
| 7.5  | Decoded I.D.A. magnetic tape  | 133     |
| 7.6  | I.D.A. data compared with theoretical tide for Eskdalemuir                      | 134     |
| 7.7  | Frequency response of Doodson-Lennon filter                                     | 136     |
| 7.8  | Power density spectrum of 85 days data at Eskdalemuir                           | 139     |
| 7.9  | Possible load vector amplitude error  | 143     |
| 7.10 | Possible error on local phase estimate of the load vector                       | 144     |
|      |   |         |
| 8.1  | Scottish secular variation network  | 148     |
| 8.2  | Fundamental bench mark  | 150     |
| 8.3  | The third geodetic levelling  | 153     |
| 8.4  | Edinburgh Linlithgow link   | 159-161 |
| 8.5  | Complete 1978 data set  | 164     |

|      |  |     |
|------|--|-----|
| 8.6  | Complete 1980 data set   | 165 |
| 8.7  | " 1981 " "   | 166 |
| 8.8  | Histogram of residual frequency  | 168 |
| 8.9  | Diagrammatic representation of 1980 and 1981 surveys                   | 170 |
| 9.1  | Summary map of the Aegean region                                       | 174 |
| 9.2  | Spatial distribution of all earthquakes for Greece since 1901          | 175 |
| 9.3  | Summary of present deformation of the Aegean area                      | 176 |
| 9.4  | Landsat lineaments from MacKenzie, 1978.                               | 178 |
| 9.5  | Station location map   | 179 |
| 9.6  | Most probable annual maximum earthquake magnitude (mode) for<br>Greece | 181 |
| 9.7  | Typical double ladder sequence drift                                   | 186 |
| 9.8  | Complete Atalanti observation sequence                                 | 187 |
| 9.9  | Difference between calibration line observations                       | 186 |
| 9.10 | Histogram of residuals; least squares network adjustment, 1981         | 190 |
| 9.11 | Histogram of residuals; " " " " 1982                                   | 192 |
| 9.12 | Observed gravity difference in the Atalanti region (1981-1982)         | 194 |
| 9.13 | Histogram of gravity differences 1981-1982                             | 195 |
| 10.1 | Typical cross section through mine workings                            | 199 |
| 10.2 | Subsidence profile with varying width                                  | 200 |
| 10.3 | Relationship between subsidence, width and depth.                      | 201 |
| 10.4 | Mine plan of survey area   | 204 |
| 10.5 | Gravity and level difference caused by extraction                      | 207 |
|      | Unit S27   |     |
|      | Unit S29   | 208 |

|   |     |
|---|-----|
| 10.7 Gravity change versus height change  | 210 |
| 10.8 Subsidence development determined gravimetrically at station<br>no. 17.      | 212 |
| 10.9 Model outline used in two dimensional gravity analysis of<br>seam extraction | 213 |
| 10.10 Results of two dimensional model studies                                    | 215 |
| 10.11 Modelled gravitational effect of seam material                              | 216 |
| 10.12 Simplified geological map of Solsgirth area.                                | 217 |

## UNITS

Despite the fundamental nature of the acceleration due to gravity there is not yet a single commonly used unit when writing about small magnitudes. I have mainly used the gravity unit (g.u.), which is in keeping with the Systeme International. One gravity unit is equal to  $10^{-6}\text{ms}^{-2}$  and is sometimes denoted  $\mu\text{ms}^{-2}$ . The most commonly occurring units are submultiples of the c.g.s. unit, the gal ( $1\text{cm.s}^{-2}$ ). The microgal ( $10^{-8}\text{ms}^{-2}$ ) has a very convenient magnitude for the discussion of accuracies and amplitudes in both earth tide studies and high precision gravimetry (hence the term microgravimetry).



## CHAPTER ONE

### INTRODUCTION

#### 1.1 Background

This thesis describes the measures undertaken to observe the acceleration due to gravity as accurately as possible using a conventional surveying instrument. Because of the nature of the subject, a range of diverse topics are considered. These include laboratory based instrumental experiments, the prediction of earth tides, and field measurements in Scotland and Greece. High precision gravity surveys are useful in several differing contexts, itemised in Chapter Two. These applications are essentially associated with local or regional investigations of the temporal variation of gravity and form the basis for the problems addressed here. In both, the data may be directly diagnostic of subsurface activity, but in the regional case the information is best considered in conjunction with other data such as geodetic levelling or earthquake distribution.

As the use of sophisticated new technologies becomes more widespread in geodesy (eg. Very Long Baseline Interferometry (VLBI), Global Positioning System (GPS)), the need for precise gravity measurements will increase. This technology is currently being tested ( Project MERIT,

sponsored by the International Union of Geodesists and Geophysicists), but ultimately geodesists would like to achieve a worldwide geodetic control point network. The 'equilibrium' measuring technique discussed in Chapters Five and Eight may be particularly useful in the direct accurate gravimetric connection of VLBI stations.

## 1.2 The Problems

The nature of the difficulties associated with precise relative gravity measurements is fully discussed in Chapter Two together with a review of the published literature. The immediate problem is one of instrumentation - the primary components of the portable gravity meter are purely mechanical and perform somewhat variably. Chapter Three discusses the constructional details of the most commonly used gravity meter and presents the environmental response curves for the Edinburgh instrument. Instrumental response can only be examined after the accurate subtraction of the force due to the Earth tides, and this is considered in Chapters Four.

After the tidal correction is applied the data is adjusted in a least squares sense to obtain the optimum solution for a particular gravity difference. Data adjustment using least squares cubic spline solutions and network analysis using specific computer programs is discussed in Chapter Five. The use of cubic splines is

illustrated with data collected during a laboratory test. Chapter Six is concerned with the problem of instrument calibration and presents two approaches, the first the result of field observations, the second based on a specially designed laboratory experiment. The predicted effect of Earth tides may be altered by the local crustal deformations caused by ocean tidal loading. The magnitude of this load correction may be calculated theoretically and verified for a particular location experimentally. The data from a Scottish Earth tide station are reduced and examined in Chapter Seven

### 1.3 Field Data

The techniques explored in Chapters Two to Six were used to good effect in field studies discussed in Chapters Eight to Ten. An established Scottish gravity network was extended and strengthened on two consecutive years. The network was observed using a novel observation technique which is designed to connect widely separated stations with the maximum possible precision. This contrasts with a new network established by the author in the Atalanti region of central Greece. The Atalanti network numbered some sixty eight stations which were observed with strongly interconnected double ladder sequences. These repeated observations have not detected any gross temporal variation in gravity. A third field study, in the nature of a well controlled experiment, was carried out

above a working coal mine. The extraction of the seam material caused surface subsidence in excess of one meter which was well resolved gravimetrically.

## CHAPTER TWO

### HIGH PRECISION GRAVITY

#### 2.1 The Meaning of High Precision

The spatial variation of the acceleration due to gravity has been measured routinely since the 1920's to determine the density structure of subsurface rocks. These early measurements were generally made using portable pendulums which were successively superceded by stable and then a stable spring balances. The most successful design originally appeared in 1934 (La Coste, 1934) and is still in use today.

The study of high precision gravity measurements is a diverse field covering several unrelated topics which can be loosely catagorised as follows:

- (1) Global secular variations of gravity
- (2) Regional deformation studies (e.g. isostatic rebound)
- (3) Local temporal gravity changes associated with tectonic mechanisms.
- (4) Engineering applications.
- (5) A non Newtonian gravitational constant, 'G'.

Figure 2.1 is a diagrammatic representation of the amplitude spectrum of such variations.

The precision of a given point value collected during conventional gravity surveying on land, undertaken by either the oil industry or a government agency, would typically be 0.5 to 1.0 g.u. (eg. NGRN73, Masson Smith et al, 1974). This is generally sufficiently accurate to resolve geological structures. Higher precision requires a further investment in both the data collection and processing judged commercially unnecessary by industry. The distinction between conventional and high precision surveying is not absolute and they may overlap in extreme cases, but a conventional survey will not attain the same degree of precision in a common area. High precision surveys involve repeated visits to all sites integrated into a carefully preplanned measuring sequence optimised to suit local conditions. All the surveys undertaken by the author required resurveying at a later date to study the temporal change of gravity and consequently each station should be permanently marked. Data reduction of the collected values includes a rigorous evaluation of earth tides and a considered representation of instrument drift.

The techniques employed in such studies are similar and comparatively recent, using for the most part relative spring balances manufactured by the La Coste and Romberg company. These meters are sufficiently small and light to

# Accuracies of absolute and relative gravimetry and related questions

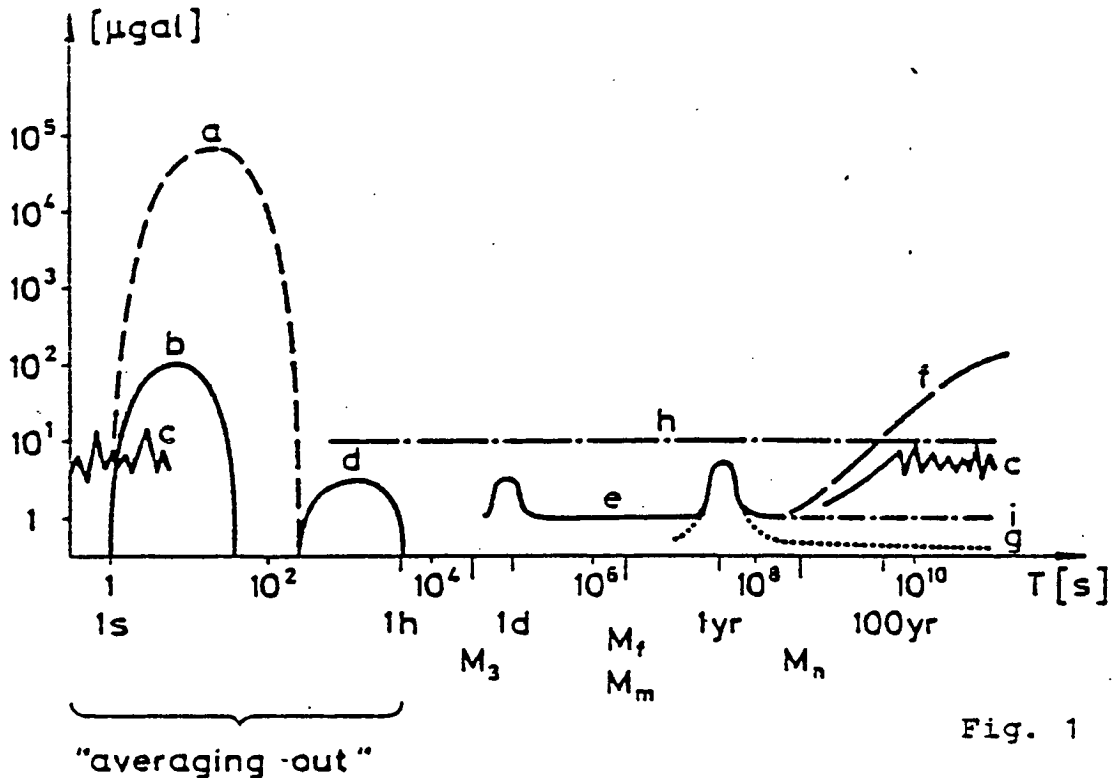


Fig. 1

tidal frequencies ( $M_3, M_f, M_m, M_n$ )

- a = earthquake activities
- b = microseismic activities
- c = manmade (artificial effects) activities
- d = eigen-vibrations of the earth
- e = hydrological and meteorological effects
- f = secular processes
- g = astronomical effects (polar motion etc.)
- h = present accuracy
- i = special techniques (short term) - 1yr

Figure 2.1 The frequency spectrum of temporal gravity variations (Elstner, 1981)

be carried by one person and the reading time at a site is less than five minutes. The La Coste and Romberg company manufactures several models, the most common being the land prospecting meter, model 'G', which has a worldwide range of 70,000 g.u.. The company also manufacture a modified land meter, model 'D', with a limited range of 2000 g.u. suitable for use in high precision surveys (Harrison and La Coste 1978). These instruments are discussed in some detail in a Chapter Three.

In addition to the La Coste instrument several transportable absolute instruments have been manufactured and several more are currently in the design phase. These are generally based on existing laboratory absolute instruments and are 'symmetric free fall' in which a corner cube reflector is projected vertically upwards, or 'free fall' instruments, where a corner cube is released at a given height, (Alasia et al, 1981, Hammond and Iliff, 1978, Sakuma, 1971 ). Several superconducting gravimeters in which a sphere is suspended over a persistent current magnet have been designed at the University of California, San Diego (Goodkind, 1981)

These absolute instruments open up many new possibilities in geodesy and geophysics, particularly the transportable instruments which may be used in conjunction with Very Long Base Line Interferometry or laser ranging. (Transportable in this context means air freighting



1000-1500 kg. of equipment to a stable, perhaps air conditioned site and up to one week for a single measurement with root mean square errors less than  $5 \times 10^{-8} \text{ms}^{-2}$ . The importance of this area of study was emphasised at the International Gravity Commission seventh session ( Res. No. 2 , Bull Geod. Vol. 115, 1975)

## 2.2 Recent Studies

It was only with the availability of reliable accurate prospecting gravimeters within research institutes that the diverse possibilities of gravimeters were explored. The very first gravity measurements to be undertaken to examine tectonic processes were undertaken as early as 1938 in Iceland (Schleusener, 1943) This survey, using Thyssen gravimeters, was of low accuracy by present day standards and the next repeat survey which took place in 1965 ignored the original measurements. In the same year, 1965, the International Association of Geodesists established two special study groups SS3.37 ('Special Techniques of Gravity Measurements') and SS3.40 (Secular Variation of Gravity) which have been instrumental in organising specialist meetings and publications in this field.

A high precision gravimetric profile of Scandinavia (figure 2.2) was proposed at the Symposium of Recent Crustal Movements in Aulanko, 1965 and the first measurements were carried out in Finland the following

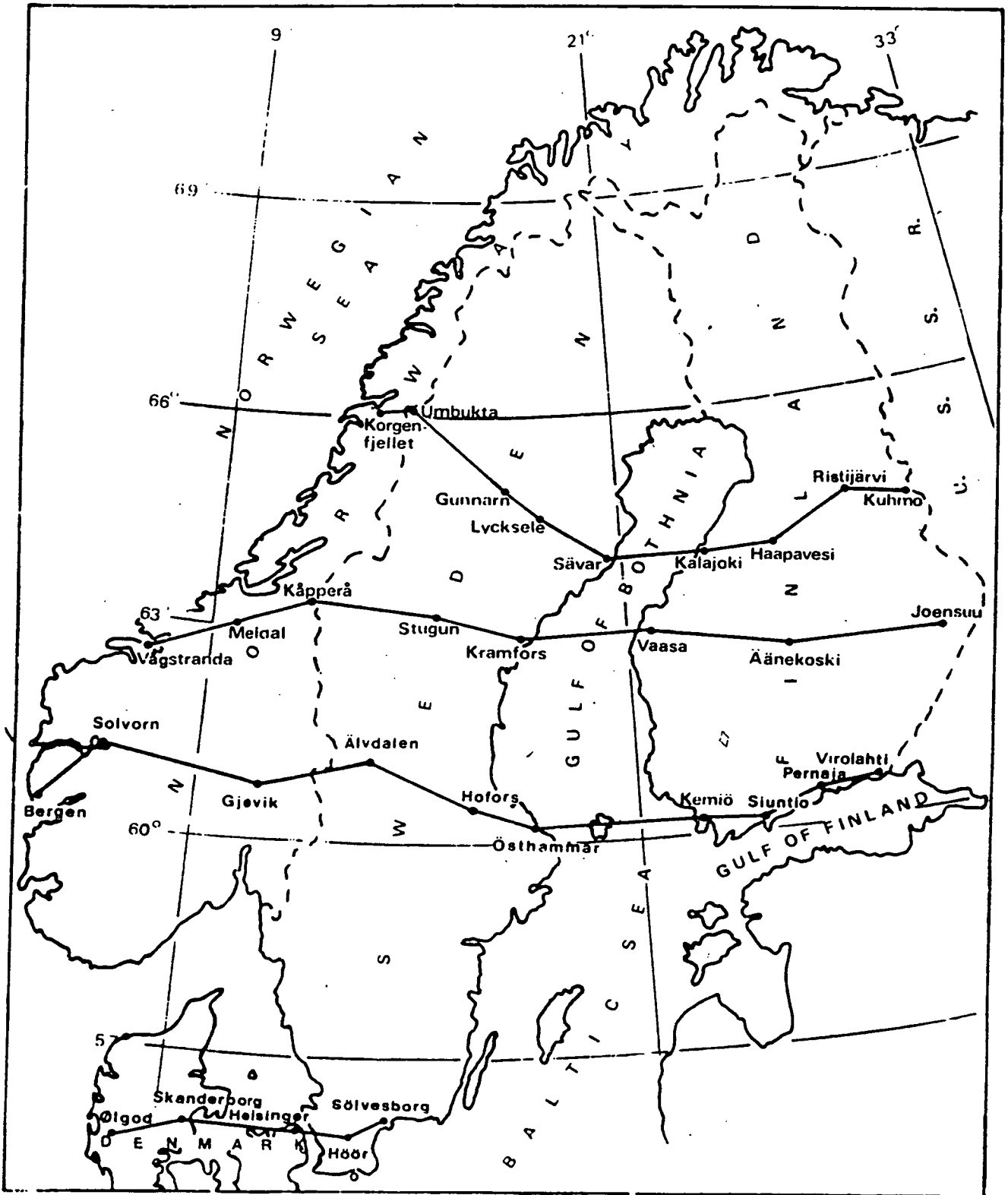


Figure 2.2 High precision gravity profiles in Scandinavia.

year. The line was subsequently extended over the Gulf of Bothnia into Sweden and Norway and is resurveyed on an annual basis. The results of these measurements are thoroughly described by Kiviniemi (1974) together with the data collection procedure. Kiviniemi obtains a standard error of 0.05 g.u. but the observed variation does not conform to the classical model of Sandanavia rebounding after the removal of the ice load. Many other institutes have collaborated with Professor Kiviniemi and the Edinburgh instrument (G-275) measured along the line during the 1978 field campaign (Hipkin, 1980). This valuable experience was utilised in the planning of network to study secular variation of gravity in Scotland. All other references to time dependent gravity variations on a regional scale have been made in tectonically active areas in an attempt to monitor either variations as a precursory phenomena or a single repeat measurement of an existing a network following an earthquake

### 2.3 Measurements in Tectonically Active Regions

There are several groups who are involved in the study of earthquake parameters and volcanology (eg. Whitcombe et al, 1980, Jachens, 1978 ) currently measuring gravity repeatedly in tectonic areas. Earthquake studies ideally involve a combined field approach with both gravity and first order levelling at common sites. Whitcomb (1976) has discussed the problems associated with geometric levelling

which is density dependent as it refers to an equipotential surface and shows that the geometric elevation change may be given as

$$\epsilon = \frac{\epsilon' \alpha / a + \Delta G}{\alpha / a - \beta}$$

$\epsilon$  obtained from levelling which gives the orthometric elevation to the first order  
 $\alpha$  the acceleration due to gravity  
 $a$  a radius of disc model, area within which dilatancy is occurring  
 $\Delta G$  measured gravity change  
 $\beta$  free air gradient

This expression does not depend on the density or thickness of the anomalous zone. The quantity  $a$  may be determined from the relation

$$\log l(\text{km.}) = 0.26M + 0.46$$

$M$  = earthquake magnitude,

$l$  = horizontal dimension of anomalous zone

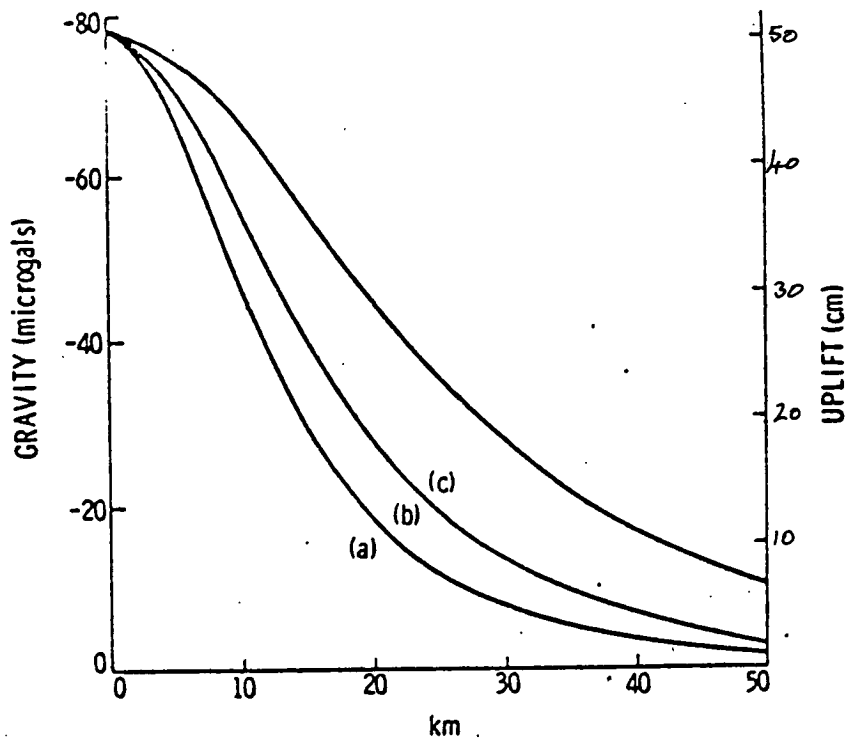
Rikitake (1975) presents several similar numerical relations from studies attempting to relate the area of deformation to earthquake magnitude.

The parameter  $\Delta G / \epsilon'$  is often used by workers, this being an approximation of  $\chi$  known as

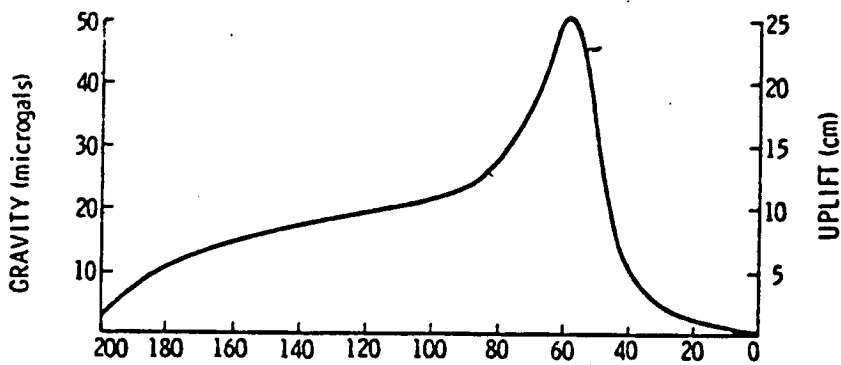
gravity gradient.

The vertical displacement caused by a dilating sphere of a given radius at some depth can be obtained by solving a Boussinesq problem and integrating. This is shown by Rundle (1979) who was investigating the so called 'Palmdale Bulge' of southern California. Figure 2.3 illustrates the uplift and associated gravity change from a 15km. radius dilating sphere at various depths and also the computed effect of thrust faulting. Such a sphere can cause a maximum gravity change of 0.8 g.u. for 0.25 metre uplift. Walsh(1975) has also discussed the theoretical gravity change associated with earth deformation and dilatancy.

Barnes (1966) describes gravity changes at 35 stations associated with the March 27, 1963 Alaska Earthquake (magnitude 8.4) and obtains a distortion gravity gradient of 2.0 g.u. per metre implying a Bouger relation rather than a free air gradient. Torge and Kangieser (1980) report a long term study of gravity variations in Northern Iceland. Measurements were taken in 1965, 1970 and 1975. Four La Coste and Romberg meters were used during the 1975 survey measuring at 176 stations with 1169 gravity differences yielding an average root mean square error of 0.07 g.u.. These gravity measurements were accompanied by geodetic surveying and the authors demonstrate a positive gravity change associated with a recent volcanic area.



Uplift and gravity change from 15 km radius dilating sphere buried at depths of a) 16 km, b) 20 km, c) 30 km.



Uplift and gravity change from thrust fault:  $\delta = 10^\circ$ ,  $\Delta U = -65$  cm,  $W = 200$  km,  $h = 10$  km,  $\rho = 2.8$  gm/cc.

$\delta$ , dip angle,  $h$ , minimum depth,  $W$ , planform width,  $\Delta U$ , dislocation displacement.

Figure 2.3 Theoretical gravitational effect of a thrust fault and a dilating sphere (after Rundle, 1978)

Torge (1981) presents results from a part of this profile (Narafjall) traversing an active rift which has been monitored annually. Figure 2.4 illustrates the gravity variation with time and indicates that activity was initiated in 1975 but now appears to have ceased.

Many gravity stations have been established for time dependent studies in Southern California and these have been remeasured at 1 - 2 month intervals (Whitcomb et al 1980) . Temporal gravity stations were established after Oliver et al, (1975) completed a remeasurement sequence in the area of the San Fernando earthquake , February 1971 (magnitude 6.5.) This study utilising 88 general sites with a high standard deviation ( $>0.6$  g.u.) shows a significant gravity change over a large area (figure 2.5) with a distorting gravity gradient of  $1.5\text{g.u. per metre}$ . In Japan, Kisslinger (1975) collated the many levelling and gravity data from the Matsushiro earthquake swarm , 1965 - 1967 and concludes that rapid dilatant expansion occurred at the source zone accompanied by high water inflow. Following the growth of a strike slip fault the surface subsided with the expulsion of water and an increase in gravity.

Repeated levelling and gravity surveys were carried out before and after the two large magnitude Chinese events of 1975, the Haicheng earthquake of February, magnitude 7.3 and the Tangshan earthquake of May , magnitude 7.8. Figure 2.6 is taken from Chen et al (1979) and illustrates

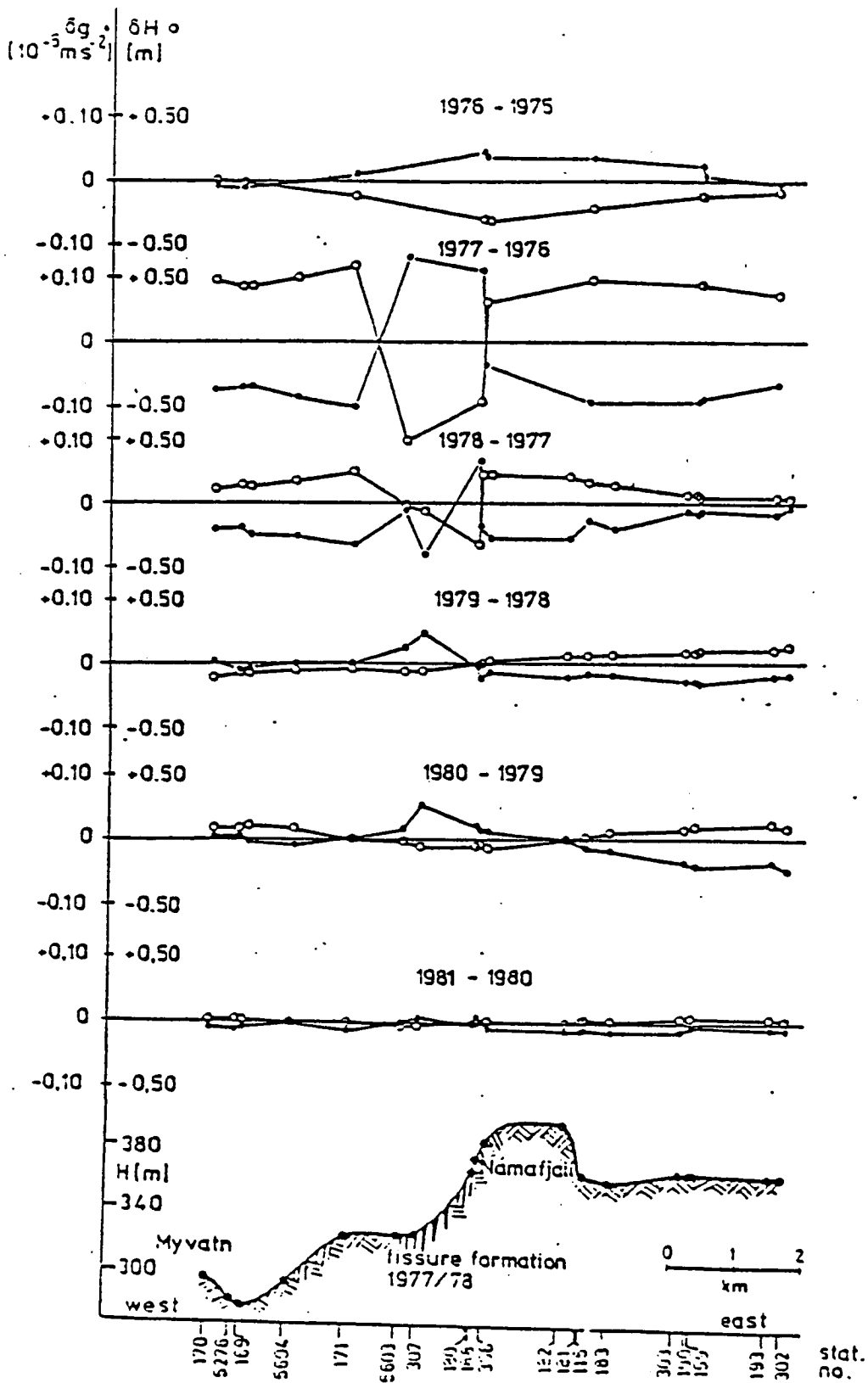


Figure 2.4 : Namafjall gravity profile :  
 Gravity and height variations between 1975 and 1981  
 (Torge, 1981)



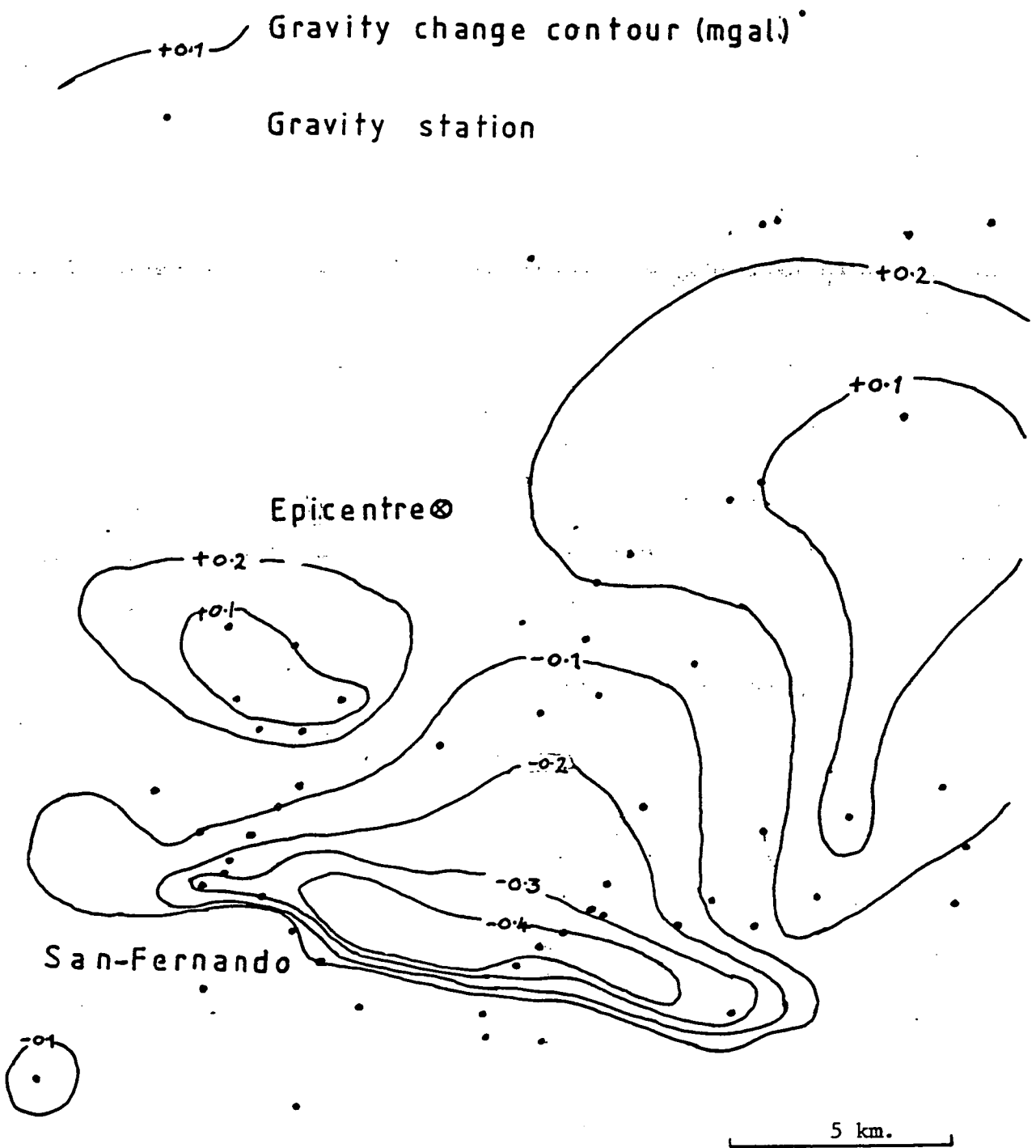


Figure 2.5 Gravity change following the San Fernando earthquake  
(after Oliver et al 1975)

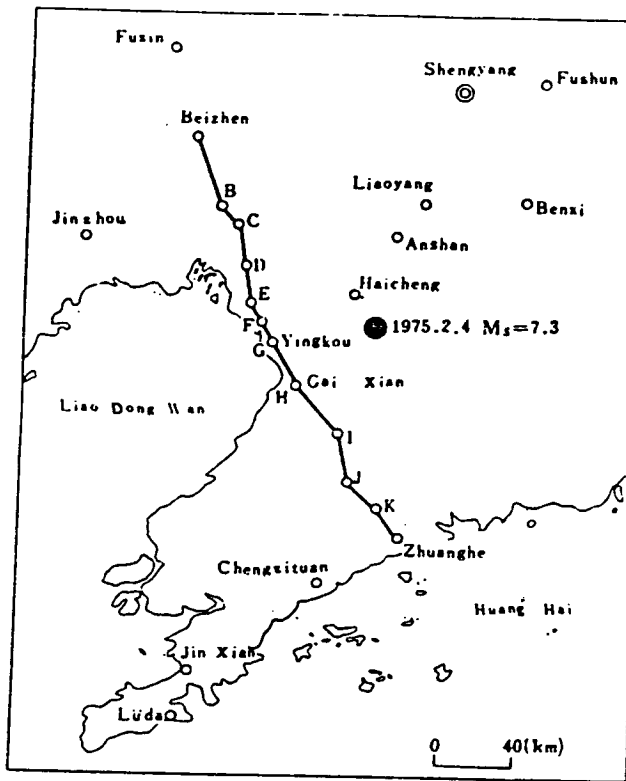


Figure 2.5 Gravity traverse from Beizhen to Zhuanghe.

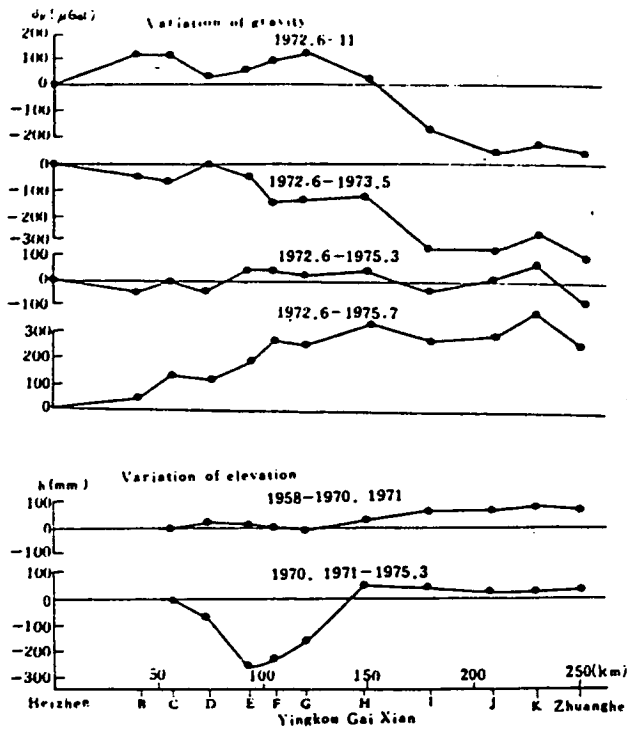


Figure 2.6 Changes of gravity and elevation along the Beizhen-Zhuanghe profile.

Figure 2.6 Gravity change after the Haicheng earthquake (from Chen et al., 1979)

the large magnitude of measured variation. In the case of the Haicheng event the gravity value dropped by a minimum of 3.52 g.u. before the shock but recovered to a slightly higher value ( 0.3 g.u.), but these measurements were made using  $ZS_2$  quartz suspension gravimeters) after the shock. The subsidence attained a maximum of only 0.26 metres. The gravity change during the Tangshan region increased to a maximum of 1.65 g.u. before the earthquake followed by a slight decrease. Chen et al. proposed very large scale mass flux in these regions (up to  $66\text{km}^3$  in the case of Haicheng)

Other examples of gravity change in the region of earthquakes are available in the literature (Jachens and Eaton, 1980 ; Hagiwara et al., 1980 ; Whitcomb et al., 1980 ; Boulanger, 1980 ) but it is only in the comparatively recent past that microgravimetric networks have been established in areas of seismic risk. Generally, reported gravity changes have been associated with large magnitude events, but with the installation of specific networks Whitcomb et al. , (1980) report the precursory response of a magnitude 5.6 event at a distance of 67km. from the calculated epicentre.

#### 2.4 Engineering Applications

This title refers to those areas of gravimetric investigation which fall outside the normal regional scale surveys involving station separations of a kilometre or

more. Engineering applications involve the use of much smaller station separations in the order of tens of metres to resolve highly localised structures perhaps associated with human activity. Such surveys require a high precision as well as close spacing and may involve the use of refined observation techniques to establish the gravity gradient.

the first reported use of gravimeters in such a way is the locating of a chromite (density =  $4400\text{kg.m}^{-3}$ ) ore bodies (Hammer et al 1945). Parasnis(1966) reviews gravimetric prospecting for ore bodies. A similar technique is used in the detection of voids which are difficult to detect geophysically and are often located by expensive high density drilling. Successful void detection is reported by Arzi (1975), Neumann(1966), and Blizkovsky(1979).

The earliest routine gravity exploration was undertaken using torsion balances which measure gravity gradients. This method was replaced with the use of the more rapid gravity meter. The vertical gravity gradient may be a more sensitive indicator of local structure (including oil bearing stratigraphic traps, Hammer and Anzoliga,1975) particularly voids. This is accomplished in the practically difficult operation of measuring at the top and bottom of a prefabricated tower (2-4 metres in height). Faklewicz (1976) reports rapid accurate (r.m.s.e. 15 Eotvos) detection of cavities. Attempts to measure the vertical gradient of gravity using a tower built at Edinburgh proved extremely

difficult and other workers have questioned Finklewicz's reported accuracies (Arzi, 1977).

## 2.5 Underground Gravity Measurements

The very first underground measurements were conducted using pendulums as early as 1854 in an attempt to determine the Newtonian gravitational constant (Airy, 1856). Subsequent underground measurements using modern gravimeters have largely been concerned with density determinations (Hammer, 1955; Hussain and Walach, 1980) and assumed the laboratory determined value of 'G'. Recent theoretical work has proposed that non-Newtonian attractive short range forces may exist and the attractive potential may be written

$$V(r) = - G_{\infty}m/r (1 + \alpha e^{-\mu r})$$

$$\alpha = 1/3, \mu^{-1} = 10 - 1000 \text{ m}$$

Stacey et al. (1981) review all the reported subsurface gravity measurements but fail to demonstrate a significant difference from the conventional value of 'G'

CHAPTER THREE  
THE MEASURING INSTRUMENT

3.1 The La Coste and Romberg Gravity Meter

The only commercially available relative gravity meter suitable for use in high precision work is manufactured by the La Coste and Romberg company of Austin, Texas. The La Coste and Romberg meter is in fact a modified long period vertical seismometer, the theory of which is well discussed in the literature (eg. Melton, 1971). A schematic diagram of the basic elements is shown in figure 3.1. An essential component of the instrument is the use of a 'zero length' spring. A zero length spring is defined as one in which the tension is proportional to the actual length of the spring (ie  $l_0 = 0$  in figure 3.2). This is accomplished by winding the spring under tension opposing the helix such that the spring is in compression when free.

Considering figure 3.1 the sensitivity may be stated as

$$S = x ( l_0 + x )^2 / l_0 a.b. \sin (\beta)$$

where  $x$  is the extension

Thus the sensitivity increases as  $l_0$  approaches zero

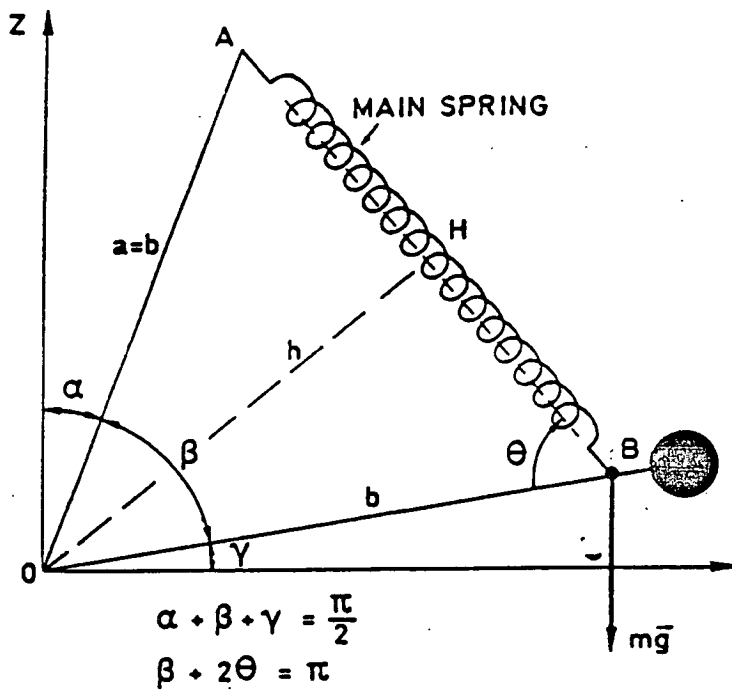


Figure 3.1 Spring arrangement of a typical grayimeter

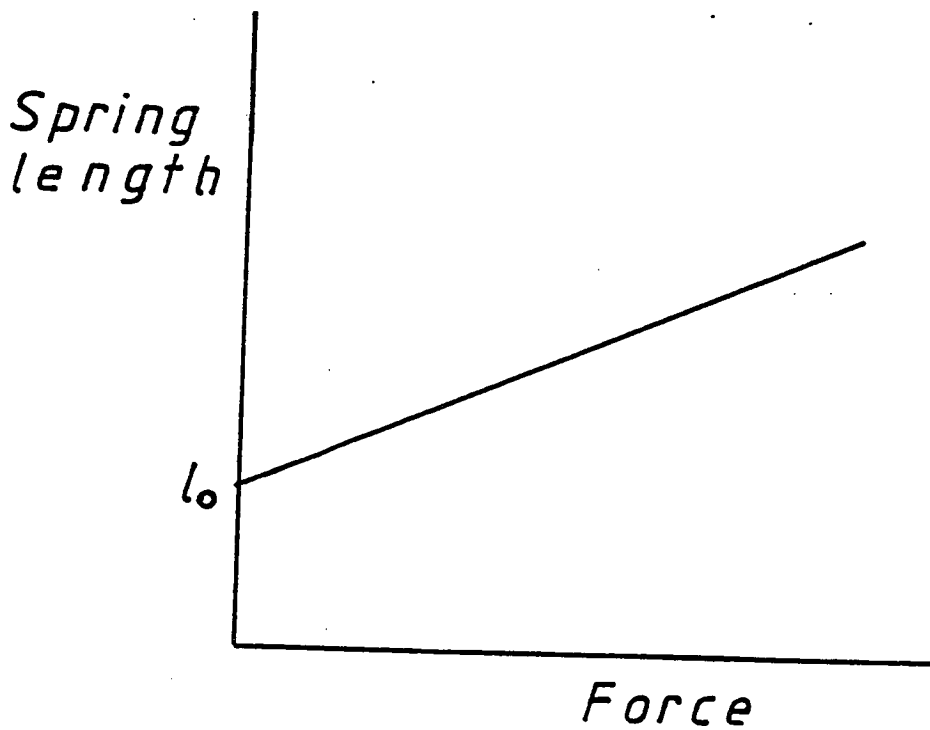


Figure 3.2 Spring extension curve.

Meters are individually produced by hand machining and for this reason it must be stressed that each meter possesses highly individual characteristics which become more apparent when the meter is taken to the limits of its precision. Exact information about the internal workings are scant and the best source of information was found to be the original patents. A diagram taken from the original patent (U.S. 2,377,889 , 1945) is shown in figure 3.3 and the design has changed only trivially (Harrison and La Coste , 1978) since that time. A negative length spring (4), with wire added to bring it to the zero length condition supports the beam (3). The beam pivots about the line joining the points of attachment of the springs (5) to the support rods (6) and theory (La Coste, 1935) shows that for equilibrium of the beam in a horizontal position the distance, A, of the upper support (35) of the zero length spring above this pivot line is proportional to g.. The meter is read by moving the support 35 vertically to bring the beam into position. The change  $dA$  in A required to do this as the meter is read first in one place and then another is proportional to gravity difference  $dg$  by the relation  $dA/A = dg/g$ . The meters are built with  $A = 2.5$  cm. so that the 70,000 g.u. range of the G meter requires moving the support 0.115 mm. and 0.01 g.u. accuracy means positioning the support to within  $2.5 \times 10^{-11}$  m.. The La Coste company has recently introduced the model 'D' meter which has many refinements to the basic design. These include improved levels which the manufacturers claim



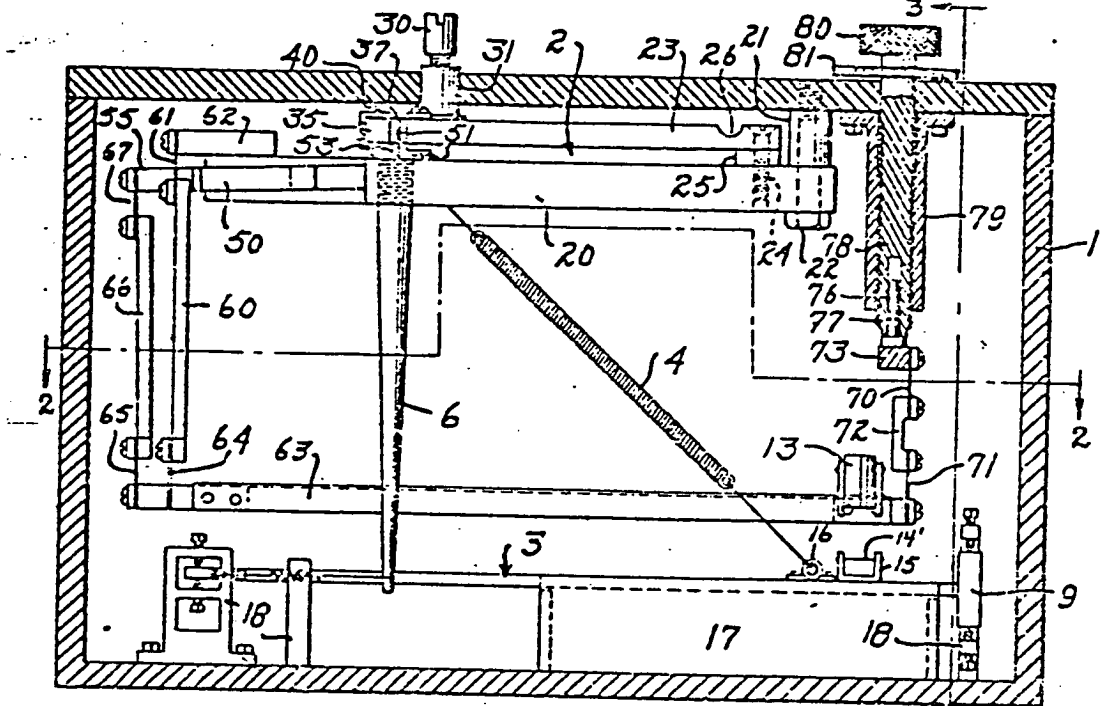


Fig. 1.

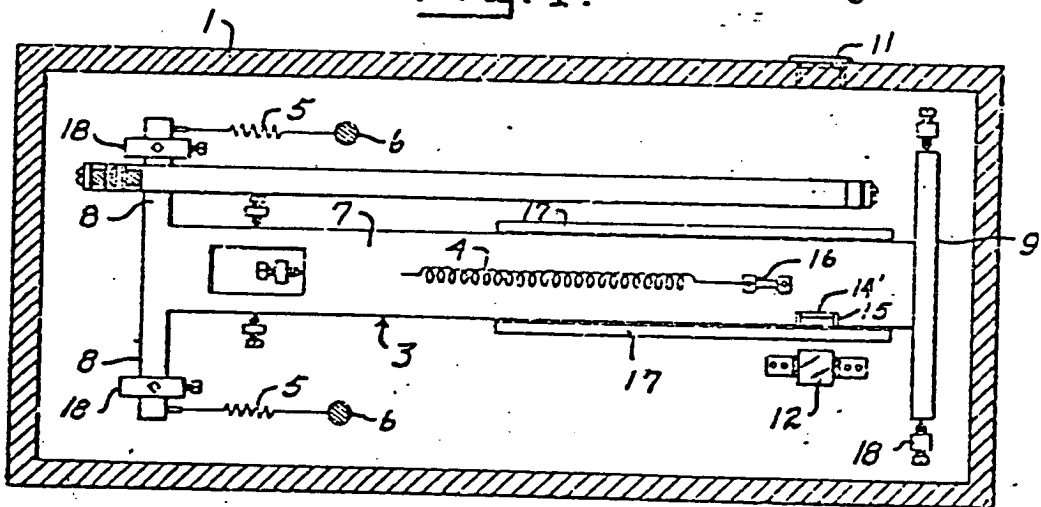


Fig. 2.

LUCIEN J. B. LACOSTE  
ARNOLD ROMBERG  
INVENTORS.

BY

Jesse R. Stone  
Lester B. Clark  
ATTORNEYS.

Figure 3.3 Extract from the 1945 La Coste and Romberg patent.

improve the accuracy of the meter and more importantly changes in the gearing system. This improvement is undoubtedly the case in some circumstances but for surveys including large gravity differences ( the D model range, without resetting is 2000 g.u.) or much transportation the intrinsic accuracies of the G and D models are similar (McConnell et al, 1975; Grannel et al. , 1982, summarise the relevant differences)

### 3.2 Instrumental Modifications

Certain external modifications were made in an effort to improve reading accuracy. The only alteration affecting the meter directly was the addition of a small vernier scale to replace the dial pointer. To improve the levelling precision it was necessary to bolt the meter on to a large secondary base plate which also incorporated improved screw feet. The meter was simply bolted to this plate using the conventional feet screw holes, thus it could be easily removed for other use. The base plate design criteria also included.

- (1) Accommodation of two nickel cadmium batteries for prolonged observation sequences
- (2) Mounting hooks for suspending the base plate during transportation to eliminate shocks and vibrations

- (3) Finely threaded screw feet at right angles , parallel and perpendicular to the direction of the meter beam ('long axis')
- (4) Mounting for improved levelling bubbles
- (5) Easy use with a sturdy tripod suitable for use on Ordnance Survey fundamental bench marks.
- (6) Use as a laboratory tilting table

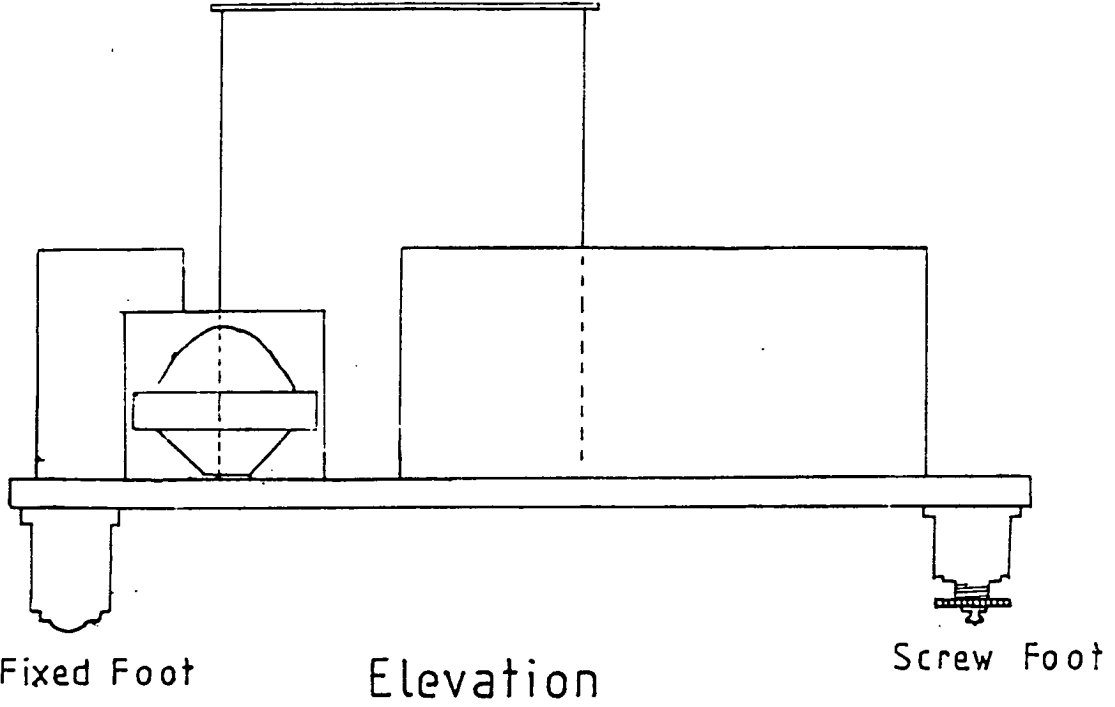
The level bubbles of the standard La Coste and Romberg instrument suffer from several disadvantages. (a) They are not adequately sensitive: one scribed division on the glass vial corresponding to 30 seconds of arc. (b) The bubbles are illuminated by festoon bulbs situated directly beneath the glass vials. When illuminated for a period of time both the fluid and the vial are heated causing bubble drift. (c) The bubbles are simply viewed from above and consequently there is a parallex error. This problem is further accentuated by uneven illumination of the bubbles from beneath.

The zeiss coincident viewing system overcomes these disadvantages and is the method used on many one second theodolites. Both ends of the bubble are view separately via a prism system and 'level' is found when the two images are coincident and appear as a single smooth curve (Bomford, 1981). Suitable levels, manufactured for use on a Cook ,Trout and Simms geodetic theodolites were obtained for use on the secondary plate. The fitted coincident

veiwing levels had the disadvantage that the instrument cannot be levelled at night , but high precision surveys should not include night time readings because of the change in the relative illumination of the beam marker image..

The secondary plate was milled from twelve millimetre aluminium plate, the plan and elevation are shown in figure 3.4. A large aluminium block, machined to a right angle , accommodates the coincident levels at right angles. The screw feet are manufactured from stainless steel with a pitch of 0.025 inches and two screw feet are mounted on brass pillars. The third support consists of a ball bearing forced into a brass pillar and is of fixed length. The screw feet are mounted eccentrically and rotation of the brass pillar causes lateral movement of the point of support. The level mounting block may also be rotated and after securing the gravity meter a series of iterative adjustments ensures that the levels and feet are parallel to the principle axis of the meter The tilt of the coincident veiwing levels may be adjusted by means of two allen screws. These were adjusted in a manner similar to that described in the La Coste and Romberg manual for the levelling of the internal levels.

A tripod was constructed with adjustable hardwood legs and a top frame of three millimetre angle aluminium (figure 3.5). The screw feet of the secondary platform rest on the



Scale ~ 1:4

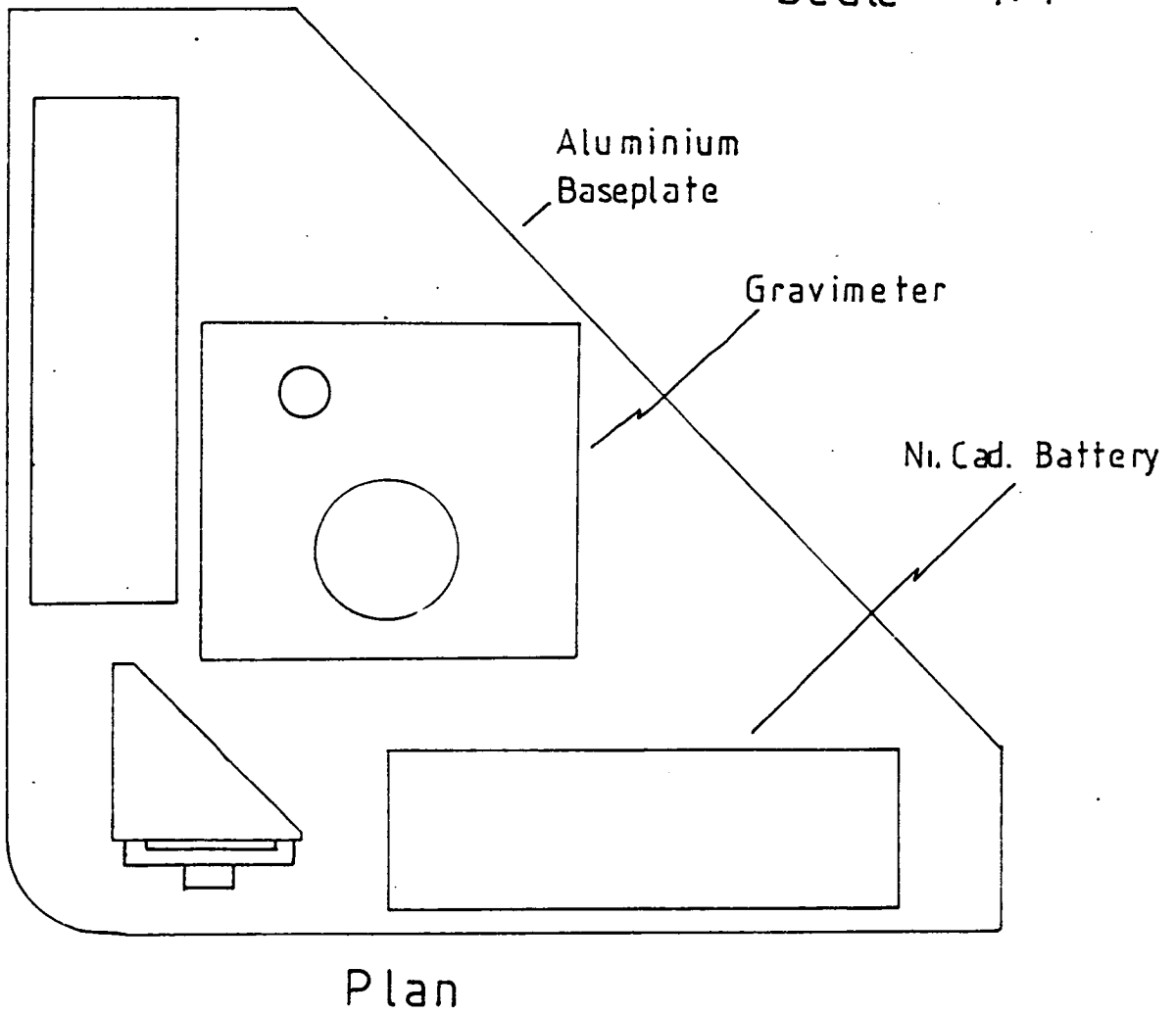


Figure (3.4) Instrumental Modifications

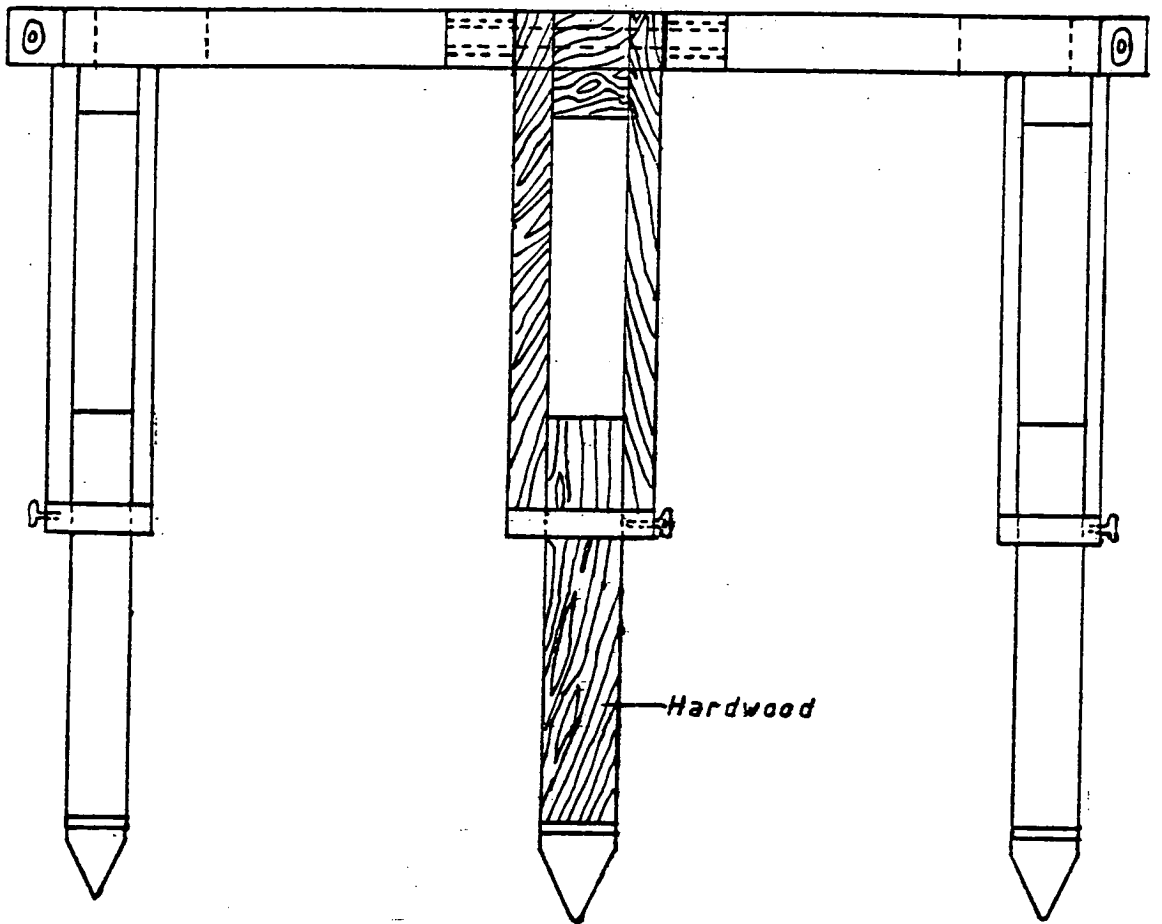
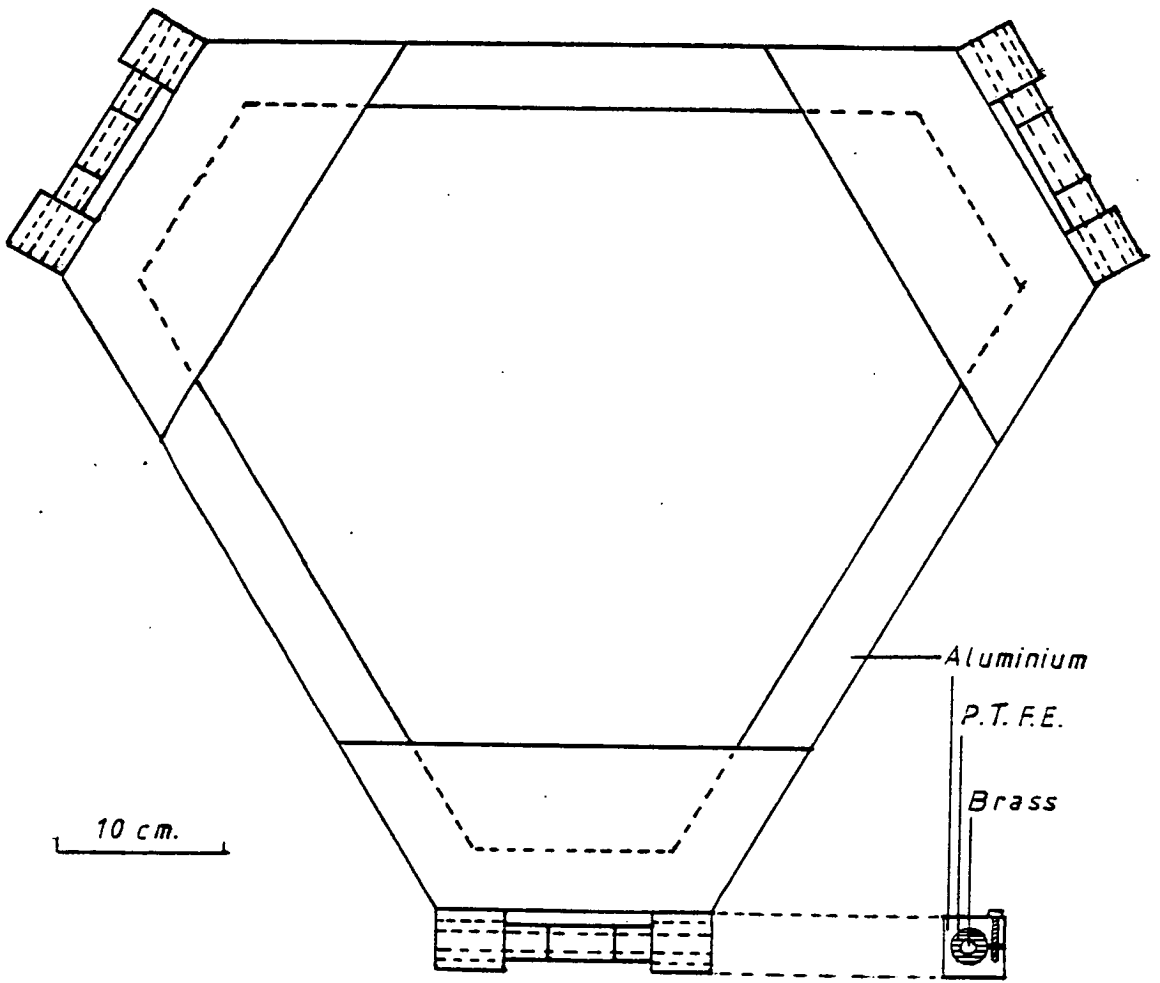


Figure 3.5 Plan and elevation of tripod



the trapezoidal corner plates. The tripod can be rapidly disassembled for storage and transportation. The tripod may be used in conjunction with a fundamental bench mark used as a third leg to provide an extremely stable measuring base. In this case one tripod leg is removed and replaced by a plate with a triangular hole cut out directly beneath the static foot, providing a three point contact with the hemispherical dome of the bench mark. Two views of the tripod in use at a fundamental bench mark (Tummel Bridge) are shown in Plates 3.1 and 3.2.

### 3.3 Instrumental Investigations

As stated above, each instrument is an individual and before high precision measurements can be undertaken it is necessary to quantify intrinsic characteristics and the instrument response to external factors.

The La Coste and Romberg meter is designed to minimise instrument drift. The mechanism is maintained at a constant temperature and typical hourly drift rates are about  $0.02 \text{ g.u.hr.}^{-1}$ . This long term drift is approximately linear and regional surveys using a La Coste and Romberg instrument usually visit a single base only twice a day. In addition to the long term drift pattern meters drift when unclamped. This effect appears to be particularly large for G -275 though other workers have not investigated the

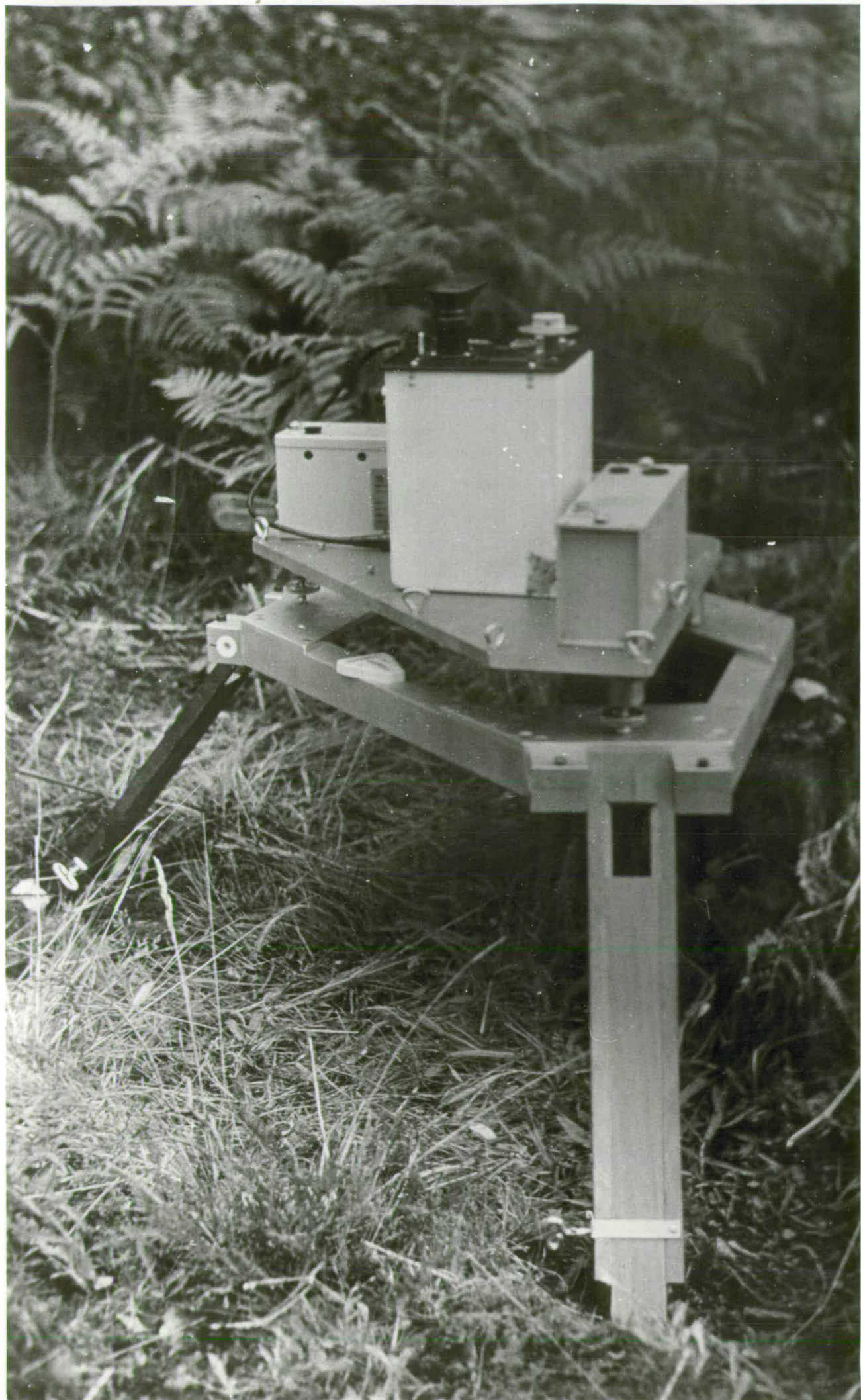
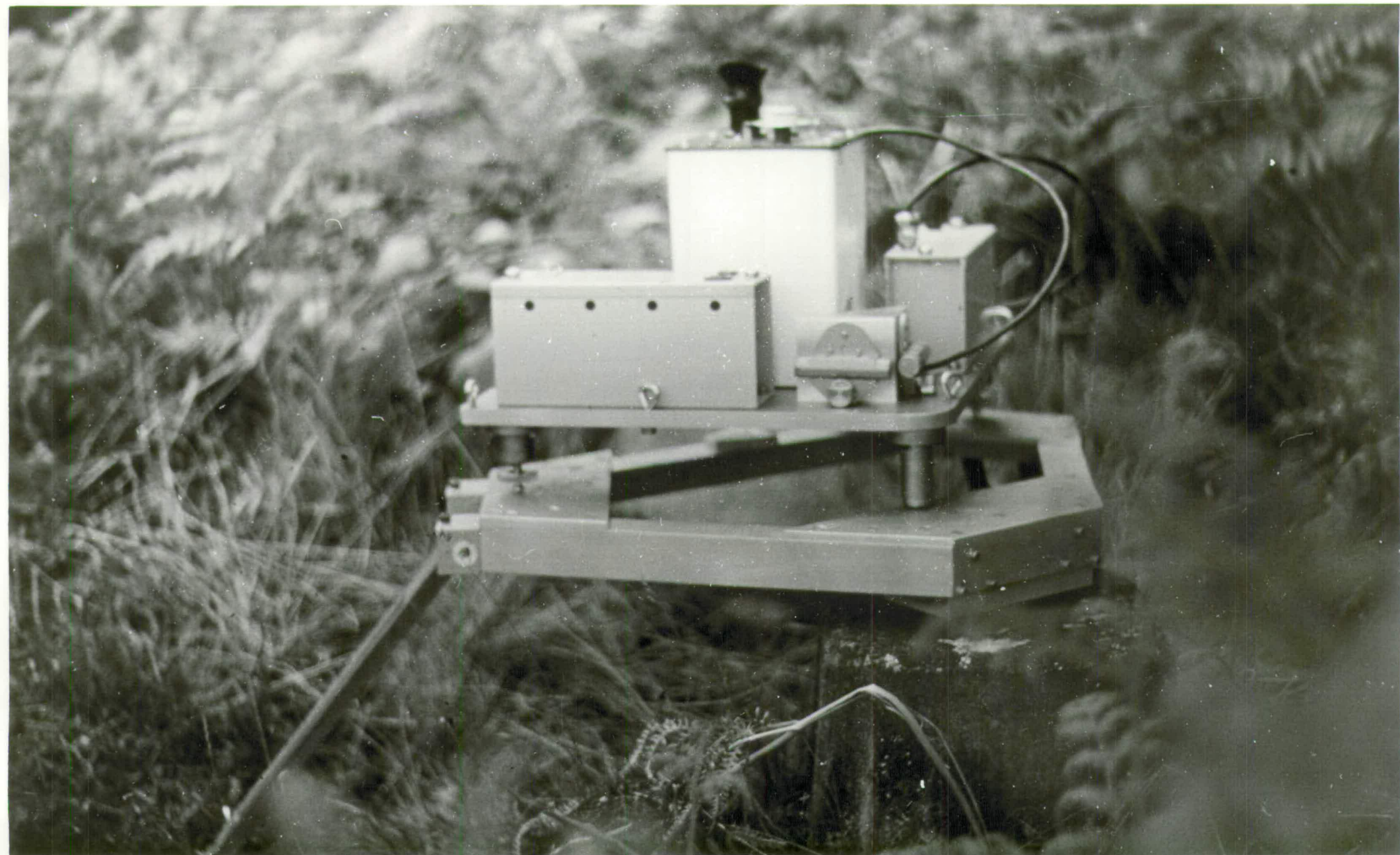




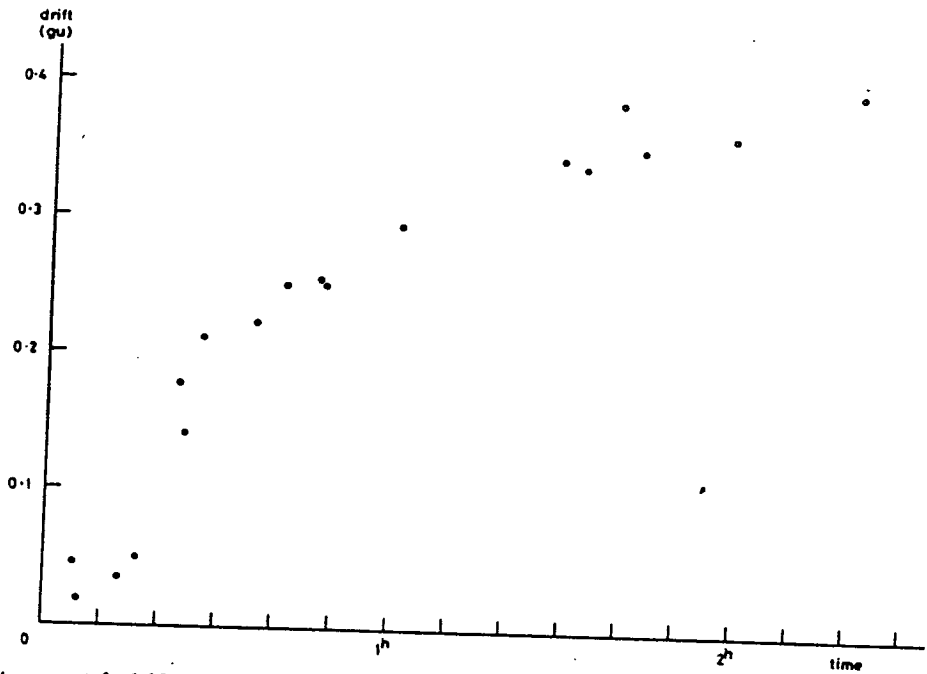
Plate 3.2: An illustration of field use of the tripod.



effect thoroughly. The Edinburgh instrument had previously undergone some testing which established a recognisable, repeatable drift curve at any site, probably associated with unclamping of the beam (Hipkin, 1980). A typical drift curve, obtained by repeated reading of the meter with the lamps continuously on and the beam unclamped, is shown in figure 3.6 . The two observation sequences illustrated in figure 3.6 differ by seven years demonstrating this is long term feature of this instrument. The readings display a rapid initial positive drift over the first thirty minutes, levelling out to an 'equilibrium' value after eighty to one hundred minutes. Such drift is not explicitly described by other workers but sharp initial drift is a recognised phenomena and is common practise to take site readings as rapidly as possible (Peterson, 1978). Indeed Sanderson (1982) illustrates a mean drift curve obtained from a set of thirty readings for G-90 , reproduced in figure 3.7, which is remarkably similar to figure 3.6. The author attributes this effect to mechanical hysteresis associated with the removal of tension from the pivotal shock eliminating springs ((5) in figure 3.3) and the main spring.

It is the experience of the author that a high precision reading can not be taken very rapidly and that the time to obtain a satisfactory reading is somewhat variable.

Since field measurements are necessarily taken in uncontrolled environments it is necessary to evaluate the effects of external agents such as (1) Temperature, (2) Air



Instrumental drift following unclamping for the LaCoste and Romberg gravity meter G-275. The zero of time is 15<sup>h</sup>03<sup>m</sup> on 23/2/76 (○) or 15<sup>h</sup>39<sup>m</sup> on 3/3/76 (●).

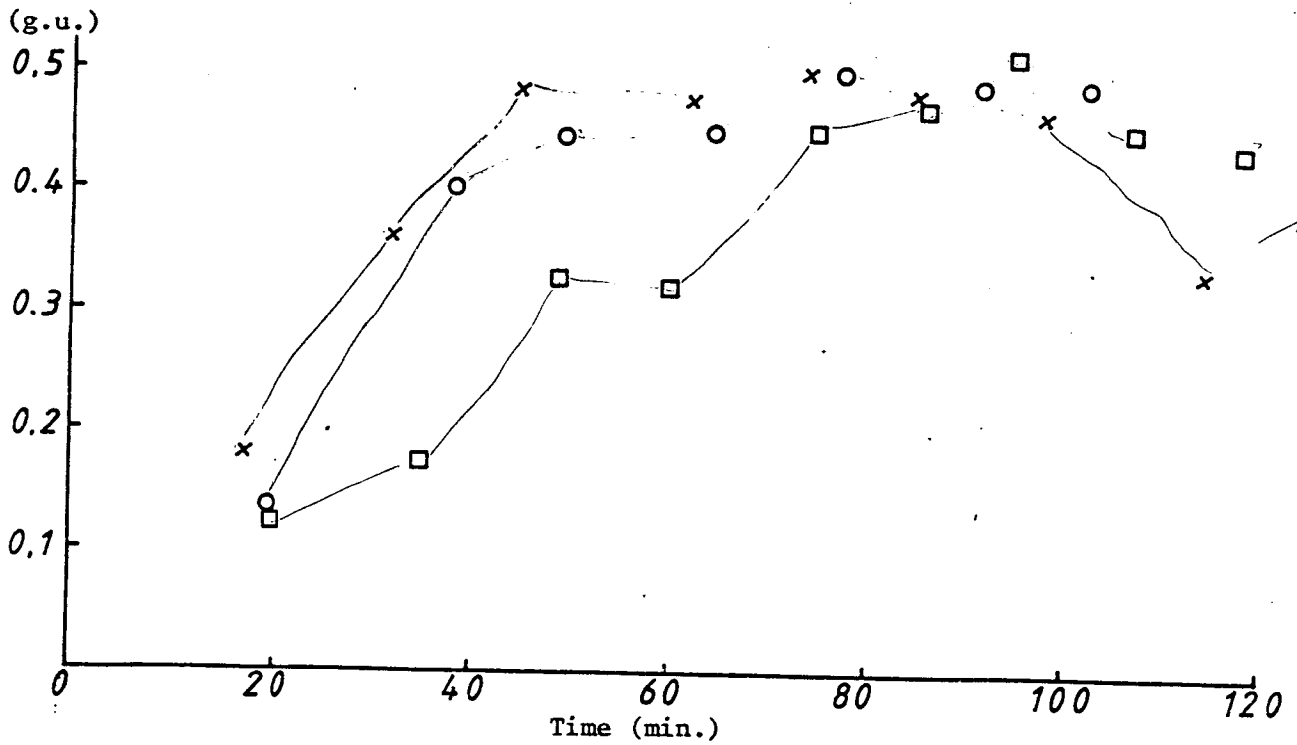


Figure 3.6 Representative drift curves for La Coste and Romberg gravimeter G-275. The upper figure is taken from Hipkin (1978), the lower set of observations (three independent sets) were observed by the author .

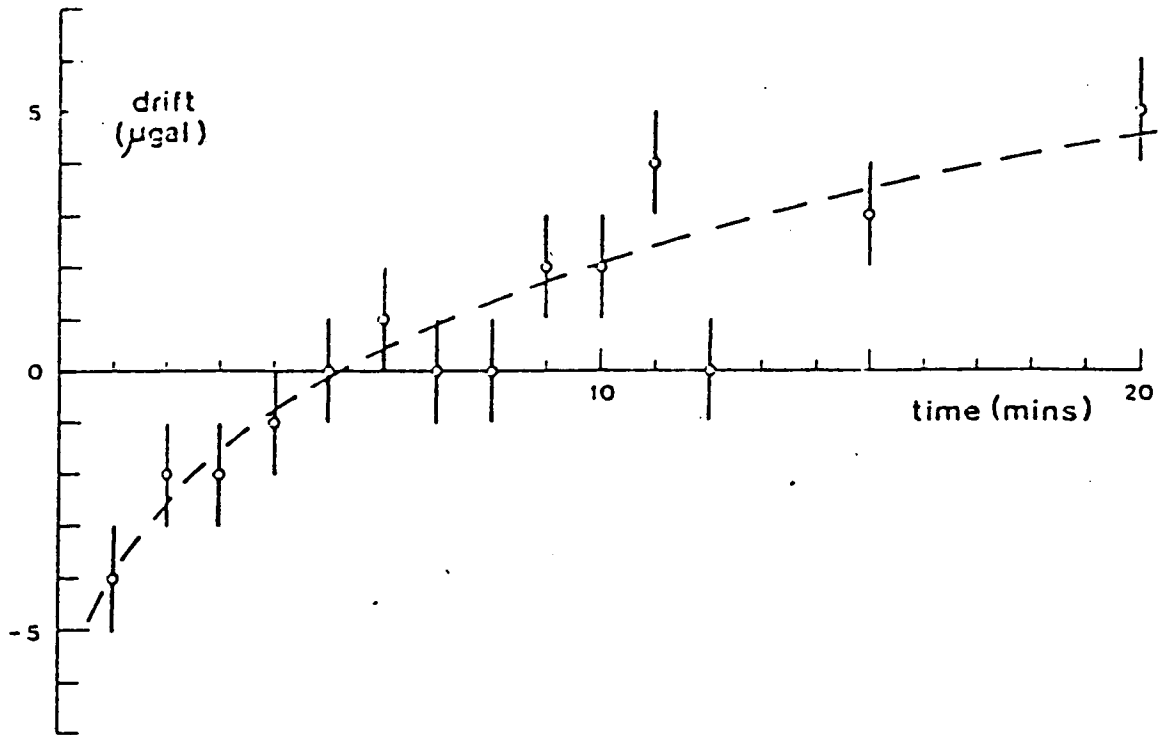


Figure 3.7 Composite drift curve taken from Sanderson (1982) for La Coste and Romberg Gravity Meter G-90. Mean of 30 independent determinations.

**Sintered Cell End Point Voltage Versus Discharge Rate**

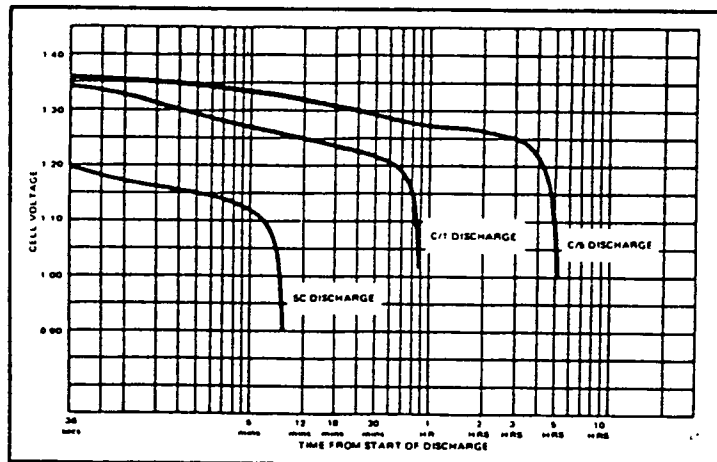


Figure 3.9 Typical Nickel-Cadmium cell discharge curves. C is the cell capacity in Ampere-hours.

Pressure, (3) Voltage Supply, (4) Magnetic Field.

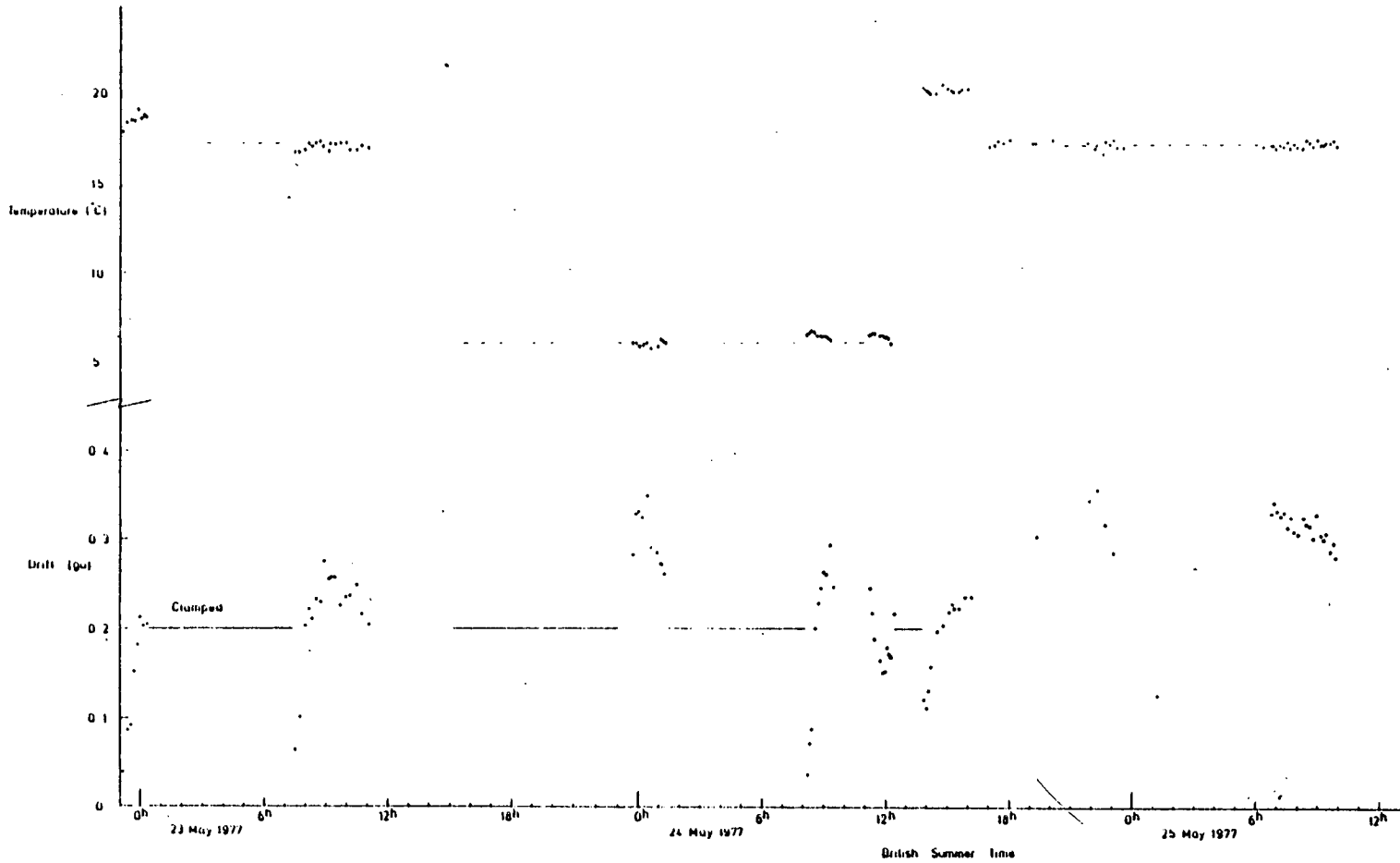
### **(1) Temperature**

It was initially postulated that the drift curve illustrated in figure 3.6 was a response to a temperature change associated with the removal of the instrument from its insulated carrying case. Hipkin (1978) describes elaborate tests on G-275 which disprove this and indicate there is no recognisable gravity change associated with a temperature variation of  $17^{\circ}\text{C}$ . (see figure 3.8 taken from Hipkin, 1978).

Table (3.1) illustrates the results presented in the literature. It can be seen that the effect is variable from meter to meter and generally small. Many observers note that the effect is indeed variable in form on a given instrument depending on the rapidity of the temperature change. Boedecker (1981) noted that it is almost impossible to model under field conditions. The effect may be particularly small for G-275 because the meter has been obtained at the working temperature of  $49.1^{\circ}\text{C}$  since its purchase in 1972.

### **(2) Air Pressure**

Variations in air pressure at a station will cause a gravity change associated with the changing Newtonian



The effect of ambient temperature on instrumental drift for the LaCoste and Romberg gravity meter G-275.

Note: (i) a voltage reduction, not affecting the gravimeter thermometer but slightly dimming the lights, occurred between 11<sup>h</sup> 28<sup>m</sup> and 11<sup>h</sup> 46<sup>m</sup> on 24/5/77. Readings between 11<sup>h</sup> 17<sup>m</sup> and 12<sup>h</sup> 25<sup>m</sup> are considered unreliable;

Figure 3.8 Effect of temperature variation on G-275 (from Hipkin, 1978)

Table 3.1

## Gravimetric Effect of Air Temperature Changes

| Author             | No. of Meters | Temperature Change | Observed<br>'Gravity Change'<br>g.u./10°C                            |
|--------------------|---------------|--------------------|--|
| Brein et al., 1977 |               |                    |  |
| GL                 | 5             | 8°C → 30°C         | -0.16 ± 0.037 to<br>+0.058 ± 0.040                                   |
|                    | 4             | 14°C → -10°C       | -0.012 ± 0.002 to<br>-0.002 ± 0.002                                  |
|                    |               |                    | Rate dependent   |
| IFAG               | ?             | ΔT = 10°C          | -0.02 max  |
| THD                | ?             | ΔT = 20°C (fast)   | 0.4 max (irregular)  |
| Boedecker, 1981    | 4             | 0 → 30°C slow      | -0.23, -0.02, +0.0<br>+0.08 and +0.1                                 |
| Nakagawa, 1975     | 8             | 20°C → -10°C       | c -0.05 → +0.1   |
| Gerstenecker, 1978 | 1             | ΔT = +12° in 3 min | ΔG = 0.08 g.u.   |
| Williams, 1983     | 7             | ± 20°C             | Optical readout av<br>0.2 ± 0.03<br>Electronic readout<br>0.1 ± 0.08 |

GL Geodettinen Laitos, Helsinki (Kiviniemi)

IFAG Institut für Angewandte Geodäsie, Frankfurt am Main (Brein)

THD Technische Hochschule, Darmstadt (Gerstenecker)



attraction of that mass of air. Theoretically this effect is  $-4.2 \times 10^{-3}$  g.u./mbar but deformation of the crust and lateral pressure variations reduce this factor. A correction of  $-3 \times 10^{-3}$  g.u./mbar is applied to observations in the program PBAS (Section 4.5)

In addition to the direct Newtonian attraction, the changing air pressure exerts a mechanical effect on the delicate balance of the instrument. Figure 3.3 shows a damping chamber attached to the main beam to minimise the effect of rapid pressure variations. Furthermore the mechanism is enclosed in a sealed chamber which though not perfect, lessens the effect of external pressure variations (Harrison and La Coste, 1978).

No facilities for controlling the air pressure in a chamber containing both the meter and an observer were available to the author. Table 3.2 presents all the published values for the mechanical effect of pressure variations located by the author.

### (3) Voltage Supply

The meter is supplied with Nickel Cadmium cells, which can supply the meter for one day under typical field conditions. The voltage of nickel cadmium cells under load drops gradually from 1.35 to 1.25 volts before the onset of very rapid loss of capacity (figure 3.9). The measurements

Table 3.2

Gravimetric Effect of Air Pressure Variations

| Author             | No. of Meters | Pressure Change    | Observed<br>'Gravity Change'<br>g.u. per 100 mbar |
|--------------------|---------------|--------------------|---|
| Brein et al., 1977 |               |                    |   |
| IFAG               | ?             | 65 mbar            | 0   |
| THD                | ?             | Fast > 20 mbar/min | $3.5 \times 10^{-4}$                              |
| GL                 | 5             | ?                  | -0.027    0.021 to<br>+0.021    0.6               |
| LMV                | 2             | ?                  | -0.027 and -0.024                                 |
| Williams, 1983     | 2             | 300 mbar           | $-3 \times 10^{-4}$ and $4 \times 10^{-4}$        |
| Boedecker, 1981    | 4             | 400 mbar           | -0.0006, -0.0014<br>-0.0014, -0.0016              |

IFAG    Institut für Angewandte Geodäsie, Frankfurt am Main (Brein)  
 THD    Technische Hochschule, Darmstadt (Gerstenecker)  
 GL    Geodeettinen Laitos, Helsinki (Kiviniemi)  
 LMV    Statens Lantmäteriverk, Gävle (Pettersson)

carried out by the author in Scotland (see Chapter Eight) required prolonged use of the cursor illuminating lights and field battery life was less than one day. The auxiliary platform accommodates two batteries which is sufficient for a twelve hour field day with repeated use of lights. In addition to these measures, an in line connector was attached to the supply cable so that a car battery could be inserted into the circuit. This alternative (a 36 ampere hour sealed lead acid battery) was used whilst the gravimeter was in the vehicle.

Laboratory tests using a stabilised power supply failed to demonstrate any gross effect caused by varying the input voltage of G-275. The results of these tests are shown in figure 3.10. In the upper case the supply voltage has been varied rapidly between converging extremes whilst in the lower case the voltage has been held at an anomalous voltage for about sixty minutes. The characteristic drift pattern discussed above is evident but no voltage effect at these extreme voltages is apparent. Table 3.3 summarises the results of several published studies.

#### **(4) Magnetic field**

Precise details of the materials used in the construction of the La Coste and Romberg gravimeter are not available but it is known that the main spring is

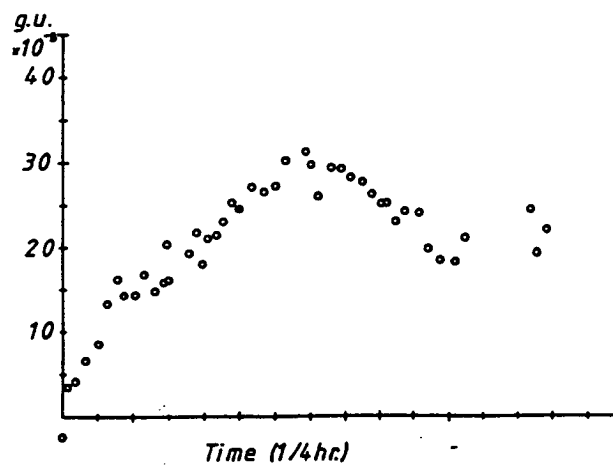
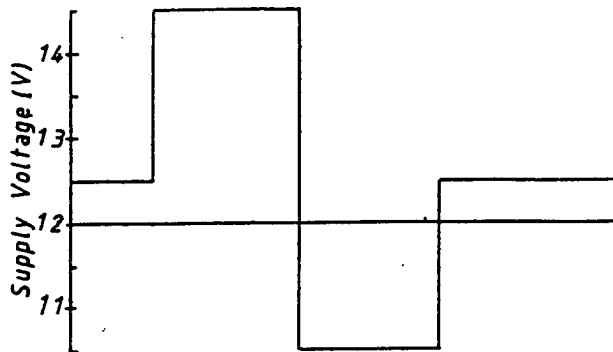
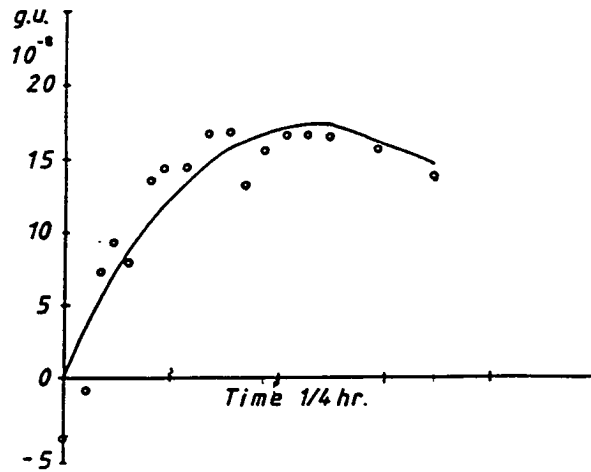
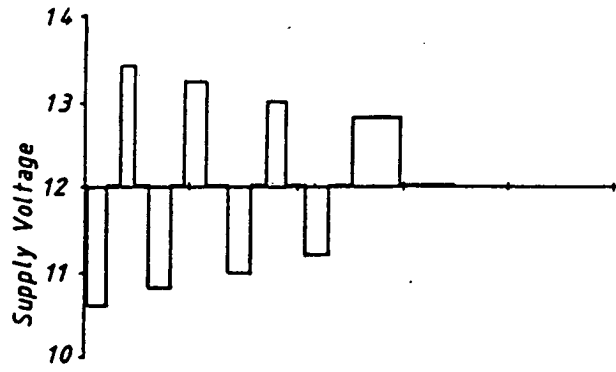


Figure 3.10 Effect of varying voltage on G-275 reading

Table 3.3

## The Effect of Supply Voltage Change on Gravity Meter Reading

| Author  | Number of meters | Voltage variation | Observed gravity change g.u. per volt                            |
|---|------------------|-------------------|--|
| Boedecker 1978  | 1                | 10 V → 12.5 V     | - 0.04   |
| Williams 1983   | 7                | 10 V → 14 V       | maximum of<br>+ 0.04 ± 0.01 optical<br>- 0.01 ± 0.005 electronic |
| (Nickel Cadmium cells recommended $\Delta V = 0.3$ V) |                  |                   |  |
| Nakogawa 1975   | 4                | 10 V → 14 V       | - 0.02, - 0.05, - 0.05,<br>- 0.05                                |

magnetic (Harrison and La Coste, 1978). The spring is demagnetised before assembly and the sealed chamber provides magnetic sheilding.

The meter was tested by placing it in the centre of a large, 2x2x2 meters, set of Helmholtz coils (figure 3.11) with the long axis of the instrument aligned east west. The magnetic field was altered by by varying the current in each set of coils independently and measured using a hand held field strength meter. The meter was read continuously, during which time the magnetic field underwent three transitions between the field states illustrated in figure 3.11. Initially the coil currents were adjusted to null the ambient field to within a few nano Tesla. The meter was then read continuously (i.e. about every four minutes, temperature and pressure were also noted) for a period before the vertical and north coil currents were switched off. Hence the earth's field was again ambient in those directions (referred to as 'H'). After a period of observation, the zeroing current was turned on again but reversed so the magnetic field of the vertical north-south plane was twice that of the Earth (referred to as '2H'). The third transition was accomplished by finally returning to zero field ('0').

Five observation sequences were undertaken and the results of four are shown in figure 3.12. These graphs clearly illustrate a correlation between magnetic field

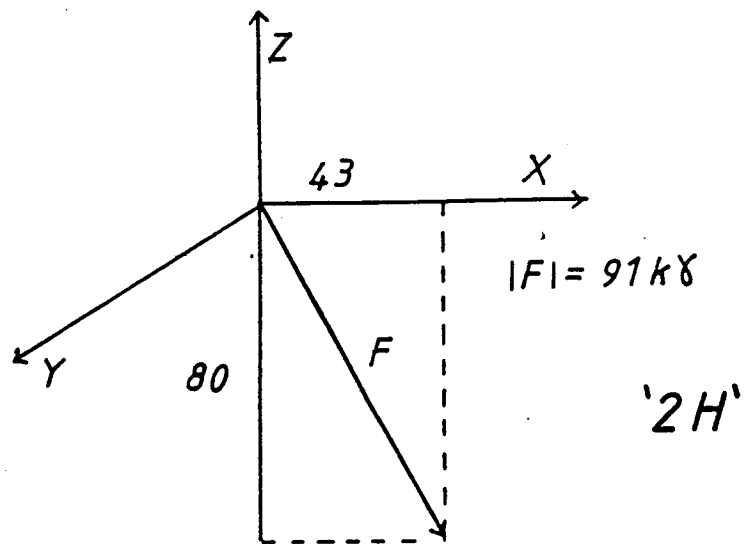
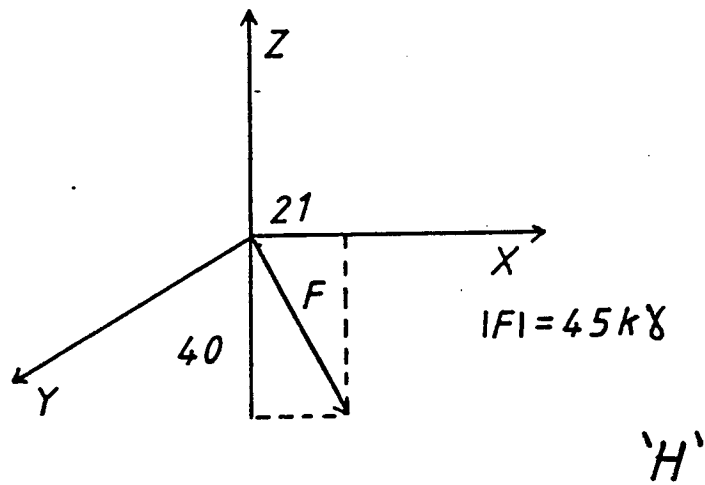
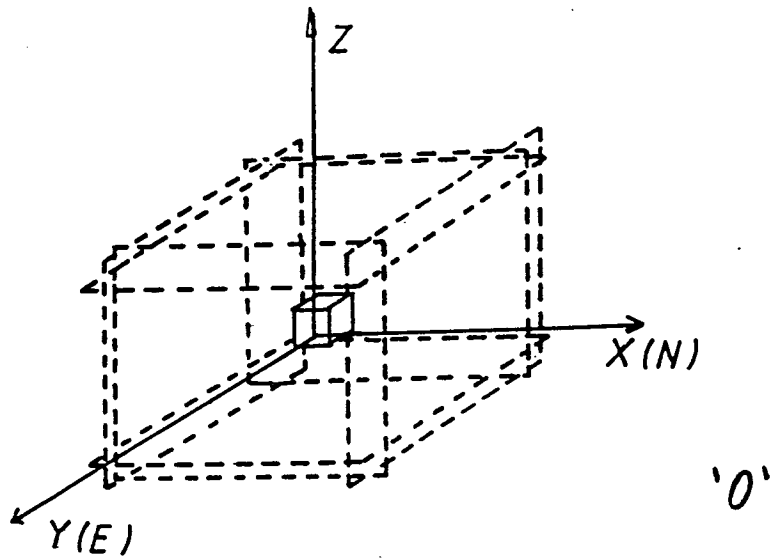


Figure 3.11 Schematic diagram of magnetic field vector

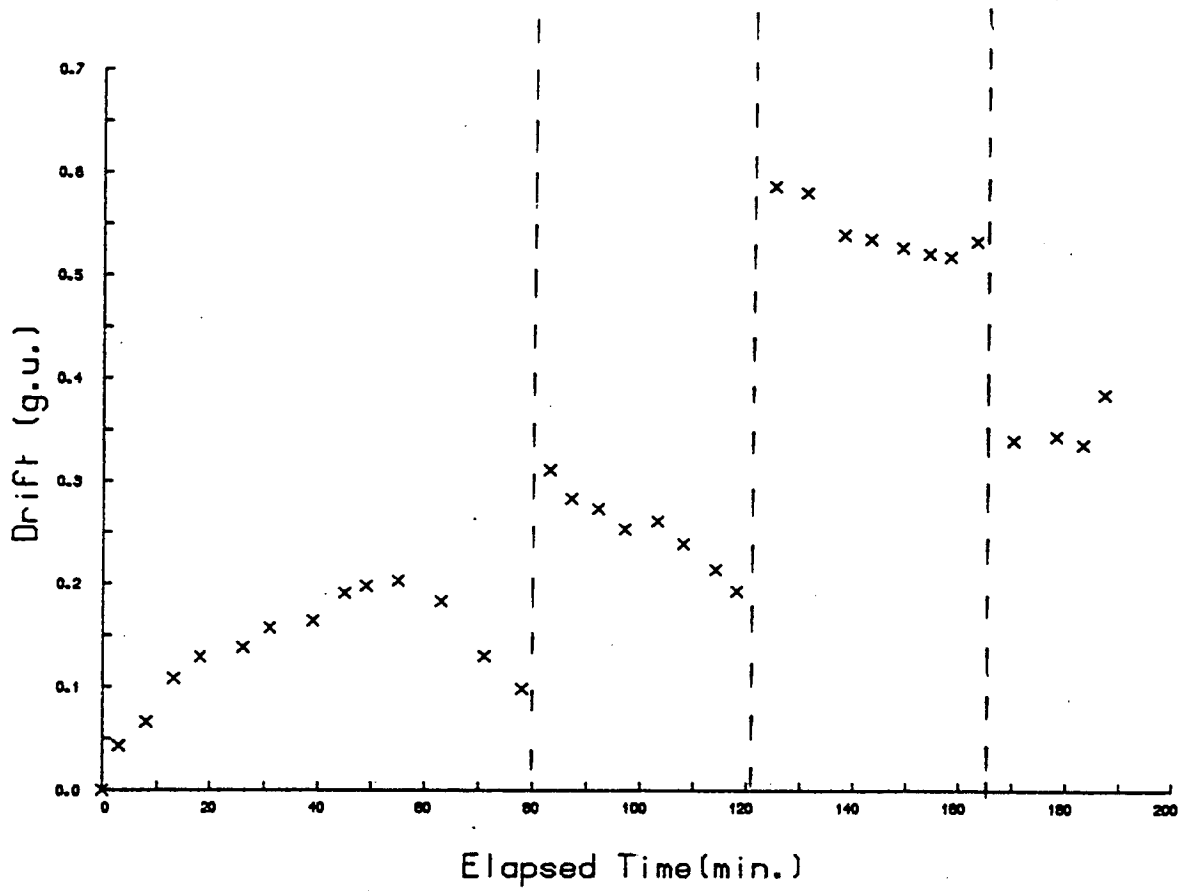


Figure 3.12(a) MAGA Observations

Magnetic Effect, 0 - H - 2H - 0

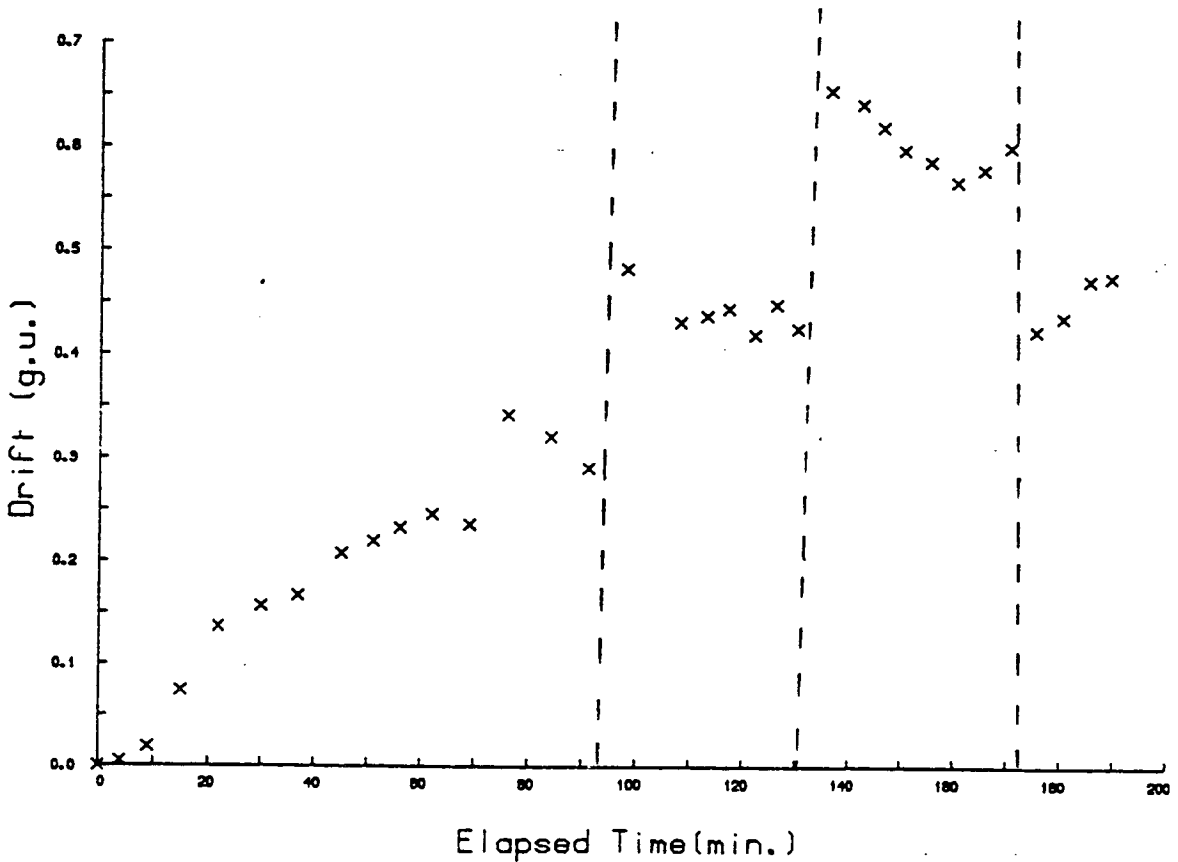


Figure 3.12(b) MAGB Observations



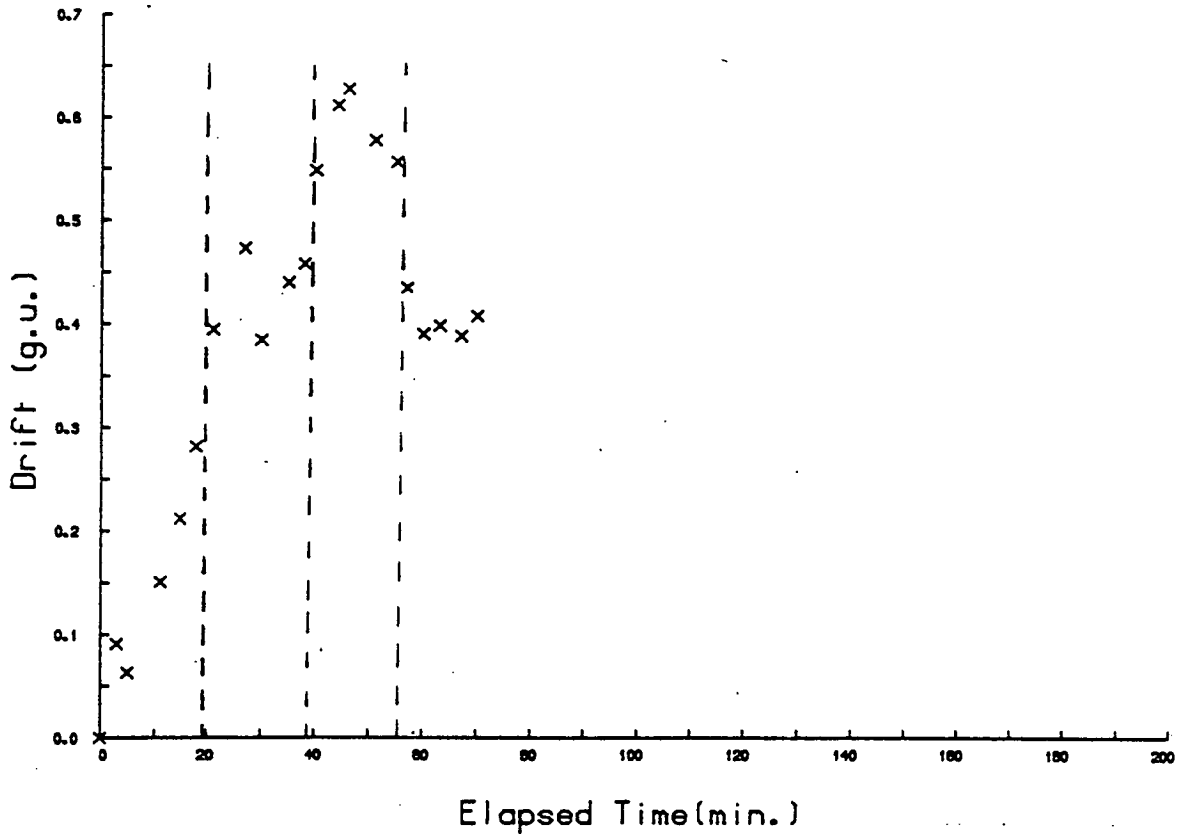


Figure 3.12(c) MAGD Observations

Magnetic Effect, 0 - H - 2H - 0

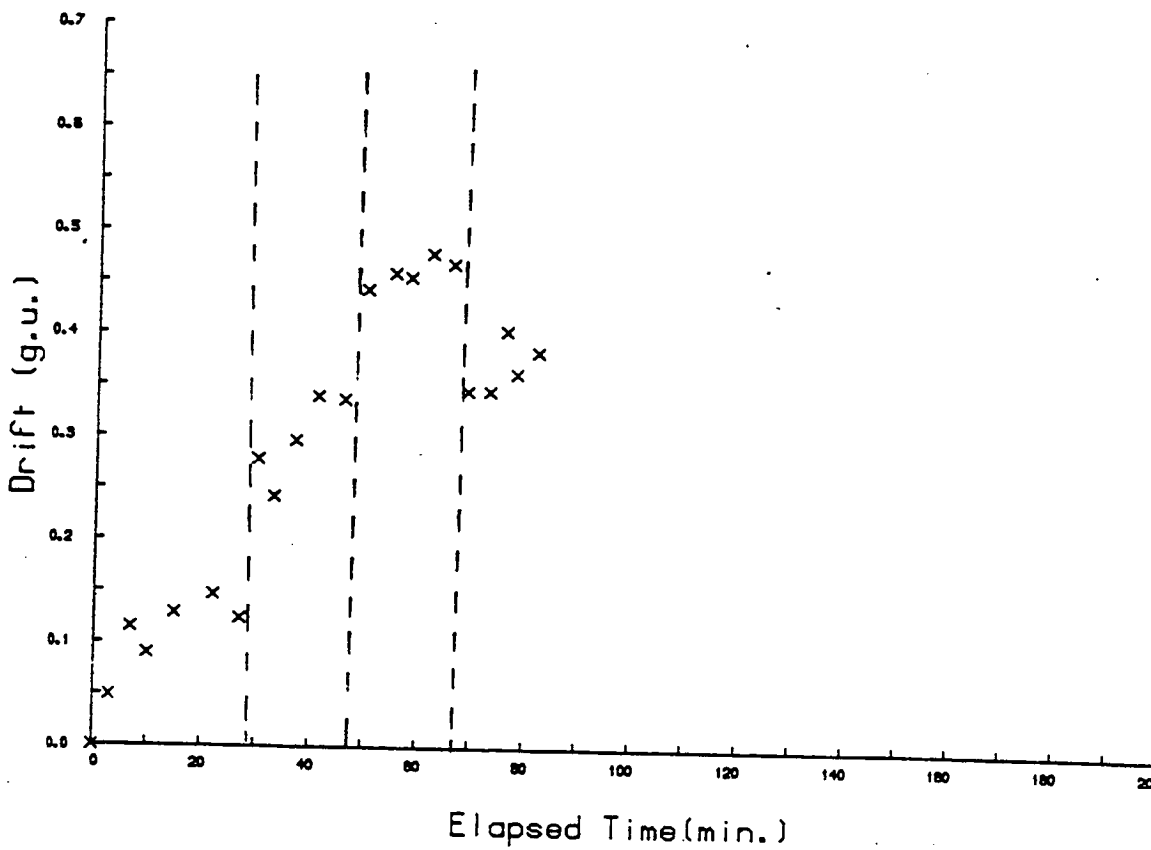


Figure 3.12(d) MAGE Observations

direction and the observed dial turns for G-275. These data were analysed using a least squares cubic spline computer program (discussed in detail in the Chapter Five) to analytically determine the effect of the applied field transitions. The results of this analysis are presented in Table 3.4. The effect is consistent but does exhibit a large scatter. The final transition (2H-0) causes a negative gravity change which does not equal the sum of the two positive steps (O-H and H-2H) possible due to magnetic hysteresis. The results of some published studies are tabulated in Table 3.5. These vary widely, for example Kivinemi notes no reading change despite a magnetic field change of five times the earth's field whereas Boedecker obtains a 0.40 g.u. change after the application of a 60 $\mu$ T. horizontal component. The values obtained for G-275 falls in between these extremes.

### 3.4 Conclusions

The effects of several environmental parameters have been studied. Temperature variations seem to have no mechanical effect on G-275. Nevertheless precautions should be taken to maintain a constant external temperature whenever possible. Level stability in particular is susceptible to direct sunlight (see section 8.3 for fieldwork experience of this phenomenon). The effect of pressure variations on G-275 was not evaluated but the literature

Table 3.4

Observed gravity change (meter G.275) due to  
magnetic field variation. (Units = g.u.)

|                  | O → H | H → 2H | 2H → O | Number<br>of<br>Observations | Fit<br>rms |
|------------------|-------|--------|--------|------------------------------|------------|
| MAGA<br>21.02.79 | 0.194 | 0.400  | -0.194 | 34                           | 0.01       |
| MAGB<br>24.02.79 | 0.150 | 0.193  | -0.119 | 34                           | 0.02       |
| MAGC<br>24.01.81 | 0.057 | 0.078  | -0.072 | 35                           | 0.03       |
| MAGD<br>29.01.81 | 0.119 | 0.139  | -0.150 | 21                           | 0.03       |
| MAGE<br>02.02.81 | 0.106 | 0.109  | -0.139 | 22                           | 0.02       |
| Average(g.u.)    | 0.125 | 0.184  | -0.135 |                              |            |
| Std.Dev(g.u.)    | 0.051 | 0.128  | 0.045  |                              |            |

Table 3.5  
Gravimetric Effect of Magnetic Field Change

| Author             | Number<br>of<br>Meters | Field Change | Observed gravity change<br>(g.u.) |
|--------------------|------------------------|--------------|-----------------------------------|
| Brein et al., 1977 |                        |              |                                   |
| GL                 | 2                      | 250 $\mu$ T  | zero                              |
| IFAG               | ?                      | 15 $\mu$ T   | .12 max                           |
| Boedecker, 1978    | 1                      | 60 $\mu$ T   | .40 max                           |
| Williams, 1983     | 2                      | 104 $\mu$ T  | < 0.01                            |

GL Geodettinen Laitos, Helsinki (Kiviniemi)

IFAG Institut fur Angewandte Geodasie, Frankfurt am Main (Brein)

suggests that these will be negligible. Large instantaneous voltage variations, substantially greater than probable under field conditions, caused no perceptible change of reading. Magnetic field variations have a demonstrable effect on reading accuracy. Observations should be taken well away from large field gradients such as large buildings, pipelines, pylons etc.. The orientation at sites should be noted and conserved when making repeat readings.

CHAPTER FOUR  
THE EARTH TIDES

4.1 Calculation of the Tidal Potential and Tidal Force

If we wish to observe gravity precisely, it is necessary to accurately correct the effect of the constantly varying tidal forces. All celestial bodies exert a Newtonian attraction upon the Earth but only the Sun and Moon need be considered. The greatest disturbing potential exerted by a planet is that of Venus and is more than four orders of magnitude smaller. These forces typically have a range of 1.5g.u. at mid latitudes with a maximum global span of some 2.5g.u.. Thus the time of each gravity reading is noted (to the nearest minute or better), and a tidal correction calculated by a computer program is applied retrospectively to the scaled dial turns.

The original development of the tide generating potential is due to Darwin (1883) (who chaired an Admiralty Committee on the problem of tidal prediction and studied the problem of tidal friction (Darwin 1879,1880); he proposed the model of the Moon ejected from the Earth. Darwin expressed the tidal potential in terms of a harmonic expansion which utilised 'old' lunar theory and



referred parameters to the Earth's equatorial plane rather than the ecliptic. Doodson (1922) used the lunar theory of Brown (1908) introducing argument numbers and extending the expansion.

Several standard texts on tidal theory and analysis exist (Godin, 1972 ; Melchior, 1978) and the subject matter is discussed in most general geophysical textbooks. The analysis here is taken from a number of sources in addition to the above (Heikkinen, 1978 ; Cartwright, 1977 ; Stacey, 1977) and principally Vanicek (1980).

We shall first consider the Earth-Moon system illustrated in figure 4.1 ; the attracting accelerations at P and O are :

$$\alpha_o = G \frac{M_m}{\rho_o^2} \quad , \quad \alpha_P = G \frac{M_m}{\rho_P^2} \quad \text{E 4.1}$$

G = Gravitational constant ( $6.67 \times 10^{-11} \text{ kg m}^3 \text{ s}^{-2}$ )  $M_m$  = Moon mass ( $7.38 \times 10^{22} \text{ kg}$ .)  
 The difference in the associated forces exert a tidal deforming stress pattern on the Earth. By application of the sine and cosine rules  $\rho_P$  may be expressed as

$$\rho_P = \rho_o \left( 1 + \left( \frac{r_E}{\rho_o} \right)^2 - 2 \left( \frac{r_E}{\rho_o} \right) \cos Z \right)^{1/2} \quad \text{E 4.2}$$

It is simpler to use the scalar potential, rather than acceleration,  $g = \text{grad } V$ .

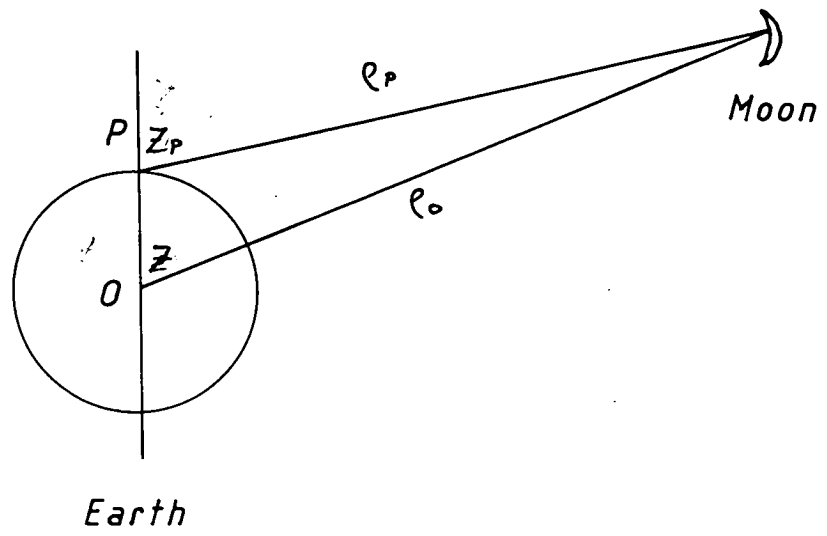


Figure 4.1

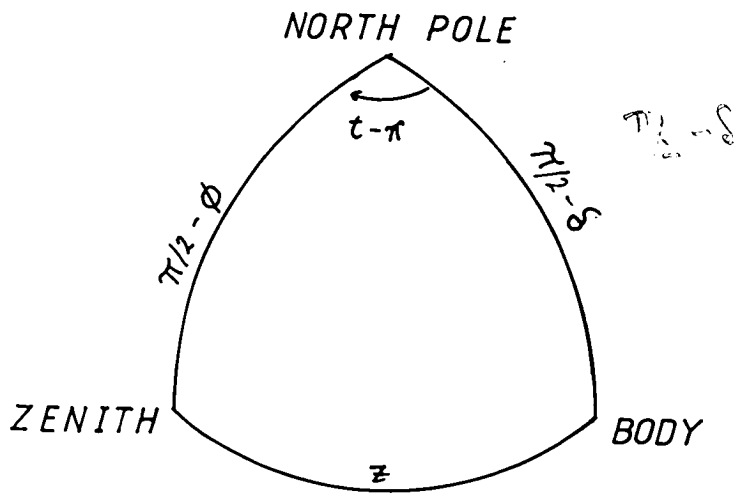


Figure 4.2



So if the tidal potential generated by the Moon at P is denoted  $V_m(P)$ :

$$\begin{aligned} V_m(P) &= \frac{GM_m}{r_p} \\ &= \frac{GM}{r_0} \left( 1 + \left( \frac{r_E}{r_0} \right) + 2 \left( \frac{r_E}{r_0} \right) \cos \phi \right)^{-1/2} \end{aligned}$$

E 4.2A

This expression may be expanded using Legendre Polynomials. The tidal potential is given by the removal of the equivalent point mass ( $n = 0$ ) and the potential of the constant force field ( $n = 1$ ). We denote this by  $W_n(P)$  for the point P

$$W_n(P) = \frac{GM_m}{r_m} \sum_{n=2}^{\infty} \left( \frac{r_E}{r_0} \right)^n P_n \cos \phi \quad \text{E 4.3}$$

A similar argument may be applied to any celestial body. In the case of the Moon  $r_E/r_m = 1.67 \times 10^{-5}$  and in that of the Sun  $r_E/r_s = 4.33 \times 10^{-5}$ ; so it can be seen that the series converges very rapidly. The first two terms in the Earth-Moon system being over 99 per cent of the total.

$$W_2(P) = \frac{GM}{2r_0} \left\{ \frac{r_E^2}{r_0} (3 \cos^2 \phi - 1) \right\} \quad \text{E 4.4}$$

$$W_3(P) = \frac{GM}{2r_0} \left\{ \frac{r_E^2}{r_0} (5 \cos^3 \phi - 3 \cos \phi) \right\}$$

E 4.5

The latitude is a locally based co-ordinate and may be

referred to geocentric and conventional astronomical co-ordinates. Consider figure 4.2, from spherical trigonometry.

$$\cos Z = \sin \phi \sin \delta + \cos \delta \cos \phi \cos t \quad \text{E 4.6}$$

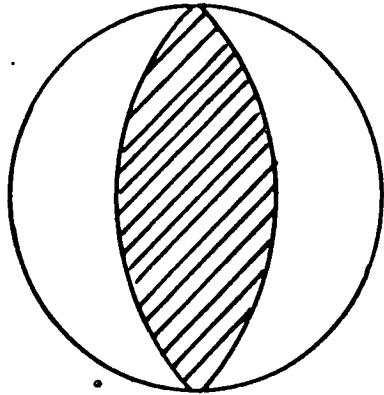
geocentric latitude,  $\delta$  = declination,  $t$  = hour angle

The expression for  $W_2(P)$  can then be separated into three distinct terms.

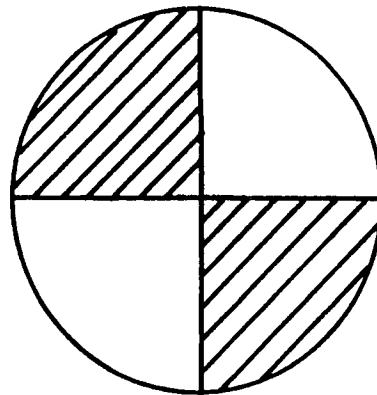
$$W_2(P) = \frac{3}{4} G M_m \frac{r_E^2}{\rho_0^3} \left\{ \begin{array}{l} \cos^2 \phi \cos^2 \delta \cos 2t \quad \text{E 4.7a} \\ + \\ \sin 2\phi \sin 2\delta \cos t \quad \text{E 4.7b} \\ + \\ 3(\sin^2 \phi - \frac{1}{3}) \cdot \\ (\sin^2 \delta - \frac{1}{3}) \quad \text{E 4.7c} \end{array} \right.$$

This decomposition into three terms is due to Laplace who demonstrated the spatial dependence of the terms, each representing a type of second order surface as shown in figure 4.3.

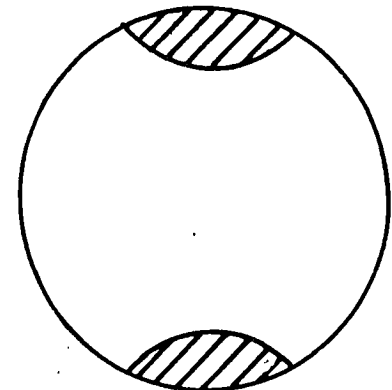
The hour angle  $t$  of the Moon increases monotonically with time as the Earth rotates, hence the sectorial term is semi diurnal and the tesseral is diurnal. The zonal term causes long term variations in the potential with the squared sine of the declination of the perturbing body, 14 days and 6 months. In practice  $\phi, \delta$  and  $t$  vary with time



*Sectorial*



*Tesseral*



*Zonal*

*Figure 4.3*

in a complex manner for both the Moon and the Sun , leading to hundreds of tidal components at discrete frequencies known as multiplets.

Since Darwin's formulation was in terms of the lunar obliquity rather than inclination, his development was quasi-harmonic. The formulation retains constituents which were really slowly variable; (lunar obliquity varies between  $18^{\circ} 18^m$  and  $28^{\circ} 46^m$  with a period of 18.6 years). Doodson's formulation utilising Brown's lunar theory derives a series expansion in terms of latitude and longitude. Doodson's purely harmonic expansion contained 386 components whose coefficients are greater than 0.0001 times the greatest. This development was in use for fifty years before being ameliorated by Cartwright and Taylor (1971, ammended Cartwright and Edden, 1973) who slightly altered certain coefficients on the basis of computer spectral analysis of three eighteen year time spans. They also used new astronomical and geodetic constants.

Doodson expressed the potential as an infinite harmonic sum of six independent variables

$$W_T = d_1 \gamma + d_2 S + d_3 h + d_4 p + d_5 N' + d_6 P_1$$

Notation as in Doodson where,

$\gamma$  = local mean lunar time

$S$  = Moon's mean longitude

$h$  = Sun's mean longitude

$p$  = longitude of the Moon's perigee

$N'$  =  $-N$  where  $N$  is longitude of the  
(Moon's ascending) node

$P_1$  = longitude of Sun's perigee

The use of such variables leads to simplified analysis and several elegant points of notation. The 'speeds' of the variables are all positive and hierarchical classification with regard to  $\tau$ , completely separates the constituents without overlapping.

Considering the argument numbers for  $W_2$ . The argument  $d_1$  may be 0, 1 or 2 while  $d_2$  to  $d_6$  may be positive, negative or zero. The tides are split into different species depending on the value of  $d_1$ , each consisting of several groups with the same value of  $d_2$ .

Doodson suggested a form of notation that is now widely accepted with the exception of Darwin's two character alphanumeric notation for the principal tidal components. For example, consider the following constituent which is a linear function of all six variables.

$$2\tau - 3s + 4h + p - 2N' + 2p_1$$

Doodson suggested the use of a datum of five (since the integer coefficients are seldom greater than 4. So five is added to all the coefficients except that of  $\tau$  (which is always positive), obtaining an argument number of 229.637.

Argument No. = 229.637

Constituent = 229

Group = 22

Species = 2

The break down of species into constituents is illustrated

in figure 4.4 taken from Doodson (1921).

## 4.2 Earth Deformation

The Earth responds to the tidal potential in a semi elastic manner. The response is complicated by indirect effects generated by the loading of oceanic water bodies. The elastic response of the real Earth was first fully treated by Love (1909) and the elastic effects can be represented by dimensionless constants (known as Love numbers) 'h' and 'k'. 'h' is the ratio of the body tide to the height of the static equilibrium tide and 'k' is defined as the ratio of the additional potential produced by the redistribution of mass to the deforming potential. A third constant,  $l$  was later introduced, and is the ratio of horizontal displacement of the crust to that of the equilibrium fluid tide (Shida , 1912).

Consider figure 4.5 which illustrates the deformation of the Earth at a point due to the vertical component of the tidal force. With the application of  $F_v$  the equipotential surface passes through C and the Earth's surface uplifts to B. This deformation causes an additional change of the equipotential so that it now passes through D.

The potential difference between the observed  $W(B)$  and the rigid Earth potential  $W(A)$  is the sum of three terms

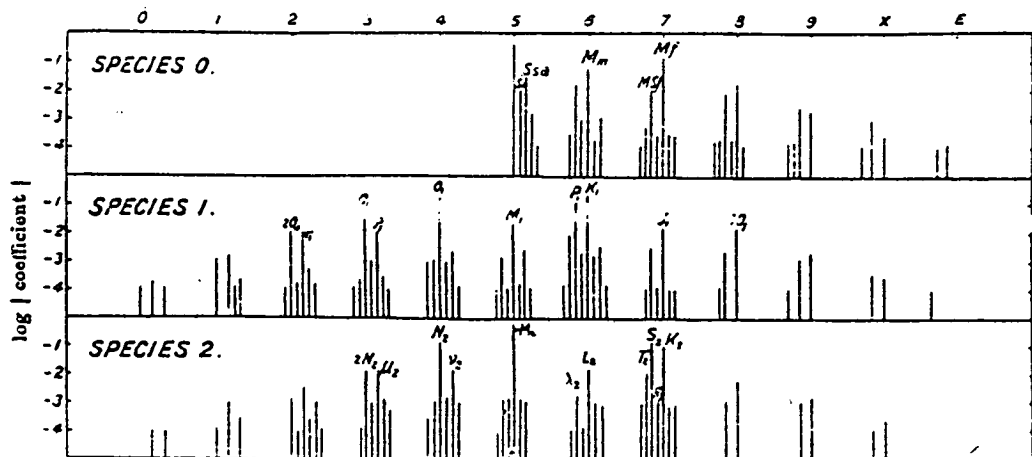


DIAGRAM A: constituents, separable in one year.

The speed scale is indicated by the figures at the top of the diagram; these, with the species-number, give the group-numbers, and the places of the constituents in the diagram can then be readily found. An increment of 1 in the group-number corresponds to an increase in speed of about  $13''$  per mean solar day; the increase in speed for an increase of 1 in the constituent-number is about  $1''$  per mean solar day.

Figure 4.4 Tidal constituents separable in one year (from Doodson, 1921)

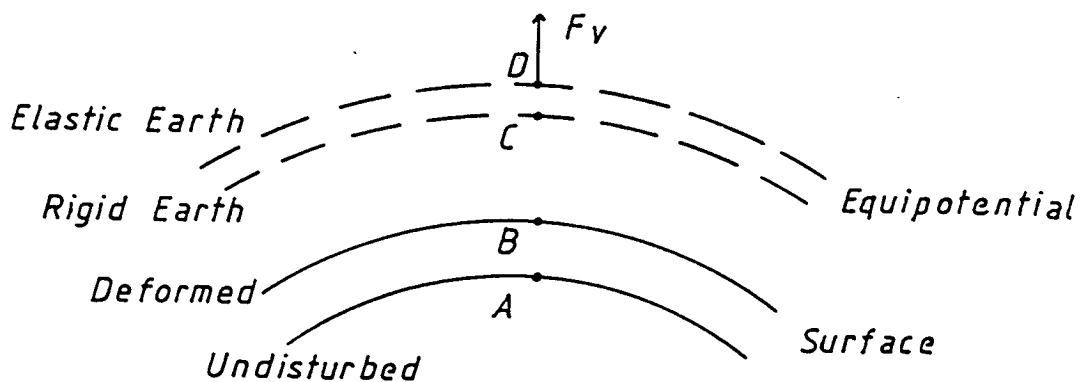


Figure 4.5  
(After Vanicek, 1973)

- (1) The tidal potential  $W_2$
- (2)  $W(u)$ , the loss in potential due to displacement  $u$ .
- (3)  $W(u)_{\text{def}}$ , the deformation potential produced by the field change

(1) is given above and the loss of potential  $W(u)$  may be simply expressed:

$$W(u) = u \frac{\partial W_A}{\partial \rho} = -u.g \quad \text{E 4.9}$$

The theoretical equilibrium height of the oceanic tide will be  $W_2/g$ . If we assume that distribution of mass is spherically symmetric and that rigidity is constant over the surface we can express the radial displacement  $u$  as the product of some function  $H(r)$  and the tidal potential:

$$W(u) = H(r).W_2 \quad \text{E 4.10}$$

$$u = H(r).W_2/g \quad \text{E 4.11}$$

The deformation potential associated with the displacement of matter may be expressed as the product of the harmonic  $W_2$  and some function of  $r$ , e.g.  $K(r).W_2$ . If we write,  $h = H(A)$ , and  $k = K(A)$ , the observed potential is given by;

$$W(B) = W(A) + W_2 + k.W_2 - h.W_2 \quad 4.12$$

The oceanic tides are diminished by the body tides by the factor

$$1 + k - h : 1$$

For a hypothetical rigid Earth both  $k$  and  $h$  would be equal to zero, and for a fluid Earth in tidal equilibrium  $h$  equals unity and  $k$  is a function of the density profile; if this



were uniform  $k = 1.5$  for the actual inferred profile  $k = 0.937$ . The elastic response of the real Earth is frequency dependent, the higher the frequency the greater the rigidity, and generally quoted values in the literature refer to  $M_2$  and  $r$  equal to  $r_E$ . By differentiating expression (4.12) and substituting (e.g. Vanicek, 1980) it can be shown:

$$g + dg = g - (1 - 3/2k + h) \delta W_2 / \delta r \quad E 4.13$$

Theoretical values for  $h$  and  $k$  can be obtained from hypothetical Earth models, the first of which was postulated by Kelvin in 1876. He demonstrated that a homogenous incompressible Earth requires a mean rigidity greater than that of steel (Lambeck, 1980). Kelvin's Earth is far removed from the real Earth but his treatment was the basis of subsequent more complex models as seismology provided further information (eg. Poincare, 1911). The first successful attempt to solve the problem for a complex heterogeneous Earth was published in 1950 (Takeuchi, 1950). Takeuchi rewrote the Love-Herglotz equations (Melchior, 1978 p91) as a function of  $r/a$  before numerical integration. The advent of modern computers has greatly facilitated the numerical calculations and the information about the elastic structure of the Earth has improved with the inclusion of free oscillations Table (4.1) illustrates the values of  $h, l$ , and  $k$  obtained from Farrell (1972) (other similar work includes Takeuchi, Saito and Kobayashi (1962), Longman(1963), Pekeris and Accad (1972)) and figure 4.6

*Theoretical Love numbers of degree  $n$  computed by Farrell (1972) for three different Earth models: Gutenberg-Bullen (G-B) Earth model (first line for each  $n$ ), an Earth model with a typical oceanic upper-mantle structure (second line for each  $n$ ), and an Earth model with a typical shield upper mantle (third line for each  $n$ )*

|                 | $n$ | $h_n$  | $l_n$  | $k_n$  |
|-----------------|-----|--------|--------|--------|
| G-B Earth model | 2   | 0.6114 | 0.0832 | 0.3040 |
| Oceanic mantle  |     | 0.6149 | 0.0840 | 0.3055 |
| Shield mantle   |     | 0.6169 | 0.0842 | 0.3062 |
|                 | 3   | 0.2891 | 0.0145 | 0.0942 |
|                 |     | 0.2913 | 0.0145 | 0.0943 |
|                 |     | 0.2923 | 0.0147 | 0.0946 |
|                 | 4   | 0.1749 | 0.0103 | 0.0429 |
|                 |     | 0.1761 | 0.0103 | 0.0424 |
|                 |     | 0.1771 | 0.0104 | 0.0427 |

Table 4.1 Love numbers calculated by Farrell(1972)  
(reproduced from Lambeck, 1980).

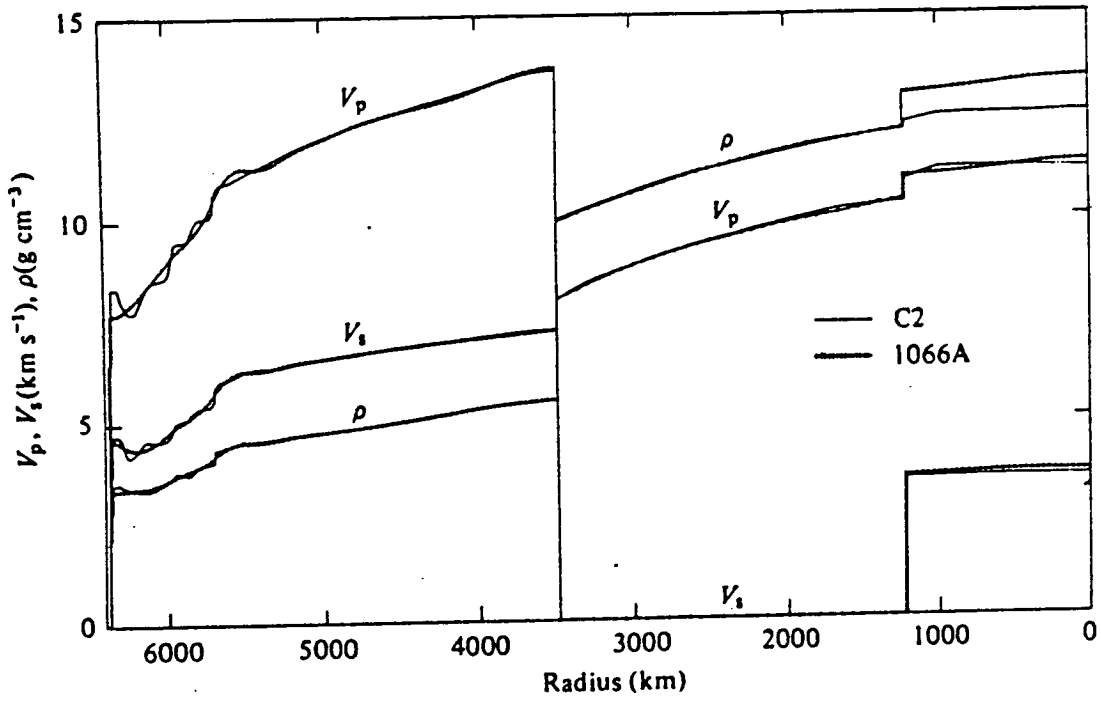


Figure 4.6 Models C2 from Anderson & Hart (1976) and 1066A from Gilbert & Dziewonski (1975) of the Earth's radial seismic velocity and density structure. (from Lambeck, 1980).

illustrates two recent Earth models. The Farrell values of the low degree Love numbers do not appear to be sensitive to mantle structure and yield a gravimetric factor of

$$1 + h - 3/2k = 1.158 \quad (n=2)$$

This is the generally accepted value for the diurnal and semi-diurnal components.

### 4.3 Ocean Loading

In the preceding discussion we have not yet considered the effect of the oceans which cover nearly three quarters of the Earth's surface. The oceans are not in equilibrium with the tidal potential and because of their irregular nature perturb the Earth tides in a complex fashion. The ocean tide loading signal consists of three components.

- (a) The change in vertical displacement of the surface due to the yielding of the crust
- (b) The redistribution of crustal mass
- (c) The direct Newtonian attraction of the water body.

Ocean loading can cause a ten per cent difference between the theoretical and observed tide and as such should be carefully evaluated to make correct tidal reductions to observations.

Little is known about the tidal parameters in the deep sea though measurements in coastal areas are commonplace.

These measurements may be used to constrain worldwide numerical models to solve Laplace's tidal equations using finite difference schemes (Hendershott, 1972 (M2); Bogdanov and Magarik ,1967,1969(M2,S2,K1,O1); Pekeris and Accad, (1970) (M2)). The most recent model study of Schwederski (1980) includes dissipative effects . The marine tide is then convolved with the Green's function of an appropriate radially stratified Earth model (such as the Gutenberg-Bullen model, determined seismically) to obtain the gravity signal (Farrell,1973). The ocean loading effect may be determined directly from the analysis of highly accurate continuously recording gravity meters (Earth tide meters ) for periods of at least sixty days at a particular location. The results from these meters (again generally manufactured by the La Coste and Romberg company), are split into tidal components and the theoretical body tide subtracted.

#### 4.4 Tidal Predictions using Computer Programs

Several computer programs to predict the vertical component of the tidal acceleration were compiled on the Edinburgh mainframe. Three programs were considered sufficiently accurate (better than  $10^{-3}$  g.u.) to reduce high precision gravity observations.

(1) CART : A program based on the harmonic expansion of Cartwright-Tayler-Edden (see section 4.2) This program was

written at Edinburgh by Dr. R. Hipkin and the author. It is a subroutine in the program PBAS listed in Appendix(4).

(2) BZS : A program based on Broucke Zurn and Schlichter (1972, kindly provided by the Earth Tides section, Institute of Oceanographic Sciences, Bidston. (A listing is not appended, but copies of the program may be requested directly from that source).

(3) HEIK : This is an exact copy of the program listed in Heikanen(1978)

The programs BZS and HEIK are generically similar but very different in programming style. They involve the use of a closed expression of the form

$$g_r = Kp^2[(\xi^{-3/2}-1)\cos z - \xi^{-3/2}]$$

where K is a constant, p is the horizontal parallax of the moon, z is the zenith angle of the moon and  $\xi$  related to the latitude of the observing station. BZS is essentially an amelioration of Longman (1959) using an improved lunar ephemeris (Eckert, Jones and Clerk, 1954). The vertical solar earth tide is in fact calculated identically to Longman. HEIK also uses the formulae of Eckert Jones and Clerk but the ephemeris of the 1972 Nautical Almanac. The solar formulae is based directly on Newcomb(1895). Heikanen corrects for the effect of polar motion, (the pole, or point where the axis of rotation passes through the Earth's surface, is in motion relative to the earth itself).

The program CART is however uses a totally different method and is based on a time harmonic expansion of the tidal potential. The analysis is taken directly from Cartwright and Tayler (1971) (see section 4.2), incorporating 504 harmonic components; (all those greater than an arbitrary level of  $4.5 \times 10^{-5}$  times the greatest coefficient). Such a harmonic development has the advantage that the amplitude and phase of each component can be varied to the value of the real earth. All three programs incorporate recent astronomical constants (I.A.U., 1964).

The program BZS was received on card format, together with a sample computation of one month's hourly predictions for the location of Bidston. The program was successfully mounted but gave very slightly different values for the test site. The difference was small with a standard deviation of  $1.2 \times 10^{-4}$  g.u. on 720 sample points. The listing was carefully checked but no transcription error was detected. The program was compiled and executed on two remote computers because of the possibility of machine error, but identical results were obtained. (The Edinburgh machine is an ICL2972, the other two machines were an IBM365 at Newcastle and a CDC7600 at Manchester.)

The program HEIK was keyed on to the mainframe computer and after many <sup>transcription</sup> corrections ran successfully. The

program agreed exactly with the five published test values, stated to  $10^{-4}$  g.u.. In addition to these values the program author Dr Heikanen kindly supplied a sample of 72 hourly values at the location of one of the Finnish secular variation sites (Vaasa, see figure 2.2). Agreement was again complete. The program BZS was executed with the same coordinates and differed with a standard deviation of  $3 \times 10^{-4}$  g.u.. The program CART was already mounted on the Edinburgh mainframe computer. It produced standard deviations of  $6.2 \times 10^{-4}$  g.u. and  $7.4 \times 10^{-4}$  g.u. respectively, when compared with the BZS values at Bidston and Vaasa.

All the programs agree within the required standard of accuracy ( $10^{-3}$  g.u.) for tidal corrections to precise gravity observations but there are other factors. If we consider central processing unit time on the Edinburgh computer (an ICL 2972) there is a considerable difference in time between the programs. BZS takes an average of one hundredth of a second to perform each calculation whereas CART takes an average of two hundredths of a second for an identical location. The program HEIK requires an astonishing 8.3 seconds making it unsuitable for many analyses (e.g. almost two hours processor time for one month of hourly values). Although BZS is the fastest program the routine CART was used in data reduction because of the facility to alter amplitude and phase of tidal component groups.



## CHAPTER FIVE

### SPLINE FITTING AND DATA ADJUSTMENT

#### 5.1 Introduction

Piecewise polynomials are ideally suited to the fitting of geophysical data which are often irregular but repeatable in nature (eg. waveform matching in seismology and palaeomagnetism). Cubic spline functions are most commonly used to approximate continuous functions of one variable because they present computational advantages. These are cubic polynomials joined such that the second derivative is continuous. Furthermore the definition of splines in terms of polynomials has the statistically important consequence that a spline function, when fitted to data by least squares conserves the first two moments of the data (Wold, 1974).

Figure 5.1 illustrates a cubic spline curve and its four composite cubic polynomials. Let us define a cubic polynomial  $f(t)$  ; the condition that  $f''(t)$  and  $f'(t)$  are continuous at the joining points (called knots or nodes) gives rise to equations that have to be satisfied. With reference to figure 5.2, within any nodal interval  $t_n < t < t_{n+1}$  the function  $f(t)$  is represented by:

$$f(t) = f_n(t) = a_n + b_n(t-t_n) + c_n(t-t_n)^2 + d_n(t-t_n)^3 \quad (5.1)$$

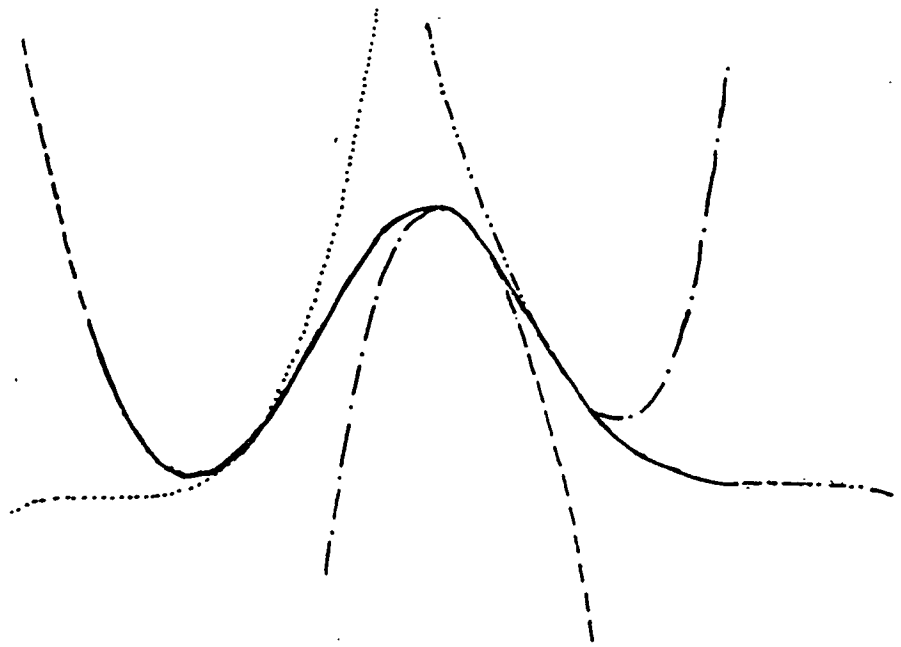


Figure 5.1 Cubic spline curve illustrating the component third degree curves.

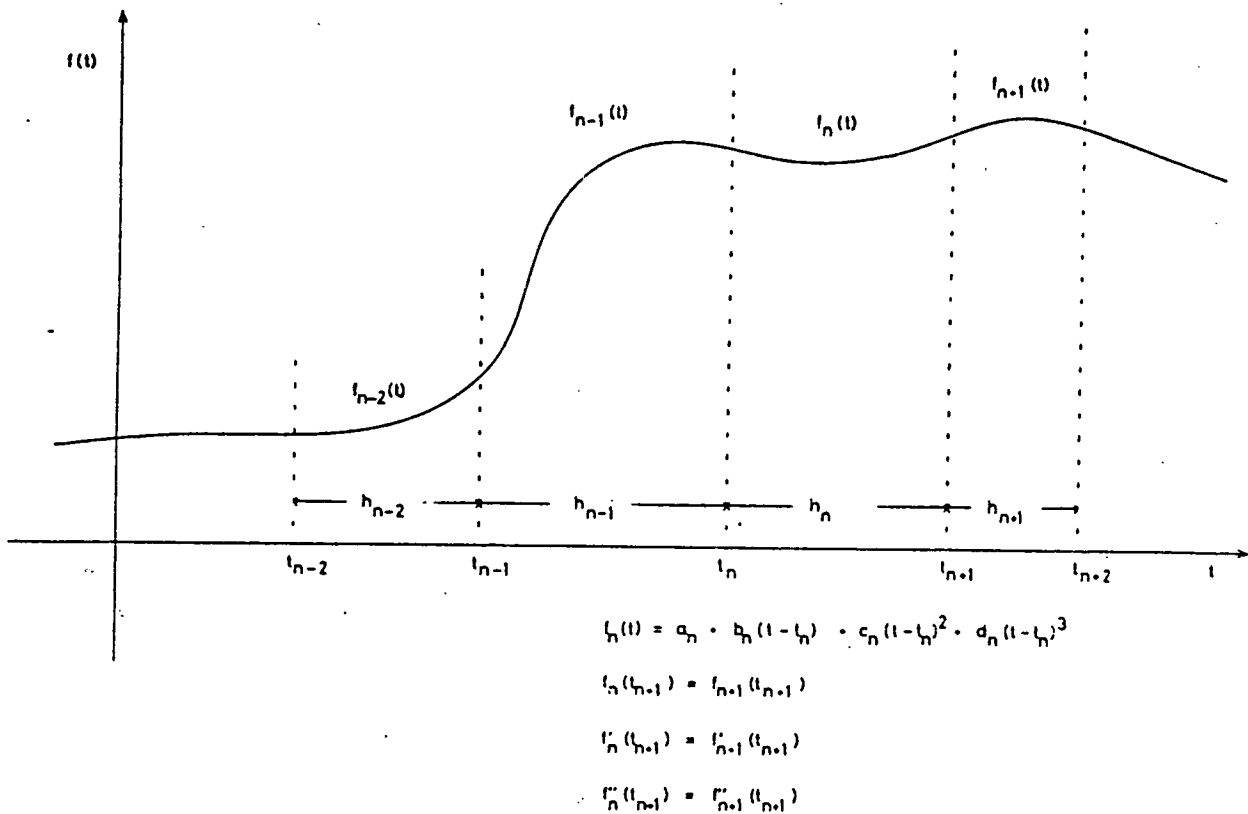


Figure 5.2 Arbitrary spline function  $f(t)$  with nodal positions  $t_{n-2}$ ,  $t_{n-1}$ , etc. indicated.

with continuity conditions

$$f_n(t_{n+1}) = f_{n+1}(t_{n+1}) \quad (5.2)$$

$$f'_n(t_{n+1}) = f'_{n+1}(t_{n+1}) \quad (5.3)$$

$$f''_n(t_{n+1}) = f''_{n+1}(t_{n+1}) \quad (5.4)$$

These continuity conditions impose recurrence relations of the form.

$$\begin{aligned} a_n = & a_1 + b_1 \{ (t_n - t_1) |_{n \geq 2} \} + c_1 \left\{ \frac{2h_1}{3} |_{n \geq 2} + h_1 (t_n - t_1) |_{n \geq 3} \right\} \\ & + c_n \left\{ \frac{h_n^2}{3} |_{n \geq 2} \right\} + c_{n-1} \left\{ \frac{1}{3} (2h_{n-1} + h_{n-2}) \cdot (h_{n-1} + h_{n-2}) |_{n \geq 3} \right. \\ & \left. + \sum_{r=2}^{n-2} c_r \left\{ \frac{1}{3} (h_r + h_{r-1}) [2h_{n-1} + h_{n-2} + 3(t_n - t_{r+1})] |_{n \geq 4} \right\} \right\} \end{aligned} \quad (5.5)$$

$$\begin{aligned} b_n = & b_1 + c_1 \{ h_1 |_{n \geq 2} \} + c_n \{ h_{n-1} |_{n \geq 2} \} \\ & + \sum_{r=2}^{n-1} c_r \{ (h_r + h_{r-1}) |_{n \geq 3} \} \end{aligned} \quad (5.6)$$

$$d_n = c_{n+1} - c_n / 3 h_n \quad (5.7)$$

where  $h_n = t_{n+1} - t_n$

Thus if there are  $N$  nodal intervals there are  $N+3$  degrees of freedom with independent parameters.

$$a_1, b_1, c_1, \dots, c_{N+1}$$

The number of degrees of freedom may be reduced to  $N+1$  (the number of knots) by the application of boundary conditions (De Boor, 1978, p54). One option is to fix the second derivative of the end points to zero.

$$f''(t_1) = f''(t_{N+1}) = 0 \Rightarrow c_{N+1} = c_1 = 0 \quad (5.8)$$

Such an end condition produces a so called natural spline

(by analogy with flexed wires whose end points are fixed).

In practise it was found that such a constraint did not greatly alter a least squares spline solution when applied to gravimetric data. The expressions given here are derived from first principles and computational advantages to be obtained by a scaled divided difference known as Basis spline or B-spline, were thought unnecessary.

## 5.2 Drift adjustment with the spline fitting program NSPL

Because of the complex and highly individual nature of any particular gravity meter's drift, cubic spline functions are well suited to the problem. ('Spline functions are the most successful approximating functions for practical applications so far discovered', Rice, 1963, p123). The observation equation has the form

$$g(t) = G(m) + f(t) + e \quad (5.9)$$

where  $G(m)$  is the gravity value at site  $m$ ,  $f(t)$  is the meter drift to be represented by a cubic spline function and the residual squared,  $e^2$  is to be minimised. With reference to the previous section the number of degrees of freedom for an unconstrained least mean squares cubic spline fit to the data is  $N + M + 3$  ( $M$  is the number of sites) with free parameters

$$a_1, b_1, c_1, \dots, c_N, c_{N+1}, G_1, G_2, \dots, G_M, e$$

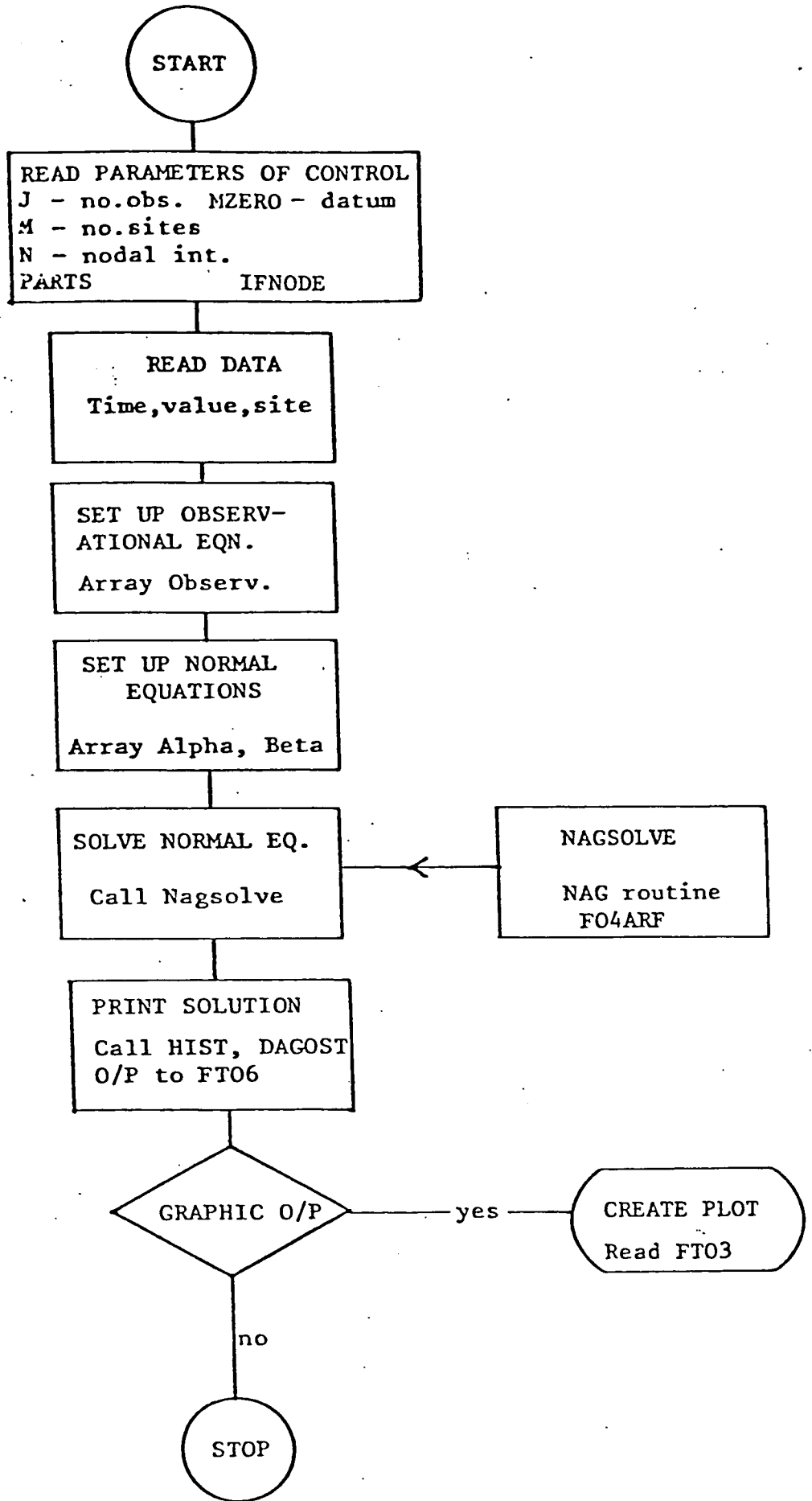
A computer program, NSPL, was written by Dr R. Hipkin and the author to evaluate these coefficients using the expressions (5.5), (5.6) and (5.7), and this is listed in Appendix (1). The program retains many different options because of the different possible measuring sequences. A flow diagram of the program is presented in figure 5.3.

There are seven control parameters which are itemised below

- (1) The number of observations, J
- (2) The number of different gravity sites, M
- (3) The number of nodal intervals, N.
- (4) A parameter controlling the least squares adjustment altered according to the observation sequence known as PARTS
- (5) Identification of the datum site, MZERO
- (6) Control of nodal spacing, IFNODE
- (7) Control of output mode, PDRIFT

The number and location of the nodes can be varied by explicit inclusion in the data set or the program may be divided into a specific fixed or increasing number of equi-spaced nodes. The parameter PARTS exists to ameliorate the adjustment of differently observed data sequences as discussed in section and has three distinct cases; PARTS = 1, PARTS <-1, PARTS >1 .

Figure 5.3 Schematic flow diagram of program NSPL



(a) PARTS = 1

This is applicable to single station continuous observation sequences such as a laboratory drift curve, when the observations are represented simply by the equation 5.9.

(b) PARTS < -1

This provision is intended to evaluate a datum shift between several independent observation sequences while calculating a single continuous spline function. In this case the data sets are joined 'head to tail' with a specified time gap between each section. This occurs when, for example, a measurement sequence is repeated at the same sites on separate occasions, the fixed gravity values constraining the adjustment. The magnitude of the time gap in relation to the nodal positions is crucial in such an application since the nodal density should be sufficiently great to accommodate gradient changes between the independent sequences.

(c) PARTS > 1

In this case it is assumed that the independent observation sequences follow the same observational routine and a common drift curve is fitted so that the initial times of the superimposed data sections are coincident. It is essential that a single observational practise is maintained and with these arguments of symmetry the drift function should be related to elapsed time only. The program calculates the appropriate least squares datum shift for each section or 'PART'.

This form of parameterisation allows the user a large degree of flexibility to select the adjustment best suited to a particular data collection pattern. The program NSPL was used extensively during the processing of data collected by the author. The number of unknowns is equal to

$$M + N + \text{PARTS} + 1$$

thus a typical observation sequence of twenty readings four times (PARTS = 4, M = 1) is well constrained since the total number of observations is eighty ( J = 4 x 20 ).

The facility to increase the number of nodes should be used with care since imprudent selection of N can lead to overfitting. Overfitting occurs when the spline function oscillates about the general trend in an attempt to minimise the error contribution of minor reading fluctuations. The solutions obtained on well constrained data sets differ only minimally as the number of nodes are initially increased. The solutions are very similar to those obtained with low order polynomials. Solutions with a single nodal interval were generally applied rather than more complex adjustments which would not be intercomparable at differing orders.

### 5.3 Adjustment of some collected data

A laboratory test was undertaken to examine the effect of transportation. This is presented in this section as an



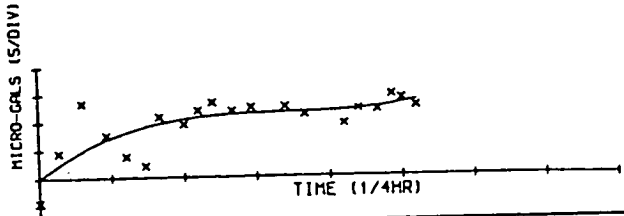
illustration of the variation of NSPL parameters and also to introduce the 'equilibrium' method of observation.

The Edinburgh instrument's characteristic drift curve attains a maximum after which the drift slope is approximately level and the meter appears to be in equilibrium with the disturbing force. Therefore it may be more accurate to use this value or the entire drift curve rather than the conventional single initial value. The meter is observed at a site for between eighty and one hundred minutes (a minimum of twenty readings), and then transported to the next site. A single link is insufficiently strong so a triple link (A-B-A-B) is completed. Such a sequence occupies a complete working day.

Four single solutions for a study in which the meter was stationary between reading sequences are shown in figure 5.4. The effect of altering the number of nodes is shown in figures 5.5 and 5.6. The latter demonstrates the problem of overfitting (to a point where the r.m.s. error is zero). A single least squares solution may be fitted to the four curves, automatically adjusting the datum level of the independent data sequences (PARTS = 4, M = 1), as shown in figure 5.7. This diagram is similar in form to the composite drift curves obtained in Chapter Eight from field data collected in Scotland (see figures 8.5,8.6,8.7).

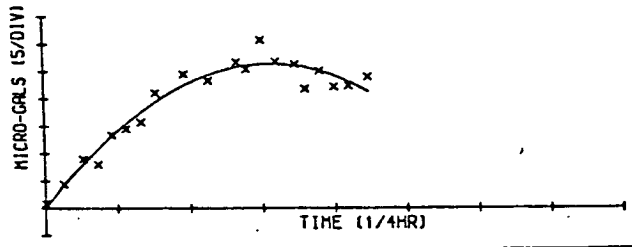
STATIC#1, OBS. SEQ. 1

|                   |   |
|-------------------|---|
| STATION #         |   |
| SPLICE PARAMETERS |   |
| NO OF RECS        | 2 |
| NO                | 1 |
| ACROSS            | 1 |
| WIDTH             | 1 |
| COND. FILE        |   |



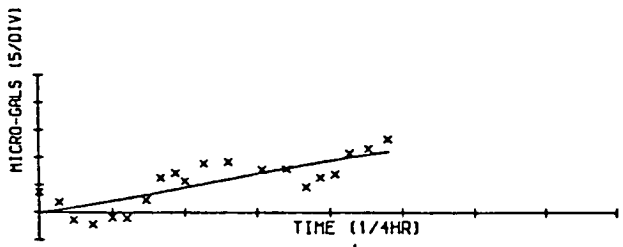
STATIC TEST#1, OBS. SEQ. 2

|                   |   |
|-------------------|---|
| STATION #         |   |
| NO OF RECS = 2    |   |
| NO VALUE = 1.80   |   |
| STATION #         |   |
| SPLICE PARAMETERS |   |
| NO                | 1 |
| ACROSS            | 1 |
| WIDTH             | 1 |
| COND. FILE        |   |



STATIC#1, OBS. SEQ. 3

|                   |   |
|-------------------|---|
| STATION #         |   |
| NO VALUE = 2.80   |   |
| STATION #         |   |
| SPLICE PARAMETERS |   |
| NO                | 2 |
| ACROSS            | 1 |
| WIDTH             | 1 |
| COND. FILE        |   |



STATIC#1 OBS. SEQ. 4

|                   |   |
|-------------------|---|
| STATION #         |   |
| NO OF RECS = 2    |   |
| NO VALUE = 1.71   |   |
| STATION #         |   |
| SPLICE PARAMETERS |   |
| NO                | 2 |
| ACROSS            | 1 |
| WIDTH             | 1 |
| COND. FILE        |   |

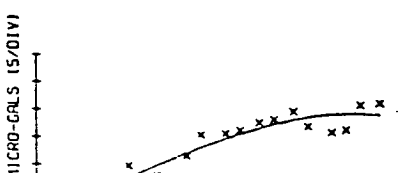


Fig.5.4  
Four  
separate  
reading  
sequence  
taken at  
the same  
site on  
the same  
day

STATIC TEST#1, OBS. SEQ. 2

NO OF NODES = 10  
RMS VALUE = 1.22  
STATIONS :

SPLINE PARAMETERS  
J: 20  
N: 1  
NZERO: 1  
PARTS: 1  
CONS: FALSE

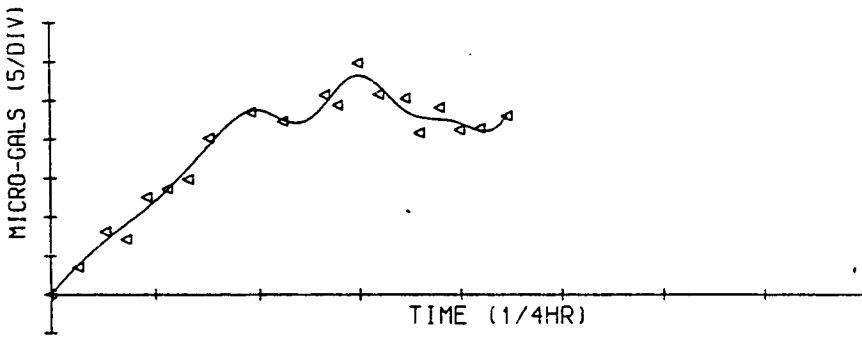


Figure 5.5 10 nodes

STATIC TEST#1, OBS. SEQ. 2

NO OF NODES = 18  
RMS VALUE = 0.00  
STATIONS :

SPLINE PARAMETERS  
J: 20  
N: 1  
NZERO: 1  
PARTS: 1  
CONS: FALSE

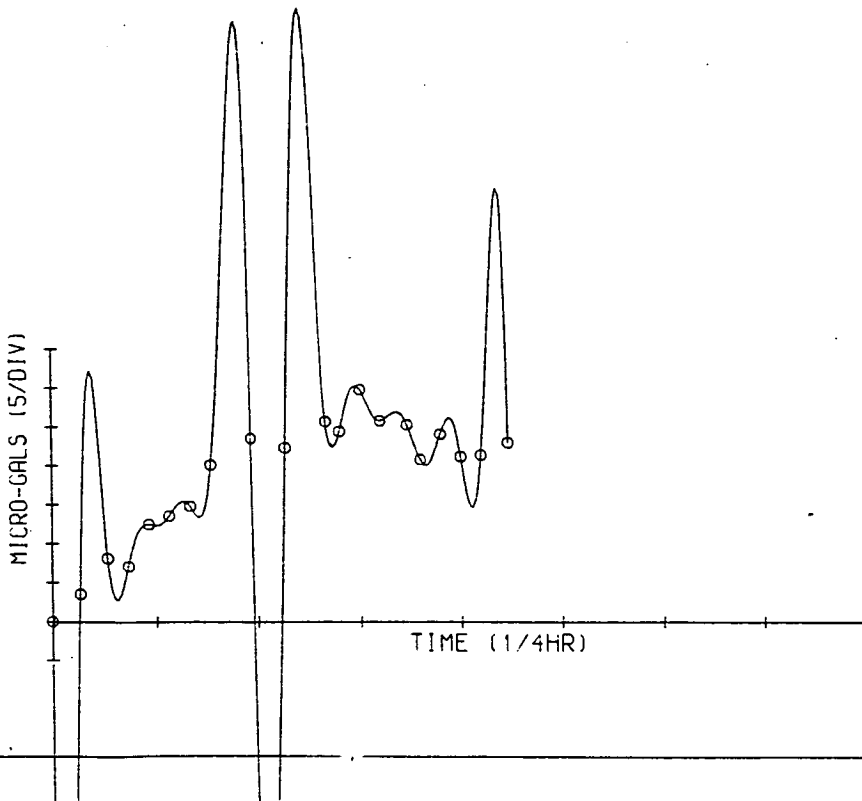


Figure 5.6 18 nodes

Table 5.1

Static / Transported Meter Test

|             | Observed gravity<br>'difference' at the same site (g.u.) | r.m.s. value (g.u.) |
|-------------|--|---------------------|
| Static 1    | -0.050   | 0.033               |
| Static 2    | +0.045   | 0.040               |
| Transport 1 | +0.093   | 0.045               |

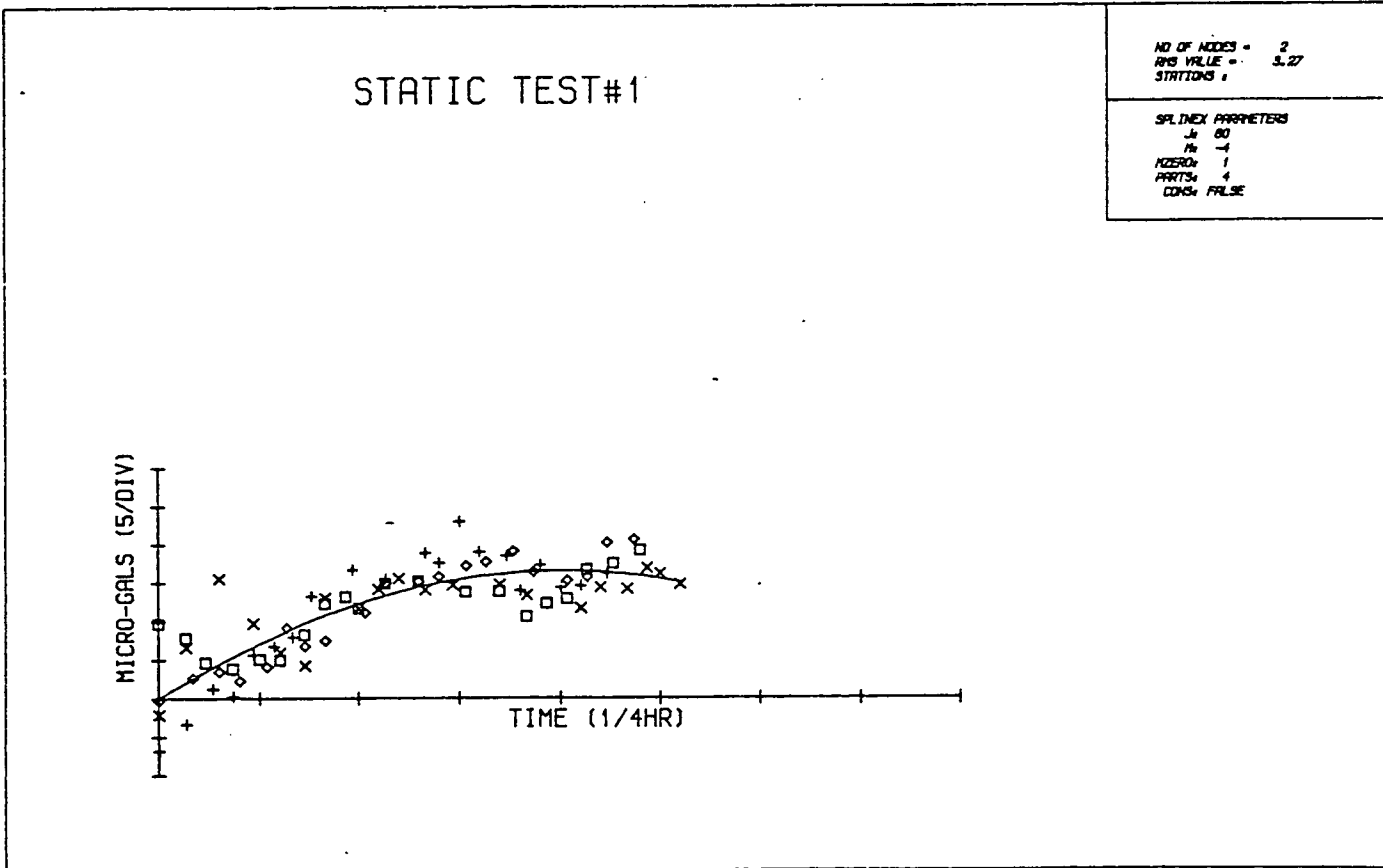


Figure 5.7 'Superposition' of data sets, PARTS = 4

Alternatively the reading sequences may be adjoined (PARTS = -4) rather than superimposed. Figure 5.8 displays the eleven node solution for the same data set as above whereas figure 5.9 demonstrates a better behaved field solution. (Field data sets often have a more pronounced maxima).

The output of adjustments with  $|PARTS| > 1$ , yields independent parameter pairs (datum and time) for each reading sequence. These form the input for a simple least squares weighted linear fit (using the program WFIT listed in Appendix (2)) to obtain the final solution. The results obtained using WFIT on the laboratory test data are given in Table 5.1 The two static test, during which the instrument remained undisturbed between reading sequences indicate gravity 'changes' which are just greater than the root mean square error bounds. These figures are tolerably zero but the observed gravity 'change' at the same site when the meter was transported between reading sequences is non zero. The transportation method was identical to that followed during field observations in Scotland (Section 8.3). The gravity meter, bolted to the secondary plate, was suspended from a rigid frame in the center of a vehicle, using elasticated cords. Thick sponge was placed beneath the baseplate to provide damping. These results are an estimate of the intrinsic accuracy of the instrument and the effect of road vibration (Hamilton

# STATIC TEST#1

NO. OF NODES = 11  
 RMS VALUE = 2.37  
 STATIONS :

SPLINEX PARAMETERS  
 J: 80  
 M: -4  
 PZERO: 1  
 PARTS: 4  
 CONS: FALSE

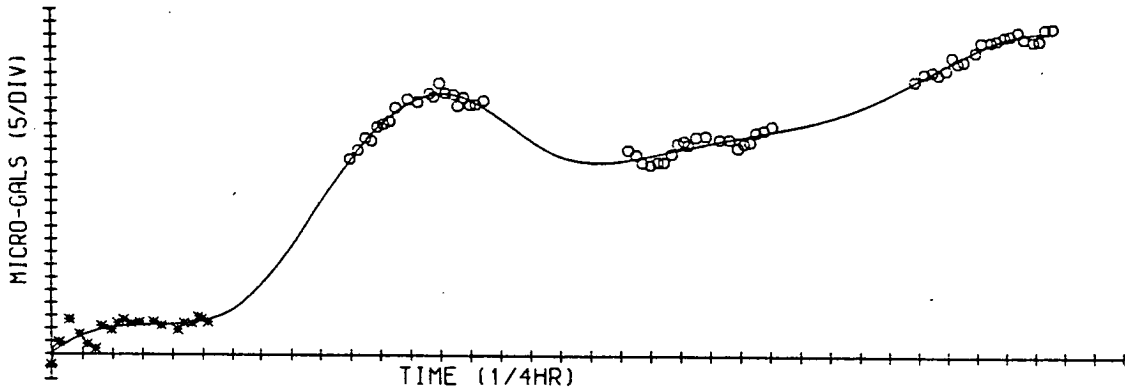


Figure 5.8 Eleven node solution for test data set.

# Edinburgh - Linlithgow 1981

NO. OF NODES = 11  
 RMS VALUE = 2.27  
 STATIONS :

SPLINEX PARAMETERS  
 J: 84  
 M: -4  
 PZERO: 1  
 PARTS: 4  
 CONS: FALSE

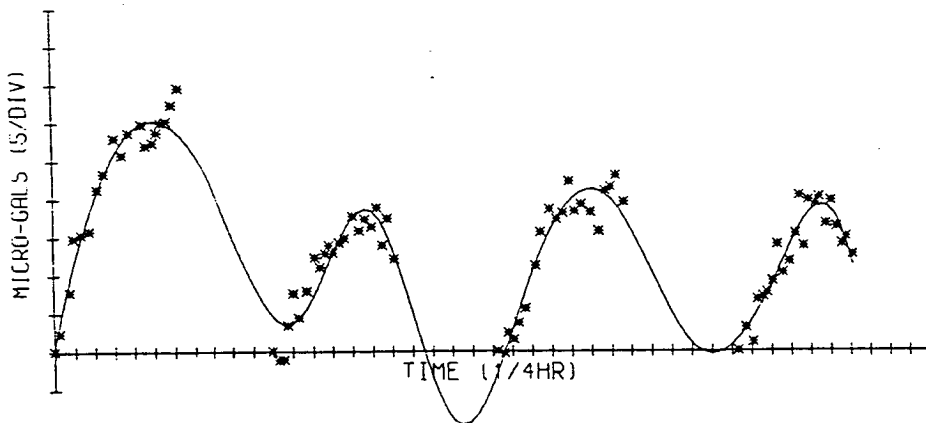


Figure 5.9 Eleven node solution for feild example

and Brule, 1963 find a resonance frequency at 49Hz for gravimeters). In fact field experience shows that instrument precision can occasionally vary quite widely without obvious reason.

### Multilinear

In addition to the spline based solution, data were adjusted using a network adjustment program MULTILINEAR (a modified version of Lagios and Hipkin, 1980). This program performs a least squares adjustment to all the data and also incorporates an independent first order fit to each observation sequence. This program was used in the adjustment of data collected in Greece (Chapter Nine) which was not observed using the equilibrium technique.

A schematic diagram of the overall data reduction procedure is given in figure 5.10. The raw data is first corrected for earth tides (using the program PBAS discussed in Chapter Four) to obtain data sets of time and relative gravity reading. These are now input to either the network program (MULTILINEAR) or spline adjustment (NSPL). The output from an independent PARTS solution is input to WFIT for a simple least squares weighted fit. The input/output channels of these programs are interconnected and graphical output may be obtained by responding to a query during an interactive terminal session.

## Standard Analysis Procedure

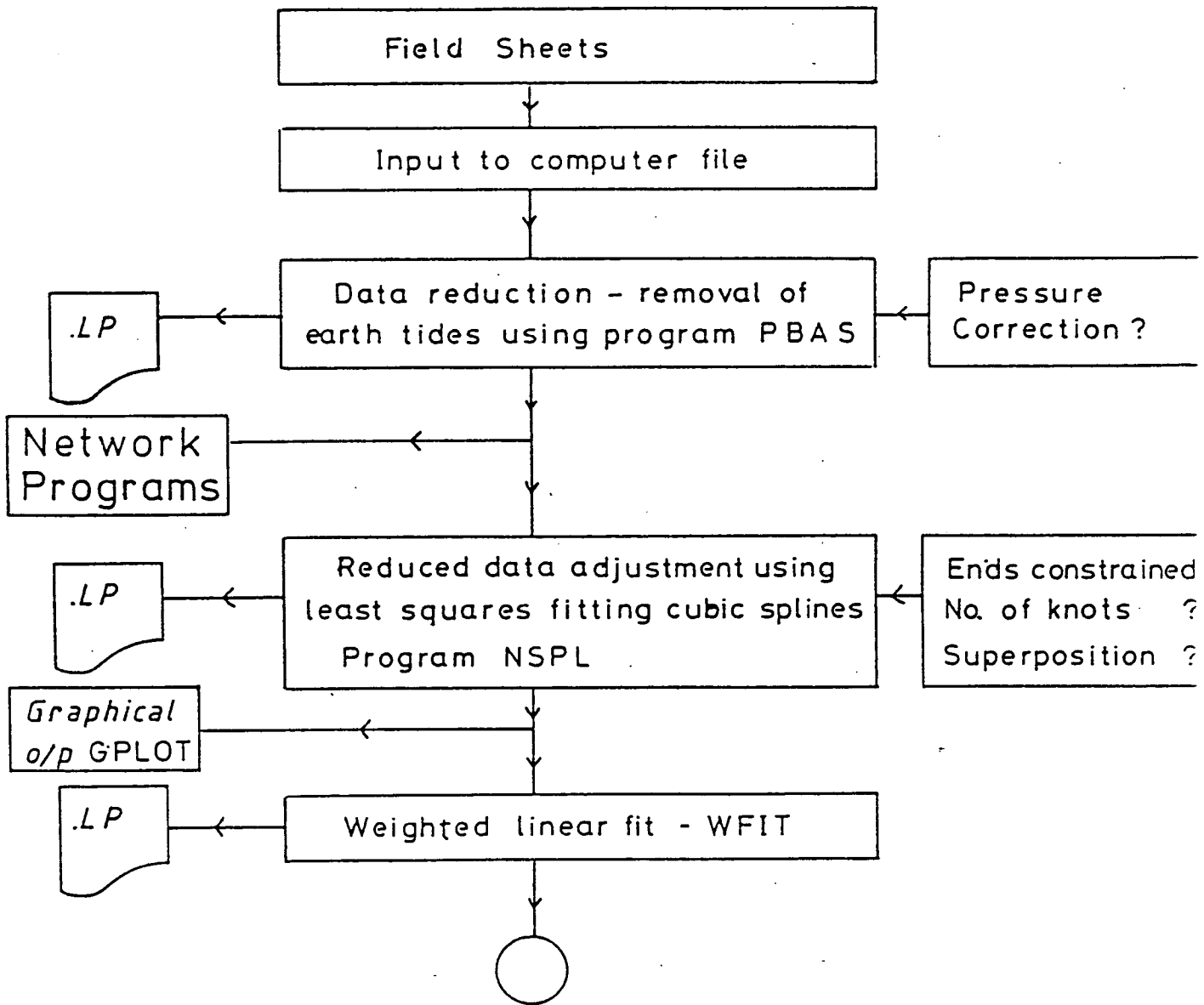


Figure 5.10 Schematic flow diagram of general data reduction procedure.



## CHAPTER 6

### INSTRUMENT CALIBRATION

#### 6.1 Introduction

The complex internal mechanism of La Coste and Romberg spring gravimeters has been discussed in section 3.1. Gravity differences are determined by differencing the noted spindle revolutions at sites, then multiplying by the calibration factor . The calibration function is continuous over the range of spindle revolutions but the manufacturer supplies a piecewise linear approximation in the form of a single factor for every hundred revolutions of the spindle. The calibration table for G-275 is reproduced in table 6.1, and shown graphically in figure 6.1. The calibration factor is given to one part in  $10^5$  whereas the 'factor interval' is rounded to 0.01mgal. Thus gravity differences between sites with gravity values lying in different table intervals will be in error if this is not considered.

Calibration in the factory is achieved by adding a small calibrating mass to the gravity meter beam to simulate gravity differences with a twenty milligal interval, known as the Cloudcroft Junior method (Lambert, 1981). Coarse adjustment is achieved by a threaded mass added along the axis of the beam (figure 6.2). This method is only possible if one has the necessary ancillary equipment and a detailed

| COUNTER READING* | VALUE IN MILLIGALS | FACTOR FOR INTERVAL | COUNTER READING* | VALUE IN MILLIGALS | FACTOR FOR INTERVAL |
|------------------|--------------------|---------------------|------------------|--------------------|---------------------|
| 000              | 000.00             | 1.05115             |                  |                    |                     |
| 100              | 105.12             | 1.05108             | 3600             | 3786.12            | 1.05337             |
| 200              | 210.23             | 1.05104             | 3700             | 3891.46            | 1.05347             |
| 300              | 315.33             | 1.05100             | 3800             | 3996.81            | 1.05356             |
| 400              | 420.43             | 1.05095             | 3900             | 4102.16            | 1.05365             |
| 500              | 525.52             | 1.05093             | 4000             | 4207.53            | 1.05374             |
| 600              | 630.62             | 1.05090             | 4100             | 4312.90            | 1.05380             |
| 700              | 735.71             | 1.05090             | 4200             | 4418.28            | 1.05385             |
| 800              | 840.80             | 1.05090             | 4300             | 4523.67            | 1.05392             |
| 900              | 945.89             | 1.05090             | 4400             | 4629.06            | 1.05399             |
| 1000             | 1050.98            | 1.05094             | 4500             | 4734.46            | 1.05405             |
| 1100             | 1156.07            | 1.05097             | 4600             | 4839.86            | 1.05411             |
| 1200             | 1261.17            | 1.05103             | 4700             | 4945.27            | 1.05415             |
| 1300             | 1366.27            | 1.05107             | 4800             | 5050.69            | 1.05417             |
| 1400             | 1471.38            | 1.05113             | 4900             | 5156.11            | 1.05416             |
| 1500             | 1576.49            | 1.05124             | 5000             | 5261.52            | 1.05415             |
| 1600             | 1681.62            | 1.05133             | 5100             | 5366.94            | 1.05412             |
| 1700             | 1786.75            | 1.05140             | 5200             | 5472.35            | 1.05407             |
| 1800             | 1891.89            | 1.05150             | 5300             | 5577.76            | 1.05402             |
| 1900             | 1997.04            | 1.05160             | 5400             | 5683.16            | 1.05395             |
| 2000             | 2102.20            | 1.05170             | 5500             | 5788.55            | 1.05386             |
| 2100             | 2207.37            | 1.05180             | 5600             | 5893.94            | 1.05380             |
| 2200             | 2312.55            | 1.05187             | 5700             | 5999.32            | 1.05372             |
| 2300             | 2417.74            | 1.05198             | 5800             | 6104.69            | 1.05364             |
| 2400             | 2522.93            | 1.05207             | 5900             | 6210.06            | 1.05355             |
| 2500             | 2628.14            | 1.05216             | 6000             | 6315.41            | 1.05344             |
| 2600             | 2733.36            | 1.05226             | 6100             | 6420.76            | 1.05330             |
| 2700             | 2838.58            | 1.05237             | 6200             | 6526.09            | 1.05315             |
| 2800             | 2943.82            | 1.05248             | 6300             | 6631.40            | 1.05297             |
| 2900             | 3049.07            | 1.05260             | 6400             | 6736.70            | 1.05275             |
| 3000             | 3154.33            | 1.05270             | 6500             | 6841.97            | 1.05253             |
| 3100             | 3259.60            | 1.05283             | 6600             | 6947.23            | 1.05227             |
| 3200             | 3364.88            | 1.05295             | 6700             | 7052.45            | 1.05200             |
| 3300             | 3470.18            | 1.05305             | 6800             | 7157.65            | 1.05163             |
| 3400             | 3575.48            | 1.05316             | 6900             | 7262.82            | 1.05115             |
| 3500             | 3680.80            | 1.05326             | 7000             | 7367.93            |                     |

\* Note: Right hand wheel on counter indicates approximately 0.1 milligals.

10-14-71  
AMS

Table 6.1 Manufacturer's Calibration Table (G-275).

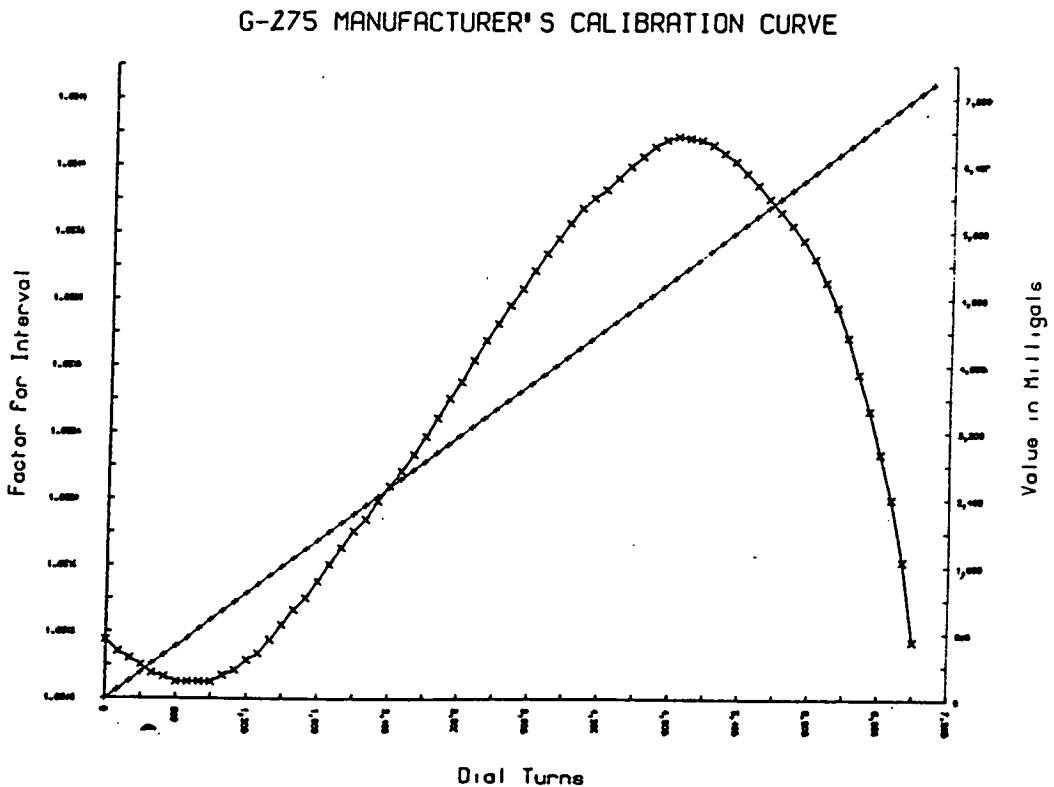


Figure 6.1 Graphical representation of the manufacturer's calibration table.

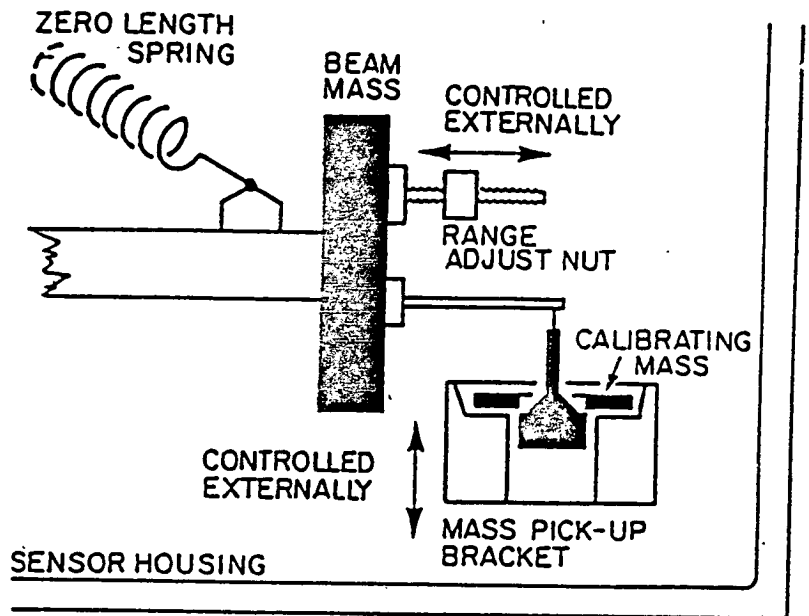


Figure 6.2 The Cloudcroft Junior method

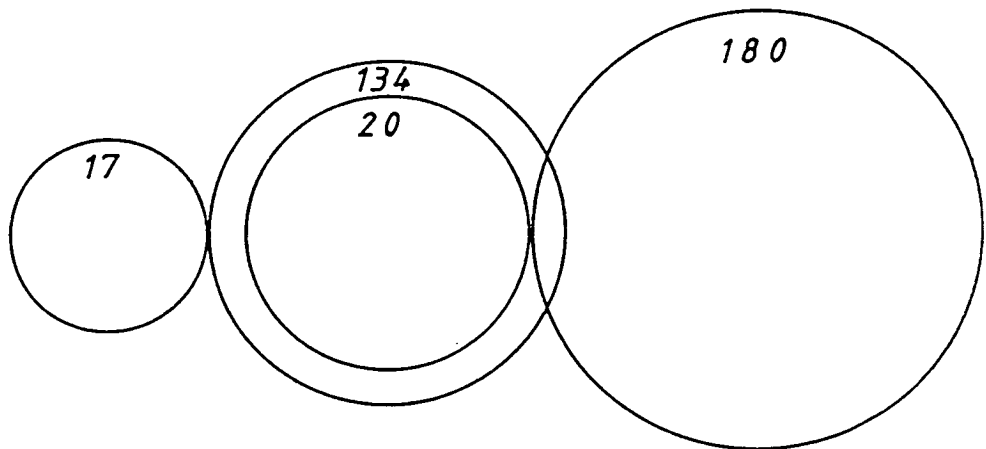


Figure 6.3 Schematic representation of model 'G' gearbox

knowledge of the internal mechanism. The normal procedure to calibrate an instrument is to observe on a well determined gravity difference which has been measured by a large number of instruments.

## 6.2 Periodic errors

Every revolution of the dial on the top plate of the gravity meter is translated into a minute movement of the measuring beam by means of reduction gears and lever arms. A schematic representation of the gear box is shown in figure 6.3. The final drive acts on a spindle (pitch 184 t.p.i.) which moves the first arm of a lever system with a reduction ratio of 77.8:1. Imperfections in the machining of the component gears may generate cyclic errors with the following periods.

1206.0, 603.0, 70.94, 35.47, 7.88, 3.94, 1.00 counter units

In addition to periodic errors, irregularities in the manufacture of the spindle may generate large local errors.

Becker (1981) reports tests on one model G (G-258) on a vertical calibration line previously observed six times with D-38. Becker obtains an amplitude of 0.027g.u. for the one dial turn period. Kanngieser and Torge (1981) have conducted extensive tests on six model G and two model D meters on special calibration lines with gravity ranges of

2, 20, 200, 2,000, 20,000, g.u.. They obtain the following average values for the respective periodicities .

| Amp. (g.u.) | Period (Dial Turns) |
|-------------|---------------------|
| 0.04        | 1                   |
| 0.01        | 3.94                |
| 0.05        | 7.89                |
| 0.05        | 35.45               |

## Part (1) Calibration by measurement of a 'known' gravity difference

### 6.3 U.K. Calibration Lines

The United Kingdom does not possess such a range of well determined gravity differences, the best possible being the two Short National Calibration Lines established by the Institute of Geological Sciences (Masson-Smith et al, 1974). These two lines are situated in north central England. The first extends from North Rode village (elev. 145.7m.) to the Cat and Fiddle inn (514.7m.), the second line links Hatton Heath (21.7m.) and Prees (85.9m.). The precision of transfer from the first to the second calibration line was degraded by the use of pressure sensitive gravity meters. After a period of time it became obvious there was a systematic difference between measurements before and after 1964 and the calibration line values were revised in 1971 after extensive remeasurement. When the United Kingdom was included in the International Gravity Standardisation Net (Morelli et al, 1971) the values were again revised to:

|       | Gravity Diff.(g.u.) | Std. Error (g.u.) |
|-------|---------------------|-------------------|
| NR-CF | 604.53              | 0.08              |
| HH-P  | 556.51              | 0.09              |

Since that date the Institute of Geological Sciences has noted ' inexplicable differences of the order of one part in one thousand' between the two lines (Masson-Smith personal communication, 1983). This fact seems to have recently emerged after analysis of the results by I.G.S. when establishing the New Long Calibration Line (1983). It is also important to note that measurements prior to 1971 were made largely with Worden meters. Until that time I.G.S. did not correct readings for earth tides but simply applied linear interpolation. Furthermore the I.G.S. has never applied pressure corrections to their observations though these will be very small.

In addition to the Short Calibration Lines there exists the New Long Calibration Line of airport stations based upon existing measurements (NGRN73 Airport Net, see figure 6.4), together with two extra stations.

Most stations lie very close to runways making measurement by private aircraft desirable.

### 6.5 University Measurements

The Edinburgh instrument, G-275 has measured on three occasions on the Hatton Heath Prees calibration line and on

four occasions on the Cat and Fiddle line. Table 6.2 illustrates the occasions on which the Edinburgh instrument G-275 has measured on the short calibration lines. Also shown are the measurement epochs of several other La Coste and Romberg meters. (Data kindly provided by Dr. P. Maguire, Dr. R. Barker, and Dr. G. Stuart of the universities of Leicester, Birmingham and Leeds respectively). Some stations of the Airport Net were measured with G-275 in conjunction with Fundamental Bench Mark and Pendulum sites as shown in figure 6.5. This line was measured in a single sequence A-B- --- -H-J on two separate days of twelve hours driving.

All these data were processed in an identical fashion, except for two sets of G-275 observations which were measured using the 'equilibrium technique'. The observation procedure was identical for all other data sets. In these the observers 'shuttle' back and forth between the two sites as often as possible in a working day (ie A-B-A...B-A-B).The dial turns were multiplied by a constant scale factor derived from the manufacturer's tables. After the removal of the Earth tides (using program PBAS, section 4.4), the reduced observations were input to the spline fitting program NSPL. A simple least squares cubic solution was obtained for each of the 'shuttle data'. The 'equilibrium' data were processed by superimposing data sets in the manner described in section 5.2.

Table 6.2

## Measurements on short calibration lines

| Meter  | Date     | Measurement Technique | Number of Observations | Gravity Difference (g.u.) | rmse  | k' (x 10 <sup>-4</sup> ) |
|--|----------|-----------------------|------------------------|---------------------------|-------|--------------------------|
| Hatton Heath - Prees (I.G.S., 556.51 (std. err. 0.09) g.u.)        |          |                       |                        |                           |       |                          |
| G275   | 26.05.79 | S                     | 8                      | 555.752                   | 0.065 | 13.68 ± 2.0              |
|  | 13.05.81 | S                     | 12                     | 555.766                   | 0.100 | 13.38 ± 3.0              |
|  | 12.05.81 | E                     | 90                     | 555.914                   | 0.093 | 10.72 ± 3.0              |
| G16*   | 02.05.81 | S                     | 13                     | 555.202<br>(556.612)      | 0.168 | 23.55 ± 4.0              |
|  | 14.06.81 | S                     | 13                     | 554.957<br>(556.367)      | 0.197 | 27.98 ± 5.0              |
|  | 21.07.81 | S                     | 14                     | 555.108<br>(556.518)      | 0.177 | 25.26 ± 4.0              |
| G545   | 28.05.81 | S                     | 13                     | 555.346                   | 0.229 | 20.96 ± 5.0              |
|  | 02.12.81 | S                     | 13                     | 555.109                   | 0.172 | 25.24 ± 4.0              |
| G471   | 14.06.81 | S                     | 11                     | 555.776                   | 0.242 | 13.21 ± 5.0              |
|  | 11.10.81 | S                     | 13                     | 556.033                   | 0.083 | 8.58 ± 3.0               |
|  | 04.07.82 | S                     | 13                     | 555.832                   | 0.097 | 12.20 ± 3.0              |
| Cat and Fiddle - North Rode (I.G.S., 604.53 (std. err. 0.08) g.u.) |          |                       |                        |                           |       |                          |
| G275   | 25.05.79 | S                     | 6                      | 604.242                   | 0.079 | 4.77 ± 2.0               |
|  | 09.01.80 | S                     | 9                      | 604.265                   | 0.063 | 4.38 ± 2.0               |
|  | 10.05.81 | S                     | 12                     | 604.138                   | 0.033 | 6.49 ± 1.8               |
|  | 11.05.81 | E                     | 99                     | 604.111                   | 0.088 | 6.95 ± 2.0               |

S - 'Shuttle', i.e. A-B-A-B.....

E - 'Equilibrium', A-B-A-B.

\* Gravity difference in brackets refer to value obtained after application of correction factor of 1.00254.

k' is the scale factor correction, (I.G.S. value - Observed / Observed)



Figure 6.4 U. K. airport net (Masson-Smith et. al.,1974)

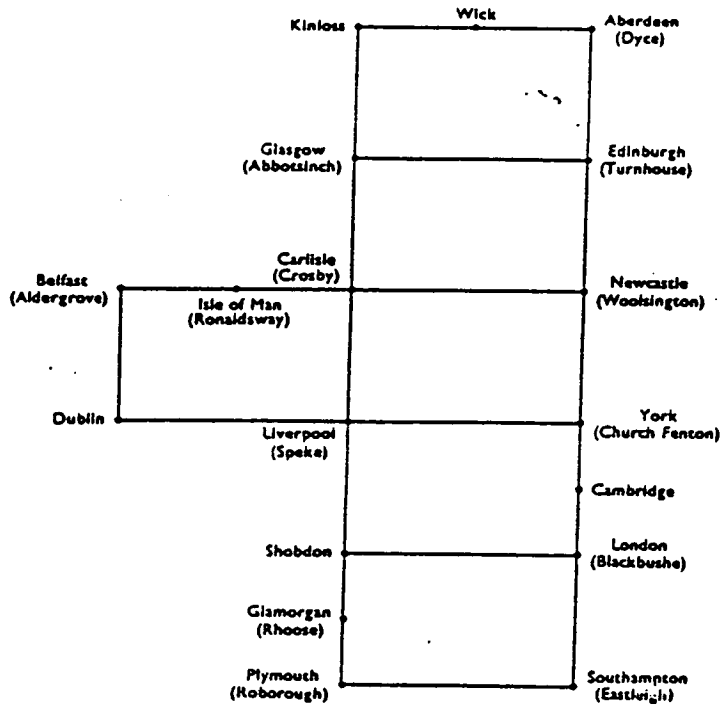
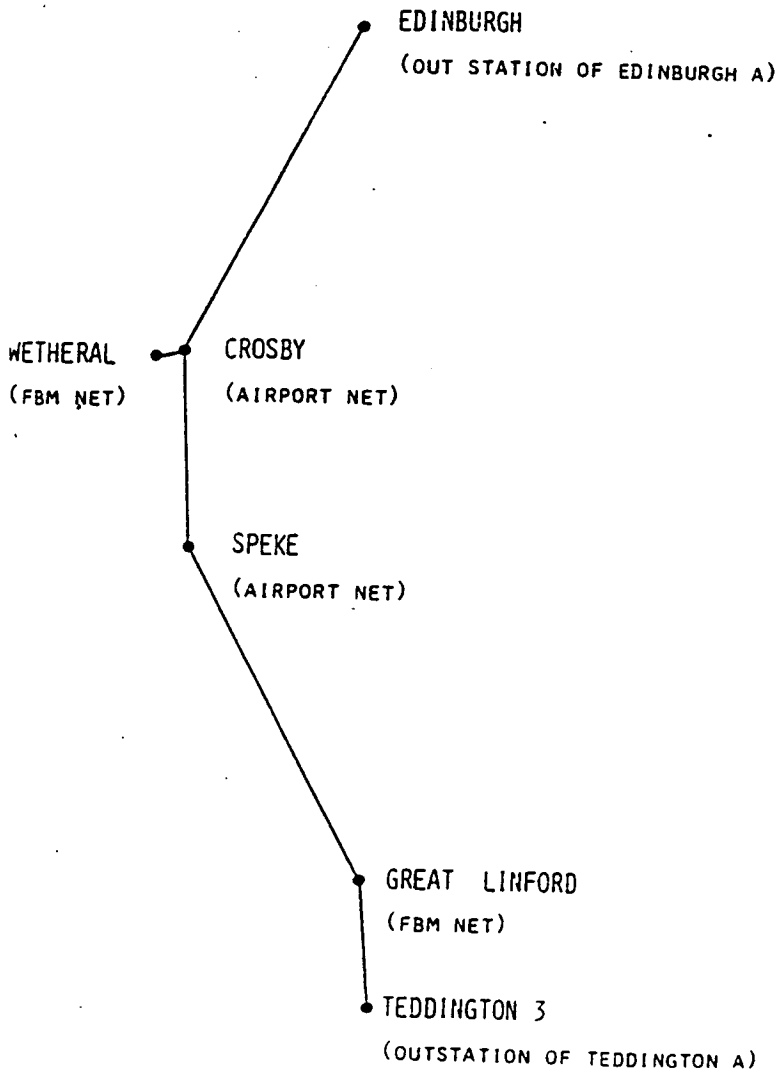


Figure 6.5 Stations measured with G-275 on long calibration run



The results of the solutions are shown in table 6.2 and they are displayed graphically in figure 6.6. It can be seen that nine independent sets of data from four different instruments processed using the manufacturer's scale factor are consistently lower than the stated NGRN73 value. (The Leicester University group mistakenly apply a 'correction' of 1.00254 on the basis of the 21-07-81 readings). The rightmost column of table 6.2 gives the scale factor error assuming the NGRN73 value. These are of the order of one or two parts in a thousand which is almost an order of magnitude greater than typical errors quoted in the literature (eg. Torge, 1971 quotes  $0.1$  to  $6.0 \times 10^{-4}$  ; Nakagawa and Satomura, 1978 obtain 2.1, 6.6, and  $6.4 \times 10^{-4}$ ).

The results obtained from the long calibration run (Table 6.3) exhibit scale factor corrections very similar to the Cat and Fiddle line. (These data were adjusted using MULTILINEAR ). All the combined evidence seems to suggest the quoted value for the Hatton Heath calibration line (the basis for the British gravity unit!) is erroneous. The calibration line is situated on the Cheshire plain where extraction and infusion of water to obtain salt is a large scale industrial operation. This may be a possible cause for the discrepancy. The results indicate that G-275 underestimates the gravity difference between sites by four parts in ten thousand. Furthermore, the Edinburgh

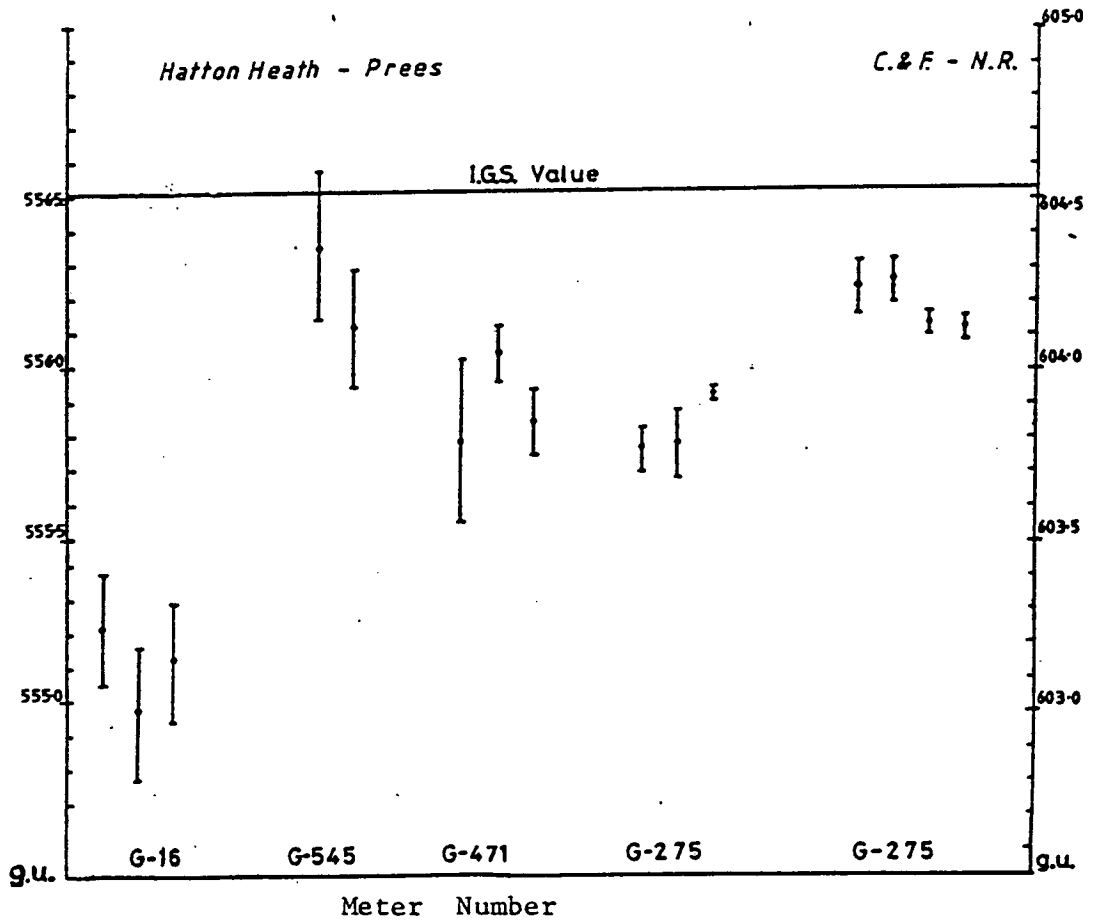


Figure 6.6 Results of university observations on U.K. short calibration lines. Four different meters observing on Hatton-Heath Prees line and one observation on Cat & Fiddle North Rode line.

Table 6.3

## Measurements on Long Calibration Line

| Station Name   | NGRN73 Value (g.u.)  | Quoted Std. Err. (g.u.) | G-275 Value (g.u.) | rmse (multi-linear) (g.u.) | Difference (NGRN-G275) (g.u.) | k' (x 10 <sup>0</sup> ) |
|--|----------------------|-------------------------|--------------------|----------------------------|-------------------------------|-------------------------|
| Edinburgh (JCMB)<br>Out station of<br>Edinburgh A <sup>o</sup> | 3967.06 <sup>+</sup> | 0.22                    | 3965.44            | 0.11                       | 1.62                          | 4.08 ± 0                |
| Crosby 1 <sup>*</sup>  | 3165.06              | 0.20                    | 3163.46            |                            | 1.60                          | 5.06                    |
| Wetheral FBM   | 3117.73              | 0.22                    | 3116.58            | 0.20                       | 1.15                          | 3.69 ± 1                |
| Speke 1 <sup>*</sup>   | 1909.01              | 0.17                    | 1908.05            | 0.02                       | 0.96                          | 5.03 ± 1                |
| Gt Linford FBM   | 540.29               | 0.31                    | 539.38             | 0.11                       | 0.91                          | 16.87 ± 7               |
| Teddington 3<br>Out station of<br>Teddington A <sup>o</sup>    | 0.00 <sup>++</sup>   | 0.17                    | 0.00               | 0.04                       |                               |                         |

Values are quoted relative to Teddington 3 (NGRN73 value 981182.038)

<sup>o</sup> Pendulum Station

<sup>\*</sup> U.K. Airport Net

k' Scale factor correction (NGRN73-G275/G275)

<sup>+</sup> Based on Edinburgh A - Edinburgh (JCMB) =  $-159.48 \pm 0.18$  g.u.  
(Lagios and Hipkin, 1981).

<sup>++</sup> Based on Teddington A - Teddington 3 =  $-2.41 \pm 0.13$  g.u.  
(Turnbull, personal communication)

meter has previously been shown to be in good agreement with other NGRN stations (Lagios and Hipkin, 1981).

## Section (2) - Calibration by Tilting

### 6.6 The Method

It is possible to simulate a variation in gravity by simply tilting the gravity meter. If the beam is assumed to be supported by a perfect pivot, and thus constrained to have one degree of freedom, the force experienced by the mass is simply  $g_0 \cos \theta$  as shown in figure 6.7. The vector  $g_0$  is the acceleration due to gravity in the direction of the local vertical. When  $\theta$  equals zero (ie the meter is levelled) the force experienced by the mass relative to the instrument case is a maximum. When the meter is tilted through small positive and negative angles ( $d\theta$ ) the acceleration change ( $dg$ ) may be expressed as.

$$dg = g_0 \cos (d\theta)$$

$$dg = g_0 (\theta/2)^2$$

This is the equation of a parabola, symmetric about the maximum value. This property is commonly used to level the glass vials by checking that the cross hair

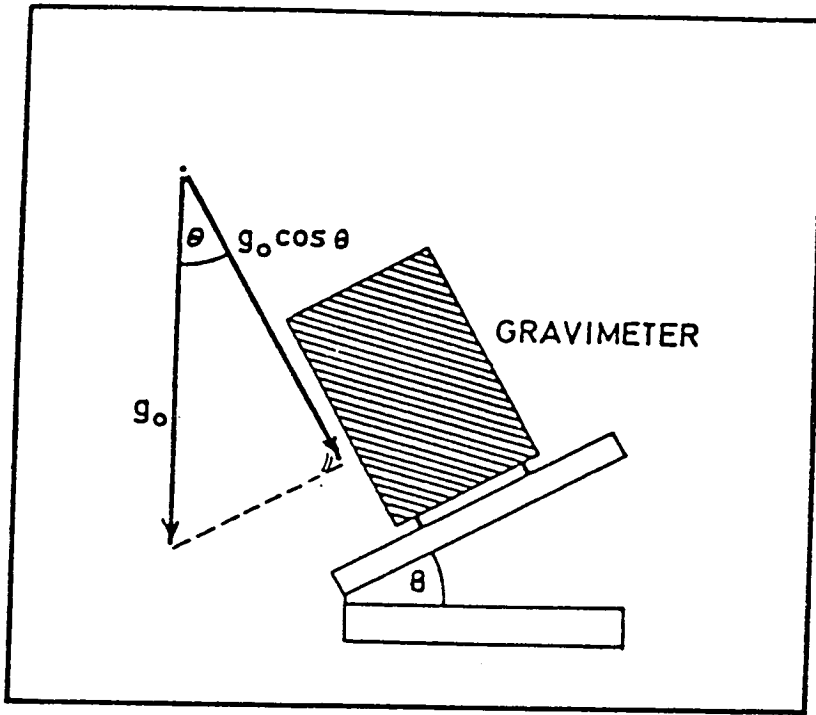


Figure 6.7 Simplified diagram of gravimeter tilting.

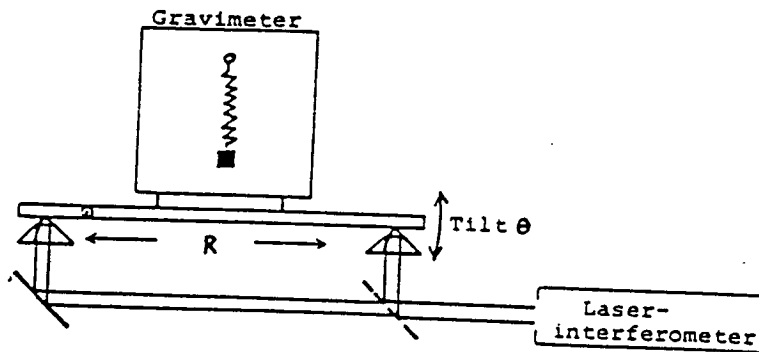


Figure 6.8 Boedecker's experimental arrangement.

displacement is equivalent when the meter is tilted one bubble division in either direction parallel to the vial. The procedure is not commonly used to determine the absolute calibration factor for model G meters but is frequently used with earth tide meters, (e.g Wenzel, 1976 describes the calibration of an Askania tide meter at Hannover, and list several references to similar work at Brussels). The tilt calibration of a fed back La Coste and Romberg observatory gravimeter is described in Moore and Farrell (1970). The instrument is tilted by a motor driven micrometer screw coupled to a metal film potentiometer to measure the number of rotations of the screw. Boedecker(1981) measured the tilt of a platform interferometrically using two corner cube reflectors (figure 6.8) to measure the vertical displacement of one reflector to the second fixed on the pivoting axis. Boedecker wished to calibrate model G meters in this way but reports 'doubtfull results'. However he used the adjustments residuals to determine periodic components as shown in figure 6.9. Despite Boedecker's reported difficulties it seemed to the author that laser interferometry is the optimum method to measure the tilting angle . Such a method is independent of a micrometre thread which may generate periodic errors and uses a well determined physical constant, the wavelength of the laser beam to determine the displacement.

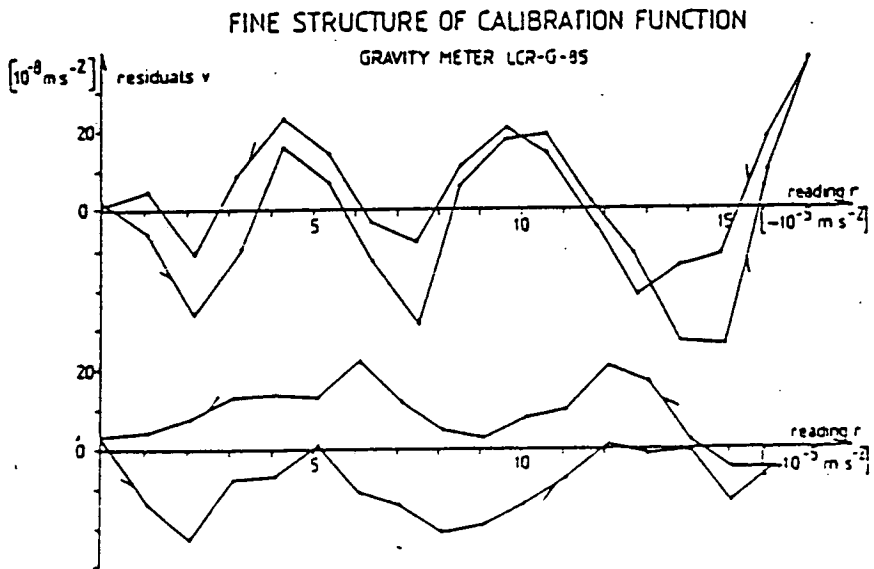
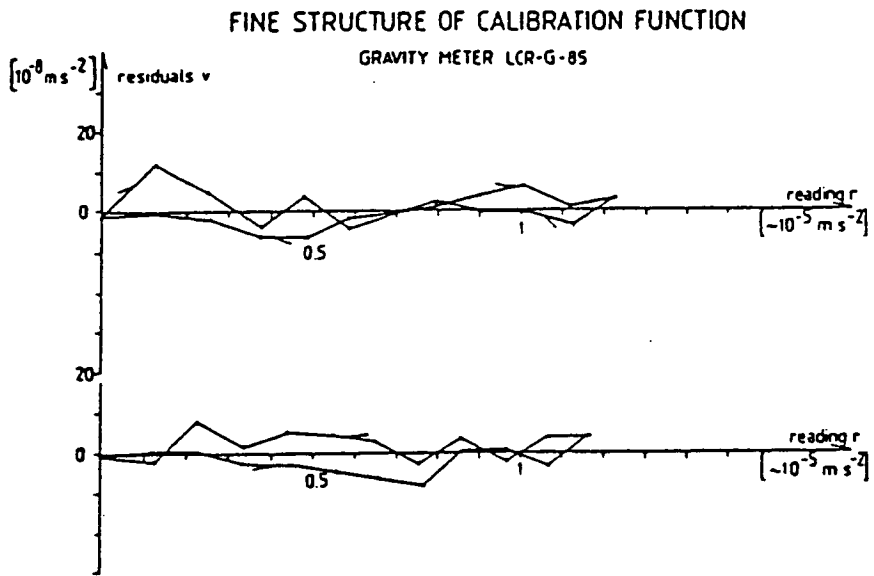


Figure 6.9 Fine structure of calibration constant,  
as observed by Boedecker.



## 6.7 Experimental Procedure

In a preliminary set of experiments the meter was mounted on the secondary platform (section 3.2) and the tilt angle adjusted and measured by means of the new screw feet. The serrated edge of the adjustable foot served as an index to count the number of rotations of the screw. A brass pointer was mounted on the barrel of the foot and every tenth count was annotated. One revolution of the screw (one fortieth of an inch) corresponds to 123 serrations. Hence one serration along the long axis approximates to 2.43 seconds of arc for small angles. Three preliminary experiments were undertaken using the foot screw to derive tilt angles. The meter was alternately tilted equal angles (ie serration counts) in opposite directions and observed. Additionally every third reading was taken in the levelled horizontal position to control drift. The drift curves (after tidal reduction) so obtained are shown in figure 6.10. After the instrumental drift is removed it is possible to plot observed gravity against the angular displacement of the platform (figure 6.11).

## 6.8 Interferometric Measurement of the Tilting Angle

Boedecker's experiment required the use of two corner cube reflectors which were both unattainable and expensive to purchase. After consultation with Mr. R. Silitto, of the Physics Department, Edinburgh University a simpler arrangement observing Newton's Rings was set up (figure

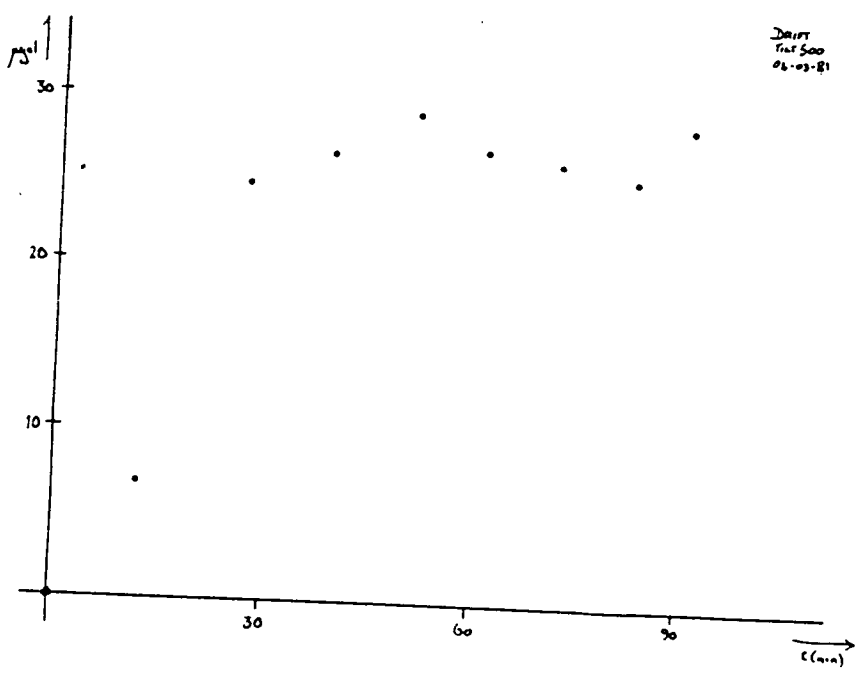
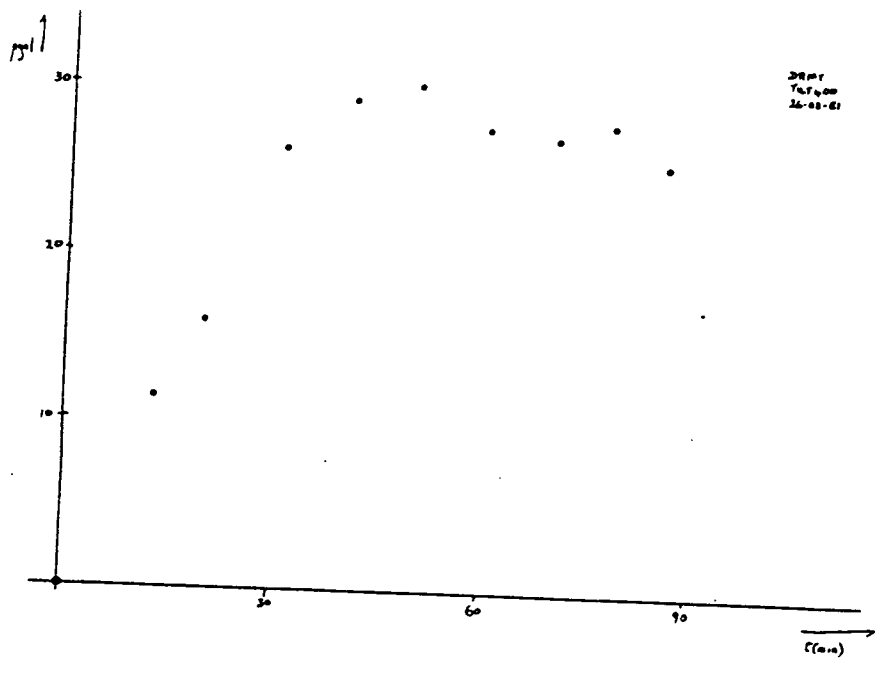
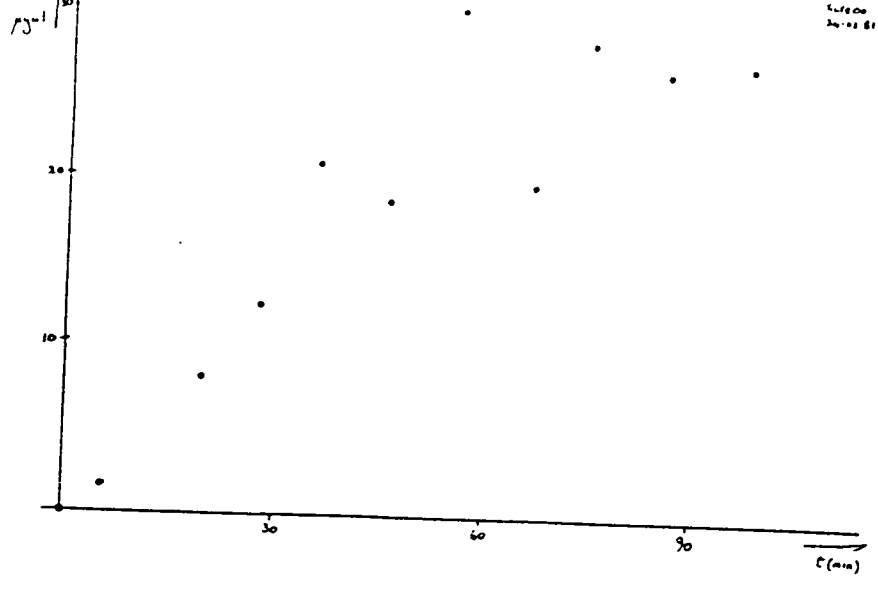
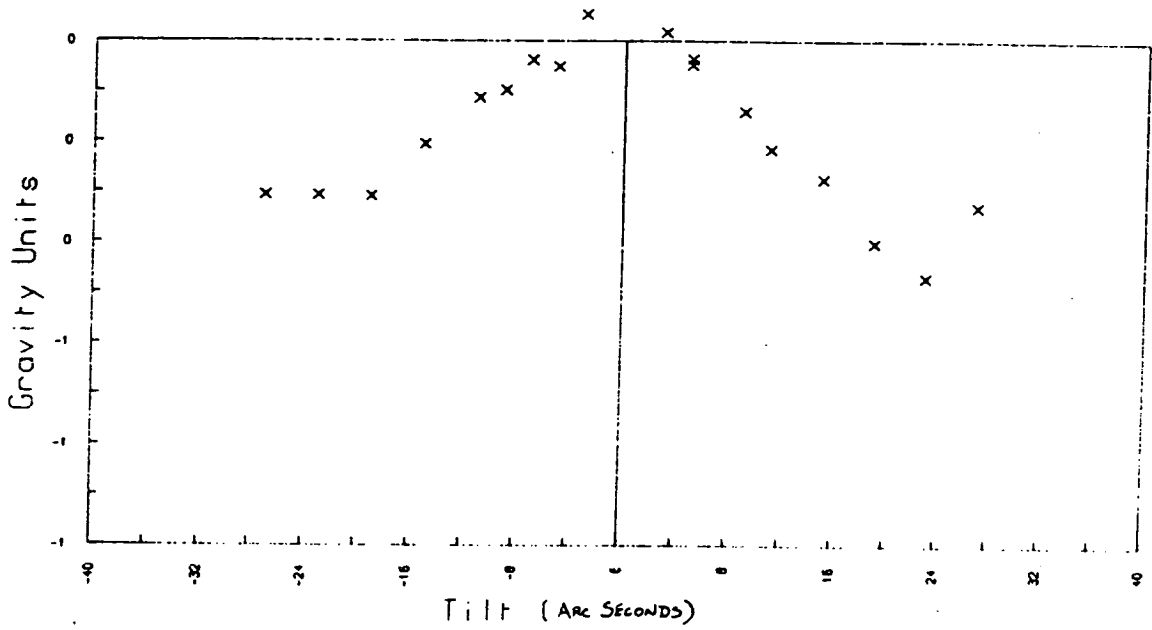


Figure 6.10 Examples of observed drift (preliminary experiments, angle estimated from screw thread).

Tilt Parabola G275, Long level (1 thread experiments)



Tilt Parabola G275, Cross level (2 thread experiments)

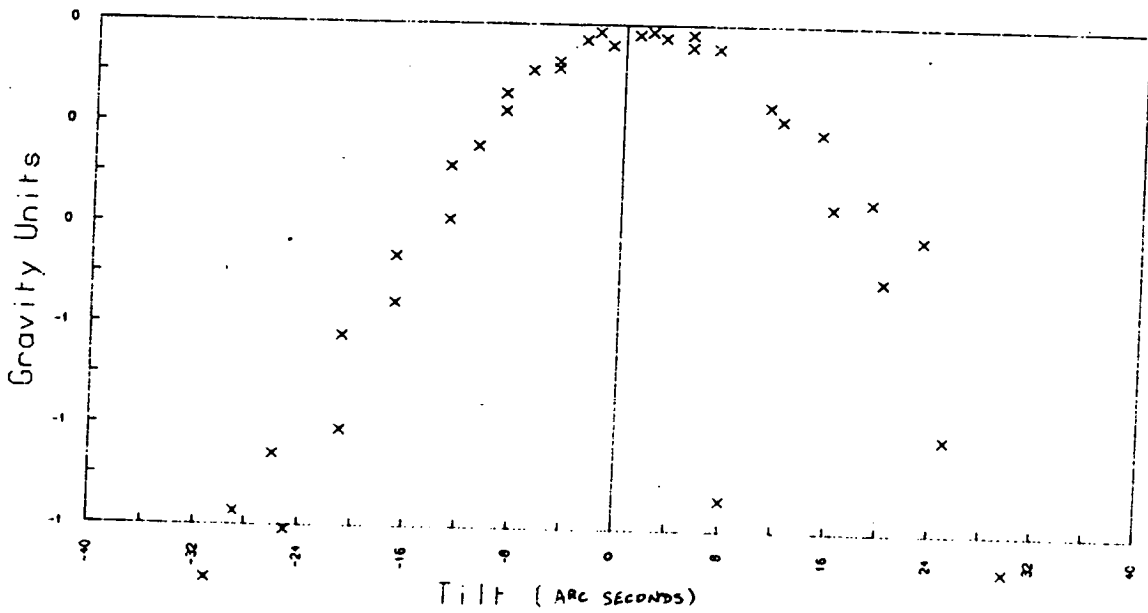


Figure 6.11 Observed tilt parabolas (preliminary experiments).

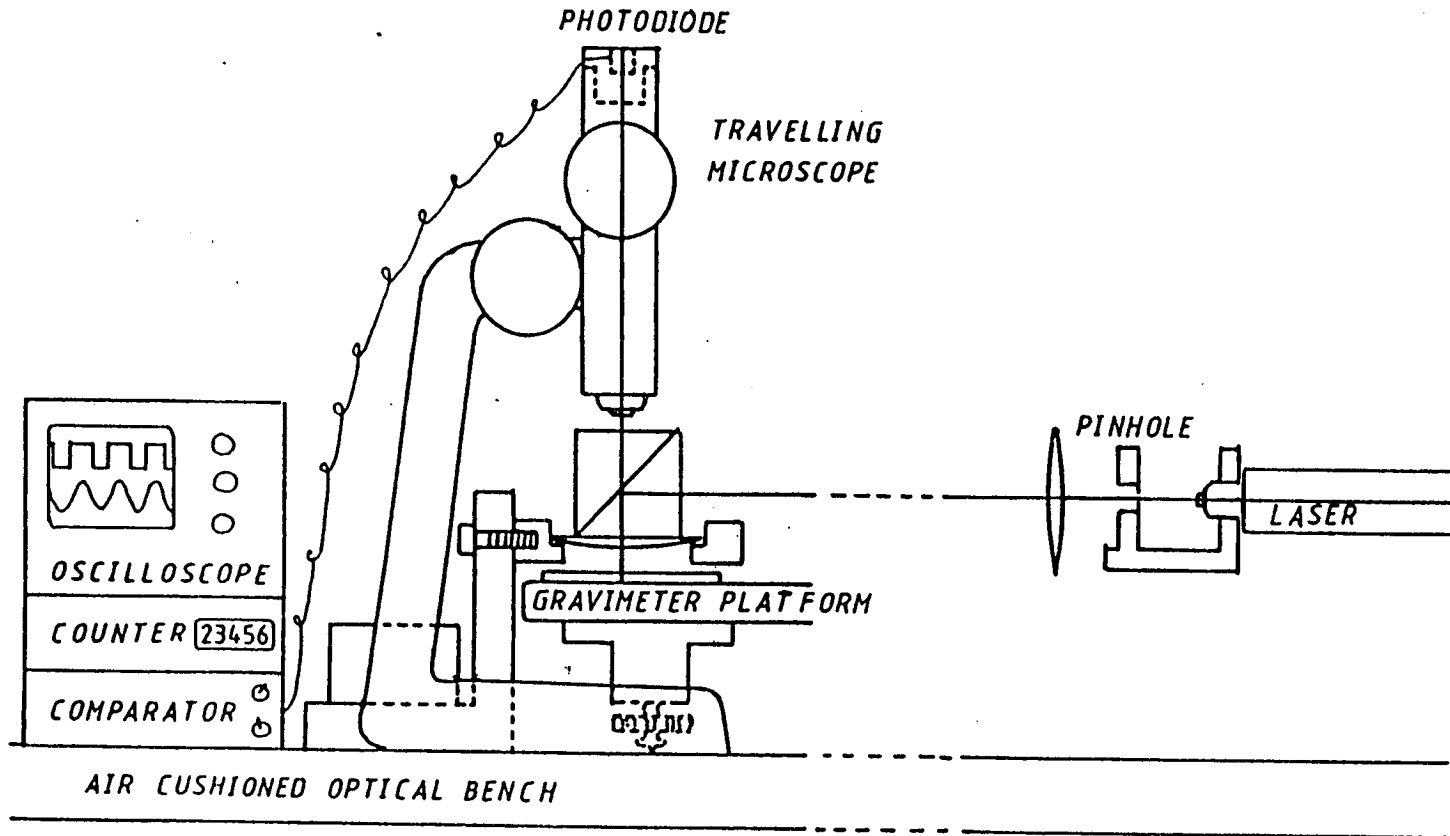
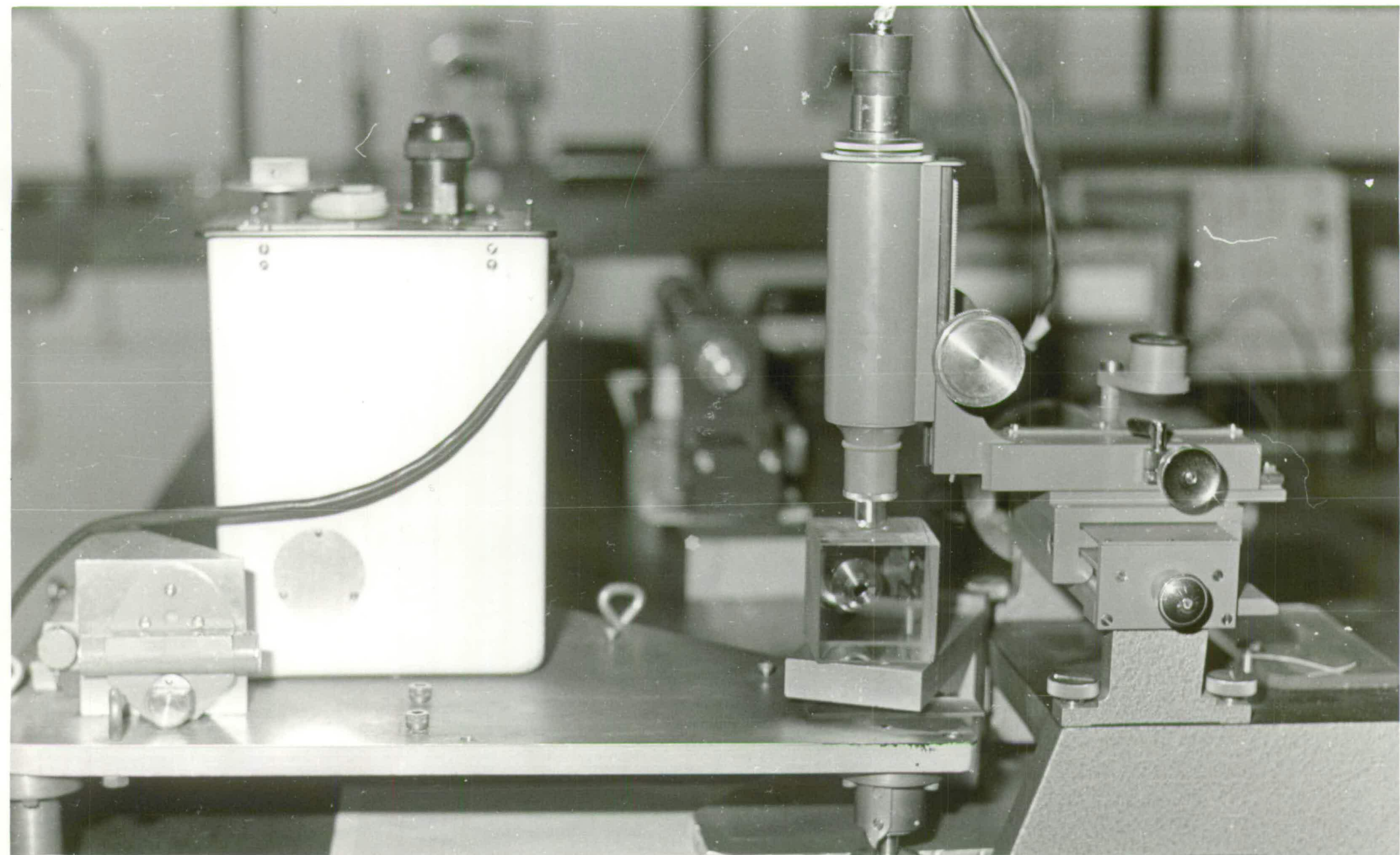


Figure 6.12 Experimental arrangement for the interferometric determination of tilting angle.

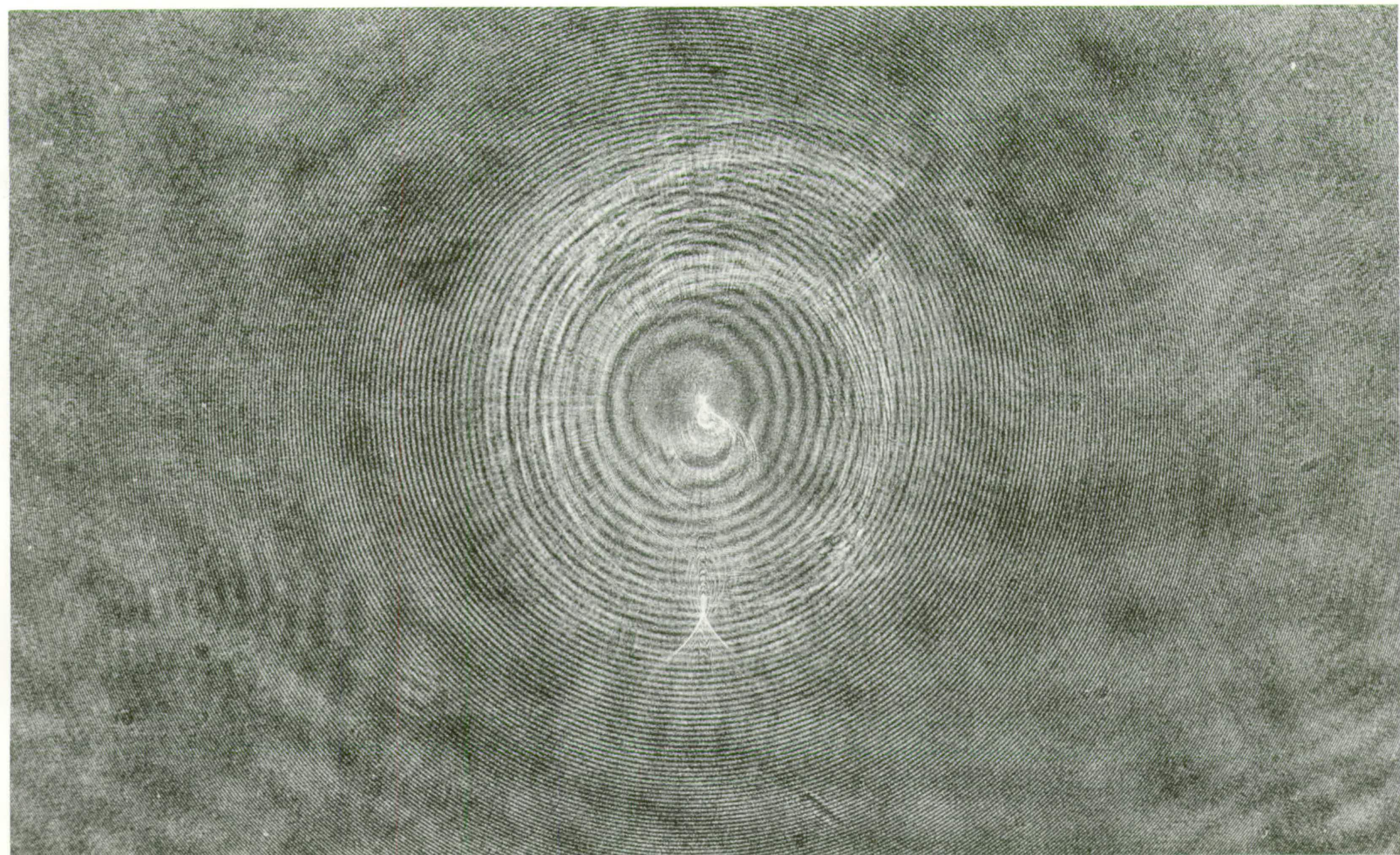


6.12 and plate 6.1). Mr Sillitto provided the necessary optical equipment and importantly the use of a stable optical bench.

Coherent light (in this case , a two milliwatt He-Ne laser) is directed on to a double prism. One ray of the split beam passes through through a planoconvex lens of long focal length and reflected perpendicularly off an optical flat resting on the surface of the platform. This is similar to the arrangement for the classic Newton's Rings experiment, the theory of which is described in any standard Physics or Optics textbook (e.g.Born and Emil, 1980). Light reflected from the top of the optical flat and the concave surface of the lens interfere to form concentric circles of maxima and minima with a large amplitude central pattern (amplitude varies radially as a sinc function). Movement of the platform alters the air gap between the lens and the optical flat changing the optical path length and the rings appear to grow outwardly from the centre or collapse in from the perimeter (depending on the direction of movement). A photograph was taken by substituting a 35mm. camera with adaptor for the microscope eyepiece (plate 6.2). This photograph was taken at an early stage of the experiment (when an inclined optical flat was used in place of a double prism) and the ring quality was rather poor.

An initial attempt to count the collapsing maxima mentally was found to be totally impractical. Apart from

Plate 6.2: An example of the eyepiece image.





numerical errors the time involved precluded repeated observation of the gravity meter. The fringes were counted electronically using a simple electronic comparator and photodiode together with a standard electronic counter. Several circuits were designed and constructed before a satisfactory arrangement was found. A diagram of the final circuit is shown in figure 6.13. This consists of two inexpensive op-amps (type 741) in a two stage amplifier, the second of which is driven to saturation, giving a square wave output. Potentiometers VR1 and VR2 determine the threshold voltage at which saturation occurs. Specific comparator integrated circuits (e.g. type 693) did not operate as well as this arrangement. Circuit performance was checked using a digital oscilloscope and a tracing from a polaroid photograph of a typical input and out trace is shown in figure 6.14. The lower trace illustrates the input signal from the photodiode (amplitude 6mv) and the upper the amplifier output (20V). The trace illustrates the screw foot being wound down to a static position; as the screw rotation rate decreases the waveform narrows. Vibrational noise was found to be a large problem but this was almost completely eliminated by supporting the optical bench on planks resting on inflated car tyres. This proved remarkably effective and most of the noise visible on figure 6.14 is electronic. The square wave pulses were counted using a Hewlett Packard model 5300B/53088A measuring system. The fringe counter is most likely to generate errors when tilting commences or

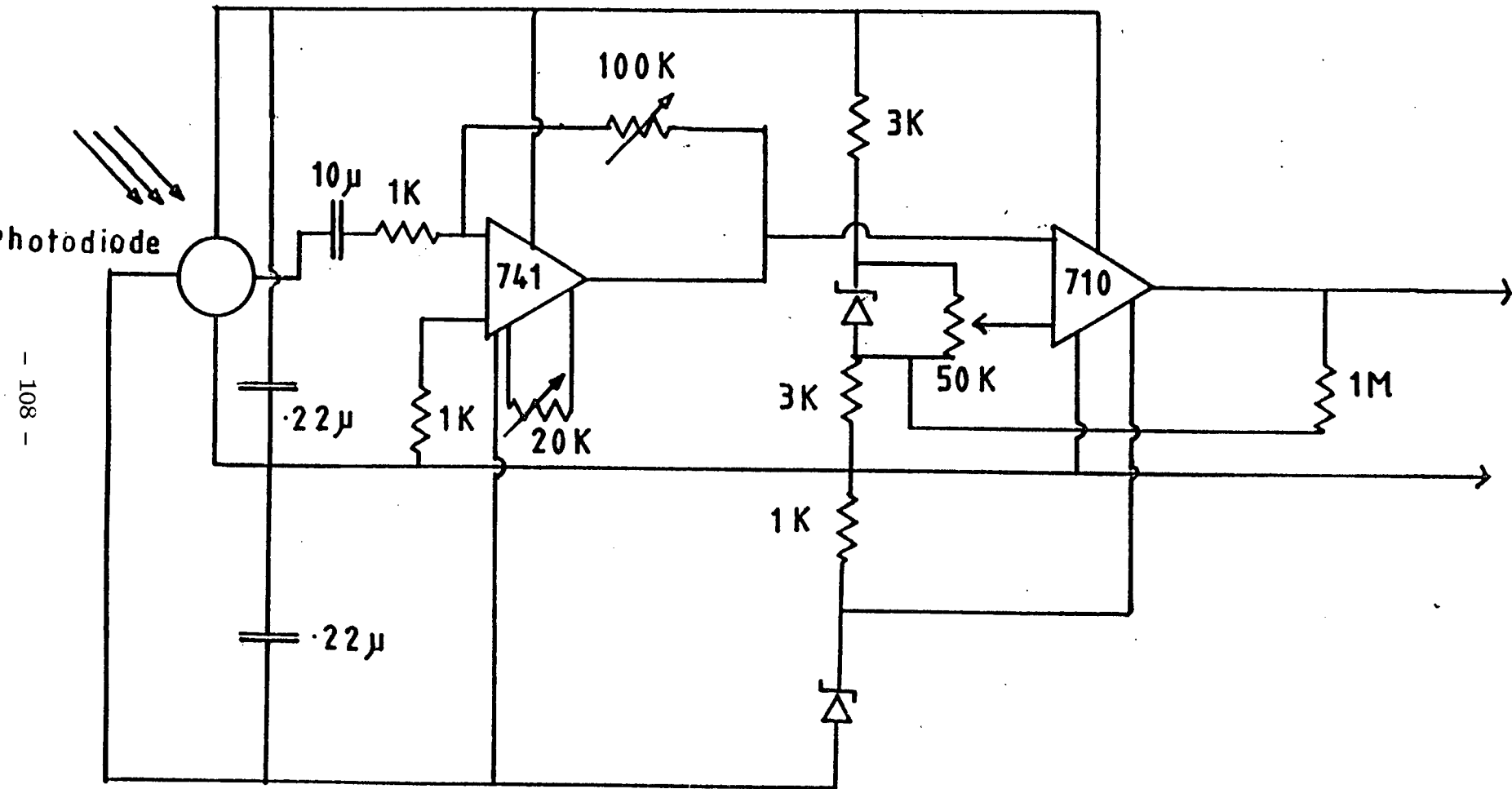


Figure 6.13 Electronic circuit diagram of comparator.

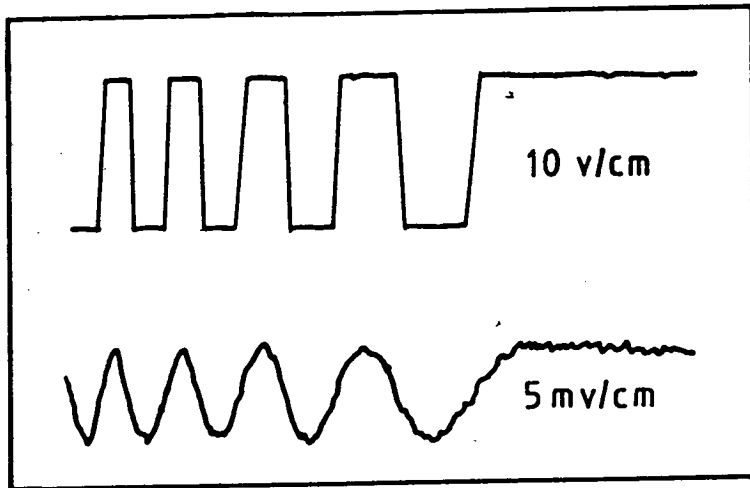


Figure (6.14)

### Dual 741 driven to power rails

Oscilloscope trace (taken from Polaroid photograph)  
of comparator input and output.

finishes as shown in figure 6.14. but repeated tests gave very satisfactory registration. The cushioning of the optical bench reduced vibration to such a small level that it was barely perceptible through the microscope eyepiece and it was possible to register zero counts when the apparatus was left unattended for several hours outside normal working hours. This was not the case during week days so all experimentation was carried out at night or weekends.

The reading procedure was similar to that outlined above, the first and every third reading was taken with the meter levelled to control instrument drift. Ten experiments were carried out, six tilting parallel to the cross axis and four parallel to the long axis, before it was necessary to vacate the optical laboratory. The position of the central interference pattern was scribed on the top surface of the secondary plate whilst sighting down the microscope. The distance to the from this point to the pivoting axis was determined on a cast iron flat bed using a vernier height guage.

### 6.9 Data Reduction and Results

The central maxima oscillates in intensity from dark to dark again as the platform is displaced one half of a wavelength. Thus for small angles

$$\theta \doteq h/R = n\lambda/2R$$

E 6.2

where  $h$  = air gap thickness

$R$  = pivot radius

$n$  = the fringe count

$\lambda$  = the wavelength of the source

The relative uncertainty in the measured angle is largely dependent on the uncertainty in fringe counting and the estimation of  $R$  since the error associated with the wavelength is negligible. The fringe count error will always be positive and a pessimistic estimate of this error would be one part in five hundred. The distance  $R$  is about 0.35m. and the error in measuring between the scribed lines using machine shop gauges is better than  $10^{-4}$ m..

If the meter is not horizontal when levelled using the vials but at a small angle  $\theta_0$ , then at some angle  $\theta_1$

$$\begin{aligned} \tilde{g} &= g_0 \cos \theta_0 - g_0 \cos \theta_1 \\ &= g_0 \{ (1 - \cos \theta_1) - (1 - \cos \theta_0) \} \\ &= g_0 \{ \sin^2 \theta_1 / 2 - \sin^2 \theta_0 / 2 \} \\ &\approx g_0 \{ \theta_1^2 / 2 - \theta_0^2 / 2 \} \end{aligned}$$

$$\tilde{g} = \theta_0 \delta\theta g_0 - \delta\theta^2 / 2$$

E 6.3

$$\delta\theta = \theta_1 - \theta_0$$

Thus the observed gravity is described by a second degree polynomial whose second coefficient relates dial turns to gravity and the first degree coefficient is related to the levelling error. The data were reduced using existing programs (PBAS) which converts the dial turns to

gravity units using the manufacturer's scale factor and relates observed gravity to the first reading. In addition to a first and second degree coefficient there is a constant term, being any error associated with the first reading. Substituting equation 6.2 into equation 6.3 and adding a constant term,  $\alpha$  gives

$$\hat{g} = \alpha + \frac{n\lambda}{2R} \theta_0 g_0 - \left(\frac{n\lambda}{2R}\right)^2 g_0 \quad \text{E 6.4}$$

The constant and first degree coefficients differ for each observation sequence but the second degree coefficient is common to those sequences tilting along the same axis.

A least squares adjustment program, LSQTILT (see appendix 5) was written to fit a common second degree coefficient to a tilting data suite. For N observation sequences there are 2N+1 unknowns, N constant coefficients, N first degree coefficients plus the common second degree coefficient. The least squares solutions for the long level data suites is shown in figures 6.15.

The cross level data suite is evidently of lower quality than that of the long level. This is also apparent on examination of tables 6.4 and 6.5, the output from the program LSQTILT. The standard deviation for the cross level set is greater than one gravity unit and the regression parameter R (Draper and Smith, 1966) is unsatisfactorily low. Tilting the meter parallel to the cross level

Tilt Parabola G275, Long level (4 experiments)

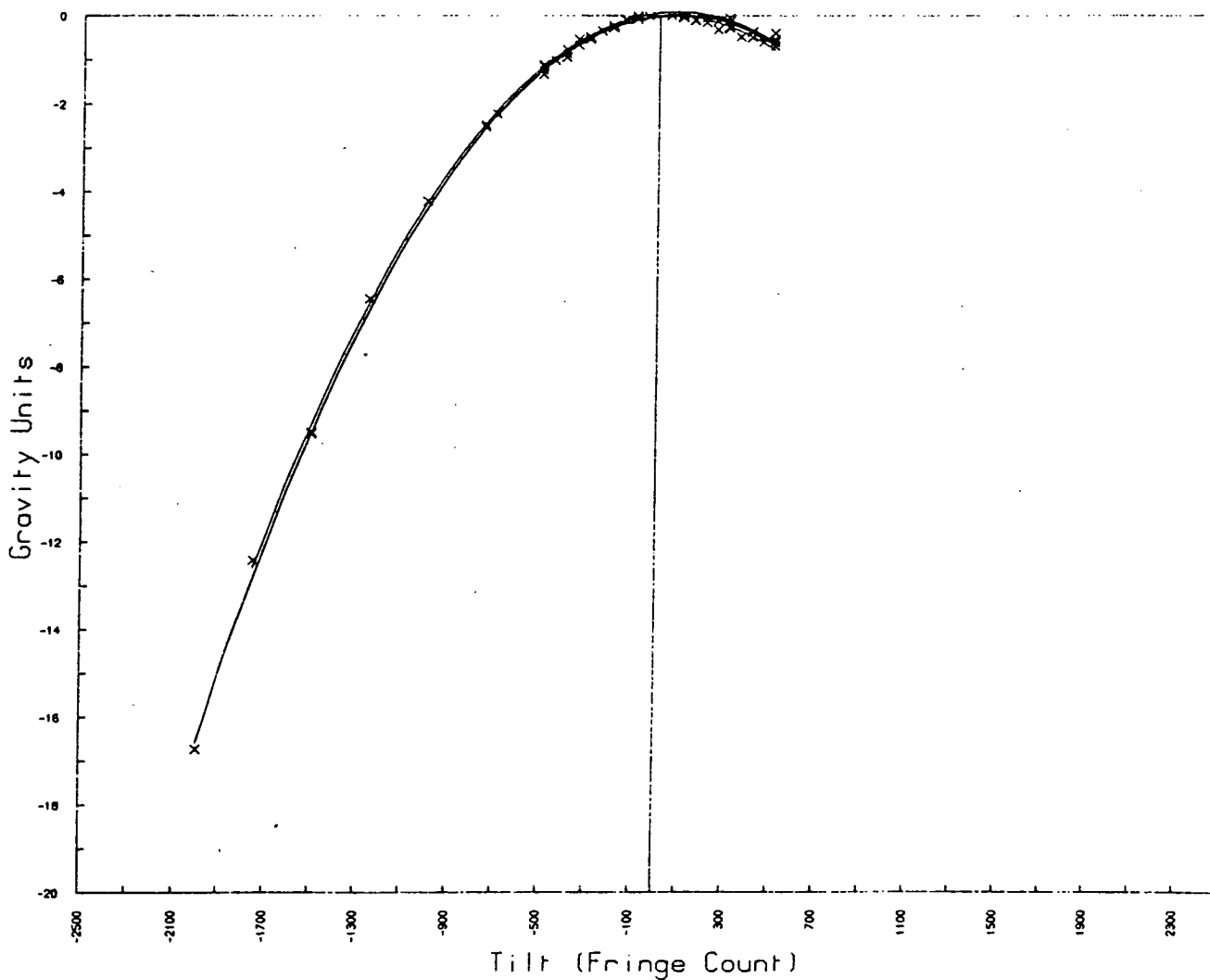


Figure 6.15 Least squares fit to long level tilt observations.

Table 6.4

Results of analysis of tilting experiment

LONG AXIS

The number of observations is 59 with 9 constraints

The estimated standard deviation of the fit is 0.0951

R squared for fit: 0.99922

The Regression Coefficients with their variances (st. err. squared) are

|   |              |             |
|---|--------------|-------------|
| 1 | -0.30340E-01 | 0.46532E-03 |
| 2 | 0.70109E-01  | 0.87535E-03 |
| 3 | 0.81648E-03  | 0.63155E-03 |
| 4 | 0.67385E-01  | 0.13580E-02 |
| 5 | 0.42231E-03  | 0.46955E-08 |
| 6 | 0.47546E-03  | 0.34683E-08 |
| 7 | 0.55704E-03  | 0.52658E-08 |
| 8 | 0.60765E-03  | 0.45869E-08 |
| 9 | -0.38598E-05 | 0.14437E-14 |

CCORRN is: 0.996139704



Table 6.5

Results of analysis of tilting experiment

CROSS AXIS

The number of observations is 92 with 13 constraints

The estimated standard deviation of the fit is 1.1313

R squared for fit: 0.96122

The Regression Coefficients with their variances (std. err. squared) are

|    |              |             |
|----|--------------|-------------|
| 1  | -0.54962E-01 | 0.80249E-01 |
| 2  | -0.12757E+00 | 0.71584E-01 |
| 3  | -0.33386E+00 | 0.19456E-00 |
| 4  | -0.15989E+01 | 0.13700E-00 |
| 5  | -0.79983E-02 | 0.80515E-01 |
| 6  | 0.10930E+01  | 0.11675E+00 |
| 7  | -0.31512E-03 | 0.60088E-06 |
| 8  | 0.12748E-02  | 0.39080E-06 |
| 9  | 0.21348E-02  | 0.34244E-07 |
| 10 | -0.10506E-02 | 0.73662E-07 |
| 11 | 0.40928E-03  | 0.45346E-06 |
| 12 | 0.42466E-03  | 0.50191E-07 |
| 13 | -0.36177E-05 | 0.14472E-13 |

CCORRN is: 1.152106255

generates greater errors because of the irregular torques placed on the pivots and leaf springs of the mechanism. Only the results from tilting parallel to the long level will be considered.

The long level observations have been successful ( $R$  equals 0.9992, a standard error of 0.09g.u.) but the standard error on the second degree coefficient is almost one percent. The variable CCORN (program line 113,119) is the ratio of the theoretical second degree coefficient to the observed value. This implies a correction factor of  $1.0039 \pm 0.0099$ , encompassing both the Hatton Heath and Cat and Fiddle correction factors. It would be necessary to increase the number of observation sequences by at least ten fold to obtain a reasonable standard error on the second degree coefficient.

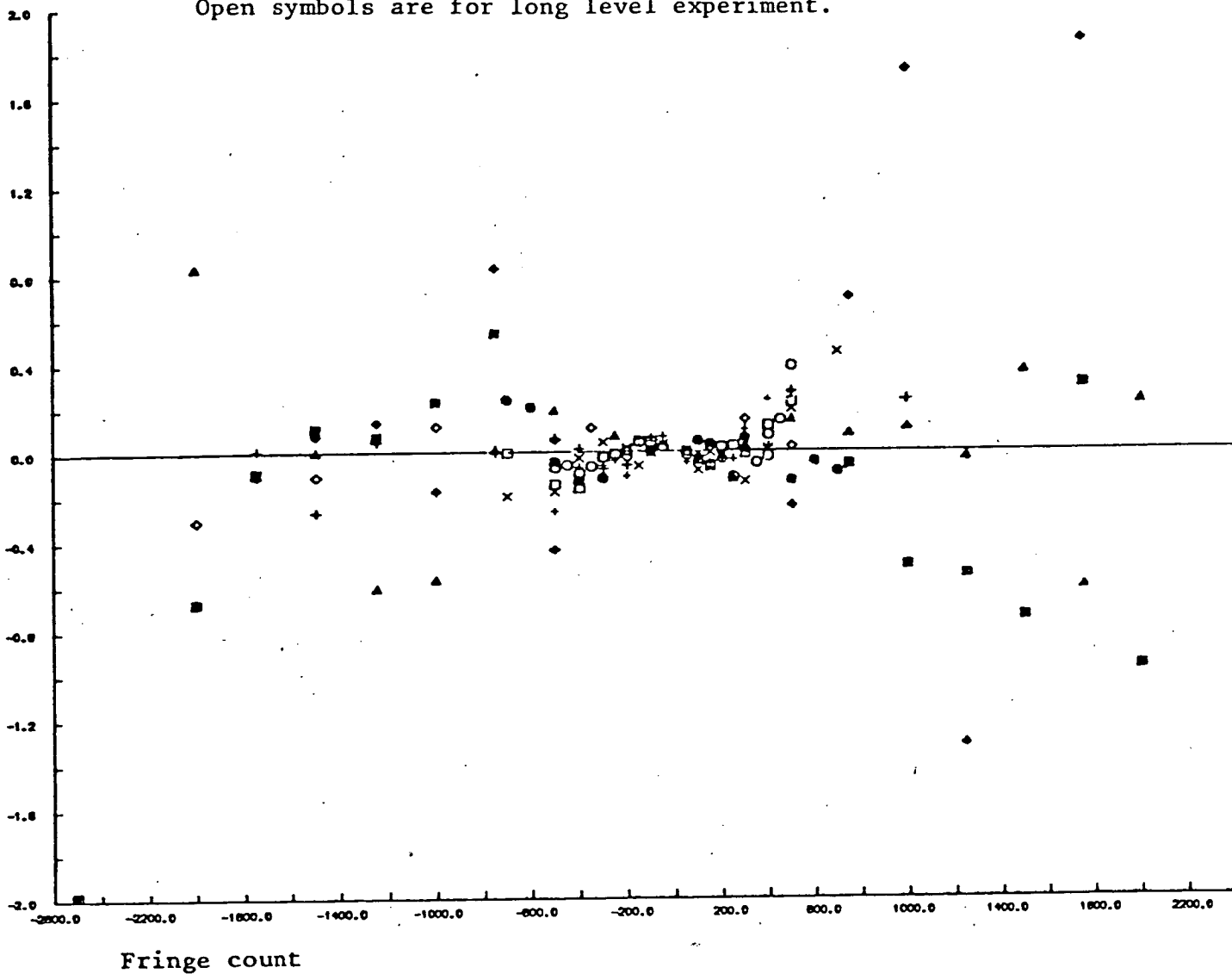
Figure 6.16 shows the quadratic fit residuals for both the cross and the long level tilting. These demonstrate the increase in error as the tilting angle is increased. Figure 6.17 is a plot of the least square solution residual against the noted gravimeter spindle position for the long level only. It is not possible to note any periodicity at the one dial turn interval because of the lack of data.

Figure 6.16

### Quadratic fit residuals

Occluded symbols are for cross level experiments.

Open symbols are for long level experiment.



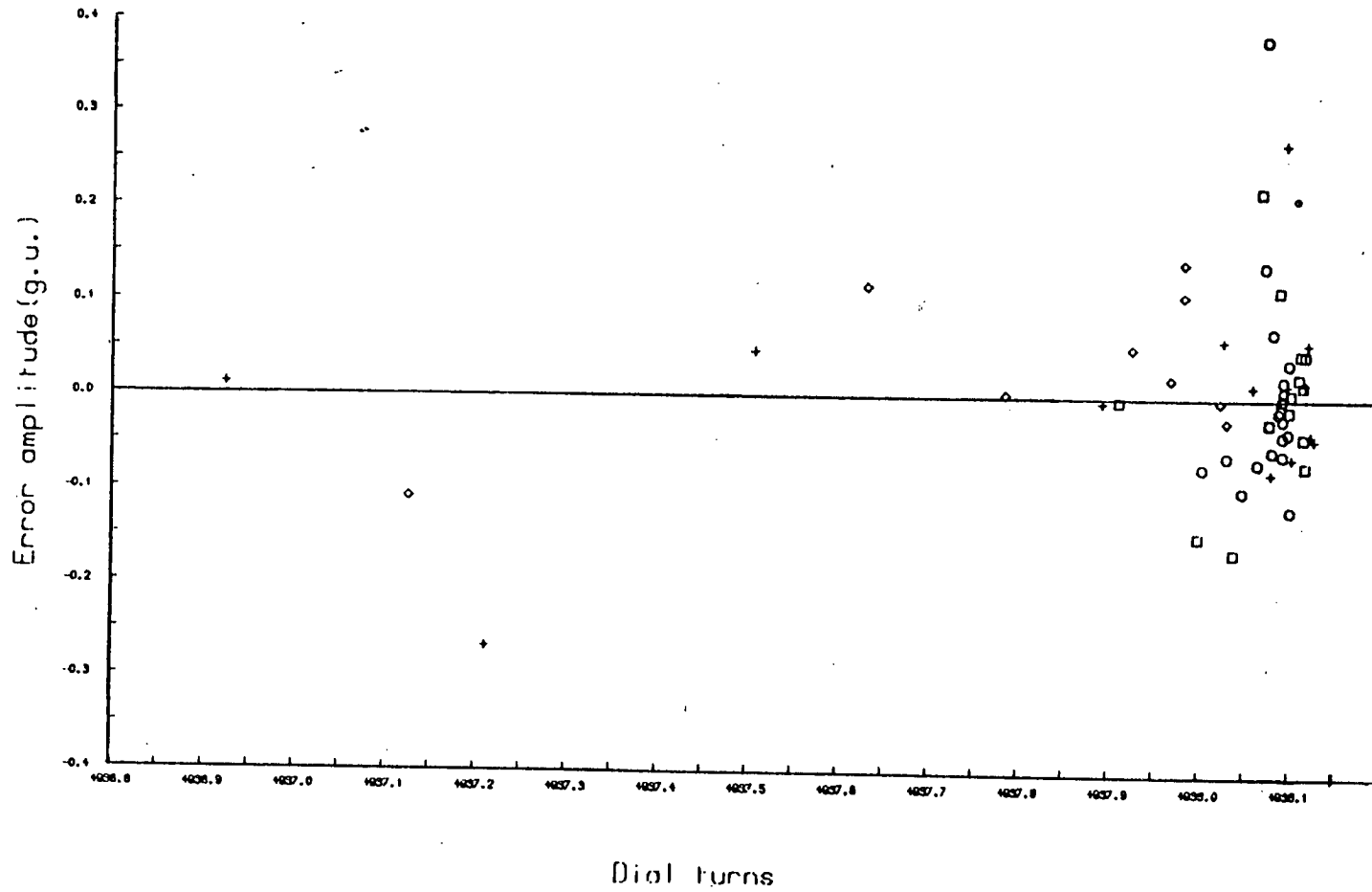


Figure 6.17

Misfit amplitude as a function of observed dial turns

## 6.10 Conclusions

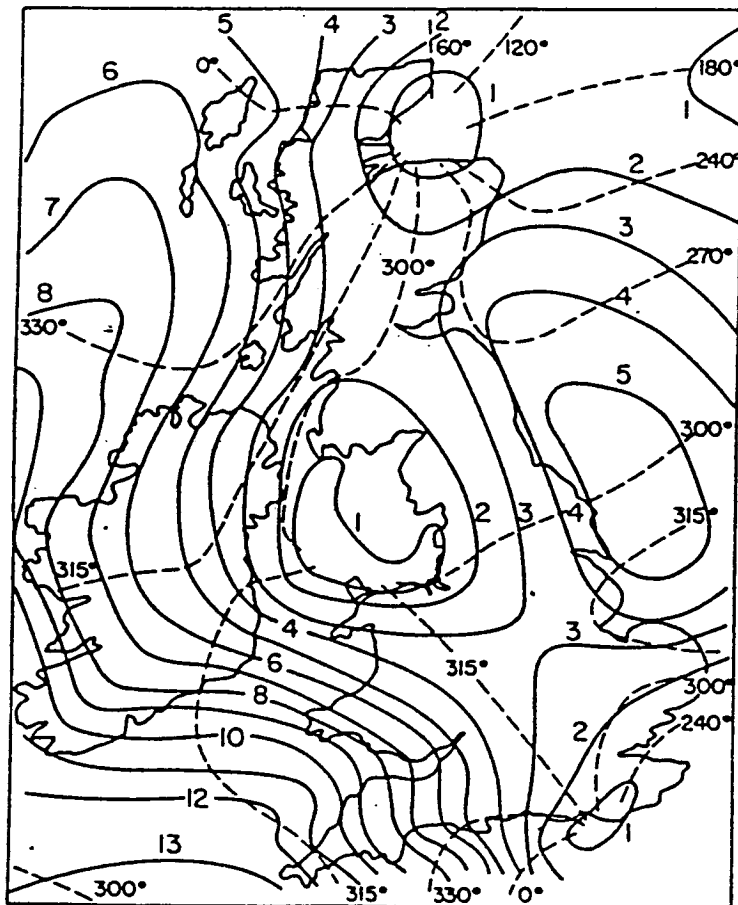
Field calibration tests with G-275 and three other gravimeters indicate that the accepted figure for the gravity difference between Hatton Heath and Press is incorrect. The scale correction factor obtained for G-275 ( $4.0 \times 10^{-4}$ ) on two independent field tests, a long calibration run and the Cat and Fiddle line are in good agreement. Laboratory test were undertaken to verify this and the field values fall within the error limits of the laboratory determined scale factor. The feasibility of a Newton's rings interferometric technique has been demonstrated but a large number of observations are required. This method has the advantage of being independent of other meter readings and network adjustments.

## CHAPTER SEVEN

### DETERMINATION OF OCEAN LOADING AT ESKDALEMUIR

#### 7.1 Introduction

As discussed in section (4.3) , the accurate determination of the Earth Tide is complicated by the ocean loading effect. Baker (1980) presents the most recent and accurate ocean load effect model for the British Isles. Figure 7.1 illustrates the theoretical  $M_2$  gravity loading obtained by Baker using the method of Farrell (1972,1973) . Baker uses the  $M_2$  ocean tide model of Hendershott and Munk (1970) for more distant water bodies together with a detailed model of the local shelf seas (Flather, 1976, numerical model B, plus sub gridding near coastal sites). Locally determined Earth models from seismic refraction surveys were used wherever possible (Blundell and Parks, 1969; Holder and Bott, 1971) but it was found that there is negligible difference between the Green's function of differing Earth models beyond seven kilometres from the load point. Baker discusses in detail the agreement of this model with the results of eight Earth tide stations, established by himself and others at locations in England and Wales. The model agreement with the observations is good (maximum residual 0.6 microgals) but the most northerly station is located at Bidston (latitude 53.3 N) which is rather unsatisfactory for the purpose of a microgravimetric investigation in central



The  $M_2$  tidal gravity loading in Britain. The full lines are the contours of the calculated loading amplitude in  $\mu\text{gals}$  and the dashed lines are contours of the phase lag of the loading with respect to the tidal potential in the Greenwich meridian.

Figure 7.1  $M_2$  tidal gravity loading in Britain (from Baker 1980)

Scotland. The only reference for Scottish studies in the literature is to an unreliable registration carried out by Tomachek, reading a Frost gravimeter hourly (Tomachek, 1958).

It was found that workers from the University of California had installed a modified La Coste and Romberg meter permanently at Eskdalemuir in Southern Scotland (latitude 55.3 N). A tidal analysis of these data was carried out to ascertain the validity of Baker's model studies at more northerly latitudes. The gravimetric factors so obtained were to be used in the tidal reduction program PBAS (section 4.4) for the reduction of gravity observations in Scotland. .

## 7.2 The I.D.A. Instrument

The gravimeter located at Eskdalemuir is part of a worldwide network of eighteen such instruments known as the International Deployment of Accelerometers (I.D.A.) (Agnew et al., 1976). The primary purpose of the I.D.A. meters is to monitor free oscillations of the Earth which have periods of one hour or less but a second channel suitable for tidal analysis is also recorded. Figure 7.2 is a block diagram of the instrument, which is essentially a modified G-meter with a three plate capacitive position sensor as described in Block and Moore (1966). Position detection is performed within a narrow band; a five kilohertz signal being applied to the outer plates and the



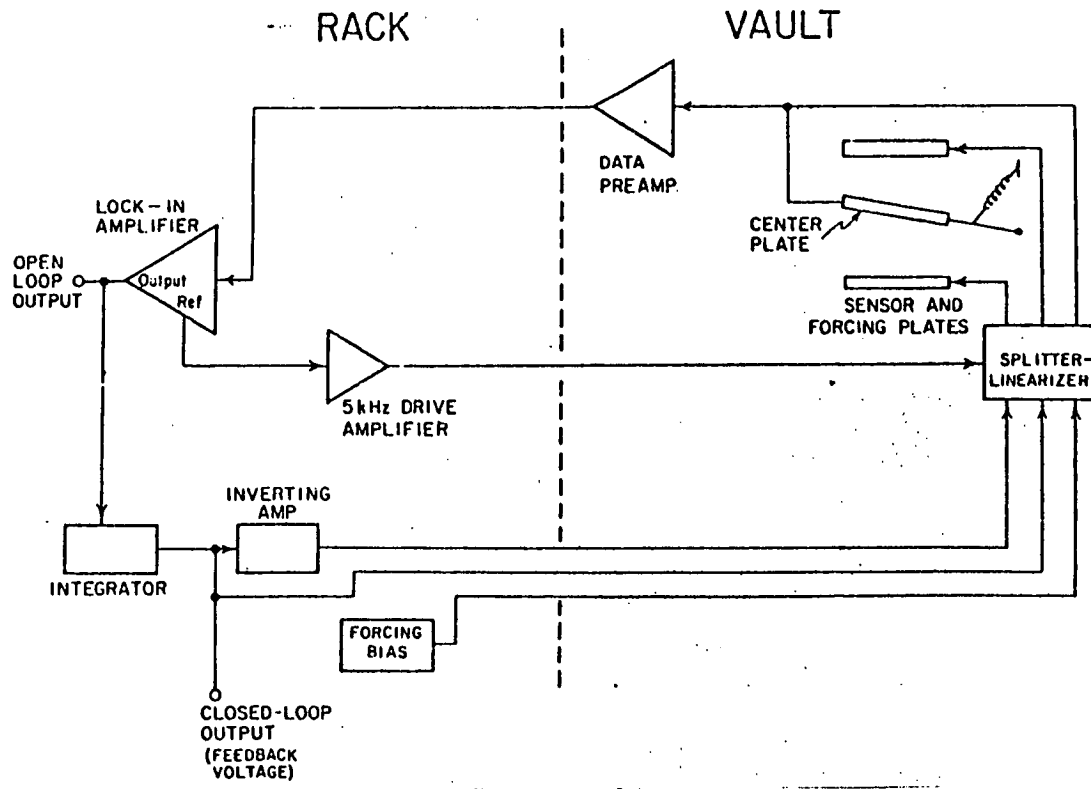


Figure 7.2 Block diagram of I.D.A. meter system

amplified voltage induced in the centre plate is input to a lock in amplifier. The lock in amplifier operates with a very narrow band width centred at five kilohertz to minimise the problems of electronic noise and outputs an equivalent bandwidth at d.c.. Negative feedback is used to centre the mass and linearise the output. Since the spring is kept at a constant extension the calibration will be stable. The instrument is hermetically sealed in a thermostatically controlled cannister which sits in a larger vessel ( 0.6 metres high, 0.46 metres diameter) filled with polystyrene beads. In this way the mechanism and preamplifiers are isolated from thermal shocks and the inner chamber is maintained at a fixed temperature  $\pm 5.10^{-4}$  C , close to the inversion point of the spring. In the case of Eskdalemuir the meter sits on an isolated concrete pier inside an earth covered bunker. The site, which includes an WWSN station is remote from all sources of manmade and coastal noise.

### 7.3 I.D.A. Instrument Response

Before digitising, the output signal undergoes analogue pre-filtering and is then written to cassette tape. The absolute gain of the instrument is measured by tilting the meter on a triangular plate having a motor driven micrometer screw at one corner. A metal film potentiometer is geared to the micrometer to gauge rotation (Moore and Farrell, 1970) . The frequency response

is measured using a cross spectral method inputting a random telegraph signal (Berger et. al.,1979). Furthermore each instrument is also run at Pinon Flat observatory for comparison with the superconducting gravimeter (see section 2.2) . The calibration funtion is given as a rational function C(f) with real coefficents, but is a complex valued funtion of frequency.

$$C(f) = A \left\{ \frac{P_0 + P_1 (i\nu) + P_2 (i\nu)^2 + \dots + P_n (i\nu)^n}{Q_0 + Q_1 (i\nu) + Q_2 (i\nu)^2 + \dots + Q_m (i\nu)^m} \right\}$$

The coefficients of C(f) are given in Table 7.1 and the amplitude and phase response are shown in Figure 7.3.

The response at tidal frequencies ( $M_2 = 28.98^{\circ}/hr$ ) is flat and can be described by two constants. The last column of the tabulated response ordinates (Table 7.2) is the group delay (i.e. the derivative of phase with respect to frequency). It is nearly constant at tidal frequencies and the phase shift can be accurately given as;

$$(-360 * 44.95) / T \quad \text{degrees} \quad T = \text{Period(sec.)}$$

The amplitude response may be stated as 0.5688 ugal per least count ( $1/1.7571 * 0.9995$ , the gain of the TIDE filter ).

The error amplitudes are obtained by examining the misfits between the smooth function C(f) and the cross spectral estimates. The response function is not

STATION: ESK  
CHANNEL: Tide

APPLICABLE 258/1/1978 TO 1

Time (and place) of calibrations:

ABSOLUTE: 255/1/1978 (ESK)  
INSTRUMENT: 257/1/1978 (ESK)  
FILTER: 117/1/1978 (LJC)

A = 1.758 ± .009 ( $10^8$  counts per  $m/s^2$ ) ( $g = 9.81 m/s^2$ )

$f_0 =$  .01 Hz  
 $\therefore (10^5 \text{ counts per } g - \text{ approx.})$   
 $\therefore (1 \text{ count per } \mu g \text{ approx.})$

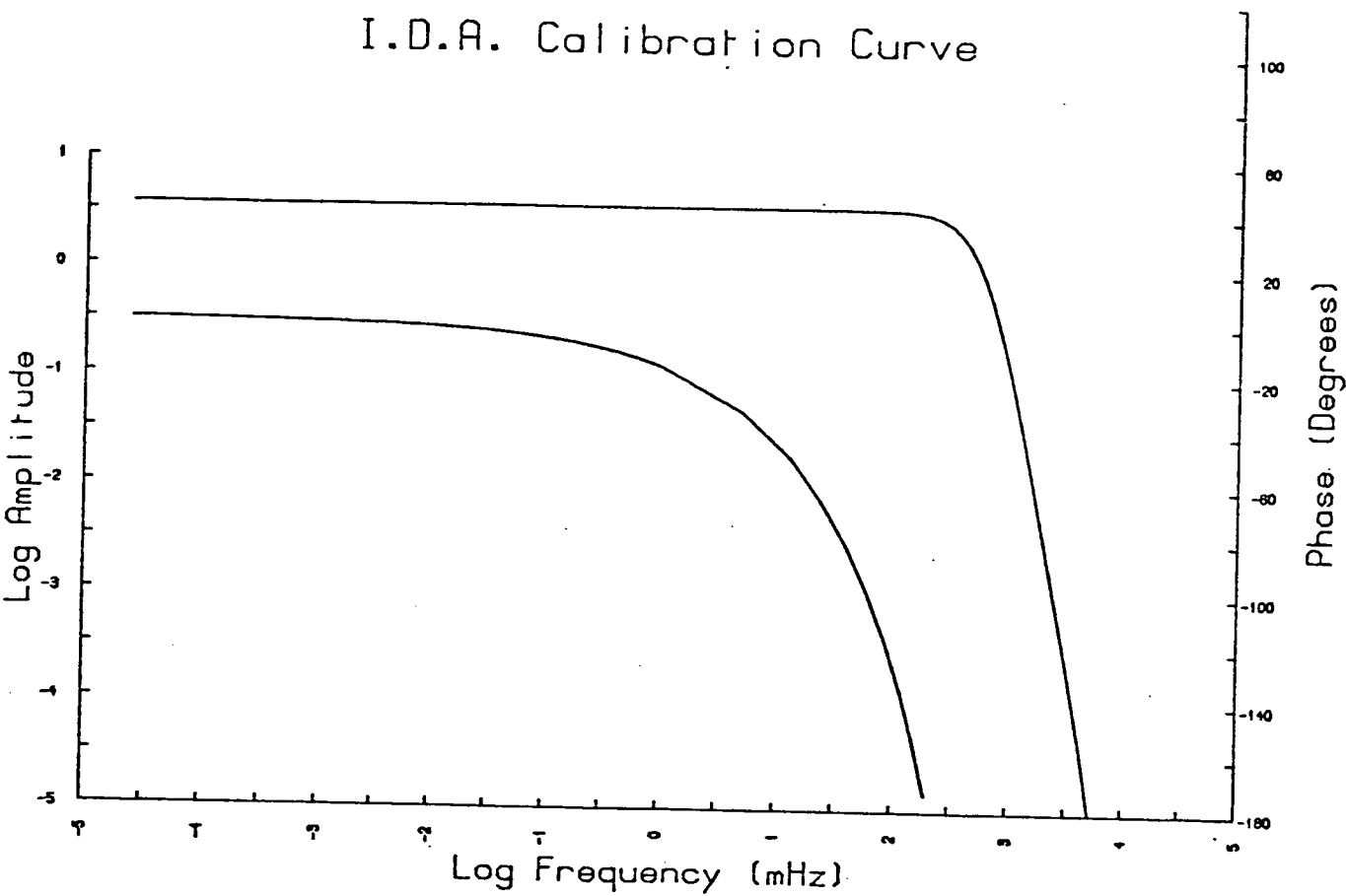
|                       |   |
|-----------------------|---|
| n = <u>1</u>          | m = <u>11</u>                                       |
| $p_0$ <u>1</u>        | $q_0$ <u>1.000490</u>                               |
| $p_1$ <u>.2315552</u> | $q_1$ <u>3.05763</u>                                |
| $p_2$ _____           | $q_2$ <u>4.649246</u>                               |
| $p_3$ _____           | $q_3$ <u>4.536808</u>                               |
| $p_4$ _____           | $q_4$ <u>3.062363</u>                               |
| $p_5$ _____           | $q_5$ <u>1.472665</u>                               |
| $p_6$ _____           | $q_6$ <u>.5018679</u>                               |
| $p_7$ _____           | $q_7$ <u>.117243</u>                                |
|                       | $q_8$ <u>.01806866</u>                              |
|                       | $q_9$ <u><math>1.717076 \cdot 10^{-3}</math></u>    |
|                       | $q_{10}$ <u><math>8.160125 \cdot 10^{-5}</math></u> |
|                       | $q_{11}$ <u><math>1.788909 \cdot 10^{-6}</math></u> |
|                       | $q_{12}$ _____                                      |
|                       | $q_{13}$ _____                                      |
|                       | $q_{14}$ _____                                      |
|                       | $q_{15}$ _____                                      |

ERROR: 2 % ( \_\_\_\_\_ % in tidal band)

REMARKS: \_\_\_\_\_  
\_\_\_\_\_  
\_\_\_\_\_

Table 7.1 Polynomial coefficients of the calibration factor for Eskdalemuir instrument (from manual).

### I.D.A. Calibration Curve



### I.D.A. Calibration Curve

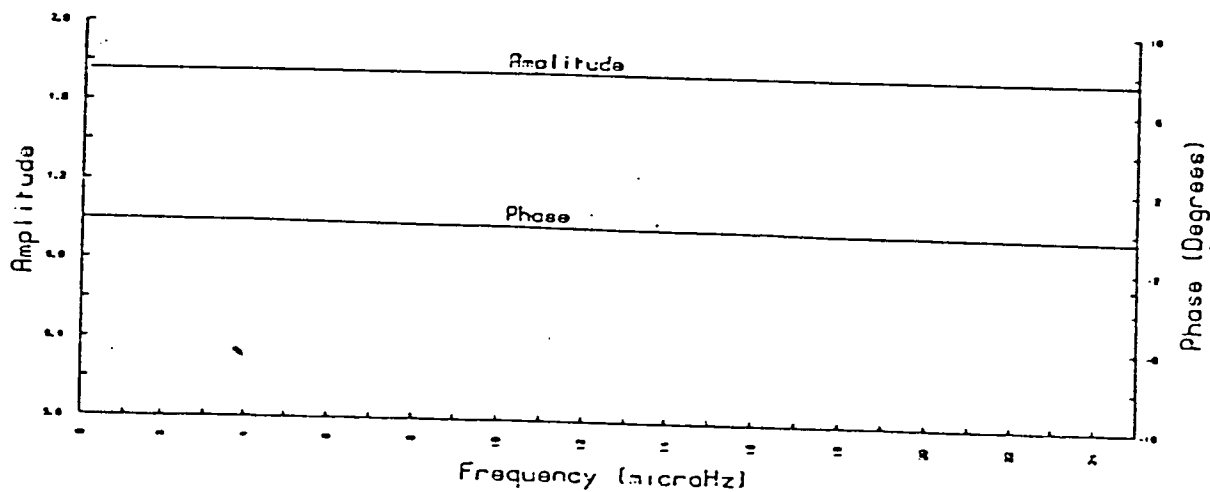


Figure 7.3 Eskdalemuir response curves

determined at tidal frequencies but is obtained by extrapolation. The tilting procedure to obtain the absolute gain is effectively carried out at d.c. and it can be seen from Table 7.2 that the response function is almost completely constant with the d.c. value at tidal frequencies. Although the response function is determined at higher frequencies the manufacturers are confident about the extrapolation to d.c. levels because of the instrument design. Being a feed back instrument the beam does not move at long periods and the rheology of the spring is not a problem. The absolute gain is determined by fitting a tilt parabola to the output voltage and in the case of this instrument the standard error was 0.5 per cent (Duncan Carr Agnew, personal communication). The overall timing error is estimated to be good to 1.2 seconds (c.  $0.01^{\circ}$  at  $M_2$  frequencies ).

#### 7.4 Data Analysis

The data were supplied on 2,400 feet, 800 bytes per inch computer tapes whose files exactly coincide with the on-site cassette tapes. Since the primary function of I.D.A. stations is to examine free oscillations of the Earth with periods typically in the range one to ten millihertz, the digitising interval is twenty seconds (this has since been amended on the tidal mode to 640 seconds). All the unpacking, binary conversion and reformatting was completed in an interactive one-stage process by the

| Frequency (mHz) | Gain (dB) | Amp. (least cnt./ (m/s <sup>2</sup> )) | Phase (deg, -ve for lag) | Delay (sec.) |
|-----------------|-----------|--|--------------------------|--------------|
| 0.0             | 164.90    | 0.17571E+09                            | -0.0000                  | -44.955      |
| 0.1             | 164.90    | 0.17571E+09                            | -1.6184                  | -44.955      |
| 0.2             | 164.90    | 0.17571E+09                            | -3.2368                  | -44.957      |
| 0.3             | 164.90    | 0.17571E+09                            | -4.8553                  | -44.961      |
| 0.4             | 164.90    | 0.17571E+09                            | -6.4740                  | -44.966      |
| 0.5             | 164.90    | 0.17571E+09                            | -8.0929                  | -44.973      |
| 0.6             | 164.90    | 0.17571E+09                            | -9.7121                  | -44.981      |
| 0.7             | 164.90    | 0.17571E+09                            | -11.332                  | -44.991      |
| 0.8             | 164.90    | 0.17571E+09                            | -12.952                  | -45.003      |
| 0.9             | 164.90    | 0.17572E+09                            | -14.572                  | -45.015      |
| 1.0             | 164.90    | 0.17572E+09                            | -16.193                  | -45.030      |
| 2.0             | 164.90    | 0.17574E+09                            | -32.440                  | -45.262      |
| 3.0             | 164.90    | 0.17577E+09                            | -48.803                  | -45.671      |
| 4.0             | 164.90    | 0.17578E+09                            | -65.348                  | -46.283      |
| 5.0             | 164.90    | 0.17573E+09                            | -82.155                  | -47.134      |
| 6.0             | 164.89    | 0.17552E+09                            | -99.316                  | -48.253      |
| 7.0             | 164.86    | 0.17494E+09                            | -116.93                  | -49.661      |
| 8.0             | 164.80    | 0.17372E+09                            | -135.11                  | -51.348      |
| 9.0             | 164.68    | 0.17142E+09                            | -153.93                  | -53.262      |
| 10.0            | 164.48    | 0.16752E+09                            | -173.47                  | -55.283      |

Table 7.2 Frequency response of Eskdalemuir calibration polynomial.

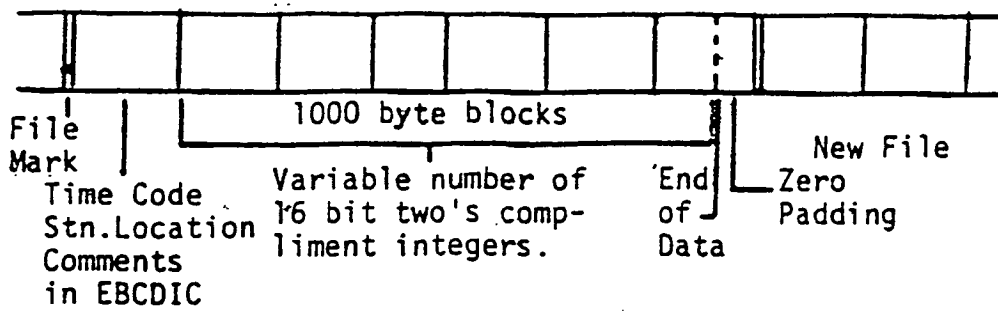
computer program NEWSM9 (listed in Appendix 6). This program is designed to run interactively on the 'Edinburgh Multi Access System' (EMAS), but could be very easily adapted to any facility supporting FORTRAN77. A fast machine is preferable to support the interactive procedures which have the advantage that the user can easily vary parameters to accommodate individual data adjustments. The output file of this program consists of hourly tidal amplitude estimates which were then input to a tidal analysis program, HYCON (Schuller, 1977). This program was implemented with assistance from Dr. R. Edge of the Earth Tides Branch, Institute of Oceanographic Sciences, Bidston.

An outline flow diagram of the program NEWSM9 is shown in figure 7.4. The data were generally smooth but a number of sample points contained random spikes, earthquake noise, binary drop outs or saturation and small offsets not uncommon with even the highest quality analogue-to-digital conversion. Those adjacent points with differences greater than twenty five uncalibrated units were examined manually and the necessary remedial action taken. This consisted of:

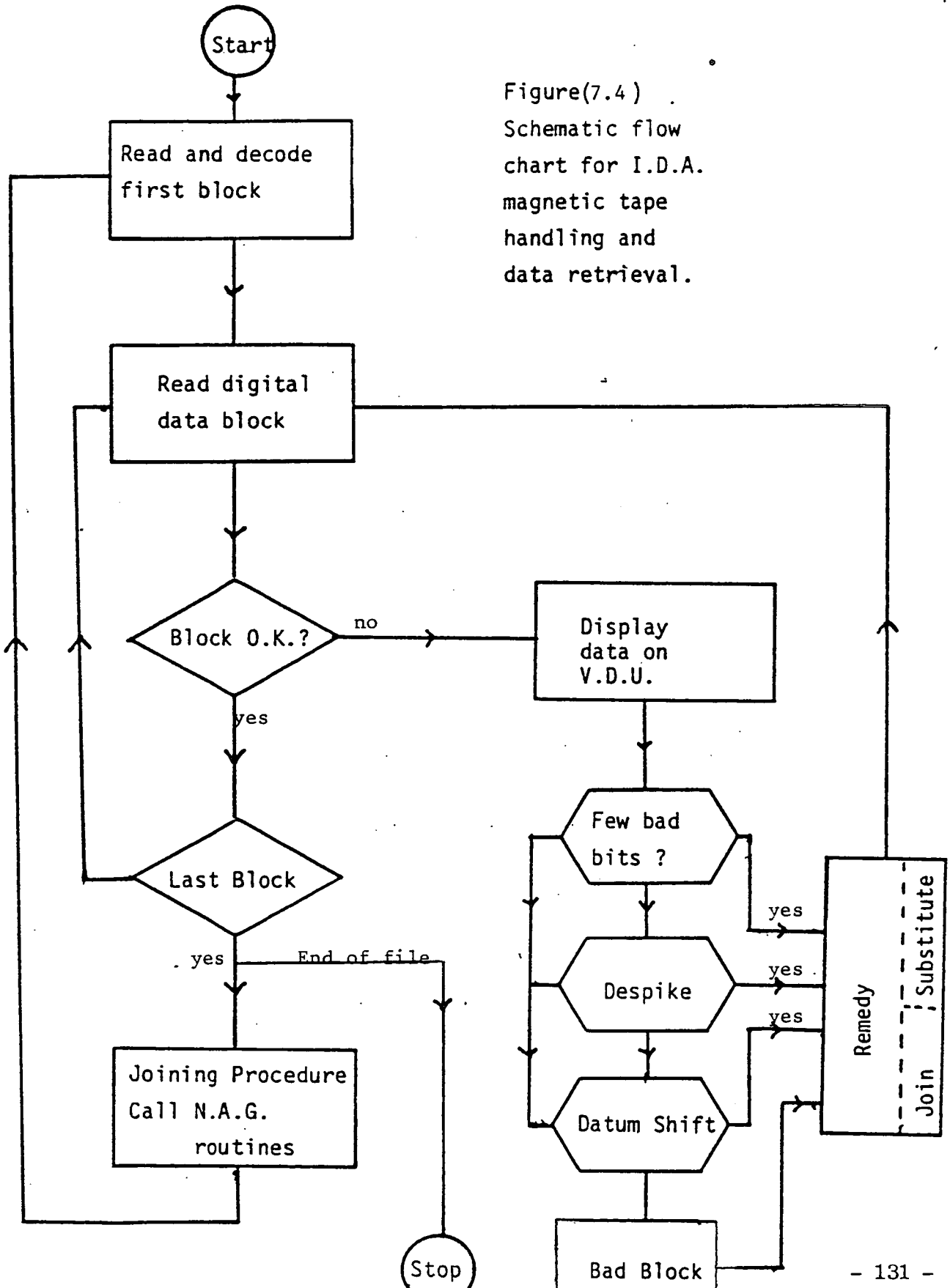
- (a) Substitution of a few data, interpolation  
judged by operator
- (b) Quadratic interpolation
- (c) Application of a datum shift . An attempt



# Magnetic Tape Structure



Figure(7.4) Schematic flow chart for I.D.A. magnetic tape handling and data retrieval.



to perform this automatically was found to be unsatisfactory and again human judgement was found to give the smoothest curve.

In addition to these error conditions it was necessary to concatenate files with a time gap between them. The data gap, being the time to change a cassette, was typically fifteen minutes (45 samples), and quadratic interpolation using N.A.G. routines EO2ADF and EO2AEF was used. The first 1000 bytes of each file contains timing information and additional comments as shown on figure 7.5. This enables the user to check the sample cursor position after each concatenation. In this manner a complete 20 second data ensemble was formed from which it was necessary to obtain hourly values suitable for Standard Earth Tide analysis procedures. This was accomplished by outputting the central value of a quadratic fit. An example of the I.D.A. instrument output together with the theoretical Earth tide (determined using the method of Browke, Zurn and Slichter) is shown in figure 7.6.

### 7.5 Tidal Analysis

After examination of a total of two years data, a continuous section (25-09-78 --> 12-05-79) consisting of a total of 5448 hourly observations was chosen. This particular section was totally free of prolonged data gaps which generally have an unpredictable effect on tidal data.



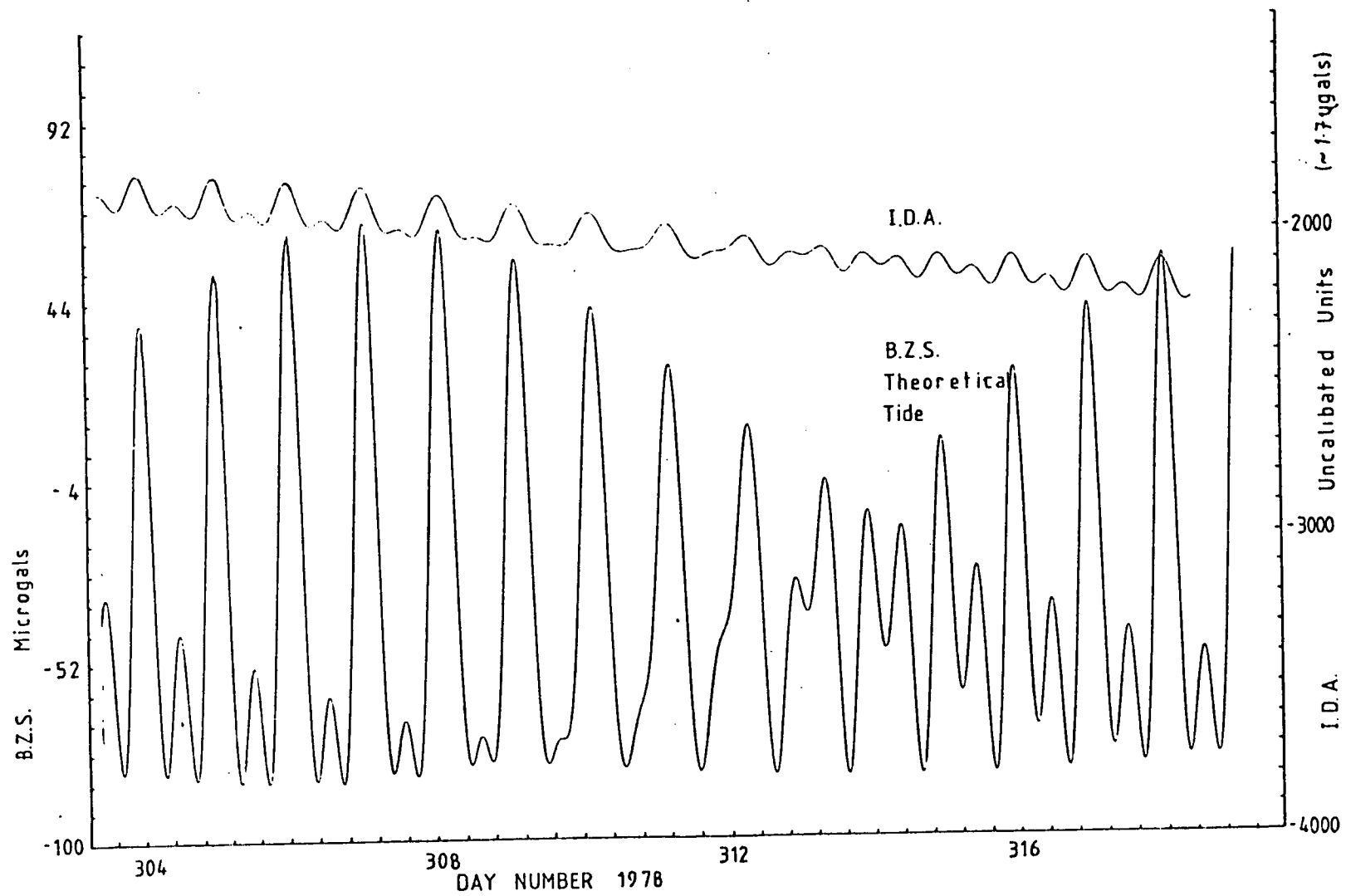


Figure 7.6 I.D.A. data compared with theoretical tide for Eskdalemuir

These data were then taken to I.O.S. Bidston for processing using the S.E.R.C. computing facilities at Daresbury.

The data were first filtered using a Doodson- Lennon Xo tidal filter which is a simple linear combination (1010010110201102112 0 ...). This filter removes long period drift, and other transient signals, (eg. exponential trends) which would otherwise produce noise at all frequencies. The Xo filter is symmetric , producing no phase shift and the Fourier amplitude spectrum is reproduced in Figure 7.7 .

The program HYCON was used to perform a standard analysis to calculate the tidal component amplitudes and phases. The analysis is completed for all 505 Cartwright-Talyer-Edden (see section 4.2) constituents in thirteen groups. It is just possible to separate  $S_2$  ( $30^\circ\text{h}^{-1}$ ) from  $K_2$  ( $30.082137^\circ\text{h}^{-1}$ ) and  $S_1$  ( $15.000002^\circ\text{h}^{-1}$ ) from  $K_1$  ( $15.041069^\circ\text{h}^{-1}$ ), but I have not attempted to do so in my analysis. The results of the analysis for the seperable groups are presented in Table 7.3 together with the results of Baker's stations. A subset of 85 days was randomly selected for fourier analysis and the power density spectrum is displayed in Figure 7.8 The data was first filtered in the time domain using a high pass filter with a 48 hour cut off.

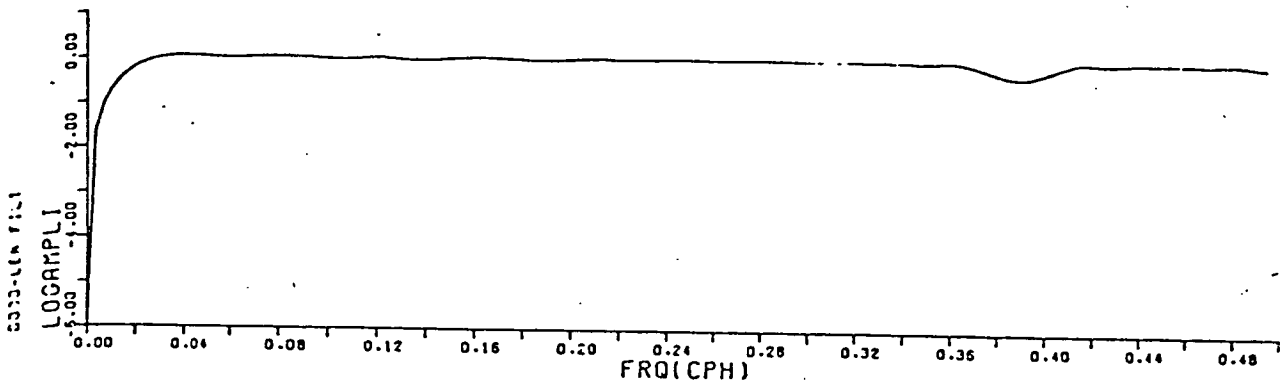
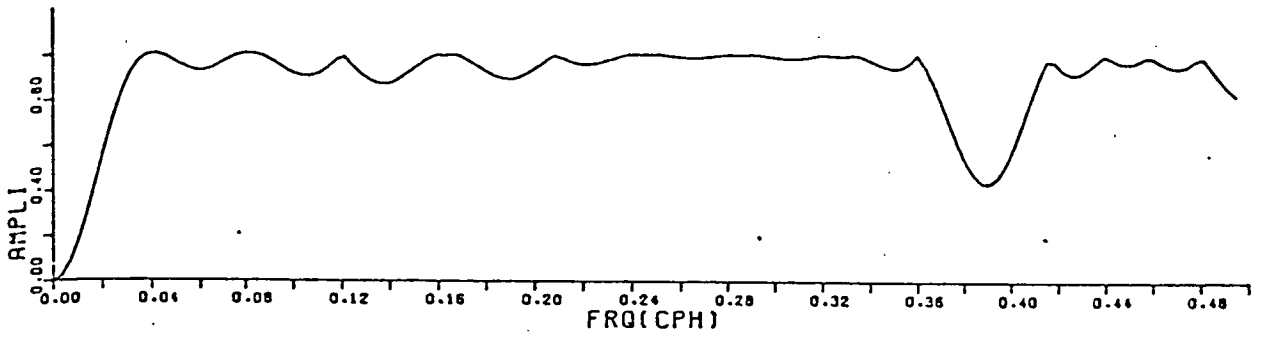


Figure 7.7 Frequency response of Doodson-Lennon filter  
 Upper - linear scale, lower - logarithmic scale.  
 (from Yaramanchi, 1979)

## 7.6 The Observed Load

The uncertainty in the amplitude of the theoretical gravity body tide is in the order of  $\pm 0.5\%$  (Baker 1980, Alsop and Kuo 1964) and that of the phase lag negligible (Zschau, 1978 from Baker, 1980). The overall residual standard deviation of the analysis is  $1.38\mu\text{gal}$  as compared with  $0.7\mu\text{gal}$  for Baker's measurements at Bidston. Tables 7.3 and 7.4 compare the parameters obtained from the Eskdalemuir analysis with those of Baker's installations. (Dr. Baker kindly provided the theoretical  $M_2$  load for the Eskdalemuir site). It can be seen that the observed load departs considerably from the model  $M_2$  load apparently outside the bounds of possible error. The problem of calculating the maximum load within given error limits is non linear. Two graphs (figures 7.9, 7.10) illustrate the effect on load amplitude and phase separately with differing observation errors. It appears that to obtain the derived load vector would require an error of one percent in the amplitude and  $-1.5^\circ$  of phase. The uncertainty associated with the standard analysis is an order of magnitude less than this (see r.m.s. figures in Table 7.4).

Dr Agnew also supplied me with the results obtained by Farrell and also Melchior (both unpublished) studying data from the same instrument. Their results are shown in Table 7.5, together with the results of model studies other than Baker. The model studies should be discounted in favour of Baker's as they use a comparatively coarse grid (Schwiderski, 1980). The results of Melchior appear to

TABLE 7.3

OBSERVED GRAVIMETRIC FACTORS ( $\delta$ ) AND PHASES ( $\kappa$  IN DEGREES)

| Station<br>and<br>Instrument | $M_2$              |                    | $N_2$             |                   | $S_2$             |                    | $O_1$             |                    | $K_1$              |                    |
|------------------------------|--------------------|--------------------|-------------------|-------------------|-------------------|--------------------|-------------------|--------------------|--------------------|--------------------|
|                              | $\delta$           | $\kappa$           | $\delta$          | $\kappa$          | $\delta$          | $\kappa$           | $\delta$          | $\kappa$           | $\delta$           | $\kappa$           |
| Eskdalemuir                  | 1.139<br>[±0.003]  | ( 3.11)<br>(±0.15) | 1.119<br>[±0.016] | ( 4.36)<br>(±0.8) | 1.171<br>[±0.006] | ( 0.3)<br>(±0.3)   | 1.083<br>[±0.003] | (-0.5)<br>(±0.1)   | 1.098<br>[±0.002]  | (-0.6)<br>(±0.1)   |
| Redruth (15)                 | 1.414<br>[±0.001]  | (13.95)<br>(±0.05) | 1.282<br>[±0.005] | ( 17.3)<br>(±0.2) | 1.442<br>[±0.003] | ( 3.2)<br>(±0.1)   | 1.127<br>[±0.001] | (-0.44)<br>(±0.07) | 1.142<br>[±0.001]  | ( 0.96)<br>(±0.04) |
| Taunton (15)                 | 1.312<br>[±0.002]  | ( 6.13)<br>(±0.07) | 1.264<br>[±0.009] | ( 7.5)<br>(±0.4)  | 1.304<br>[±0.003] | (-0.05)<br>(±0.1)  | 1.304<br>[±0.002] | (-0.23)<br>(±0.09) | 1.138<br>[±0.002]  | ( 0.24)<br>(±0.08) |
| Newtown (15)                 | 1.246<br>[±0.002]  | ( 4.72)<br>(±0.08) | 1.182<br>[±0.008] | ( 6.2)<br>(±0.4)  | 1.252<br>[±0.003] | ( 0.6)<br>(±0.2)   | 1.138<br>[±0.005] | ( 0.5)<br>(±0.3)   | 1.148<br>[±0.004]  | ( 0.7)<br>(±0.2)   |
| Llanryst (13)                | 1.207<br>[±0.002]  | ( 1.99)<br>(±0.08) | 1.170<br>[±0.008] | ( 3.6)<br>(±0.4)  | 1.218<br>[±0.003] | (-0.7)<br>(±0.2)   | 1.143<br>[±0.004] | ( 0.2)<br>(±0.2)   | 1.157<br>[±0.003]  | ( 0.2)<br>(±0.1)   |
| Cambridge (721)              | 1.196<br>[±0.004]  | ( 3.99)<br>(±0.2)  | 1.136<br>[±0.02]  | ( 2.7)<br>(±1.0)  | 1.119<br>[±0.007] | (-0.5)<br>(±0.4)   | 1.119<br>[±0.009] | (-0.8)<br>(±0.4)   | 1.118<br>[±0.006]  | (-4.5)<br>(±0.3)   |
| London (15)                  | 1.186<br>[±0.002]  | ( 3.08)<br>(±0.08) | 1.159<br>[±0.008] | ( 3.3)<br>(±0.4)  | 1.196<br>[±0.005] | ( 0.9)<br>(±0.2)   | 1.140<br>[±0.002] | (-0.2)<br>(±0.1)   | 1.136<br>[±0.001]  | ( 0.41)<br>(±0.06) |
| Herstmon. (721)              | 1.132<br>[±0.0008] | ( 0.66)<br>(±0.04) | 1.142<br>[±0.004] | ( 0.4)<br>(±0.2)  | 1.156<br>[±0.002] | ( 1.8)<br>(±0.08)  | 1.152<br>[±0.002] | (-0.4)<br>(±0.1)   | 1.146<br>[±0.002]  | ( 0.09)<br>(±0.08) |
| Bidston (13)                 | 1.153<br>[±0.0008] | ( 0.68)<br>(±0.04) | 1.152<br>[±0.004] | ( 0.0)<br>(±0.2)  | 1.173<br>[±0.002] | ( 0.5)<br>(±0.08)  | 1.138<br>[±0.001] | ( 0.22)<br>(±0.08) | 1.149<br>[±0.001]  | ( 0.18)<br>(±0.05) |
| Bidston (15)                 | 1.147<br>[±0.0009] | ( 0.77)<br>(±0.04) | 1.140<br>[±0.005] | ( 0.7)<br>(±0.2)  | 1.165<br>[±0.002] | ( 0.86)<br>(±0.09) | 1.132<br>[±0.001] | ( 0.13)<br>(±0.06) | 1.144<br>[±0.0008] | ( 0.50)<br>(±0.04) |
| Bidston (721)                | 1.148<br>[±0.001]  | ( 0.68)<br>(±0.05) | 1.156<br>[±0.006] | ( 0.1)<br>(±0.3)  | 1.174<br>[±0.002] | ( 0.6)<br>(±0.1)   | 1.138<br>[±0.002] | (-0.4)<br>(±0.1)   | 1.149<br>[±0.002]  | (-0.17)<br>(±0.07) |

Errors for Eskdalemuir are r.m.s. values; other stations are taken from Baker (1980) and errors are standard errors



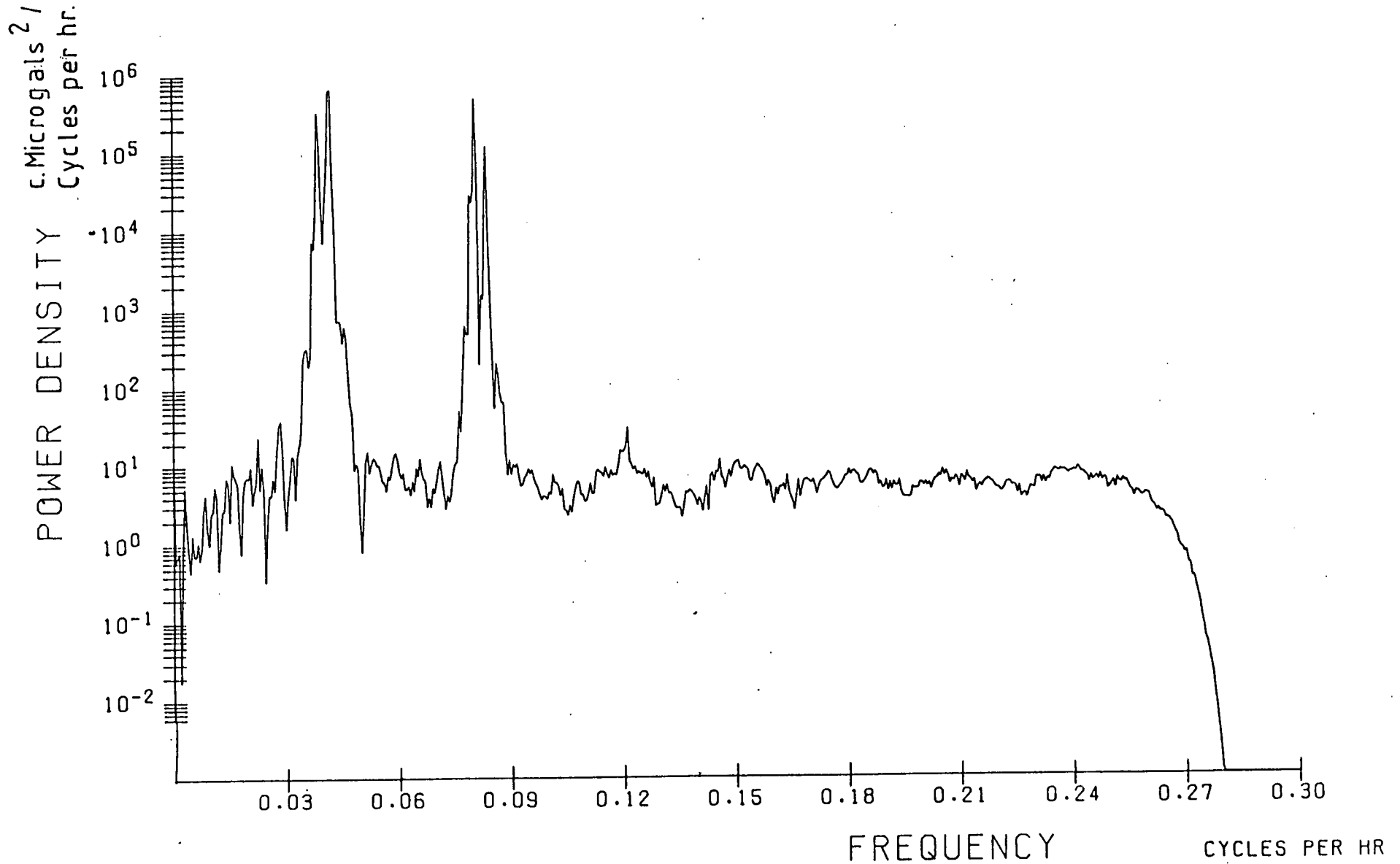


Figure 7.8 Power density spectrum of 85 days data at Eskdalemuir.

The uncertainty in the amplitude of the theoretical gravity body tide is in the order of +0.5% (Baker 1980, Alsop and Kuo 1964) and that of the phase lag negligible ( Zschau, 1978 from Baker, 1980). The overall residual standard deviation of the analysis is 1.38ugal as compared with 0.7ugal for Baker's measurements at Bidston. Tables 7.3 and 7.4 compare the parameters obtained from the Eskdalemuir analysis with those of Baker's installations. (Dr. Baker kindly provided the theoretical  $M_2$  load for the Eskdalemuir site). It can be seen that the observed load departs considerably from the model  $M_2$  load apparently outside the bounds of possible error. The problem of calculating the maximum load within given error limits is non linear. Two graphs (figures 7.9,7.10) illustrate the effect on load amplitude and phase separately with differing observation errors. It appears that to obtain the derived load vector would require an error of one percent in the amplitude and  $-1.5^\circ$  of phase. The uncertainty associated with the standard analysis is an order of magnitude less than this (see r.m.s. figures in Table 7.4).

Dr Agnew also supplied me with the results obtained by Farrell and also Melchior (both unpublished) studying data from the same instrument. Their results are shown in Table 7.5 , together with the results of model studies other than Baker. The model studies should be discounted in favour of Baker's as they use a comparatively coarse grid (Schwidorski, 1980 ). The results of Melchior appear to

TABLE 7.4

M<sub>2</sub> OBSERVATIONS AND THEORETICAL CALCULATIONS (AMPLITUDES IN μGALS AND GREENWICH PHASE LAGS IN DEGREES)

| Station       | Observed<br>(O)<br>Amp. Phase | Theoretical Body<br>(B)<br>Amp. Phase | Observed Load<br>(L)<br>Amp. Phase | Theoretical Load<br>(L)<br>Amp. Phase | Observed -<br>total theoretical<br>(R = L' - L)<br>Amp. Phase |
|---------------|-------------------------------|---------------------------------------|------------------------------------|---------------------------------------|---|
| Eskdalemuir   | 27.63 ( 3.30)                 | 28.24 ( 6.41)                         | 1.63 (253.07)                      | 2.26 (288.7)                          | 1.74 (325)  |
| Redruth       | 43.49 (-3.48)                 | 35.67 (10.47)                         | 12.35 (312.4)                      | 12.31 (312.0)                         | 0.10 ( 17)  |
| Taunton       | 39.01 ( 0.00)                 | 34.50 ( 6.13)                         | 5.98 (321.9)                       | 6.28 (322.2)                          | 0.30 (147)  |
| Newtown       | 34.68 ( 1.91)                 | 32.29 ( 6.63)                         | 3.64 (315.1)                       | 3.81 (316.3)                          | 0.19 (161)  |
| Llanrwst      | 32.68 ( 5.64)                 | 31.40 ( 7.63)                         | 1.70 (325.6)                       | 1.92 (317.0)                          | 0.35 ( 91)  |
| Cambridge     | 33.77 (-4.22)                 | 32.75 (-0.23)                         | 2.53 (291.5)                       | 2.44 (305.2)                          | 0.60 (217)  |
| London        | 34.53 (-2.81)                 | 33.78 ( 0.27)                         | 1.98 (290.8)                       | 1.88 (302.2)                          | 0.40 (221)  |
| Herstmonceux  | 33.88 (-1.33)                 | 34.72 (-0.67)                         | 0.93 (204.3)                       | 0.82 (170.6)                          | 0.52 (266)  |
| Bidston (13)  | 30.80 ( 5.46)                 | 30.99 ( 6.14)                         | 0.42 (248.4)                       | 0.64 (253.6)                          | 0.23 ( 83)  |
| Bidston (15)  | 30.65 ( 5.37)                 | 30.99 ( 6.14)                         | 0.54 (236.3)                       | 0.64 (253.6)                          | 0.20 (126)  |
| Bidston (721) | 30.67 ( 5.46)                 | 30.99 ( 6.14)                         | 0.49 (234.8)                       | 0.64 (253.6)                          | 0.24 (115)  |

| RESULTS FOR<br>ESKDALEMUIR         | M2 THEORY |        | M2 OBSERVED |         | M2 LOAD   |         | O1 THEORY |        | O1 OBSERVED |         | O1 LOAD   |         | Installed 10-09-79                 |
|------------------------------------|-----------|--------|-------------|---------|-----------|---------|-----------|--------|-------------|---------|-----------|---------|------------------------------------|
|                                    | GREENWICH | LOCAL  | GREENWICH   | LOCAL   | GREENWICH | LOCAL   | GREENWICH | LOCAL  | GREENWICH   | LOCAL   | GREENWICH | LOCAL   |                                    |
| Lyness                             |           | 28.235 |             | 27.6212 |           | 1.62    |           | 33.745 |             | 31.478  |           | 2.29    | 230 days                           |
|                                    |           | 0.00°  |             | -3.11°  |           | 113.77  |           | 0.00°  |             | -0.50   |           | 186.96° | 25-09-78<br>12-05-79               |
| Farrell                            |           |        |             |         |           | 2.16    |           |        |             |         |           | 1.8     | 118 days                           |
|                                    |           |        |             |         |           | 120°    |           |        |             |         |           | 178°    | 23-12-78<br>10-05-79               |
| Melchior                           |           |        |             | 27.5    |           | 3.71    |           |        |             | 31.45   |           | 7.48    | Same Data<br>Set as Farrell        |
|                                    |           |        |             | -7.49°  |           | -104.5° |           |        |             | -12.56° |           | -114°   | Melchior notes<br>a timing problem |
| Baker<br>(Model)                   |           | 28.235 |             |         |           | 2.26    | 2.26      |        |             |         |           |         | Fine mesh<br>ocean                 |
|                                    |           | 0.0°   |             |         |           | 288.7*  | 77.7°     |        |             |         |           |         | model with<br>refinements          |
| Ducarme<br>and Melchior<br>(Model) |           |        |             |         |           | 4.1     |           |        |             |         |           | 0.41    | Schwiderski                        |
|                                    |           |        |             |         |           | 62°     |           |        |             |         |           | 151°    | Ocean Model                        |
| Agnew<br>(Model)                   |           |        |             |         |           | 3.8     |           |        |             |         |           | 0.39    | "                                  |
|                                    |           |        |             |         |           | 57°     |           |        |             |         |           | 154°    |                                    |

\* Phase lags  
positive

Table (7.5) Comparison of results obtained by different workers analysing Eskdalemuir I.D.A. Data (Duncan C. Agnew, personal comm.) Upper figure is vector magnitude, lower is phase in degrees.

# Load variation with hypothetical error

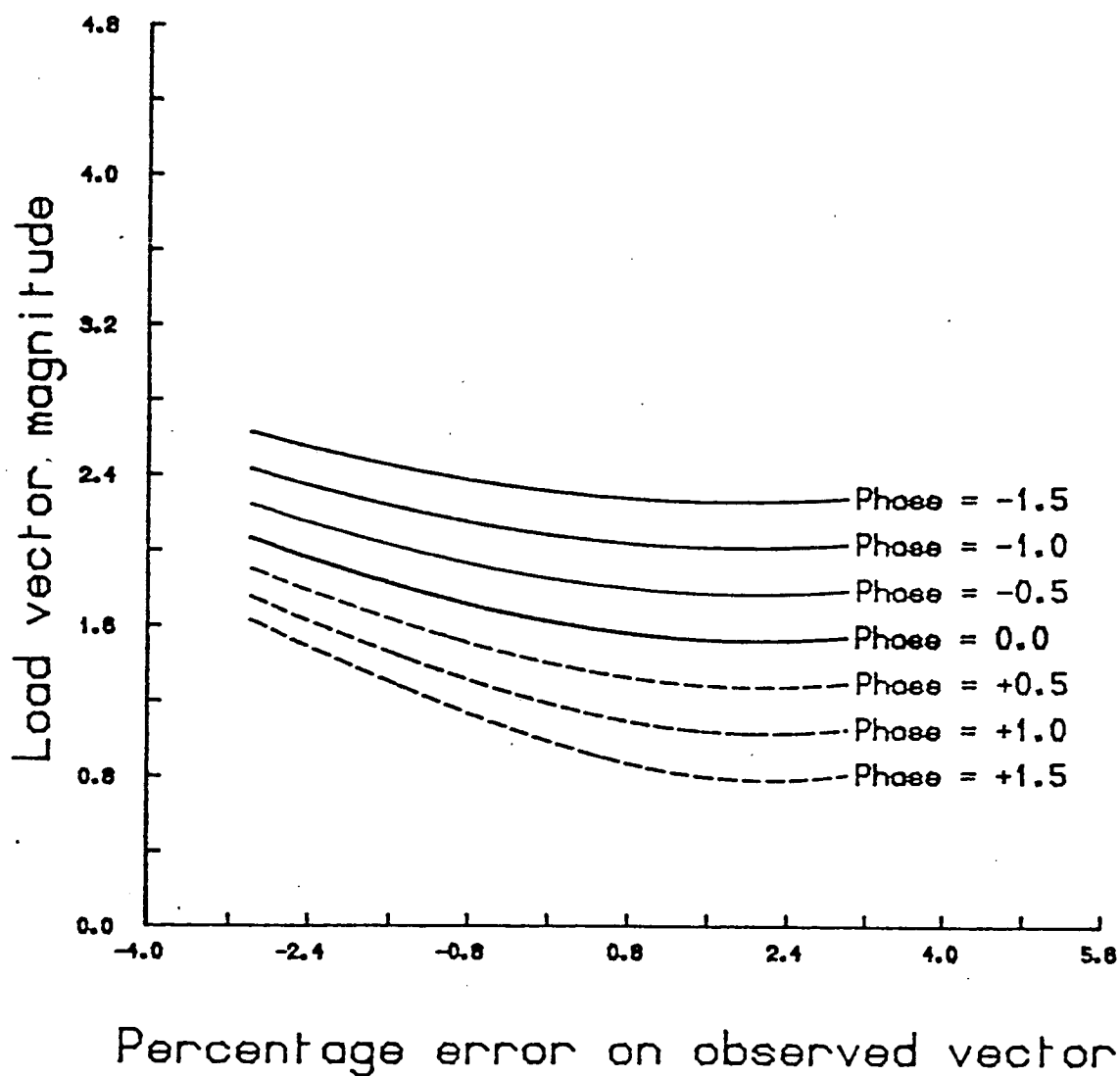


Figure 7.9 Possible load vector amplitude error..

Observed vector error ranges  $\pm 3\%$  magnitude,  $\pm 1.5^\circ$  phase.

# Load variation with hypothetical error

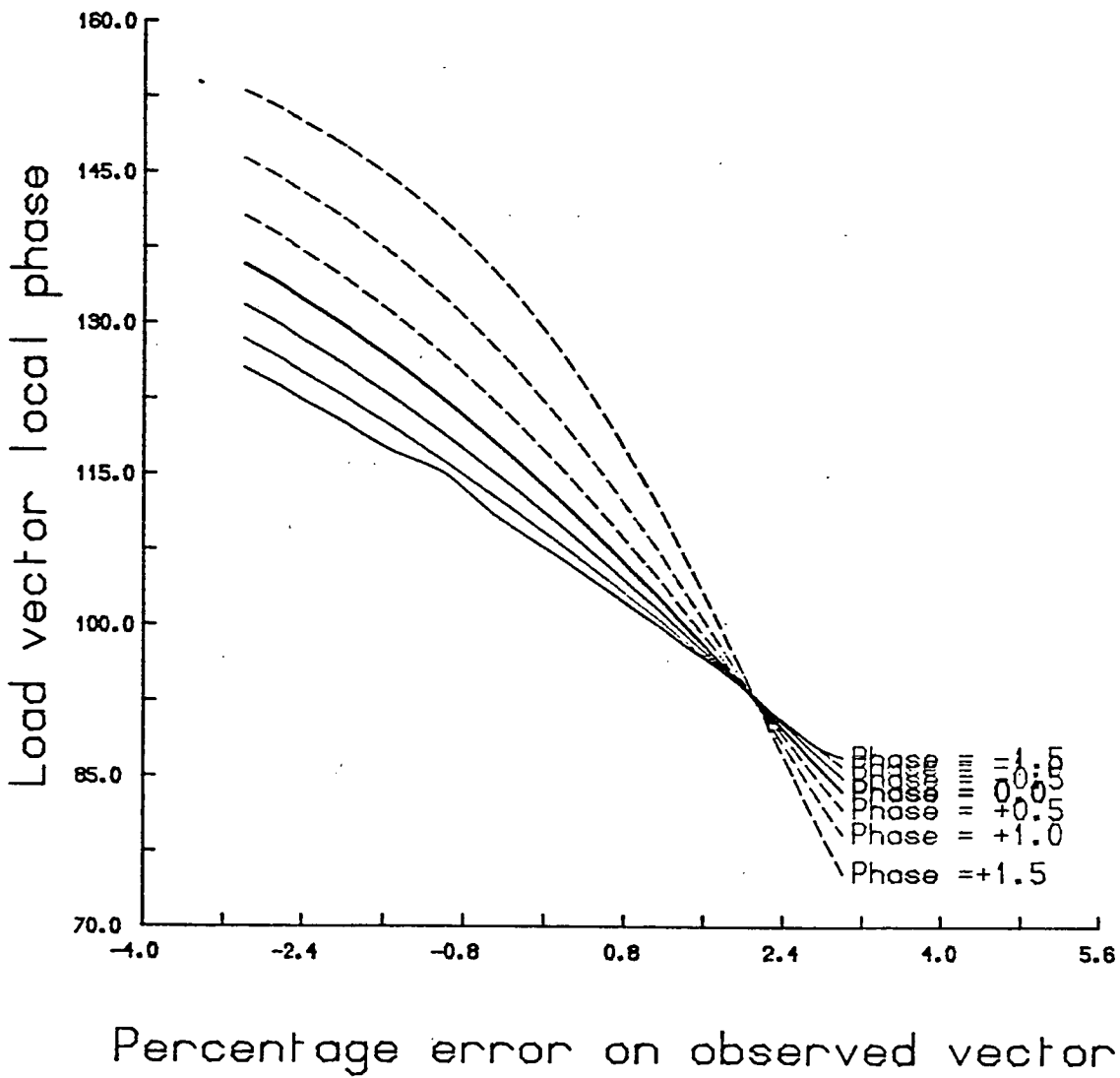


Figure 7.10 Possible error on local phase estimate of the load vector.  
Observed vector error ranges  $\pm 3\%$  magnitude,  $\pm 1.5^\circ$  phase.

be in error and Agnew notes that there is the possibility of a timing error. Agreement with Farrell is moderate but there is a significant discrepancy when compared to the  $M_2$  model of Baker which has been shown to be consistent elsewhere. Furthermore the  $O_1$  gravimetric factor of  $1.083 \pm 0.003$  is significantly lower than all other  $O_1$  values shown on Table 7.4 or any published values for western Europe (eg. Melchior, p.376).

One is forced to conclude that the Eskdalemuir instrument is currently operating with an error unacceptably high for the purposes of Earth tide registration. The probable error magnitudes involved are not sufficient to concern most users of this instrumentation; seismologists studying free oscillations of the Earth. Errors could be due to, off levelness, a build up of charge on the position sensor plates or thermal drift in the electronics. The large variation in derived tidal parameters obtained by different workers may be due to different analysis techniques ( the figures of Melchior are particularly perplexing, though he does note a timing problem) or an unstable instrument response rather than a simple systematic error.

The results of this analysis indicate that the I.D.A. determined gravimetric factor and phase lag are not suitable for use in tidal prediction programs. The analysis of the Scottish secular variation sites was carried out

using gravimetric factors and phases derived from Baker (1980).



## CHAPTER EIGHT

### SECULAR GRAVITY STUDIES IN SCOTLAND

#### 8.1 Introduction

Laboratory tests indicate that it may be possible to successfully evaluate gravity differences in the order of a few microgals. Field measurements do not generally attain this degree of precision but Hipkin (1978) describes a field measurement (using G-275) with a standard error of 0.018 gravity units. This link between Ordnance Survey fundamental bench marks at Edinburgh and Linlithgow was the pilot study for the establishment of a larger network of secular gravity sites in Scotland. This link was expanded to the stations shown in figure 8.1 which were all measured by the author in 1980 and 1981. In addition to these measurements more limited observations took place in 1977 and 1978. The observations were made under a strictly controlled regime of symmetry from year to year to eliminate random factors. The measuring technique is identical to that described in section 5.3; it makes use of well determined instrument response of G-275 and requires a large number of readings (c. 20) over a period of 80 minutes at a single site.

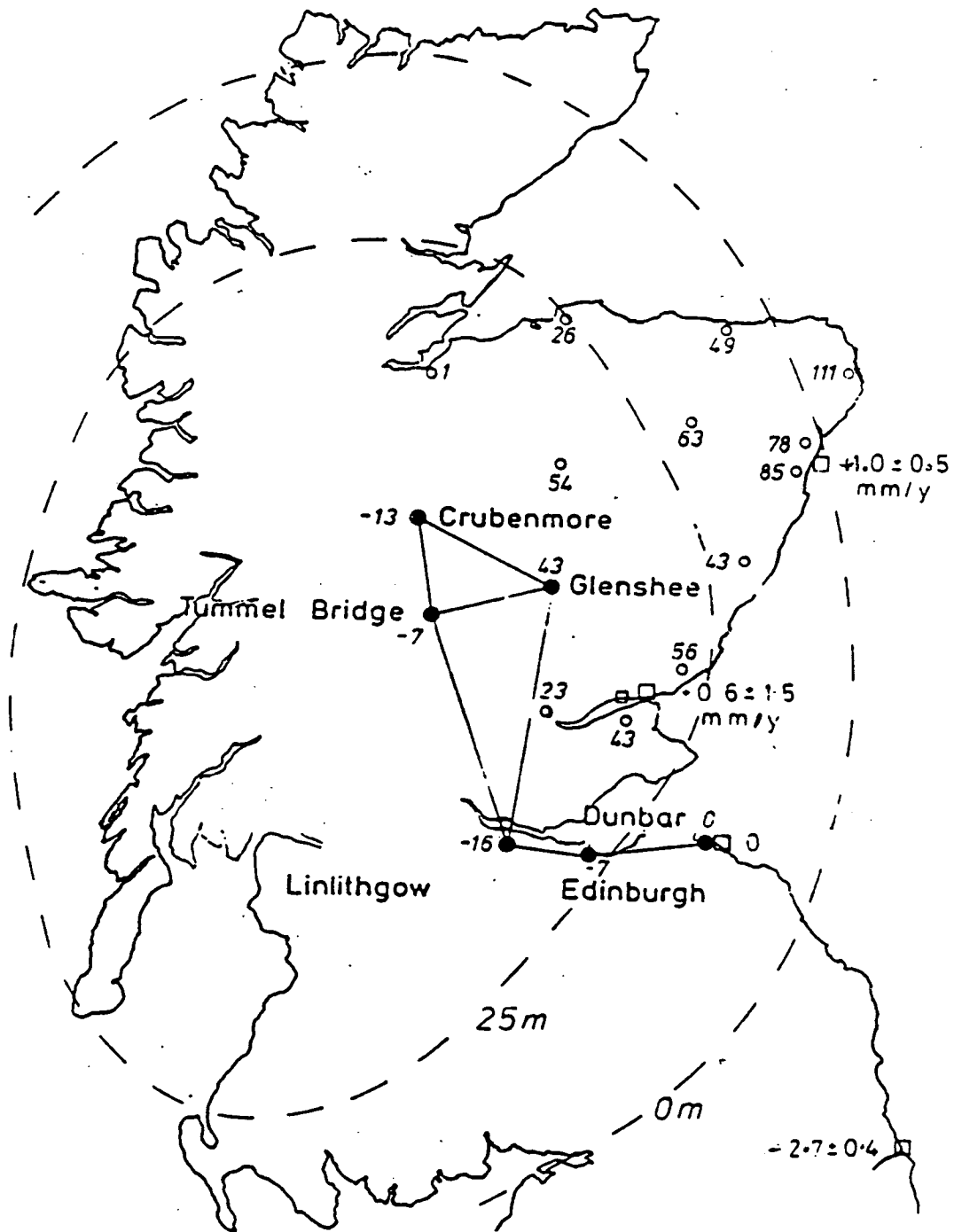


Figure 8.1 Scottish secular variation network

- Station locations
- Fundamental bench marks with uplift (mm.) between second and third geodetic levellings relative to Dunbar. Uplift since the last ice age derived from geomorphological studies. (Sissons, 1967).
- Tidal gauges (relative uplift rates from Rossiter, 1972)

## 8.2 Scotland as a Test Bed

All the stations are located on fundamental bench marks. These form part of the Ordnance Survey geodetic levelling network and provide uniquely stable and permanent monumentation of a very high quality (Figure 8.2) together with well determined positions. The primary constraint was that the stations should form a network with gravity differences lying almost within a single dial turn. Additionally stations are a reasonable driving distance from one another (maximum two and a half hours). All the stations are situated on low permeability metamorphic or igneous rocks to minimise the affects of ground water variations.

Secular gravity studies in Scandanavia suggest a cumultative gravity difference of 0.35 g.u. in five years (Kivinemi, 1974; Petterson, 1974). Mareographic evidence from the Gulf of Bothnia indicates contemporary rates of uplift as high as 10mm. per annum. This is at the centre of a rebounding depression resulting from the removal of the load of the last ice sheet. Geomorphological data (Sissons ,1976) presents a similar picture for the Holocene in Scotland as shown by the dashed contours in figure 8.1 Other studies; mareographic, archaeological and geodetic agree qualitatively that Northern Britain is rising relative to Southern Britain.

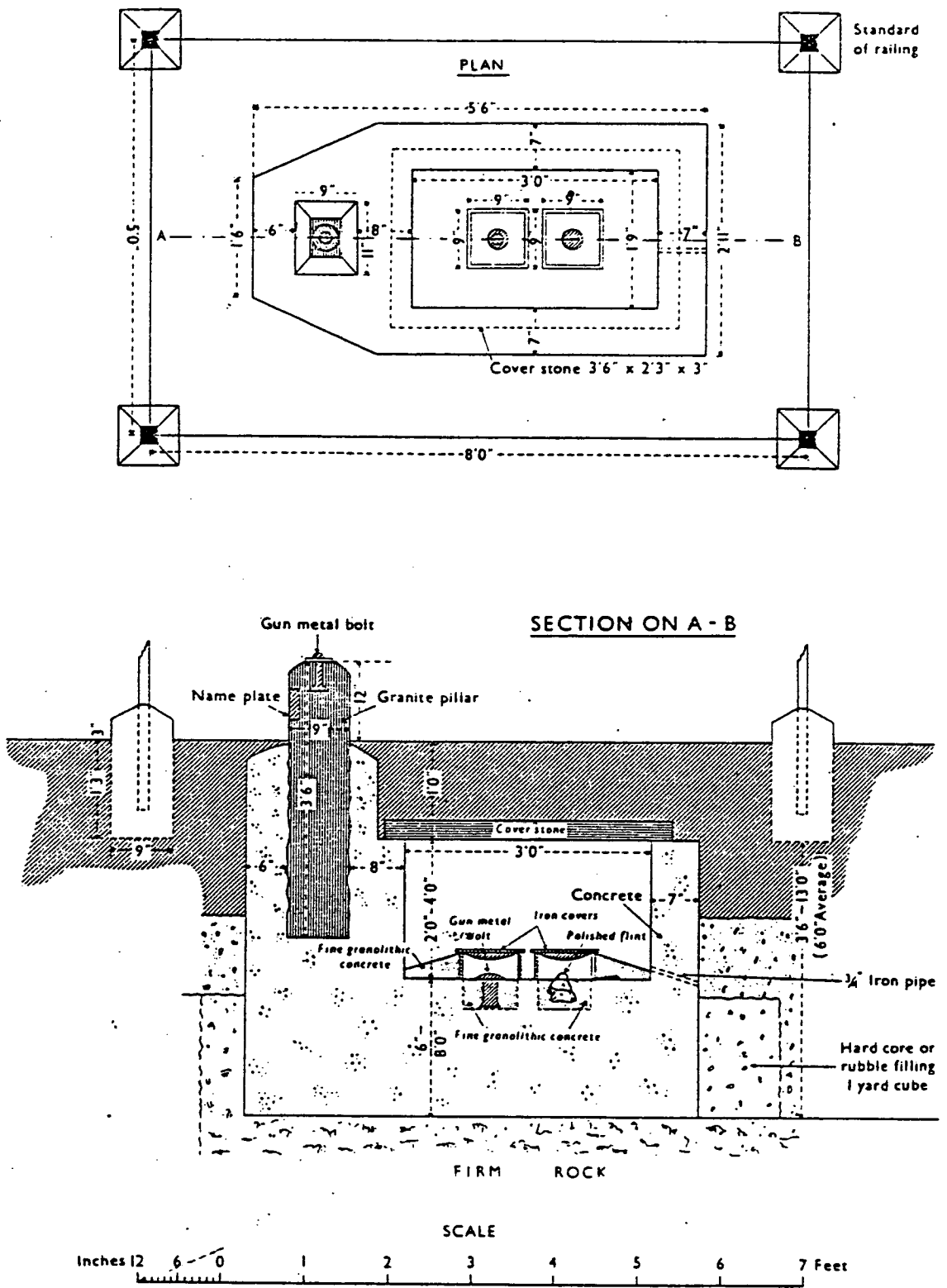


Figure 8.2 Fundamental Bench Mark

Rossiter (1972) has examined all the available tide guage records for Great Britain up to 1970. The observations are of extremely variable quality and continuity, the longest record dates back to 1830 (Sheerness) but even this has considerable gaps. Aberdeen and Dunbar are amongst the most consistent stations and Rossiter suggests an uplift in eastern Scotland of the order 0.5mm. per annum. This is compared to an observed subsidence of the order 1mm. per annum in southern England and along the French and Dutch coasts.

Three geodetic levellings of Great Britain have taken place. The first geodetic levelling of Great Britain was carried out during 1840 - 1860 (Jolly and Wolff, 1922). The datum for this survey , mean sea level at Liverpool derived from a ten day tide guage record is unfortunately inadequate for comparison with subsequent levellings. The second geodetic levelling took place between 1912 and 1921 in England and Wales (including Dunbar) but was not extended to the remainder of Scotland until the period 1936 - 1952. The Ordnance Survey established tidal observatories; Dunbar in 1913, Newlyn in 1915 and Felixstowe in 1917 to control the survey. (Rossiter comments that these Ordnance Survey maintained guages yeild the highest quality data in Europe .) The third geodetic levelling of England , Wales and Scotland was carried out between the years 1951 and 1959 using Newlyn

mean sea level as a datum as did the second levelling. Figure 8.3 is taken from Kelsey (1972) and presents the difference between third and second levellings. The probable error of each levelling is given as 1.8mm. km.for the second and  $1.2\text{mm.}/\sqrt{\text{km.}}$  for the third geodetic levellings. The observed uplift in Scotland exceeds the probable error and the values for the bench marks common to the gravity network are listed below.

|            |         |
|------------|---------|
| Dunbar E.  | 149 mm. |
| Edinburgh  | 142 mm. |
| Linlithgow | 133 mm. |
| Crubenmore | 192 mm. |
| Tummel B.  | 142 mm. |
| Glenshee   | 203 mm. |

These represent a rate of uplift between four and five millimetres per year for Scottish stations. Differential rates of uplift for the Grampians with respect to southern Scotland are in fact greater than this based on an examination of the exact acquisition dates.

Geodetic data would therefore seem to suggest rates of uplift of an order of magnitude greater than mareographic analysis. Thompson (1980) analyses the data from 29 tide guages evenly spaced around the British Isles, for the period 1960 - 1975 (here again record sections were not always complete). Thompson observes a latitudinal slope of

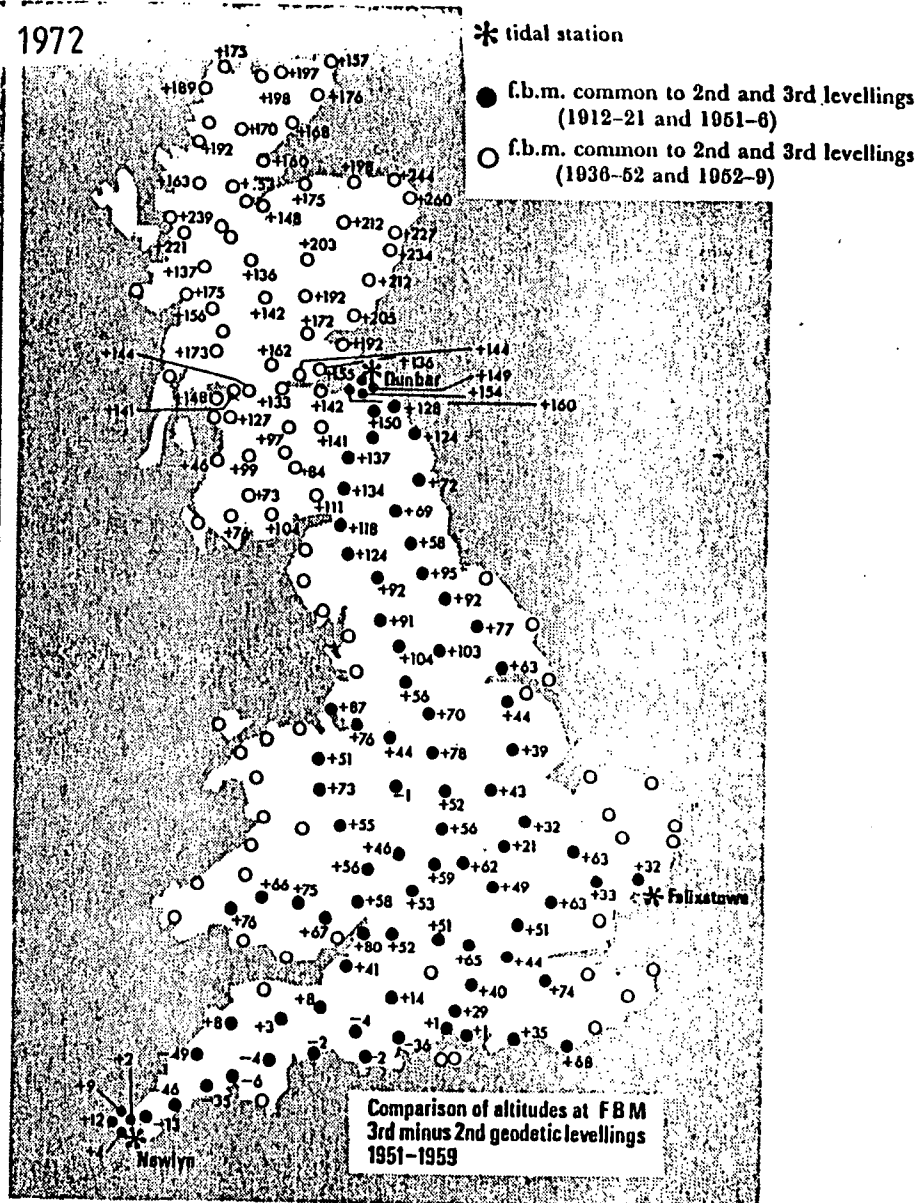
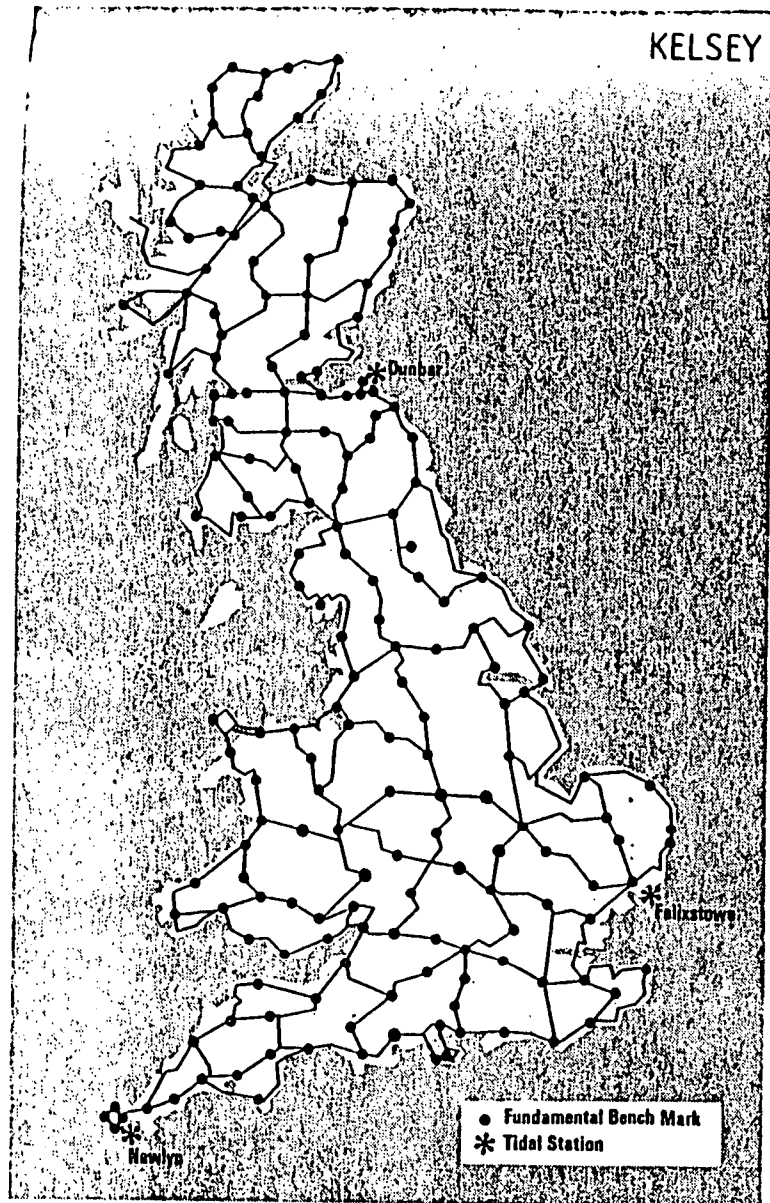


Figure 8.3 The third geodetic levelling comparison of altitudes at fundamental bench marks: third minus second geodetic levellings 1951-9 in mm.

5.3 ± 0.4 centimetres per degree on both the east and west coasts. This is difficult to explain oceanographically and for this reason suggests a systematic error in the third geodetic levelling. Such a systematic error would almost eliminate the supposed uplift of northern Britain and reduce all figures to less than the probable error.

Mareographic and geodetic observations are the only available sources for the derivation of modern uplift rates. This recent evidence suggests a maximum rate of uplift of five millimetres per year and probably much less than this figure. The Scottish network is therefore located in a tectonically stable area suitable for studying temporal gravity variations with the hypothesis of zero change. Archeological and geomorphological (river terraces, peat dating etc.) agree that Scotland has risen in the Holocene period but are also inconsistent quantitatively.

### 8.3 The Observations

Observations were made between the fundamental benchmarks shown in figure 8.1 over the period 1976 - 1981 as follows:

|      |             |
|------|-------------|
| 1976 | E-L         |
| 1977 | E-L         |
| 1978 | E-L,E-D,T-L |



1980 E-L,E-D,T-L,C-G,C-T,T-G,T-L,L-G

1981 E-L,E-D,T-L,C-G,C-T,T-G,T-L,L-G

E:Edinburgh, L:Linlithgow, D:Dunbar, C:Crubenmore,  
T:Tummel Bridge , G:Glenshee

Observations made prior to 1980 were carried out by levelling the gravity meter directly on the hemispherical surface of the bench mark. Subsequent observations were carried out using the tripod described in section 3.2. The use of the tripod as shown in plate 3.1 means that the height and orientation can be recovered with extreme accuracy from year to year. Furthermore, when in transport, the meter was suspended using elasticated cords during the 1980 and 1981 measurement sequences. During the 1976 - 1978 measurement sequences the meter sat on one observer's lap in the front passenger seat of the vehicle (a Renault 4 )whilst in 1980 - 1981 the meter was suspended as close to the vehicle's centre of gravity as possible.

Meter readings were taken alternately by one of two observers whilst the second noted the air temperature and pressure to 0.1K and 0.1mbar respectively. Twenty to twenty four readings were taken at each site over a period of approximately eighty minutes with an average reading interval of four minutes. The reading procedure is as described in section 3.2. After a sequence of readings

on one fundamental bench mark, the apparatus was carefully loaded into the car and driven to the second site where the reading process was repeated. The first site was then revisited followed by the second (ie. ABAB ). Thus each day's observations is a treble link consisting of four 80 minute reading sequences and three driving sequences. Each connection can be measured in a long day (10 - 14 hours fieldwork). All the measurements to be undertaken were made in June or July when meteorological conditions are fairly stable and the long days permit all the observations to be undertaken with natural light. This is particularly necessary with the use of coincident image spirit levels which were used in 1980 and 1981. The difference between the La Coste and ancillary platform levels was noted in 1981.

The meter proved trouble free during the fieldwork period and the batteries maintained their capacity despite the unusually heavy demands placed upon them. A sun shade was acquired for the 1981 fieldwork season, as direct sunlight had proved to be the major problem during the 1980 campaign. Sunlight shining directly on the level bubbles caused them to drift and some form of shading is necessary. The tripod was found to act as a stable and secure measuring base.

#### 8.4 Data Reduction and Results

The data reduction procedures have already been thoroughly outlined in section 5.3. All data collected on Scottish fundamental bench marks, including that collected between 1976 and 1978 was reduced using spline fitting (program NSPL) and ancillary adjustment routines. Earth tide reductions were made using the program PBAS (section 5.3) using tidal parameters extrapolated from Baker (1980) as shown in Table 8.1.

The data from each day was initially adjusted individually to examine the data quality and conformability to the classic G-275 drift pattern. Figure 8.4 illustrates the observations of the Edinburgh Linlithgow link between the year 1976 and 1982 and provide a typical example of data quality. ( The spline program parameters are shown in the inset box .) The root mean square error of these daily spline fits with two knots does not exceed 0.05 g.u. and is generally in the range 0.015 g.u. to 0.030g.u.. The daily drift curves for the 1981 survey are remarkably consistent, whereas those for 1980 exhibit some inconsistencies attributable to the inadequate shading mentioned above. Daily spline fits were found to provide robust solutions for all years. Increasing the number of nodes did not significantly alter the spline solution or reduce the root mean square error. Table 8.2 illustrates the solution variation with an increasing number of nodes for the Linlithgow - Glenshee link. Because of this , the simplest solution sets generated using two unconstrained nodes

| Station | Lat.<br>(°) | Long.<br>(°) | Height<br>(m) | M <sub>2</sub><br>Theory<br>(μ gals) | Load<br>Amp.<br>(μ gals) | Vector<br>G. Phase<br>(°) | Local Phase<br>(°) | M <sub>2</sub><br>Observed<br>(μ gals) | δ <sub>M<sub>2</sub></sub> | κ <sub>M<sub>2</sub></sub><br>(°) |
|---------|-------------|--------------|---------------|--------------------------------------|--------------------------|---------------------------|--------------------|--|----------------------------|-----------------------------------|
| EDN     | 55.953      | 3.152        | 60.05         | 27.396                               | 2.8                      | 285                       | 81                 | 27.834                                 | 1.179                      | 5.70                              |
| CRU     | 56.984      | 4.216        | 318.84        | 25.953                               | 2.2                      | 317                       | 51                 | 27.331                                 | 1.221                      | 3.59                              |
| LIN     | 55.956      | 3.656        | 101.55        | 27.393                               | 2.6                      | 295                       | 72                 | 28.196                                 | 1.194                      | 5.03                              |
| GLE     | 56.729      | 3.405        | 296.47        | 26.308                               | 2.1                      | 298                       | 69                 | 27.061                                 | 1.193                      | 4.15                              |
| TUM     | 56.708      | 4.020        | 149.60        | 26.337                               | 2.3                      | 310                       | 58                 | 27.556                                 | 1.214                      | 4.05                              |
| DUN     | 55.998      | 2.499        | 5.94          | 27.332                               | 2.5                      | 273                       | 92                 | 27.245                                 | 1.156                      | 5.26                              |

Table ( 8.1 ). Position of Scottish secular variation sites and M<sub>2</sub> tidal parameters inferred from Baker (1980)

# SECULAR VARIATION - SVB EL76

NO OF NODES - 2  
 RMS VALUE - 2.56  
 STATIONS :

SPLINEX PARAMETERS  
 J: 80  
 N: -4  
 NZERO: 1  
 PARTS: 4  
 CONS: FALSE

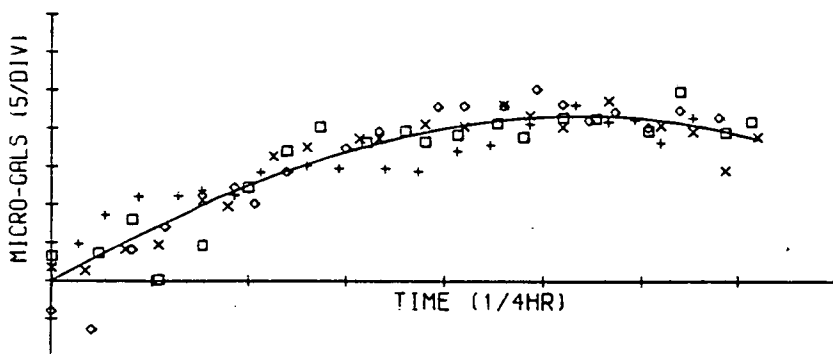


Figure 8.4(a) Edinburgh - Linlithgow link, 1976

# SECULAR VARIATION - SVB EL77

NO OF NODES - 2  
 RMS VALUE - 2.08  
 STATIONS :

SPLINEX PARAMETERS  
 J: 79  
 N: -4  
 NZERO: 1  
 PARTS: 4  
 CONS: FALSE

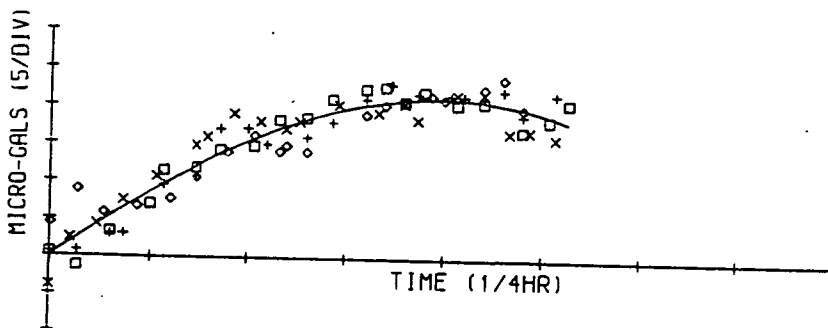
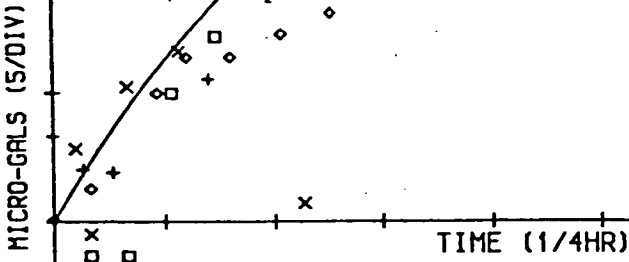


Figure 8.4(b) Edinburgh - Linlithgow link, 1977

SVB\_EL78

NO OF NODES = 2  
 RMS VALUE = 3.06  
 STATIONS :

SPLINE PARAMETERS  
 J: 80  
 K: -4  
 KZERO: 1  
 PARTS: 4  
 CONS: FALSE



SECULAR VARIATION - SVB EL80

NO OF NODES = 2  
 RMS VALUE = 1.72  
 STATIONS :

SPLINE PARAMETERS  
 J: 80  
 K: -4  
 KZERO: 1  
 PARTS: 4  
 CONS: FALSE

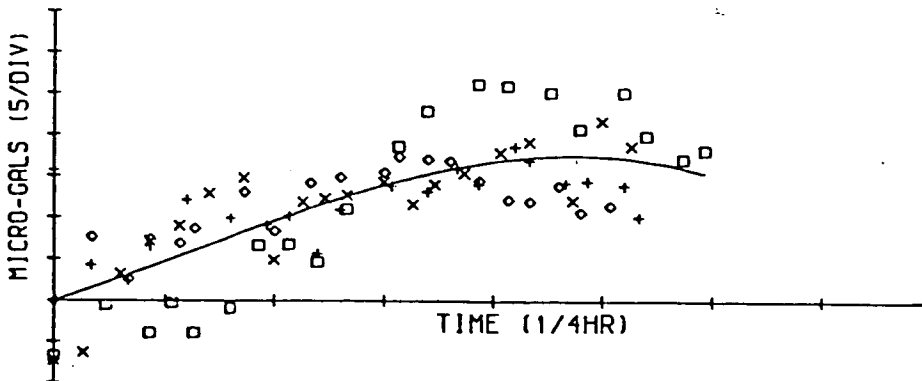


Figure 8.4(d) Edinburgh - Linlithgow link, 1980

SECULAR VARIATION - SVB EL81

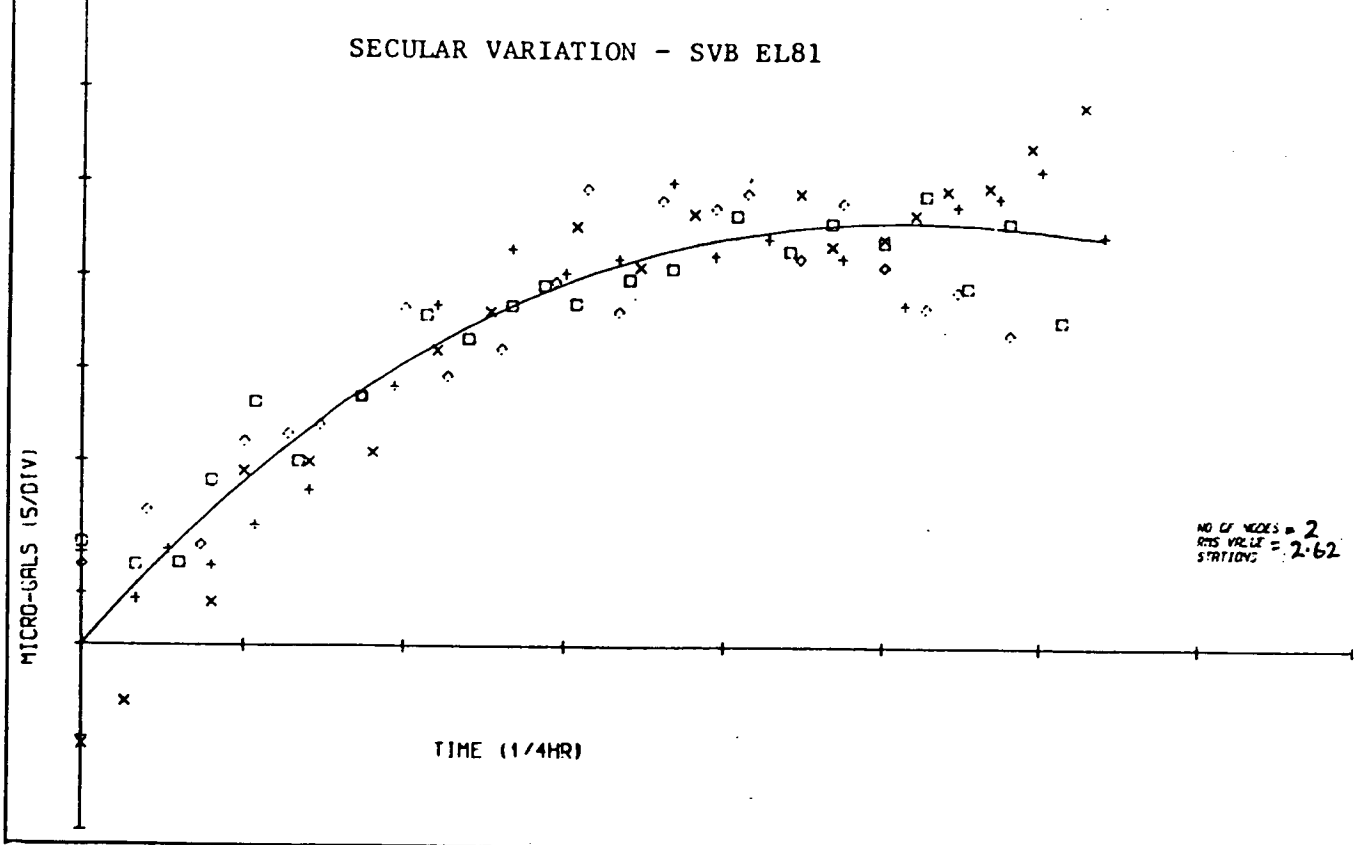


Figure 8.4(e) Edinburgh - Linlithgow link, 1981

Table 8.2

Effect of increasing number of nodes  
(Spline solution with 'superimposed' data sets)

| Number of<br>Nodes | Linlithgow-Glenshee 1980     |       | Linlithgow-Glenshee 1981     |       |
|--------------------|------------------------------|-------|------------------------------|-------|
|                    | Gravity Difference<br>(g.u.) | rmse  | Gravity Difference<br>(g.u.) | rmse  |
| 2                  | 49.071                       | 0.076 | 49.205                       | 0.071 |
| 3                  | 49.071                       | 0.076 | 49.205                       | 0.071 |
| 4                  | 49.070                       | 0.076 | 49.205                       | 0.070 |
| 5                  | 49.071                       | 0.075 | 49.205                       | 0.070 |
| 6                  | 49.070                       | 0.075 | 49.205                       | 0.070 |
| 7                  | 49.070                       | 0.075 | 49.205                       | 0.070 |
| 8                  | 49.070                       | 0.075 | 49.205                       | 0.070 |
| 9                  | 49.070                       | 0.075 | 49.206                       | 0.070 |
| 10                 | 49.071                       | 0.075 | 49.206                       | 0.070 |
| 11                 | 49.071                       | 0.074 | 49.205                       | 0.070 |
| 12                 | 49.071                       | 0.074 | 49.205                       | 0.069 |



were used throughout. This avoided the possibility of overfitting the data.

All the data from one year's field measurements were adjusted by a common drift function for all 80 minute measurement sequences solution in a least squares sense; the a priori assumption being that each observation sequence measured at a fundamental bench mark would conform to a similar drift response (as observed in the laboratory). Figures 8.5 , 8.6 and 8.7 illustrate the drift curves so obtained for the years 1978,1980 and 1981 respectively. Each observation sequence is represented by a different symbol. Thus if we consider the 1981 diagram of figure 8.7, 58 different measuring sequences of 80 to 90 readings are shown (a total of 598 readings). The low root mean square error and observational consistency demonstrate the validity of the model assumption.

Such a universal adjustment is independent of the site observation sequence and network. A simple weighted least squares linear fit was applied to each day's observations (weights equal to the reciprocal root mean square error of the spline fit). The final solution after a daily linear fit is shown in Table 8.3. It can be seen that the observed annual gravity change is quite variable, attaining a maximum of 0.24 g.u. on the Tummel Bridge - Glenshee link. A histogram of the gravity change between consecutive years is shown in figure 8.8. This distribution with twelve

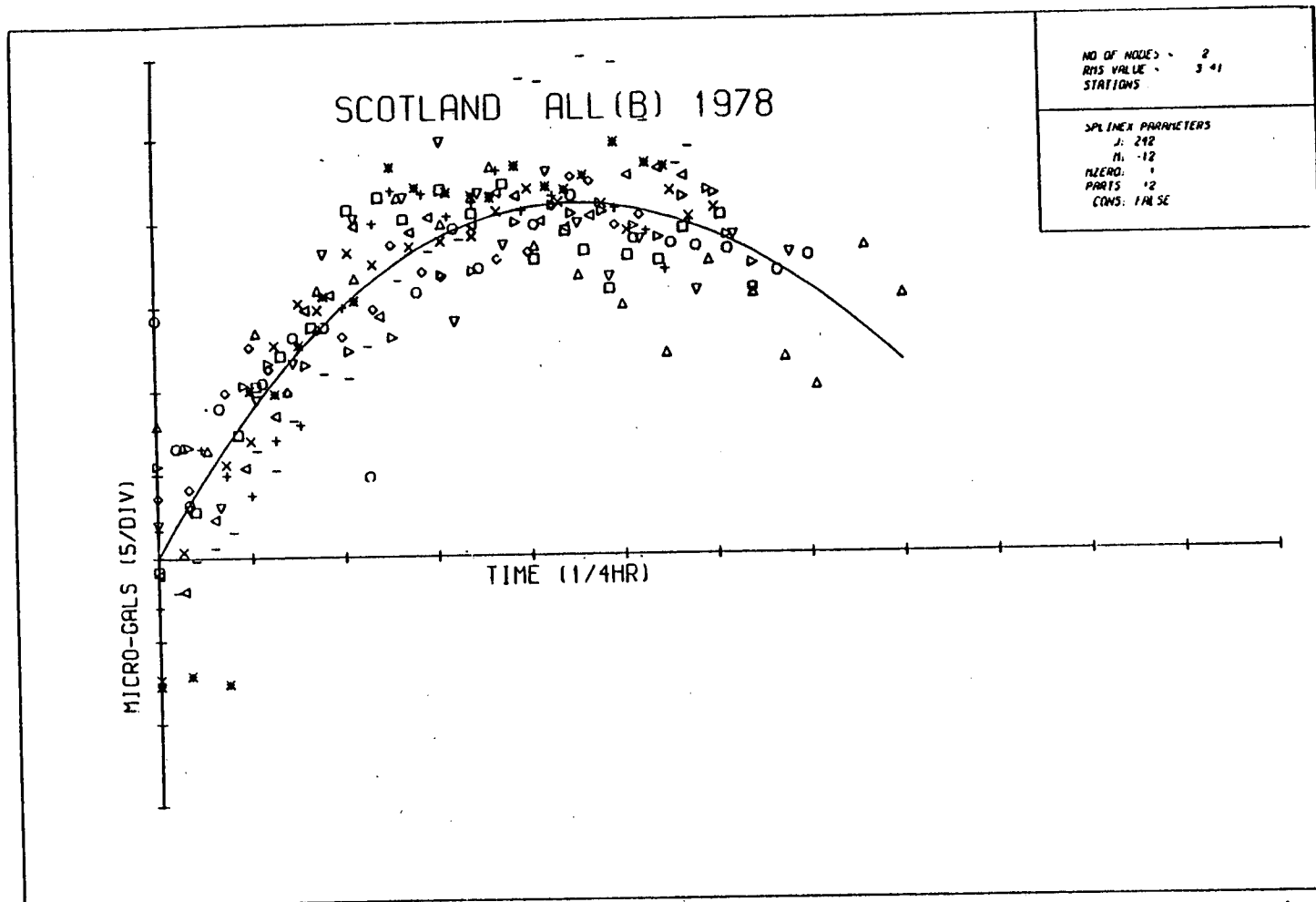


Figure 8.5 Complete 1978 data set. Station drift curves superimposed.  
 242 observations, 12 data sequences 4 x 3 days readings

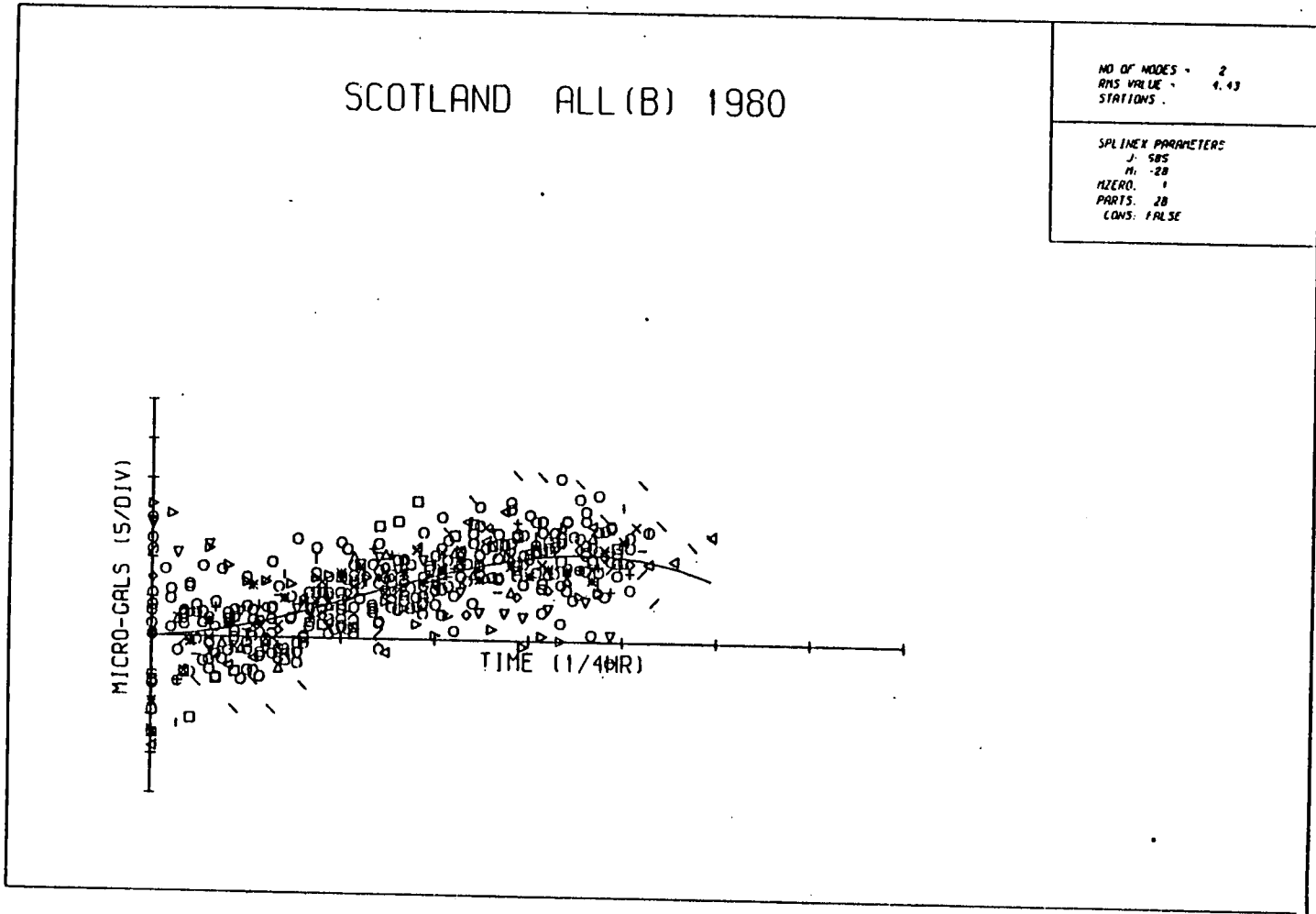


Figure 8.6 Complete 1980 data set. Station drift curves superimposed.

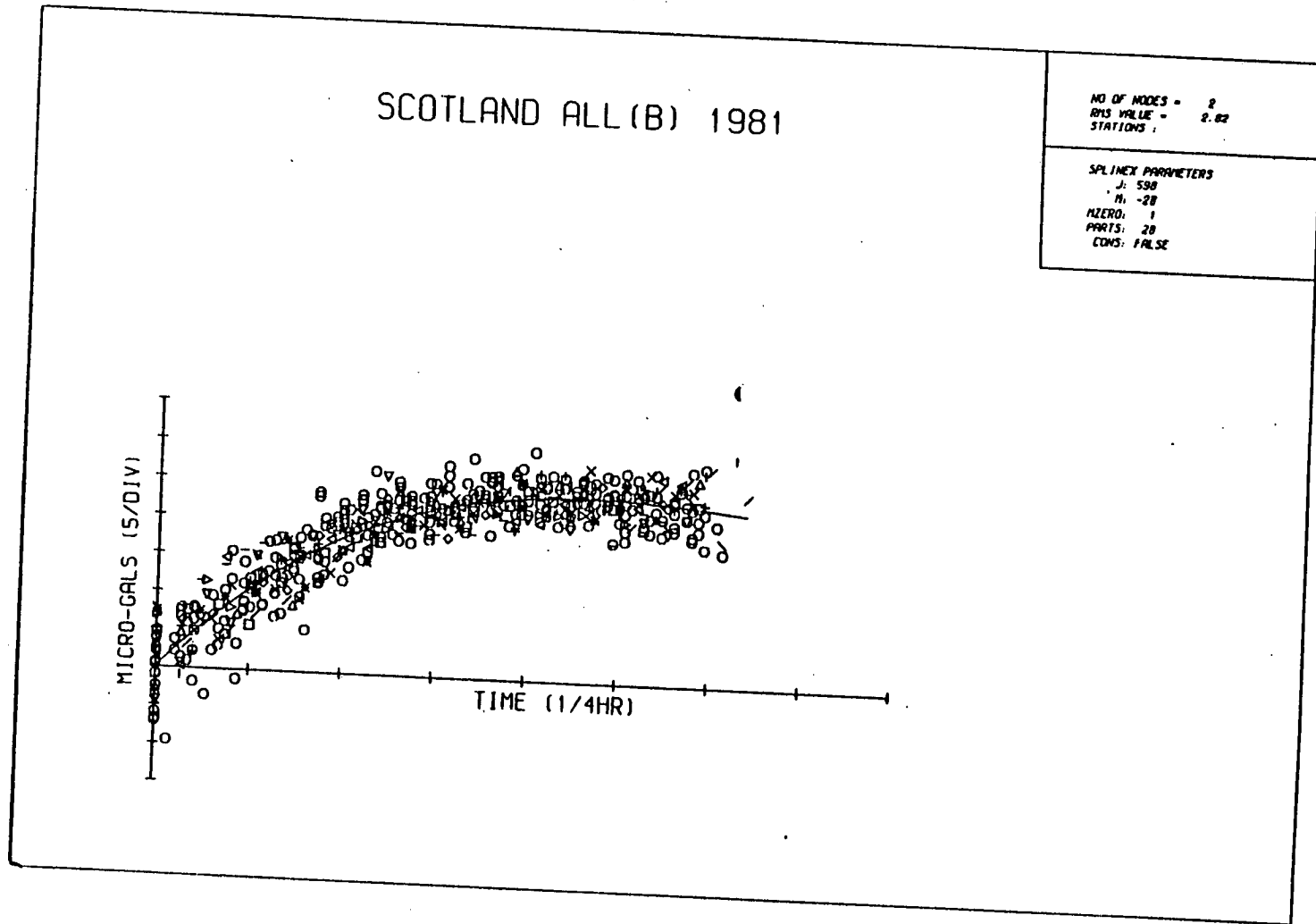


Figure 8.7 Complete 1981 data set. Station drift curves superimposed.

TABLE 8.3

Scottish Secular Variation Network - Results

| Link                          | Year | Gravity<br>diff.<br>(g.u.) | rmse<br>(WFIT only) | rmse<br>(NSPL only) | $(\text{rmse}_w^2 + \text{rmse}_N^2)^{1/2}$ |
|-------------------------------|------|----------------------------|---------------------|---------------------|---|
| Crubenmore -<br>Glenshee      | 1980 | 62.295                     | 0.044               | 0.081               | 0.092                                       |
|                               | 1981 | 62.316                     | 0.040               | 0.042               | 0.058                                       |
| Crubenmore -<br>Tummel Bridge | 1978 | 44.557                     | 0.010               | 0.047               | 0.048                                       |
|                               | 1980 | 44.507                     | 0.014               | 0.079               | 0.080                                       |
|                               | 1981 | 44.439                     | 0.026               | 0.053               | 0.059                                       |
| Edinburgh -<br>Dunbar         | 1980 | -24.727                    | 0.017               | 0.058               | 0.060                                       |
|                               | 1981 | -24.677                    | 0.037               | 0.057               | 0.068                                       |
| Edinburgh -<br>Linlithgow     | 1976 | - 5.534                    | 0.014               | 0.046               | 0.048                                       |
|                               | 1977 | - 5.531                    | 0.011               | 0.043               | 0.044                                       |
|                               | 1978 | - 5.563                    | 0.026               | 0.072               | 0.076                                       |
|                               | 1980 | - 5.439                    | 0.005               | 0.090               | 0.090                                       |
|                               | 1981 | - 5.628                    | 0.009               | 0.052               | 0.053                                       |
| Linlithgow -<br>Glenshee      | 1980 | 49.066                     | 0.003               | 0.074               | 0.074                                       |
|                               | 1981 | 49.184                     | 0.042               | 0.066               | 0.078                                       |
| Tummel Bridge -<br>Glenshee   | 1980 | 17.654                     | 0.011               | 0.081               | 0.082                                       |
|                               | 1981 | 17.895                     | 0.011               | 0.065               | 0.066                                       |
| Tummel Bridge -<br>Linlithgow | 1978 | -31.291                    | 0.051               | 0.081               | 0.096                                       |
|                               | 1980 | -31.413                    | 0.006               | 0.069               | 0.069                                       |
|                               | 1981 | -31.368                    | 0.009               | 0.055               | 0.056                                       |

rmse - root mean square error

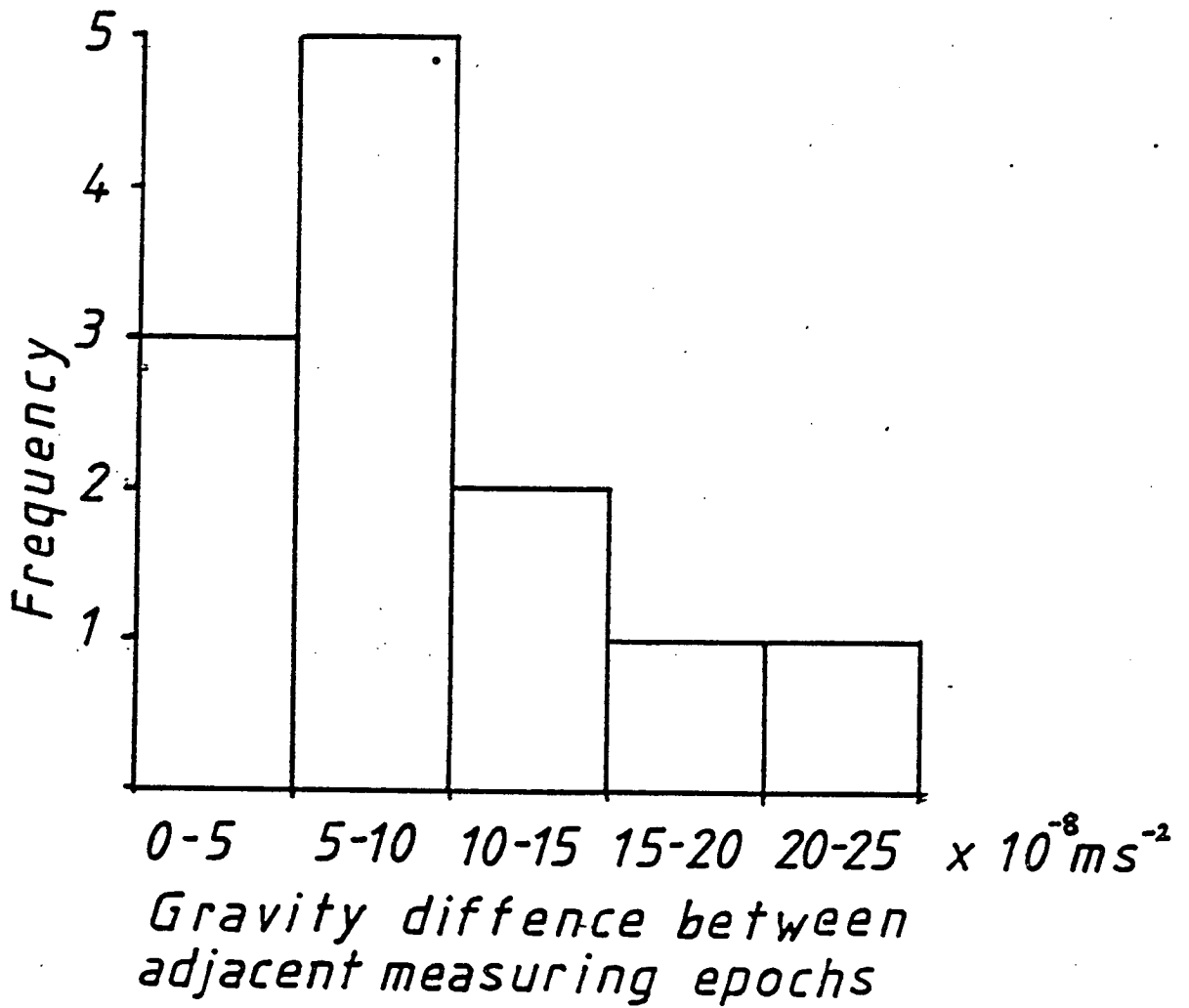


Figure 8.8 Histogram of residual frequency.

members possess a mean of 0.081 g.u. with a standard deviation of 0.073 g.u.. The last column of Table 8.3 is an estimate of the root mean square error for each individual link. This is obtained by taking the square root of the mean square error on the site drift function plus the weighted linear fit.

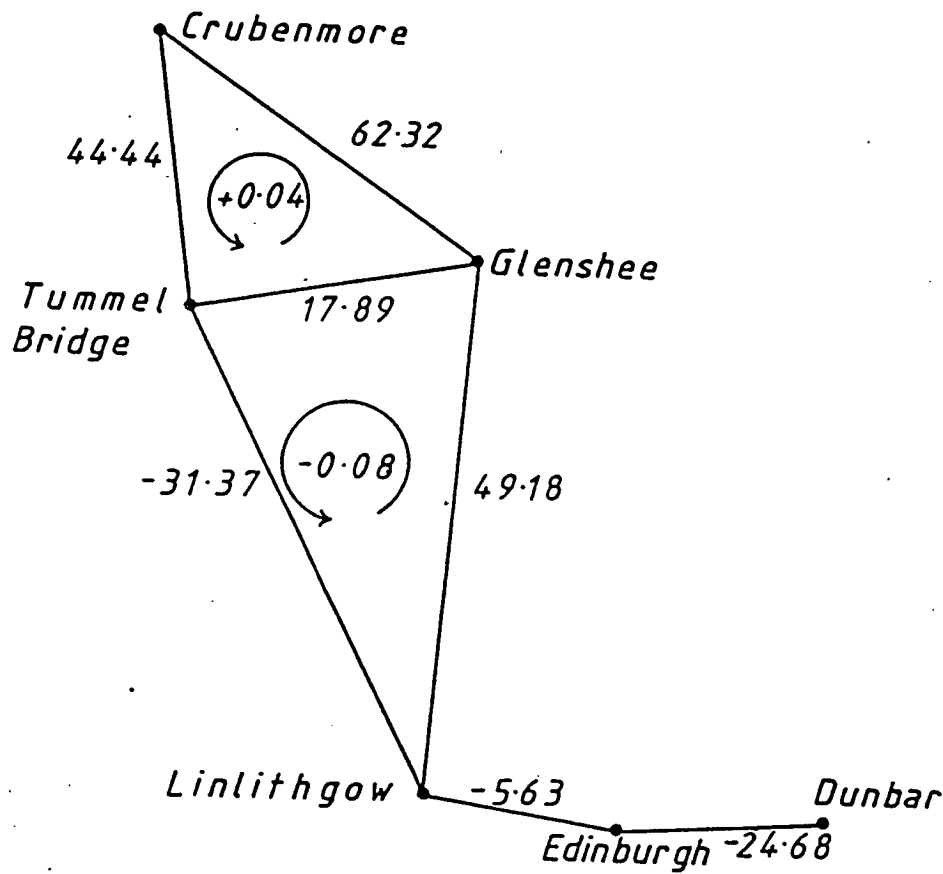
Five of the sites chosen form a simple network of two triangles with a common side. This simple network was completely measured during the 1980 and 1981 fieldwork seasons only. The misclosures are shown diagrammatically in figure 8.9. The largest observed gravity change of 0.24g.u. (more than double the estimated r.m.s. error of 0.105g.u. , ie.  $0.082^2 + 0.066^2$ ) is observed on the network's common link, Tummel Bridge - Glenshee.

### 8.5 Conclusions

In conclusion the Scottish gravity secular variation net has attained levels of precision comparable to but not better than conventional high precision surveys. But it has proved successful in linking distant stations precisely without a dense network. It would be particularly interesting to apply this method to the much observed Fennoscandia (figure 2.3) secular variation profile where stations are similarly separated by large distances. The time involved in measuring the network in this fashion is

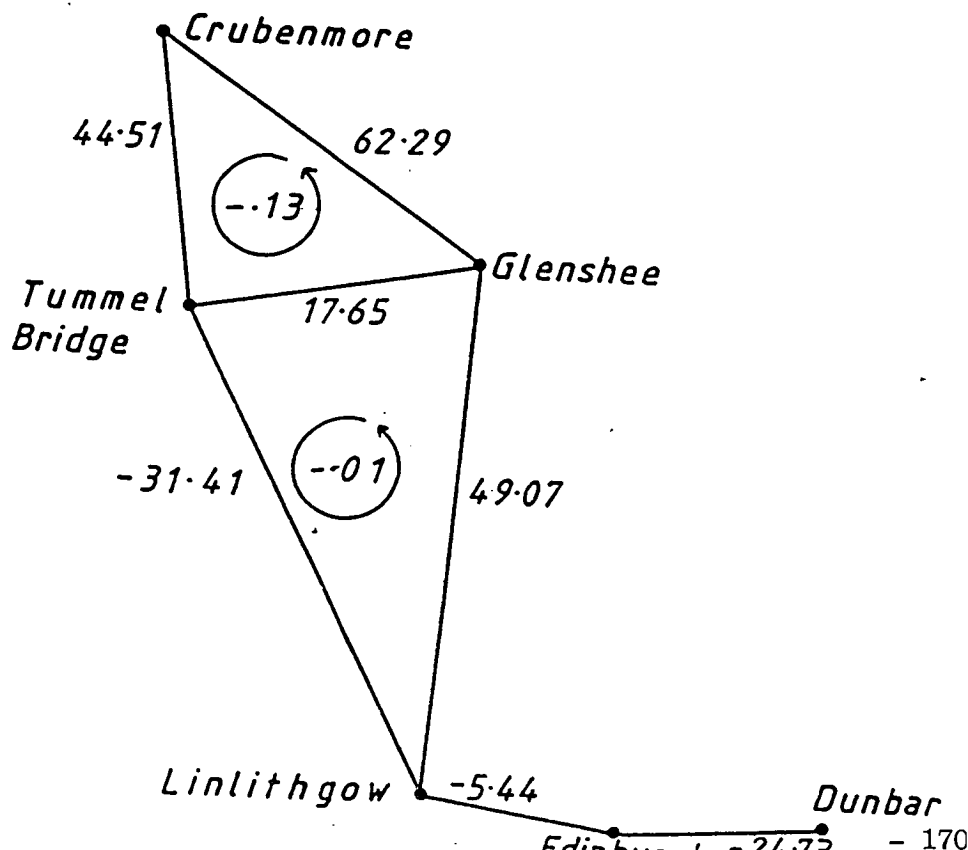
Scottish High Precision Gravity Net

1981



Scottish High Precision Gravity Net

1980





greater than conventional surveying involving forward looping or a double or treble ladder sequence. One important link (Tummel Bridge) unfortunately appears to be less accurate than the others reducing the precision of the network and increasing the network misclosures. Since this is the only common link it would be invalid to adjust it without an independent reason.

The technique of fitting a characteristic drift curve to field data has proved robust (as evidenced in figures 8.5, 8.6, and 8.7). This indicates success in overcoming time dependent environmental and time dependent systematic effects. The failure to improve the accuracy of the final solution to the level generally attained at individual sites suggest inter-site effects such as irregular transport drift (see section 5.3, Table 5.1). This could be controlled by increasing the density of the network, or reducing the areal extent of the network, hence shortening the distance between stations. But this would lose the advantage that sites are currently almost within a dial turn range.

## CHAPTER NINE

### GRAVITY MEASUREMENTS IN EAST CENTRAL GREECE

#### 9.1 Introduction

A local (c.80km. x 20km.) microgravimetric network was established in East Central Greece using two gravimeters G-275 (Edinburgh University) and G496 (Athens University) in 1981. A total of 69 stations were established with an approximate station spacing of two kilometres. This study is incorporated in a regional remeasurement of the Greek National gravity base network undertaken by members of the Seismological Laboratory of the University of Athens. The network is located in an area of potential seismic hazard and will be remeasured on an annual basis

A series of major shocks occurred in the Gulf of Corinth during February and March, 1981 ( $M_S$  6.7, 6.4, 6.4, U.S.G.S.). These shocks were followed by increased seismic activity in the area North of Thibes (max  $M_S$  4.5, Athens University). Seismic stations were immediately installed in the area using Sprengnether drum recording instruments which were withdrawn with the introduction of a local telemetered network. (VOLOSNET, installed and maintained by members of the Global Seismology Unit, Institute of Geological Sciences, using Willmore Mark III seismometers and 'Geostore' analogue tape-recorders).

A map of the principle morphological trends in the Hellenides is shown in figure 9.1. The particular area that is of interest gravimetrically is the coastal strip west of the island of Evia centred on the Atalanti Fault. It is firstly necessary to consider the tectonic background of the region.

## 9.2 Greek Tectonics

Greece and Turkey are the most seismically active counties in Europe (Karnik,1969), the annual earthquake energy release in Greece accounting for two per cent of the world's total and equivalent to a single event of magnitude 7.2. The most probable annual mode is  $M_s = 6.4 \pm 0.1$  with an upper bound of  $8.7 \pm 0.6$  for surface wave magnitude (Makropoulos 1979, Galanopoulos 1960, 1961; Richter 1958). Because of this, the area has been the subject of much study including a UNESCO multidisciplinary group during the period 1972-1976. Figure 9.2 illustrates the spatial distribution of all Greek earthquakes compiled by Makropoulos and Burton (1981) on the basis of UNESCO and other data.

Examination of this figure in conjunction with figure 9.3 illustrates the main tectonic structures of the region. The Mediterranean ridge is an irregular feature stretching from the Ionian Sea to Cyprus but is not thought to be a

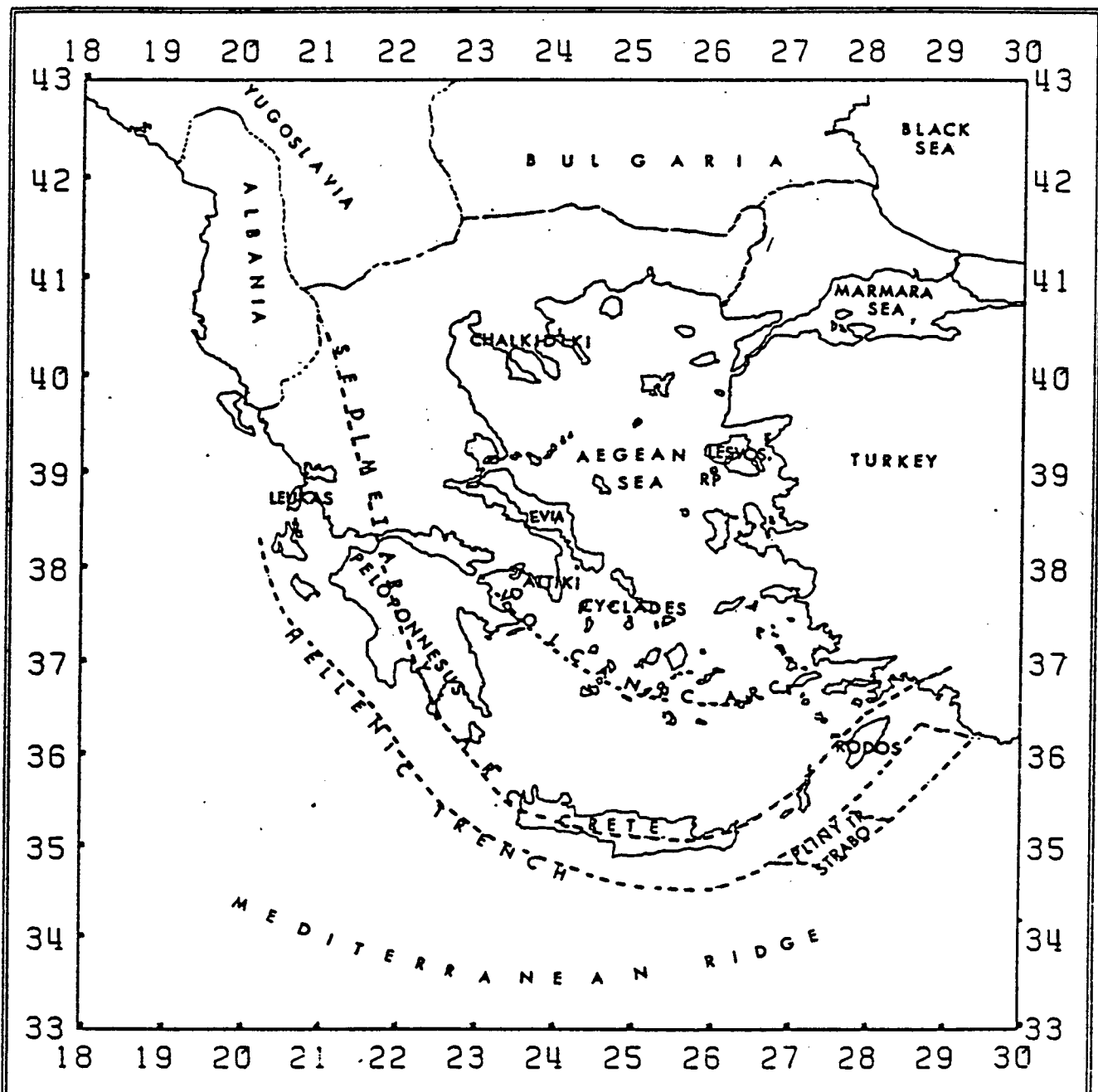
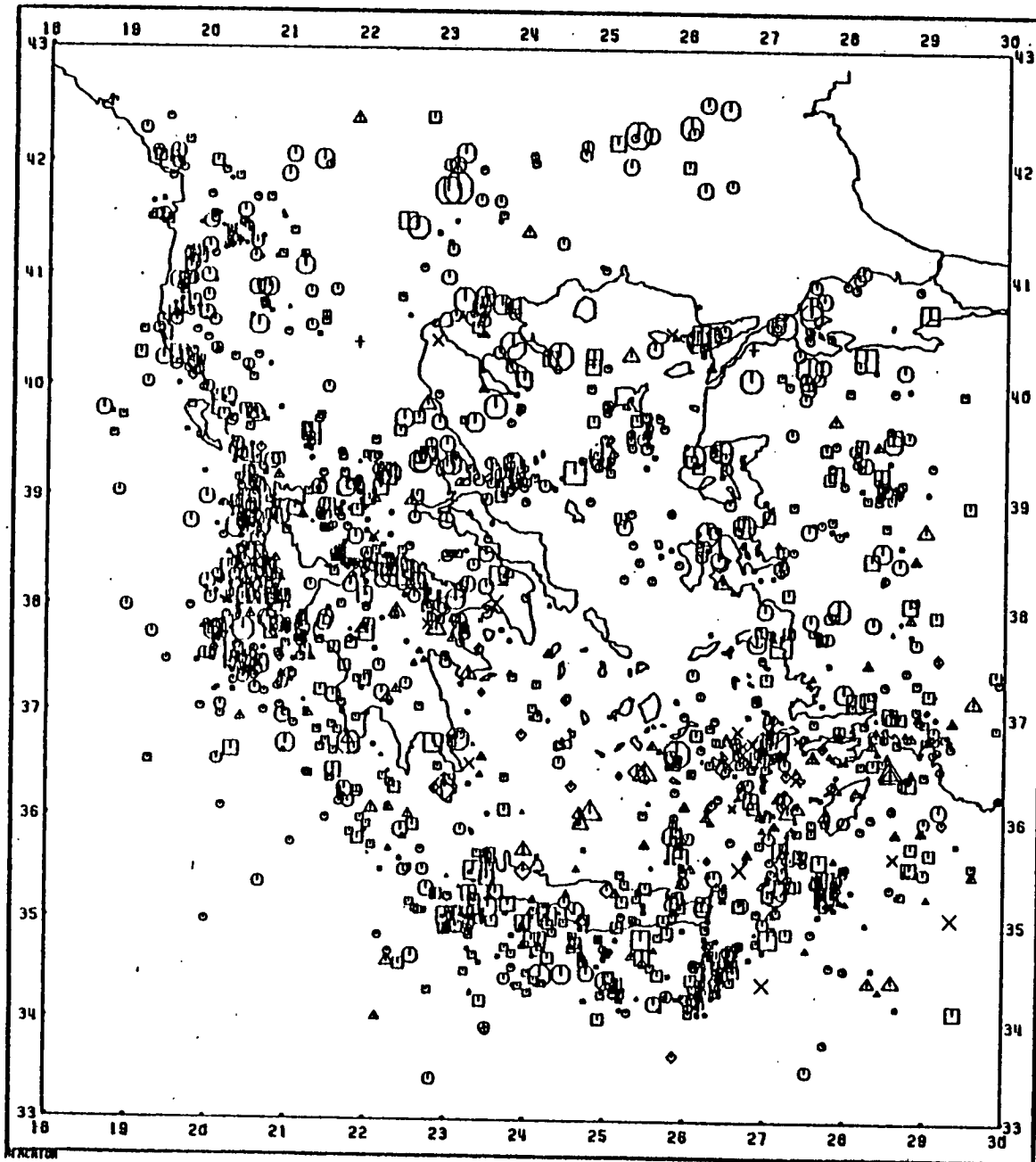


Figure 9.1  
 Summary map of the Aegean region, showing morphologic and geologic trends in a schematic way.  
 (from Makropoulos, 1978)



| KEY TO SYMBOLS            |                   |
|---------------------------|-------------------|
| DEPTHS (SYMBOL TYPES)     |                   |
| ○                         | UP TO 30.00       |
| □                         | 30.00 TO 60.00    |
| △                         | 60.00 TO 100.00   |
| ◇                         | 100.00 TO 140.00  |
| ×                         | 140.00 TO 200.00  |
| +                         | 200.00 OR GREATER |
| MAGNITUDE (SYMBOL RADIUS) |                   |
| •                         | UP TO 4.50        |
| •                         | 4.50 TO 5.00      |
| •                         | 5.00 TO 5.50      |
| •                         | 5.50 TO 6.00      |
| •                         | 6.00 TO 6.50      |
| •                         | 6.50 TO 7.00      |
| •                         | 7.00 TO 7.50      |
| •                         | 7.50 OR GREATER   |

Figure 9.2  
 Spatial distribution of all  
 earthquakes for Greece since  
 1901.  
 (from Makropoulos and Burton, 1981)

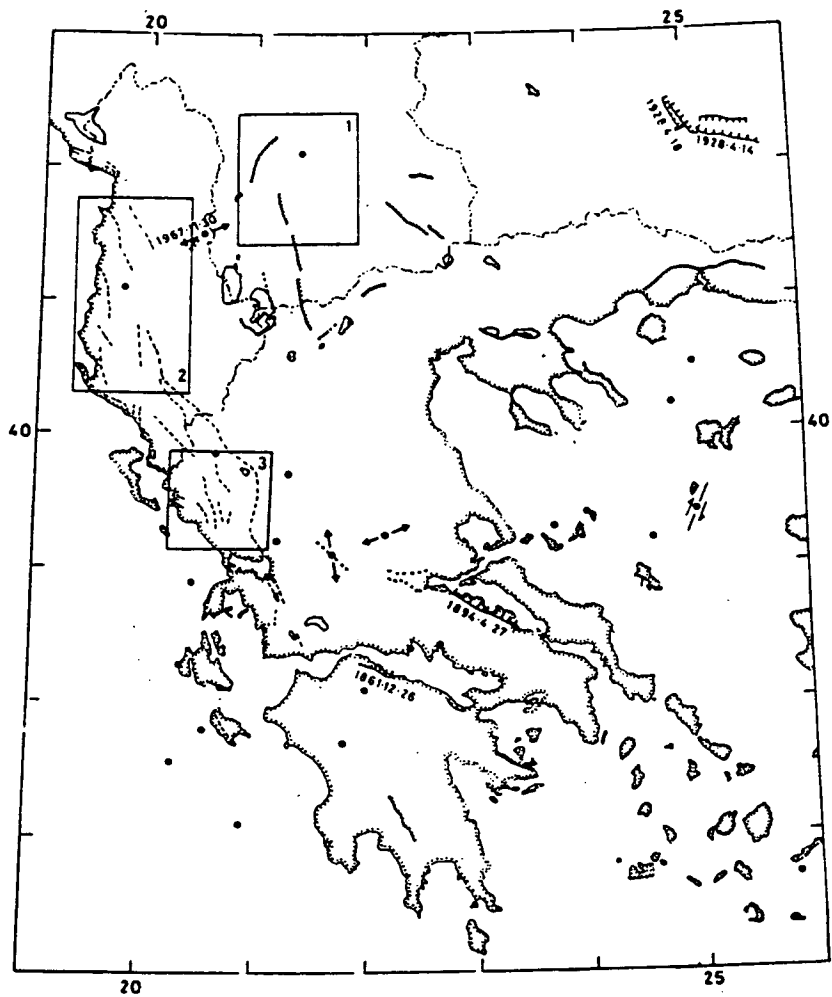


Fig 9.3 Summary of the present deformation of the Aegean area after McKenzie (1978). (Long curved lines show normal faults. Lines with open semicircles show thrust faults. Solid dots mark epicentres of shocks for which mechanisms are used. Arrows show the direction of motion obtained from fault plane solutions. The long heavy arrow shows the direction of relative motion between the Aegean and Africa. Heavy Vs mark sites of recent volcanism.)

mid-ocean ridge (Finetti, 1976). The Hellenic trench consists of a series of depressions to a depth of 5100 metres paralleling a sedimentary (Hellenic) arc. Between the Hellenic and volcanic arcs lies the Cretan Trough where the water depth attains a maximum of 2000 metres.

Seismic refraction studies (Makris, 1977) have shown the crustal thickness in the Aegean to be 22 to 32 km. , whereas the thickness beneath Greece and Turkey is between 40 and 50 km.. Several tectonic models for this complex region have been proposed. A common feature of the models is the underthrusting of the African plate along the Hellenic arc with a dip of  $c.35^{\circ}$ . Figure 9.4 is taken from McKenzie (1978), and demonstrates the major fault lines as determined from Landsat images, refraction studies and fault plane solutions. McKenzie postulates that the crustal thinning beneath the Aegean is evidence of stretching by a factor of about two and the direction of relative motion between the Aegean region (microplate) and Africa is  $211^{\circ}$ .

The extensional deformation in Northern Greece is evidenced by diffuse normal faults characterised by shallower dips at depth than those at the surface (McKenzie, 1977). One such feature trending NWW - SEE is clearly seen West of Evia in the Atalanti region (Figure 9.3, and 9.4 ). Figure 9.5 shows the region in greater detail, and the epicentres of large magnitude events which



Surface breaks and faults visible on the *Landsat* images (see Fig. 10 for details). Projection that of Fig. 14. The fault breaks are taken from 1861.12.26 Richter (1958), 1894.4.27 Richter (1958) 1928.4.14 and 1928.4.18 Richter (1958), 1967.11.30 Sulstarova & Kociaj (1969) and Ambrasey (private communication).

Figure 9.4 Landsat lineaments from Mckenzie, 1978



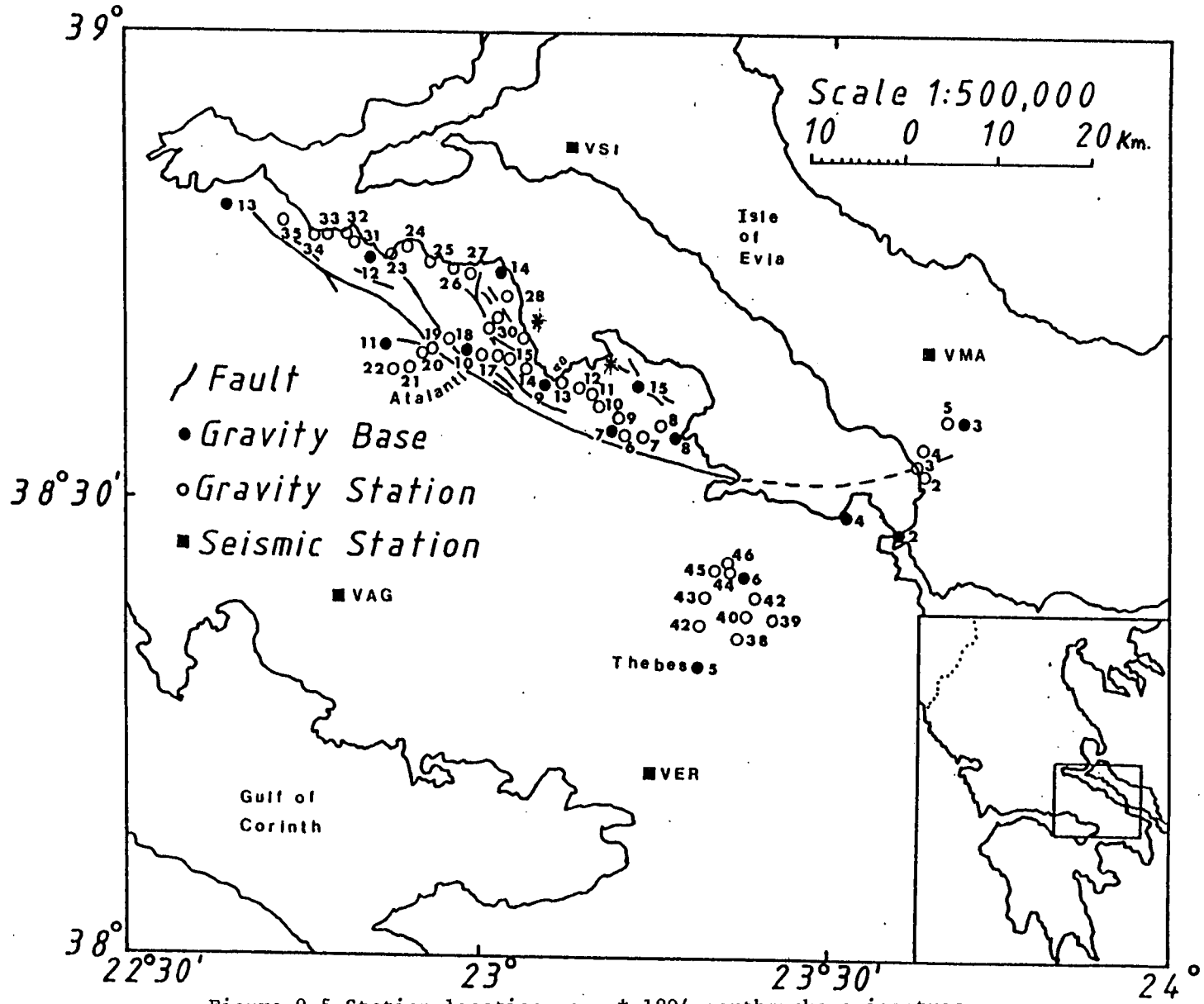


Figure 9.5 Station location map. \* 1894 earthquake epicentres.

occurred in 1894. These earthquakes caused much loss of life (greater than 300; Karnik 1969) and several villages where submerged following subsidence. The small islands just North of Scalade were once mainland.

Following the Gulf of Corinth earthquakes several rough hewn stone buildings collapsed during shocks centred around the hamlet of Ψπατον. This is slightly south of the Atalanti Fault but led to fears it may be reactivated. The 1894 shocks were the last major events and the elapsed time of 89 years exceed the return period (82 years, Makropoulos, 1979 ) of a magnitude 6.5 event for this locality. Figure 9.6 is taken from Makropoulos (1979), and illustrates the most probable annual maximum earthquake magnitude using the Extreme Value method (Gumbal, 1966), based on a catalogue of 1860 events. A peak is quite apparent in the Atalanti area.

### 9.3 The Atalanti Network

A Network of 68 stations , with a total of 370 observations of two La Coste and Romberg 'G' meters was established by the author and Dr. E. Lagios. These stations were first occupied in September 1981, (Table 9.1 lists collection dates), and have been remeasured during July 1982. The stations were observed using G-275 (Edinburgh University) and G-496 (Athens University) during

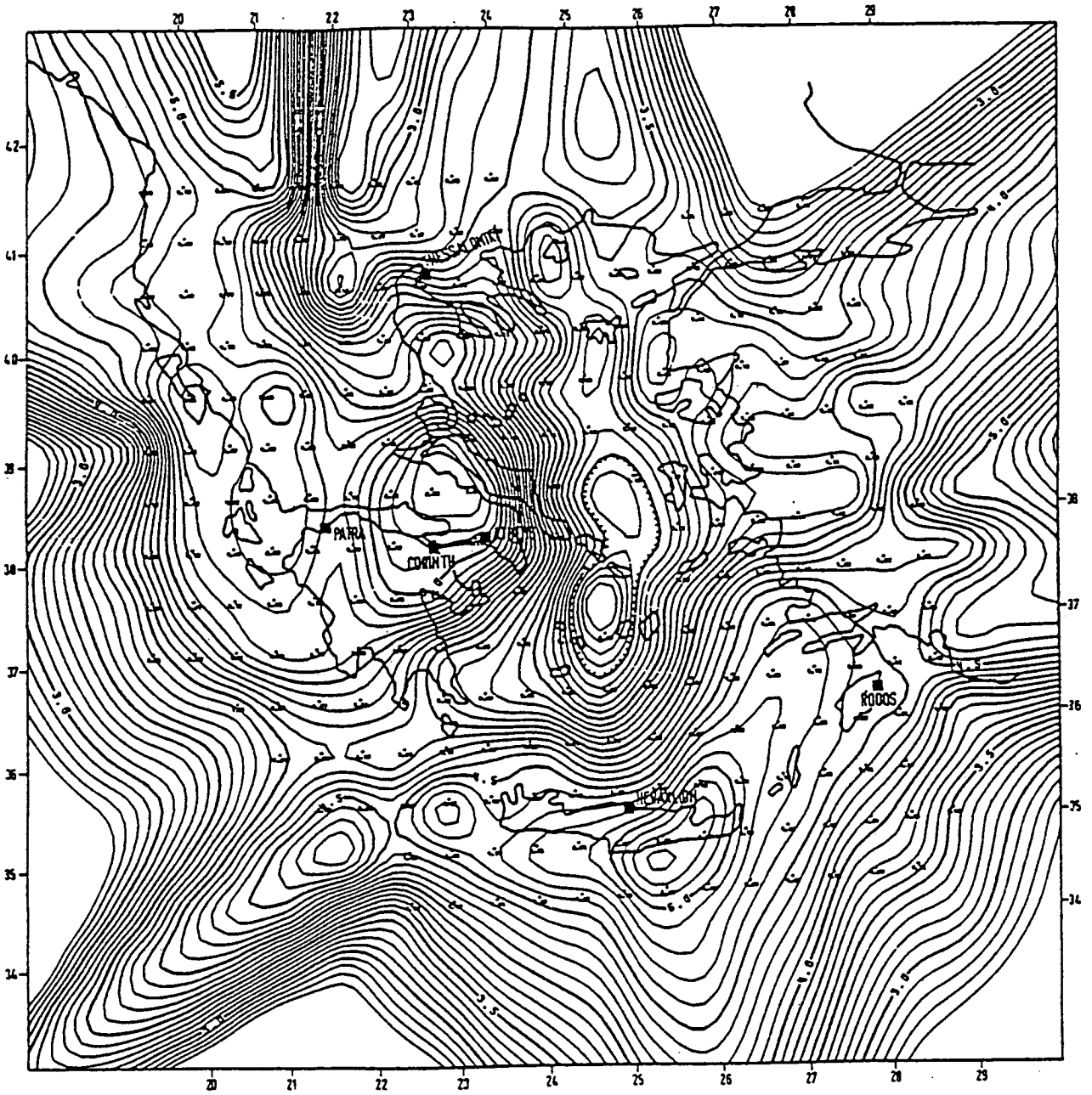


Fig 9.6 Most probable annual maximum earthquake magnitude (mode) for Greece.

(from Makropoulos, 1978)

APPENDIX 7

Published Paper : Geophys. J. R. astr. Soc. (1984) 77, 875-882

A microgravimetric network in East Central Greece -  
an area of potential seismic hazard

|       | B0   | B1   | B1A  | B2   | B3  | B4 | B5 | B6   | B7   | B8    | B9  | B10   | B11  | B12 | B13  | B14  | B15  | S1   | S2   | S3   | S4   | S5   | S6   | S7   | S8   | S9   | S10  | S11  | S12  | S13  | S14  | S15   | S16   | S17   |  |  |
|-------|------|------|------|------|-----|----|----|------|------|-------|-----|-------|------|-----|------|------|------|------|------|------|------|------|------|------|------|------|------|------|------|------|------|-------|-------|-------|--|--|
| 5-09  | 1,15 | 2,14 | 3    |      |     |    |    |      |      |       |     |       |      |     |      |      |      |      |      |      |      |      |      |      |      |      |      |      |      |      |      |       |       |       |  |  |
| 6-09  | 1    |      |      | 3,14 | 8,9 |    |    |      |      |       |     |       |      |     |      |      |      | 2,15 | 4,13 | 5,12 | 6,11 | 7,10 |      |      |      |      |      |      |      |      |      |       |       |       |  |  |
| 7-09  |      |      |      | 1    | 2   | 3  |    | 5,14 | 9,10 |       |     |       |      |     |      |      | 4,15 |      |      |      |      |      | 6,13 | 7,12 | 8,11 |      |      |      |      |      |      |       |       |       |  |  |
| 8-09  |      |      |      |      |     |    |    | 2,25 | 8,19 | 13,14 |     |       |      |     |      |      | 1,26 |      |      |      |      |      |      |      |      | 3,24 | 4,23 | 5,22 | 6,29 | 7,20 | 9,18 | 10,17 | 11,16 | 12,15 |  |  |
| 9-09  | 12   | 11   |      | 10   | 9   |    |    | 2,7  | 1,8  | 3,6   | 4,5 |       |      |     |      |      |      |      |      |      |      |      |      |      |      |      |      |      |      |      |      |       |       |       |  |  |
| 12-09 | 1    | 2    |      |      |     |    |    |      |      |       |     |       |      |     |      |      |      | 3,16 | 9,10 |      |      |      |      |      |      |      |      |      |      |      |      |       |       |       |  |  |
| 14-09 |      |      |      |      |     |    |    |      |      |       |     | 11,12 | 1,22 |     |      | 7,16 |      |      |      |      |      |      |      |      |      |      |      |      |      |      |      |       |       |       |  |  |
| 15-09 |      |      |      |      |     |    |    |      |      |       |     |       |      |     |      |      |      | 1,16 | 7,10 |      |      |      |      |      |      |      |      |      |      |      |      |       |       |       |  |  |
| 16-09 |      |      |      |      |     |    |    |      |      |       |     | 4,11  | 6,9  | 7,8 | 2,13 | 1,14 | 3,12 |      |      |      |      |      |      |      |      |      |      |      |      |      |      |       |       |       |  |  |
| 17-09 |      |      |      |      |     |    |    | 2,11 | 7    |       |     |       |      |     |      |      |      |      |      |      |      |      |      |      |      |      |      |      |      |      |      |       |       |       |  |  |
| 18-09 |      |      |      |      |     |    |    | 1,14 | 7,8  |       |     |       |      |     |      |      |      |      |      |      |      |      |      |      |      |      |      |      |      |      |      |       |       |       |  |  |
| 01-10 |      | 1,14 | 2,13 |      |     |    |    |      |      |       |     |       |      |     |      |      |      |      |      |      |      |      |      |      |      |      |      |      |      |      |      |       |       |       |  |  |

|       | S18  | S19  | S20  | S21  | S22  | S23 | S24  | S25  | S26  | S27  | S28  | S29  | S30  | S31   | S32 | S33 | S34 | S35 | S36 | S37 | S38 | S39 | S40 | S41 | S42 | S43 | S44 | S45 | S46 | GNCL1 | GNCL2 | GNCL3 | G4 | G5 |  |      |      |      |      |     |
|-------|------|------|------|------|------|-----|------|------|------|------|------|------|------|-------|-----|-----|-----|-----|-----|-----|-----|-----|-----|-----|-----|-----|-----|-----|-----|-------|-------|-------|----|----|--|------|------|------|------|-----|
| 5-09  |      |      |      |      |      |     |      |      |      |      |      |      |      |       |     |     |     |     |     |     |     |     |     |     |     |     |     |     |     |       |       |       |    |    |  | 4,13 | 5,12 | 6,11 | 7,10 | 8,9 |
| 6-09  |      |      |      |      |      |     |      |      |      |      |      |      |      |       |     |     |     |     |     |     |     |     |     |     |     |     |     |     |     |       |       |       |    |    |  |      |      |      |      |     |
| 7-09  |      |      |      |      |      |     |      |      |      |      |      |      |      |       |     |     |     |     |     |     |     |     |     |     |     |     |     |     |     |       |       |       |    |    |  |      |      |      |      |     |
| 8-09  |      |      |      |      |      |     |      |      |      |      |      |      |      |       |     |     |     |     |     |     |     |     |     |     |     |     |     |     |     |       |       |       |    |    |  |      |      |      |      |     |
| 9-09  |      |      |      |      |      |     |      |      |      |      |      |      |      |       |     |     |     |     |     |     |     |     |     |     |     |     |     |     |     |       |       |       |    |    |  |      |      |      |      |     |
| 12-09 | 4,15 | 5,14 | 6,13 | 7,12 | 6,11 |     |      |      |      |      |      |      |      |       |     |     |     |     |     |     |     |     |     |     |     |     |     |     |     |       |       |       |    |    |  |      |      |      |      |     |
| 14-09 |      |      |      |      |      |     | 2,21 | 3,20 | 4,19 | 5,18 | 6,17 | 8,15 | 9,14 | 10,13 |     |     |     |     |     |     |     |     |     |     |     |     |     |     |     |       |       |       |    |    |  |      |      |      |      |     |
| 15-09 |      |      |      |      |      |     |      |      |      |      |      |      |      |       |     |     |     |     |     |     |     |     |     |     |     |     |     |     |     |       |       |       |    |    |  |      |      |      |      |     |
| 16-09 |      |      |      |      |      |     |      |      |      |      |      |      |      |       |     |     |     |     |     |     |     |     |     |     |     |     |     |     |     |       |       |       |    |    |  |      |      |      |      |     |
| 17-09 |      |      |      |      |      |     |      |      |      |      |      |      |      |       |     |     |     |     |     |     |     |     |     |     |     |     |     |     |     |       |       |       |    |    |  |      |      |      |      |     |
| 18-09 |      |      |      |      |      |     |      |      |      |      |      |      |      |       |     |     |     |     |     |     |     |     |     |     |     |     |     |     |     |       |       |       |    |    |  |      |      |      |      |     |
| 01-10 |      |      |      |      |      |     |      |      |      |      |      |      |      |       |     |     |     |     |     |     |     |     |     |     |     |     |     |     |     |       |       |       |    |    |  |      |      |      |      |     |

Table 9.1 Atalanti network measurement timetable. Stations measured in double ladder sequence.

the 1981 field campaign and using G-496 and G-478 (National Technical University of Greece) during 1982. The stations will continue to be occupied annually or more frequently depending on seismic activity.

The station locations are shown on Figure 9.5 They are situated in the the area of faulting stretching from Larymna (B8) to Molos (B13), and on the island of Evia where the main Atalanti fault terminates. A group of ten stations are located a few kilometres North of Thibes where the tremors mentioned in section 9.2 were felt. Few stations exist West of the main fault because of logistic difficulties; here the terrain is rugged and only one minor road to Zelion (B11) traversed the fault line. (Fault location derived from Philipson(1930) and Mercier(1977)).

The measurements were made in a ladder sequence with base stations (marked '●' in figure 9.5) occupied on more than one ladder circuit and also measured on a separate base station only circuit. Car transport was used throughout with G-275 resting on the operator's lap in the rear passenger accomodation and G-496 secured with a safety belt in the front passenger seat. Station positions can be relocated from a large masonry pin and a circle of red paint, together with photographs. The height and latitude were taken from 1:50,000 maps supplied by the Hellenic Military Geographic Service. The resurvey of 1982 failed to locate station 'S7' and only station 'B14' had been

destroyed.

In addition to the stations located in the study area measurements were taken on the Greek National Calibration Line before and after the field campaign. The calibration line consists of five stations ascending Mount Parnis , near Athens. This calibration line overlaps only part of the gravity range of the network. It serves to demonstrate possible variations in the scale factor before and after the field campaign and to relate different measuring epochs.

#### 9.4 Data Analysis

The general procedure is similar to that outlined in section 5.3. Pressure and temperature were taken during the 1981 survey but not during the 1982 survey,(because of the lack of a suitable barometer). Therefore no pressure corrections were were applied but it should be noted that pressure systems in Greece during the summer months are extremely stable. The pressure difference upon return to a station during the 1981 survey was often less than one millibar.

The data were first corrected for earth tides using the harmonic expansion of Cartwright and Tayler (1971) as ammended by Cartwright and Edden (1973), using the computer progam PBAS (Appendix (4) ), with standard

gravimetric factors. The data were examined as separate daily sequences using the spline fitting program (NSPL) to construct daily drift curves, for each instrument. A typical set of curves with two nodes is shown in Figure 9.7. This daily analysis was performed to identify tares, misreadings and observation sequences with anomalous drift. In general the root mean square error of a daily linear fit was less than two microgals. A total of 370 readings were taken with each instrument during 1981, but less than ten were excluded. In the case of G-275 one day, the first observation of the calibration line, exhibited a very high drift rate caused by battery failure during the ladder sequence. In the case of the 1982 readings the observations using G-496 were similar to the previous year but those observations taken with G-478 were of very poor quality. This instrument had presented difficulties in the field with the beam sticking firmly in the mid position. The readings of this instrument were rejected and the data for 1982 consists solely of that collected using G-496.

In addition to an appraisal of the daily drift characteristics the splining program was used to obtain graphs of the complete data set as shown in figure 9.8. Low order spline solutions were very similar to those obtained using the multi-linear technique but suffered from instability with decreasing nodal intervals.



# Typical daily drift

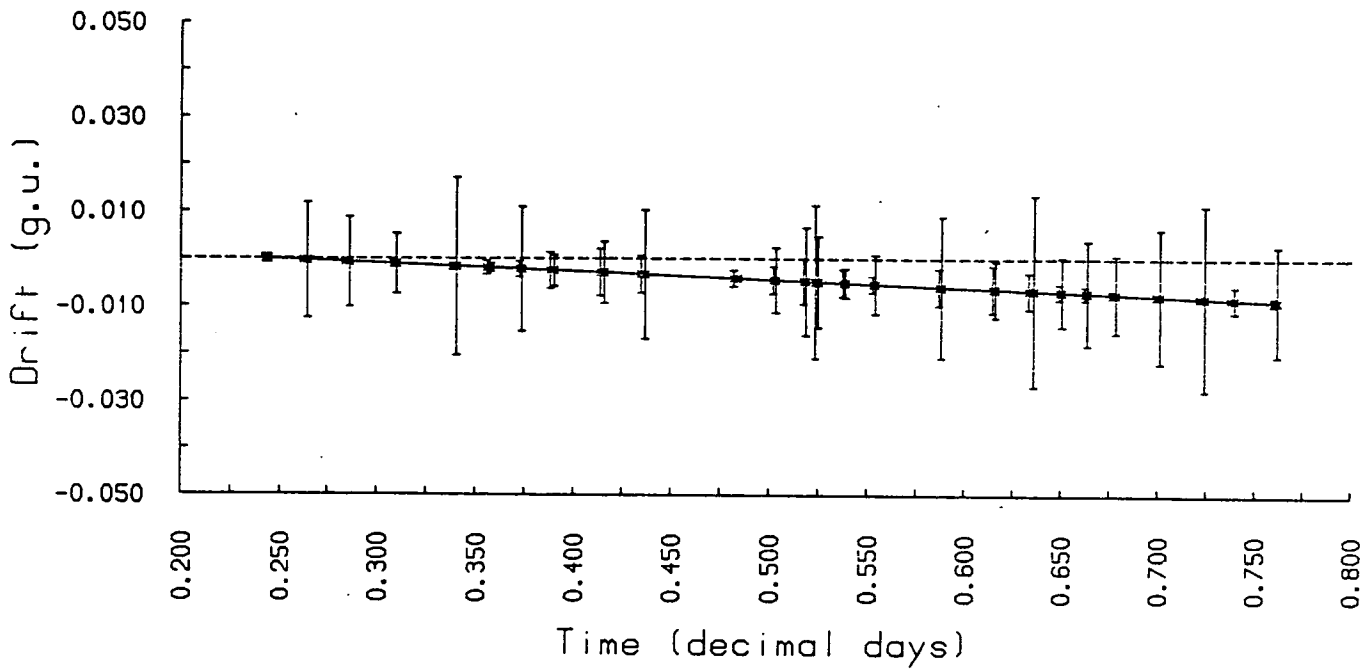


Figure 9.7 Typical double ladder sequence drift.

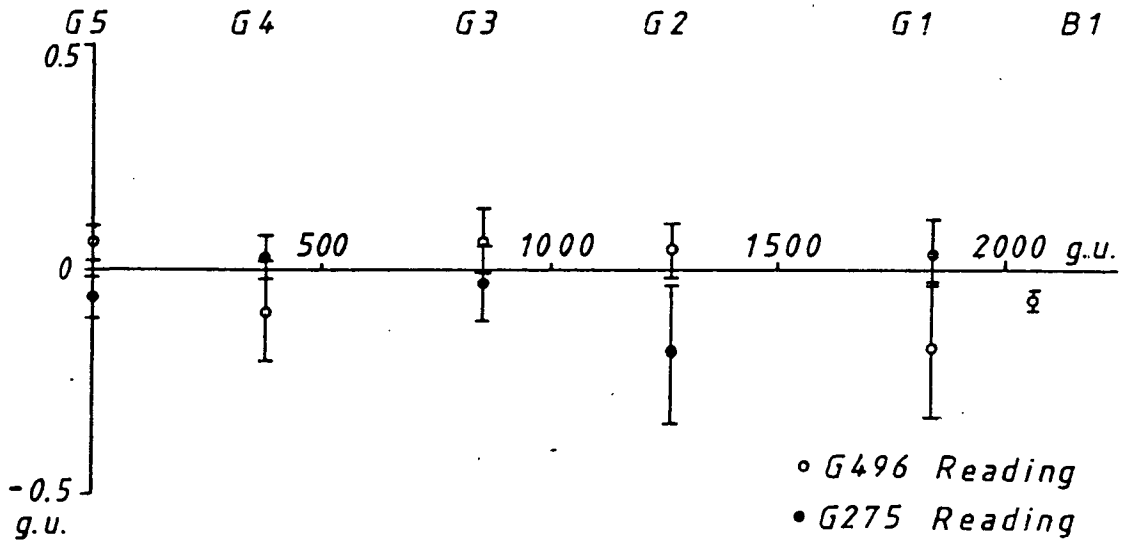


Figure 9.9 Difference between calibration line observations before and after field campaign.

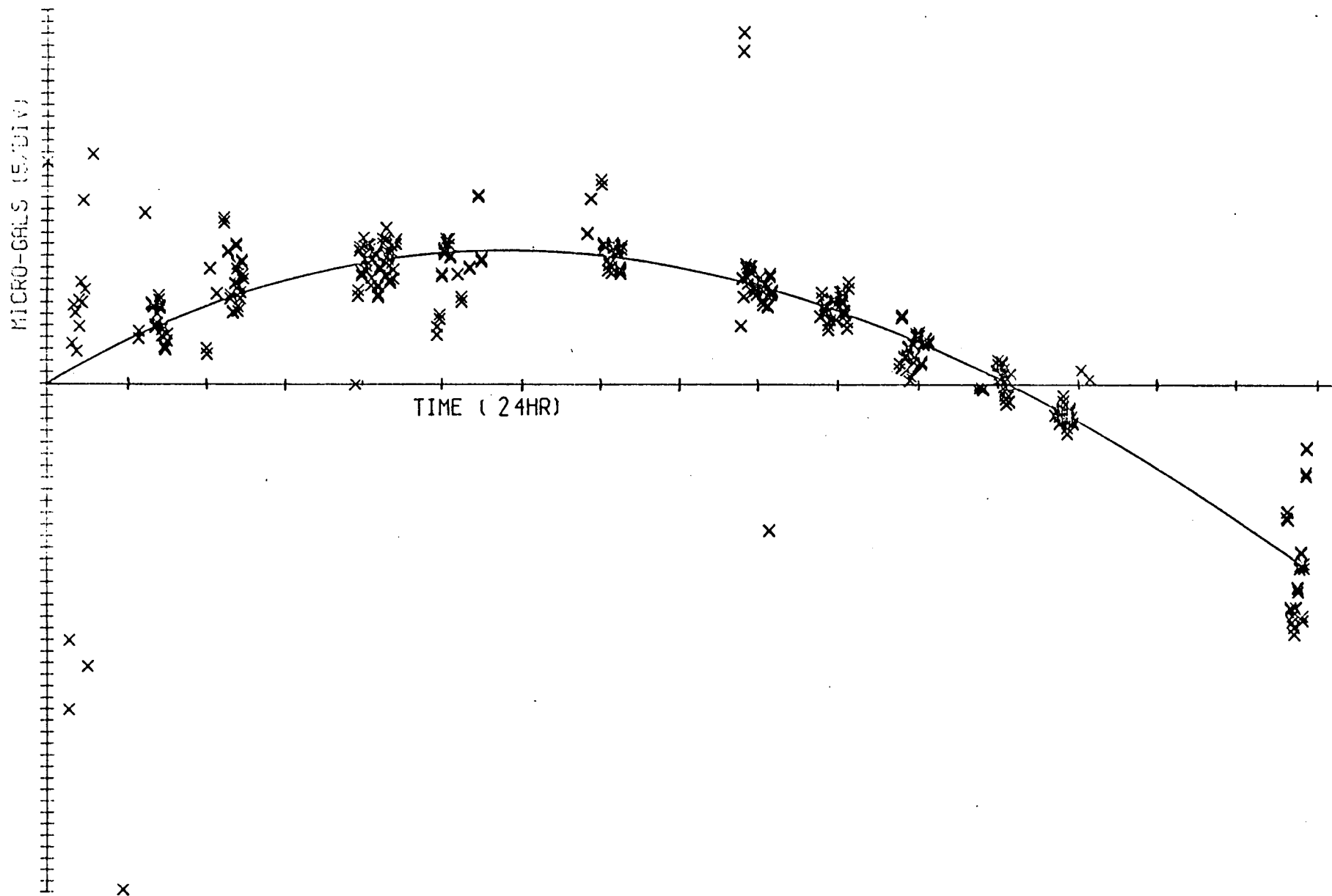


Figure 9.8 Complete Atalanti observation sequence (instrument - G275,1981) . Unconstrained 2-node cubic spline fit.

025505 1981 G 275 UNCONSTRAINED

The network adjustment program was now applied to the culled data sets in order to obtain a comparison of the 1981 and 1982 data. More than half the total observations are repeat readings at a base station (i.e. stations occupied on more than one day) and every third day includes a remeasurement of base stations only. These repeat measurements control the long term drift and strengthen the network adjustment.

### 9.5 Data Results

The difference between the calibration line observation before and after a fieldwork period of ten days is shown in figure 9.9. The gravity values are obtained from a straight line fit to each days' observations. The residuals have a standard deviation of nine microgals and do not appear to exhibit any systematic trend. The instruments' calibration has remained stable throughout the fieldwork period and a constant calibration factor adopted. The manufacturer's calibration tables were used since there are few well observed gravity stations in Greece with which to observe the stated scale factors. (The established values on the calibration line have yet to be released by the military authorities). The values derived from the combined 1981 adjustment solution are shown in Table 9.2. A histogram of the adjustment residuals compared with the

TABLE 9.2  
 Network adjustment values for 1981, combined instrument data set (G275 and G496)  
 Gravity values are with respect to station GNCL5 (Mount Parnis summit).

NETWORK ADJUSTMENT USING MULTILINEAR DRIFT

| BASE  | NO. | GRAVITY   | R.M.S. | NUMBER OF OBSERVATIONS |
|-------|-----|-----------|--------|------------------------|
| B0    | 1   | 2217.7047 | 0.0948 | 9                      |
| B1    | 2   | 2027.1463 | 0.0479 | 12                     |
| B1A   | 3   | 2025.8122 | 0.0984 | 5                      |
| B2    | 4   | 2506.1729 | 0.1180 | 6                      |
| B3    | 5   | 2462.7353 | 0.0742 | 6                      |
| B4    | 6   | 2443.0636 | 0.0659 | 6                      |
| B5    | 7   | 1844.7906 | 0.0987 | 12                     |
| B6    | 8   | 2129.8871 | 0.0849 | 4                      |
| B7    | 9   | 2030.2629 | 0.1418 | 14                     |
| B8    | 10  | 2659.0361 | 0.0864 | 8                      |
| B9    | 11  | 2592.0611 | 0.0961 | 12                     |
| B10   | 12  | 2383.1582 | 0.0797 | 20                     |
| B11   | 13  | 1405.9868 | 0.0959 | 9                      |
| B12   | 14  | 2249.9390 | 0.0947 | 12                     |
| B13   | 15  | 2057.3322 | 0.0390 | 8                      |
| B14   | 16  | 2441.3197 | 0.0592 | 8                      |
| B15   | 17  | 2158.4494 | 0.2683 | 9                      |
| GNCL1 | 18  | 1219.4743 | 0.1398 | 6                      |
| GNCL2 | 19  | 1249.4719 | 0.1530 | 6                      |
| GNCL3 | 20  | 846.1349  | 0.1132 | 6                      |
| GNCL4 | 21  | 379.1207  | 0.1187 | 6                      |
| GNCL5 | 22  | 0.0000    | 0.1165 | 6                      |
| S1    | 23  | 1536.7090 | 0.1148 | 2                      |
| S2    | 24  | 2462.1675 | 0.0114 | 4                      |
| S3    | 25  | 2532.4780 | 0.0268 | 4                      |
| S4    | 26  | 2529.3812 | 0.0741 | 4                      |
| S5    | 27  | 2542.7419 | 0.0357 | 4                      |
| S6    | 28  | 2164.5282 | 0.0343 | 4                      |
| S7    | 29  | 2482.2106 | 0.0735 | 4                      |
| S8    | 30  | 2508.9265 | 0.0474 | 4                      |
| S9    | 31  | 2129.4279 | 0.1112 | 4                      |
| S10   | 32  | 2110.1665 | 0.0850 | 4                      |
| S11   | 33  | 2428.2421 | 0.0605 | 4                      |
| S12   | 34  | 2558.1029 | 0.0313 | 4                      |
| S13   | 35  | 2546.4565 | 0.0669 | 4                      |
| S14   | 36  | 2554.5499 | 0.0838 | 4                      |
| S15   | 37  | 2530.5140 | 0.0882 | 4                      |
| S16   | 38  | 2464.7316 | 0.0343 | 4                      |
| S17   | 39  | 2450.0753 | 0.0596 | 4                      |
| S18   | 40  | 2221.5581 | 0.0435 | 4                      |
| S19   | 41  | 2044.1075 | 0.0506 | 4                      |
| S20   | 42  | 1555.5728 | 0.0624 | 4                      |
| S21   | 43  | 1901.3959 | 0.1052 | 4                      |
| S22   | 44  | 1709.4675 | 0.0770 | 4                      |
| S23   | 45  | 2285.9367 | 0.0882 | 4                      |
| S24   | 46  | 2283.7400 | 0.0579 | 4                      |
| S25   | 47  | 2386.0833 | 0.0604 | 2                      |
| S26   | 48  | 2411.5037 | 0.0794 | 4                      |
| S27   | 49  | 2448.3446 | 0.0612 | 4                      |
| S28   | 50  | 2483.0587 | 0.0860 | 4                      |
| S29   | 51  | 2503.7961 | 0.0328 | 4                      |
| S30   | 52  | 2479.4364 | 0.0537 | 5                      |
| S31   | 53  | 2258.3677 | 0.0941 | 4                      |
| S32   | 54  | 2210.5666 | 0.0613 | 4                      |
| S33   | 55  | 2228.5183 | 0.0057 | 4                      |
| S34   | 56  | 2233.4579 | 0.0615 | 4                      |
| S35   | 57  | 2032.6949 | 0.0795 | 4                      |
| S36   | 58  | 1909.0742 | 0.1164 | 4                      |
| S37   | 59  | 2638.6121 | 0.1347 | 4                      |
| S38   | 60  | 2002.1738 | 0.0716 | 4                      |
| S39   | 61  | 1998.6606 | 0.0270 | 4                      |
| S40   | 62  | 2116.9104 | 0.0913 | 4                      |
| S41   | 63  | 1534.3864 | 0.0501 | 4                      |
| S42   | 64  | 2025.1805 | 0.0686 | 4                      |
| S43   | 65  | 2143.6459 | 0.0190 | 4                      |
| S44   | 66  | 2192.9777 | 0.0075 | 4                      |
| S45   | 67  | 2220.8270 | 0.0379 | 4                      |
| S46   | 68  | 2176.5633 | 0.0579 | 4                      |

HISTOGRAM 1

Standard Deviation of best fitting Normal Distribution 0.083 g.v.

Number of Degrees of Freedom 9  
Chi squared is 5.01977

|           |   |   |   |   |   |   |    |    |    |    |    |    |    |    |   |   |   |   |   |   |
|-----------|---|---|---|---|---|---|----|----|----|----|----|----|----|----|---|---|---|---|---|---|
| NORMAL    | 0 | 0 | 0 | 0 | 2 | 6 | 16 | 34 | 55 | 70 | 70 | 55 | 34 | 16 | 6 | 2 | 0 | 0 | 0 | 0 |
| FREQUENCY | 0 | 0 | 0 | 1 | 2 | 5 | 20 | 29 | 47 | 74 | 80 | 53 | 30 | 15 | 6 | 3 | 0 | 3 | 0 | 0 |

EACH 80 EQUALS 2 POINTS

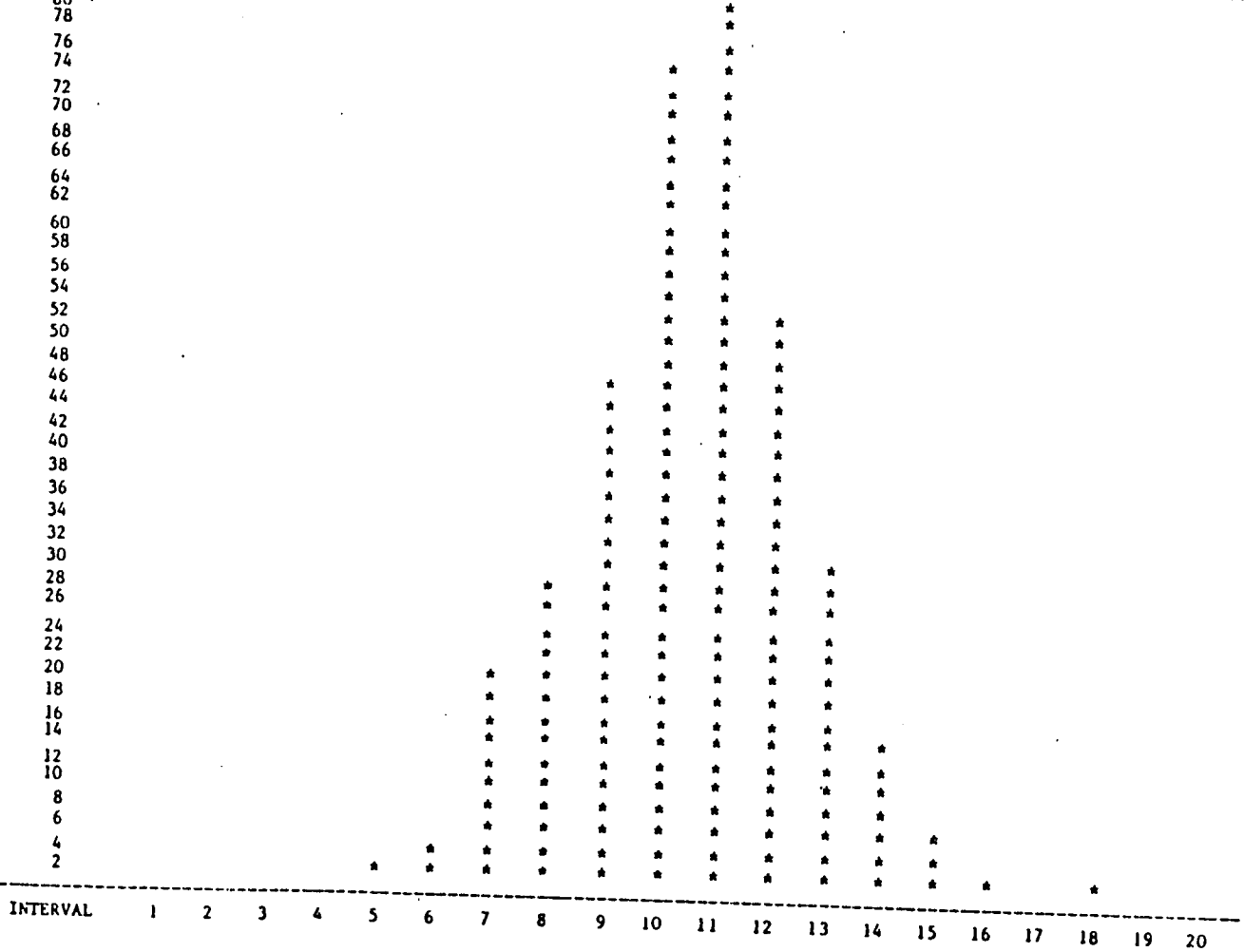


Figure 9.10 Histogram of residuals ; least squares network adjustment , 1981

best fitting normal curve is shown in figure 9.10 . This yields a standard deviation of 8.3 mcrogals and the chi-squared test (  $P(X_9^2 < 5.02) = 0.84$  ) indicates that the residuals are normally distributed . Similarly the 1982 adjustment given in Table 9.3 and figure 9.11 yields a standard deviation of 7.7 microgals and a high probability of normality (  $P(X_8^2 < 3.5) = 0.93$  )

These two solution sets were differenced to assess if any change in gravity greater than the limits of accuracy had taken place. A graph of the differences, adjusted with zero change in the mean is shown in figure 9.12. Some individual measurements, with their associated error bars appear to exhibit a significant gravity change. However analysis of the total data suite reveals that these are normally distributed random fluctuations with the anticipated standard deviation for the differenced data set. A histogram of the difference distribution (Figure 9.13) indicates a high probability of normality and  $P(X_4^2, 0.21) = 0.27$ . The data set has a standard deviation of 11 microgals. This figure is in agreement with the combination of standard deviations of the 1981 and 1982 adjustment solutions,  $(8.3^2 + 7.7^2)^{1/2} = 11.3$  microgals.

Therefore the residuals of the differenced adjustment solutions are strongly consisted with the hypothesis of no change in gravity over the observation period , within the limits of accuracy of the instruments. Should the

TABLE 9-3  
 Network adjustment values for 1982 (one instrument, 6496)  
 Values are with respect to station GNCL5 (Mt. Parnis summit)

NETWORK ADJUSTMENT USING MULTILINEAR DRIFT

| BASE  | NO. | GRAVITY   | R.M.S. | NUMBER OF OBSERVATIONS |
|-------|-----|-----------|--------|------------------------|
| B0A   | 1   | 1783.1309 | 0.1872 | 13                     |
| B2    | 2   | 2508.1494 | 0.0780 | 5                      |
| B3    | 3   | 2462.7348 | 0.0248 | 2                      |
| B4    | 4   | 2443.1700 | 0.0019 | 2                      |
| B5    | 5   | 1884.8924 | 0.1034 | 6                      |
| B6    | 6   | 2189.8727 | 0.0644 | 4                      |
| B7    | 7   | 2030.3029 | 0.1098 | 11                     |
| B8    | 8   | 2659.2562 | 0.0555 | 4                      |
| B9    | 9   | 2592.1728 | 0.1153 | 6                      |
| B10   | 10  | 2383.2155 | 0.1009 | 13                     |
| B11   | 11  | 1405.9323 | 0.0361 | 3                      |
| B12   | 12  | 2250.0188 | 0.0675 | 9                      |
| B13   | 13  | 2057.6007 | 0.0688 | 5                      |
| B14   | 14  | 2445.0141 | 0.0394 | 4                      |
| B15   | 15  | 2158.5636 | 0.0000 | 1                      |
| GNCL2 | 16  | 1249.4116 | 0.0371 | 2                      |
| GNCL3 | 17  | 846.0662  | 0.0397 | 2                      |
| GNCL4 | 18  | 378.9722  | 0.0402 | 2                      |
| GNCL5 | 19  | 0.0000    | 0.0417 | 2                      |
| S2    | 20  | 2462.1121 | 0.1338 | 2                      |
| S3    | 21  | 2532.2922 | 0.0775 | 2                      |
| S4    | 22  | 2529.4584 | 0.0172 | 2                      |
| S5    | 23  | 2542.7302 | 0.0440 | 2                      |
| S6    | 24  | 2164.6837 | 0.0455 | 2                      |
| S7    | 25  | 2482.3571 | 0.0206 | 2                      |
| S8    | 26  | 2509.0710 | 0.0486 | 2                      |
| S9    | 27  | 2129.2906 | 0.0129 | 2                      |
| S10   | 28  | 2110.0377 | 0.0122 | 2                      |
| S11   | 29  | 2428.2570 | 0.0226 | 2                      |
| S12   | 30  | 2558.1355 | 0.0175 | 2                      |
| S13   | 31  | 2546.6121 | 0.1116 | 2                      |
| S14   | 32  | 2554.8588 | 0.1283 | 2                      |
| S15   | 33  | 2530.7908 | 0.0247 | 2                      |
| S16   | 34  | 2464.9904 | 0.1057 | 2                      |
| S17   | 35  | 2450.2973 | 0.0566 | 2                      |
| S18   | 36  | 2221.5656 | 0.1317 | 2                      |
| S19   | 37  | 2044.0626 | 0.1115 | 2                      |
| S20   | 38  | 1955.6690 | 0.0555 | 2                      |
| S21   | 39  | 1901.5440 | 0.0583 | 2                      |
| S22   | 40  | 1709.4970 | 0.0191 | 2                      |
| S23   | 41  | 2286.0340 | 0.0161 | 2                      |
| S24   | 42  | 2283.8371 | 0.0136 | 2                      |
| S25   | 43  | 2386.1138 | 0.0260 | 2                      |
| S26   | 44  | 2411.6521 | 0.0111 | 2                      |
| S27   | 45  | 2448.4386 | 0.0380 | 2                      |
| S28   | 46  | 2483.0646 | 0.0450 | 2                      |
| S29   | 47  | 2503.7081 | 0.0410 | 2                      |
| S30   | 48  | 2479.3901 | 0.0385 | 2                      |
| S31   | 49  | 2258.4051 | 0.0181 | 2                      |
| S32   | 50  | 2210.6348 | 0.0332 | 2                      |
| S33   | 51  | 2228.6292 | 0.0193 | 2                      |
| S34   | 52  | 2233.4803 | 0.0130 | 2                      |
| S35   | 53  | 2032.8591 | 0.0253 | 2                      |
| S36   | 54  | 1509.2080 | 0.0654 | 2                      |
| S37   | 55  | 2638.8019 | 0.0000 | 1                      |
| S38   | 56  | 2002.0920 | 0.0417 | 2                      |
| S39   | 57  | 1598.5929 | 0.0565 | 2                      |
| S40   | 58  | 2116.7805 | 0.0767 | 2                      |
| S41   | 59  | 1934.4465 | 0.0339 | 2                      |
| S42   | 60  | 2025.2360 | 0.0662 | 2                      |
| S43   | 61  | 2143.8366 | 0.0873 | 2                      |
| S44   | 62  | 2192.9331 | 0.0313 | 2                      |
| S45   | 63  | 2220.8516 | 0.0408 | 2                      |
| S46   | 64  | 2176.5271 | 0.0128 | 2                      |
| B1    | 65  | 2027.1961 | 0.0366 | 2                      |
| B1A   | 66  | 2025.7775 | 0.0081 | 2                      |

Each class interval is half the estimated standard deviation of 0.0766  
 Result of Dagostinos test : D = 0.19673Y = -39.65202

TOTAL NUMBER OF OBS. = 193

HISTOGRAM 1

Standard Deviation of best fitting NormalDistribution 0.04  
 Chi squared is 3.49476

|           |   |   |   |   |   |   |   |    |    |    |    |    |    |    |    |   |   |   |   |
|-----------|---|---|---|---|---|---|---|----|----|----|----|----|----|----|----|---|---|---|---|
| NORMAL    | 0 | 0 | 0 | 0 | 1 | 3 | 8 | 18 | 29 | 37 | 37 | 29 | 18 | 8  | 3  | 1 | 0 | 0 | 0 |
| FREQUENCY | 0 | 1 | 2 | 1 | 5 | 7 | 6 | 14 | 27 | 31 | 36 | 25 | 14 | 10 | 13 | 1 | 0 | 0 | 0 |

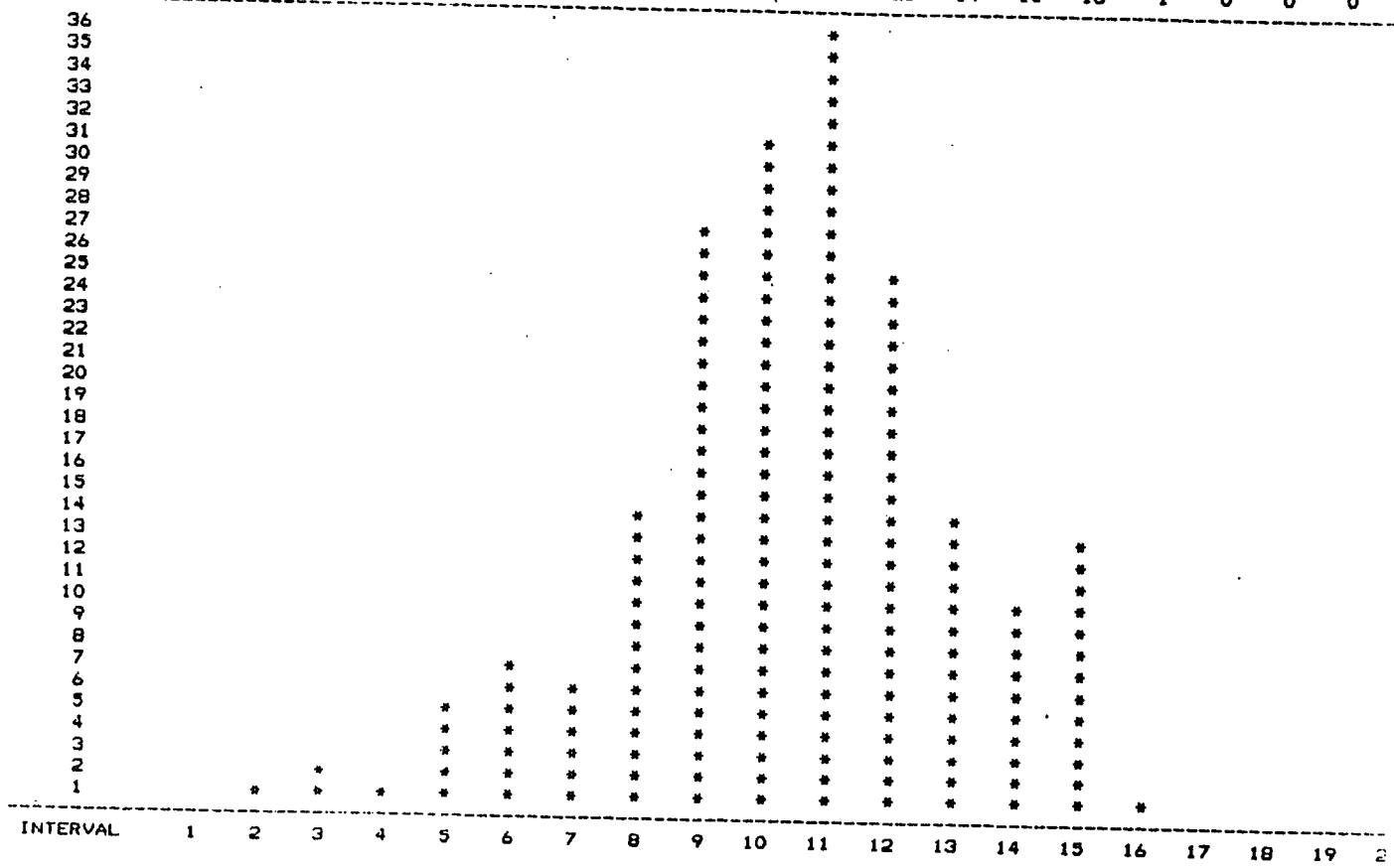


Figure 9.11 Histogram of residuals, least squares network adjustment, 1982



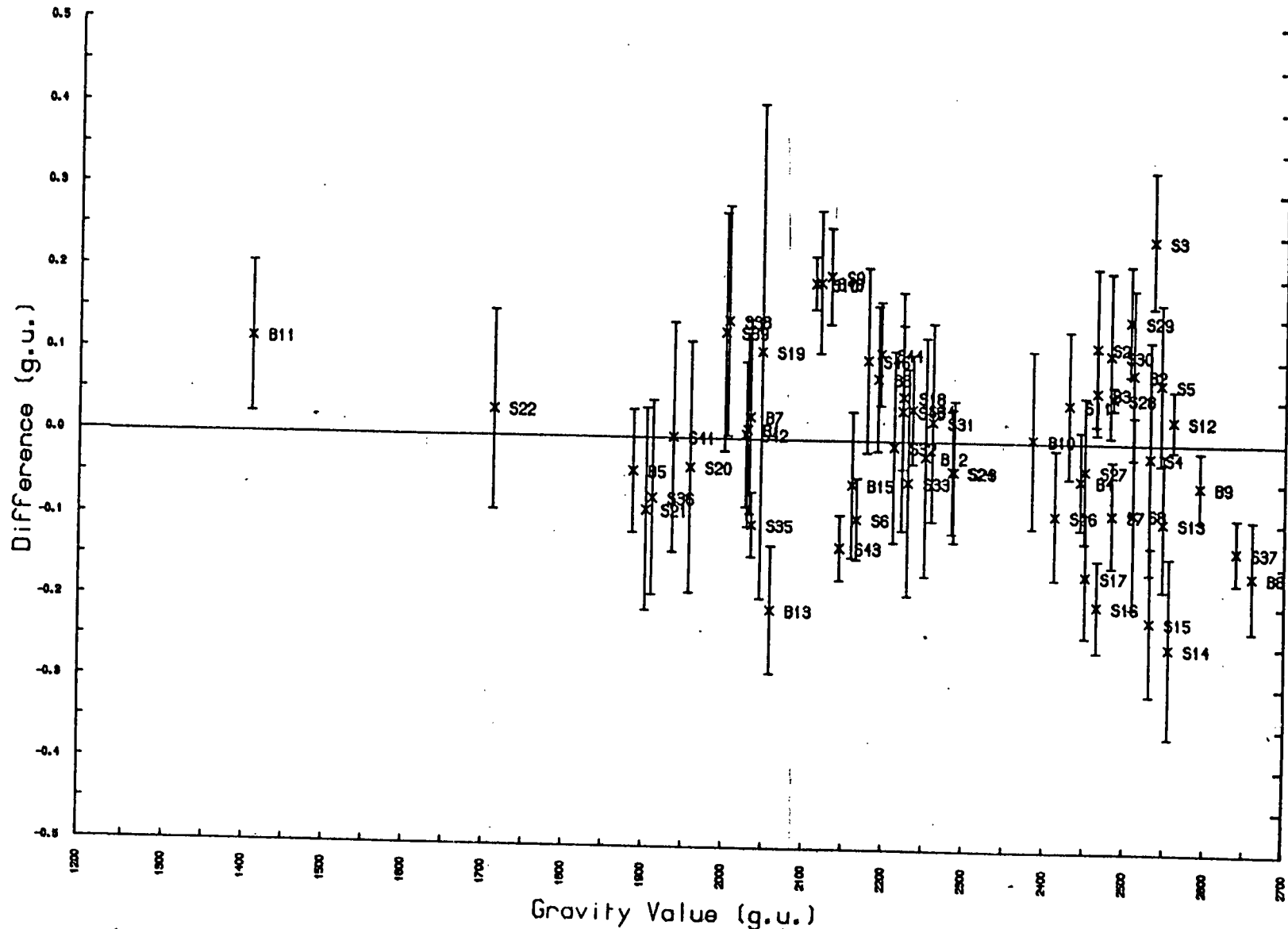


Figure 9.12 Observed gravity difference in the Atalanti region (1981 - 1982)

TOTAL NUMBER OF OBS. = 58  
 Standard Deviation = 0.110 g.u.  
 Number of Degrees of Freedom 4  
 Chi squared is 0.23790

| NORMAL FREQUENCY | 0 | 0 | 0 | 0 | 0 | 1 | 3 | 5 | 9 | 11 | 11 | 9  | 5  | 3  | 1  | 0  | 0  | 0  | 0  | 0  |
|------------------|---|---|---|---|---|---|---|---|---|----|----|----|----|----|----|----|----|----|----|----|
| 12               | 0 | 0 | 0 | 0 | 0 | 1 | 3 | 5 | 9 | 11 | 11 | 9  | 5  | 3  | 1  | 0  | 0  | 0  | 0  | 0  |
| 11               |   |   |   |   |   |   |   |   |   | *  | *  |    |    |    |    |    |    |    |    |    |
| 10               |   |   |   |   |   |   |   |   |   | *  | *  |    |    |    |    |    |    |    |    |    |
| 9                |   |   |   |   |   |   |   |   |   | *  | *  |    |    |    |    |    |    |    |    |    |
| 8                |   |   |   |   |   |   |   |   |   | *  | *  | *  |    |    |    |    |    |    |    |    |
| 7                |   |   |   |   |   |   |   |   | * | *  | *  | *  |    |    |    |    |    |    |    |    |
| 6                |   |   |   |   |   |   |   |   | * | *  | *  | *  |    |    |    |    |    |    |    |    |
| 5                |   |   |   |   |   |   |   |   | * | *  | *  | *  |    |    |    |    |    |    |    |    |
| 4                |   |   |   |   |   |   |   |   | * | *  | *  | *  | *  |    |    |    |    |    |    |    |
| 3                |   |   |   |   |   |   |   | * | * | *  | *  | *  | *  | *  |    |    |    |    |    |    |
| 2                |   |   |   |   |   | * | * | * | * | *  | *  | *  | *  | *  | *  |    |    |    |    |    |
| 1                |   |   |   |   |   | * | * | * | * | *  | *  | *  | *  | *  | *  | *  |    |    |    |    |
| INTERVAL         | 1 | 2 | 3 | 4 | 5 | 6 | 7 | 8 | 9 | 10 | 11 | 12 | 13 | 14 | 15 | 16 | 17 | 18 | 19 | 20 |

Figure 9.13 Histogram of gravity differences 1981-1982

difference distribution have been non normally distributed or possessed a higher standard deviation, there would be grounds for an immediate remeasurement of the network.

CHAPTER TEN  
SUBSIDENCE MEASUREMENTS

10.1 Introduction

As previously discussed in Chapter Two, high precision gravity surveys have proved to be a useful technique in the detection of underground voids. A further application of the technique (with certain commercial possibilities) is the detection of elevation changes caused by mining subsidence. This is presently carried out by conventional levelling which is costly and time consuming, particularly in the absence of thoroughfares.

Subsidence caused by underground coal workings is a common problem in Great Britain and is of two kinds:

- (1) Old workings, where the subsidence is often sudden and unpredictable
- (2) Current workings, in which the subsidence is predictable both in time and space

Old workings may exist as voids or be infilled with uncompacted rubble. They often occur in urban areas where they present a considerable hazard to existing and planned buildings. Unfortunately locations are not well documented

and often inaccurate, making a controlled survey impossible. One possible site was investigated without result and it was thought best to concentrate on current workings

Most coal seams in the United Kingdom are mined by panel working, which is suited to mechanised extraction. In this system the roof in the area of extraction is supported over the entire length of the working face by a continuous bank of hydraulic jacks. The jacks are moved forward immediately after the cutter has passed before them, allowing the goaf behind to collapse. In this way, total extraction is achieved and 90 per cent of the subsidence occurs within days (Orchard, 1964). A comprehensive study of the associated subsidence at many mines has resulted in graphical methods for the prediction of subsidence (Subsidence Engineers Handbook, National Coal Board 1975)

Fig (10.1) illustrates the standard notation for subsidence and slope. The amplitude (i.e. the vertical displacement) and shape of the subsidence profile are related to the width ( $w$ ) and the depth( $h$ ) of the seam. The subsidence for a given depth of seam is found to attain a maximum when the ratio  $w/h$  is equal to 1.4 (Weir, 1969) , a situation termed 'critical' (see Fig.10.2). Figure (10.3) illustrates the relationship of subsidence to width and depth. Support by various methods of waste infill will alter the subsidence amplitude but these are

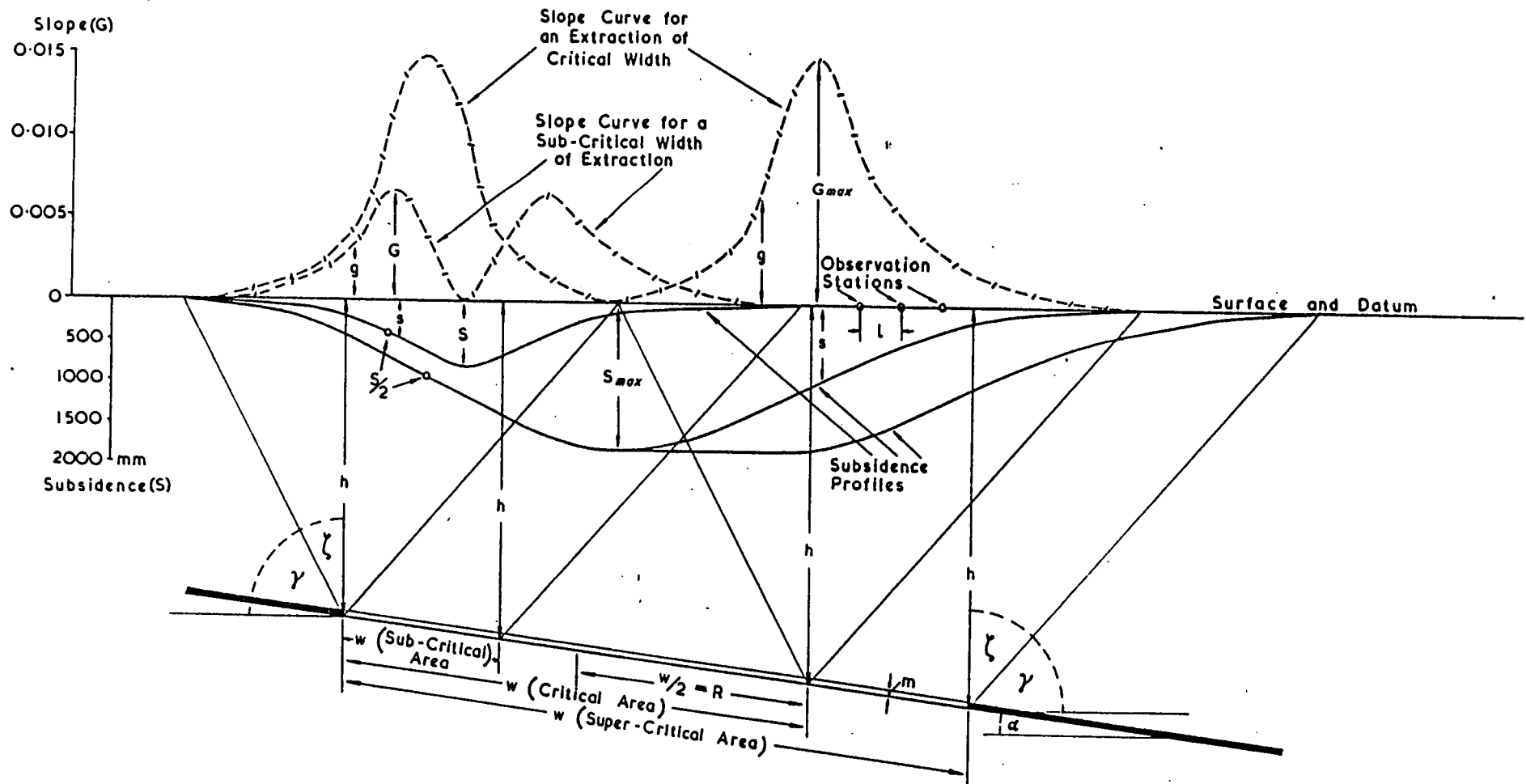
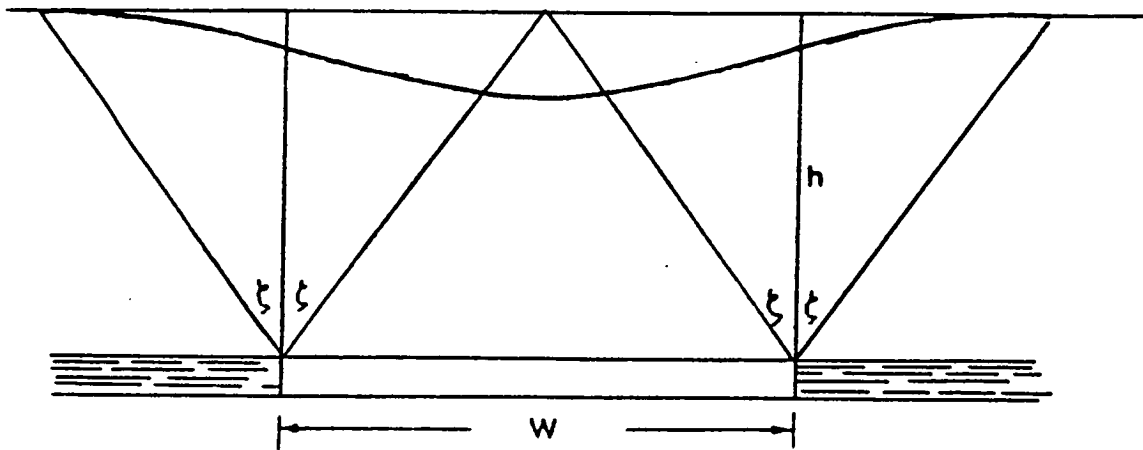
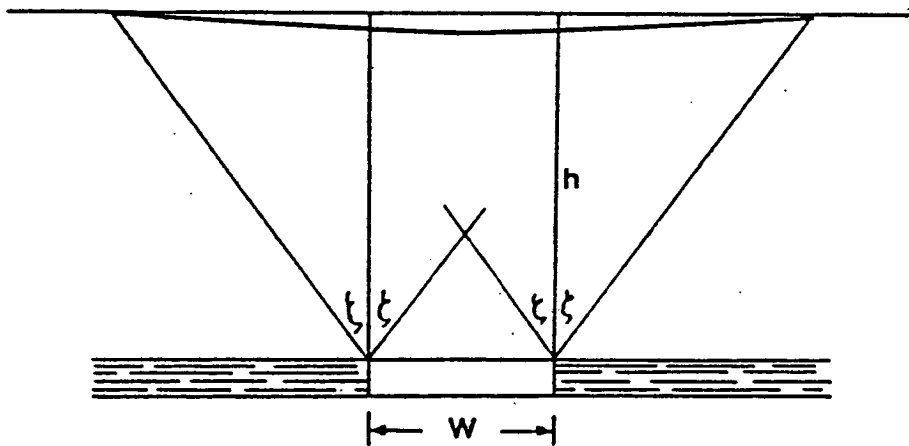


Figure 10.1 Typical section through workings, illustrating standard symbols for subsidence and slope.  
(National Coal Board, 1975)

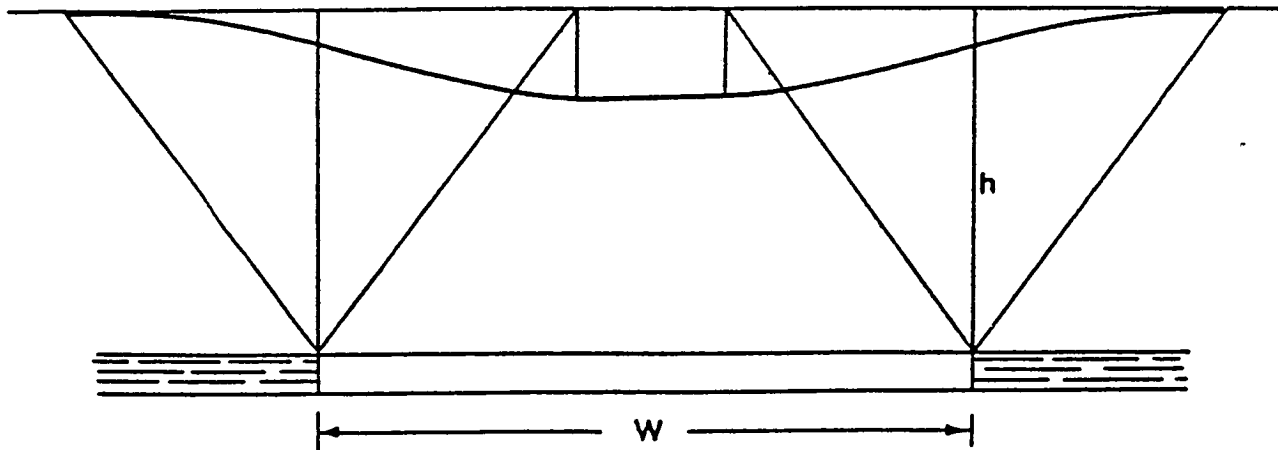


W = width; h = depth;  $\xi$  = limit angle.

CRITICAL AREA



PARTIAL OR SUB-CRITICAL AREA



SUPER - CRITICAL AREA

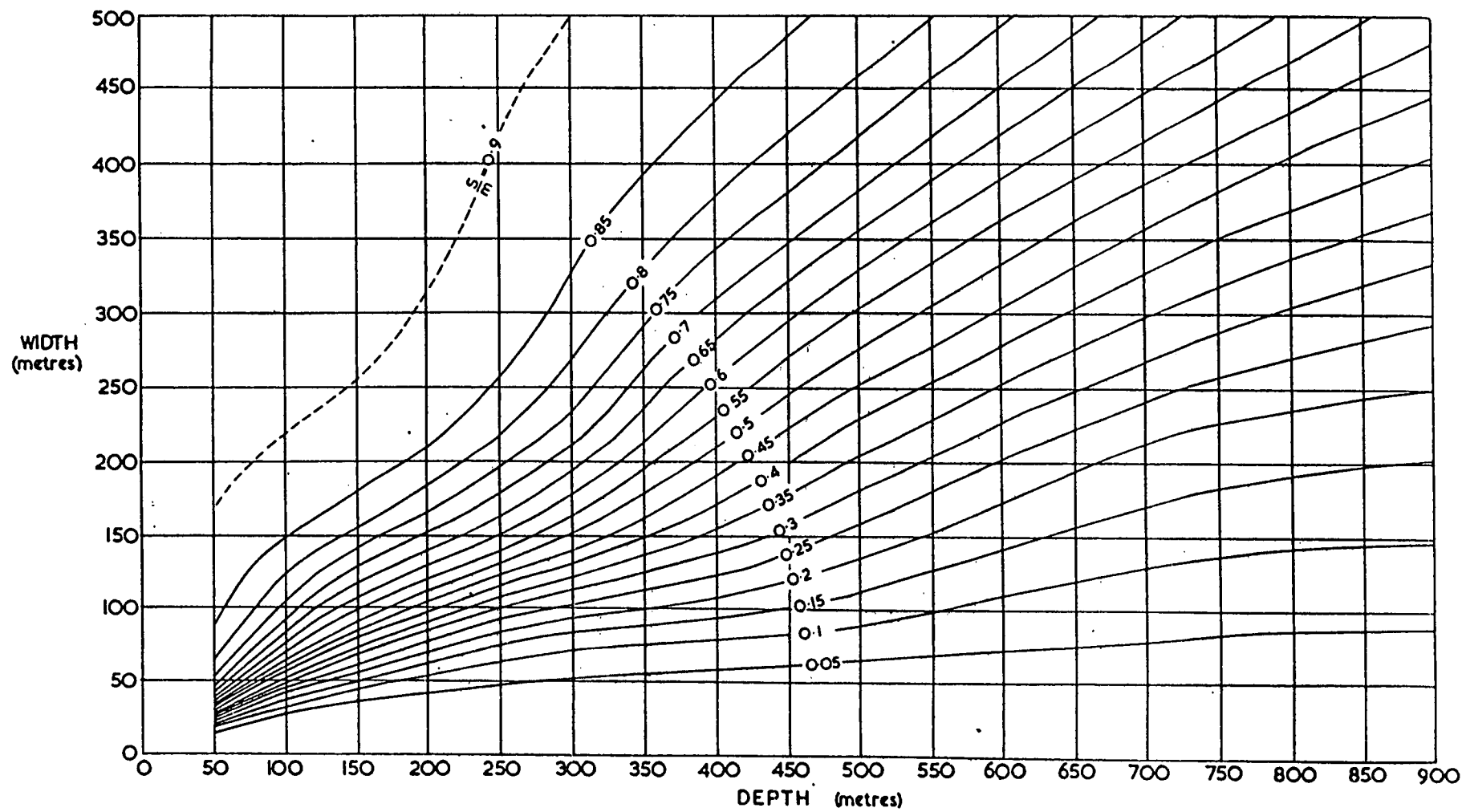


Figure 10.3 Relationship between subsidence and width and depth



expensive and only the most costly, pneumatic stowing, which can reduce subsidence by 50 per cent, has a marked effect.

## 10.2 Field area

For the purposes of this investigation it was desirable that the field area should satisfy the following conditions.

(1) Large possible subsidence to evaluate the relationship between height and gravity change with the maximum resolution. (2) A road perpendicular to the direction of mining to ease levelling. (3) Within 100km. of Edinburgh as the site was to be visited repeatedly

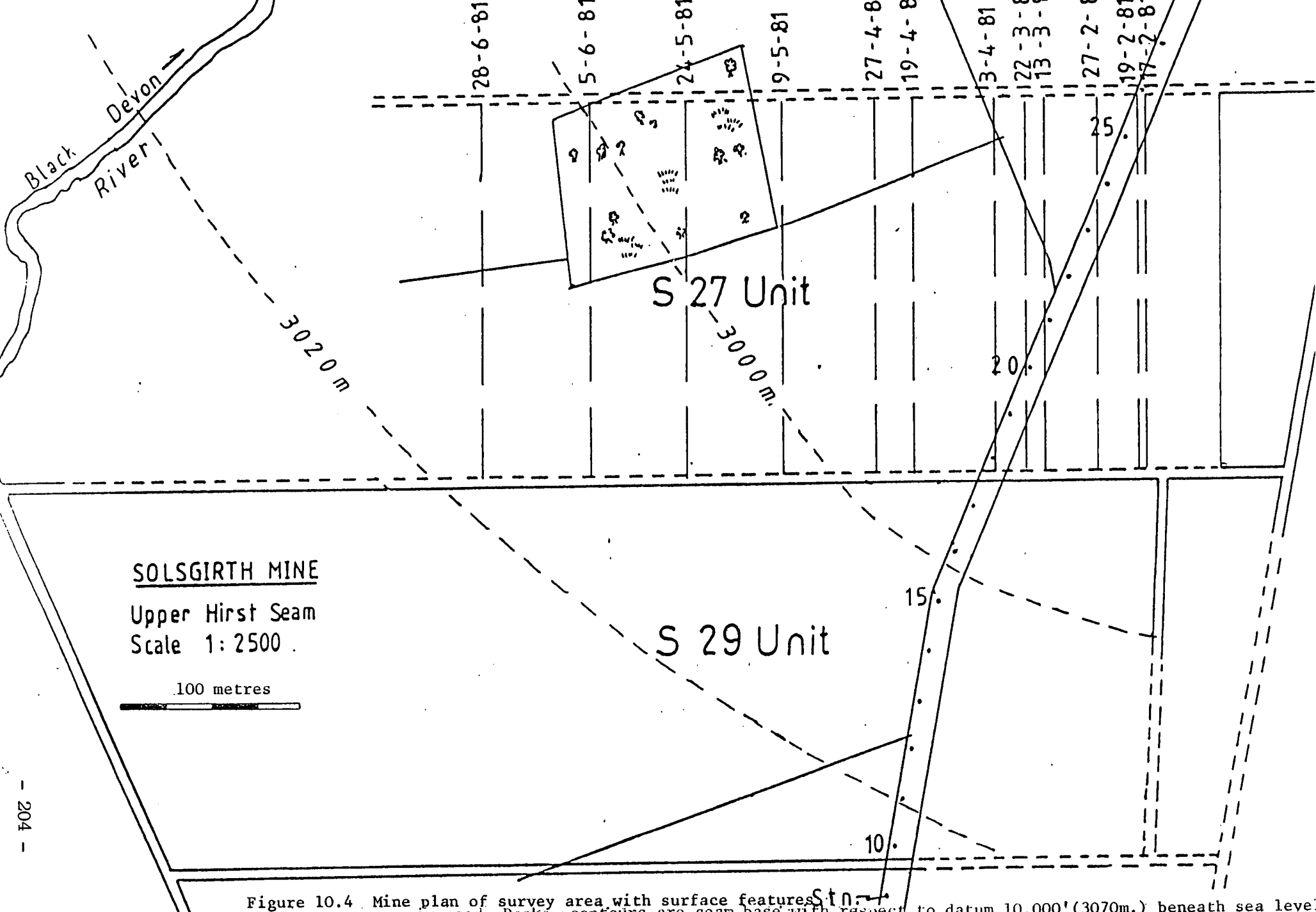
A highly suitable site was selected near Saline, Fife after consultation with National Coal Board engineers (George Archibald, Robert Longmore, Green Park, Scottish Area Headquarters). Coal is being extracted, from the Solsgirth colliery, Fife at a depth of 107m.-122m. from the Upper Hirst Seam in the Upper Limestone Series of the Carboniferous. The seam is extracted in 'panels' about 200m. wide and 1.68m thick. These are shallow workings (the average depth of coal workings in Scotland is in excess of 400m.) and as a result the half width of the subsidence profile is comparatively narrow.

Figure (10.4) is a mine plan of the survey area together with some surface features. The contours show the height of the seam with reference to a datum 3048 metres ( the metric equivalent of 10,000 feet) below mean sea level. Measurements were made along the road which roughly traverses the panels.

### 10.3 Measurements

The stations marked on Figure (10.4) were levelled on four separate occasions and gravity measurements made on a total of fourteen occasions to examine the surface displacement caused by the extraction of units S27 and S29. The dates of the data acquisition are shown on Table (10.1). Each station was positioned to one side of the tarmacadammed road and located with a washer and a round headed masonry pin driven . into the surface. The pin was both the level station and the gravity site.

The first levelling sequence was completed using a Watts microptic level fitted with a parallel plate micrometer, measuring in a ladder sequence (Close, 1965). This method, though accurate was found time consuming and subsequent surveys were carried out with a Zeiss Ni02 automatic level, using forward looping.



**SOLSGIRTH MINE**

Upper Hirst Seam

Scale 1:2500

100 metres



Figure 10.4 Mine plan of survey area with surface features superimposed. Dashed contours are seam base with respect to datum 10,000' (3070m.) beneath sea level.

---

Data Acquisition - Solsgirth

---

| Date     | Day No. | Survey<br>Type and No. |             |
|----------|---------|------------------------|-------------|
| 10.02.81 | -07     | Levelling # 1          |             |
| 17.02.81 | 00      | Gravimetric # 1        |             |
| 19.02.81 | 02      | Gravimetric # 2        |             |
| 27.02.81 | 10      | Gravimetric # 3        |             |
| 13.03.81 | 24      | Gravimetric # 4        |             |
| 22.03.81 | 33      | Gravimetric # 5        |             |
| 03.04.81 | 45      | Gravimetric # 6        | Unit<br>S27 |
| 19.04.81 | 61      | Gravimetric # 7        |             |
| 27.04.81 | 69      | Gravimetric # 8        |             |
| 09.05.81 | 81      | Gravimetric # 9        |             |
| 24.05.81 | 94      | Gravimetric #10        |             |
| 03.06.81 | 108     | Levelling # 2          |             |
| 05.06.81 | 110     | Gravimetric #11        |             |
| 28.06.81 | 133     | Gravimetric #12        |             |
|          |         |                        |             |
| 01.12.81 | 288     | Levelling # 3          |             |
| 02.12.81 | 289     | Gravimetric #13        | Unit<br>S29 |
| 27.04.82 | 438     | Levelling # 4          |             |
| 28.04.82 | 439     | Gravimetric #14        |             |

---

TABLE 10.1

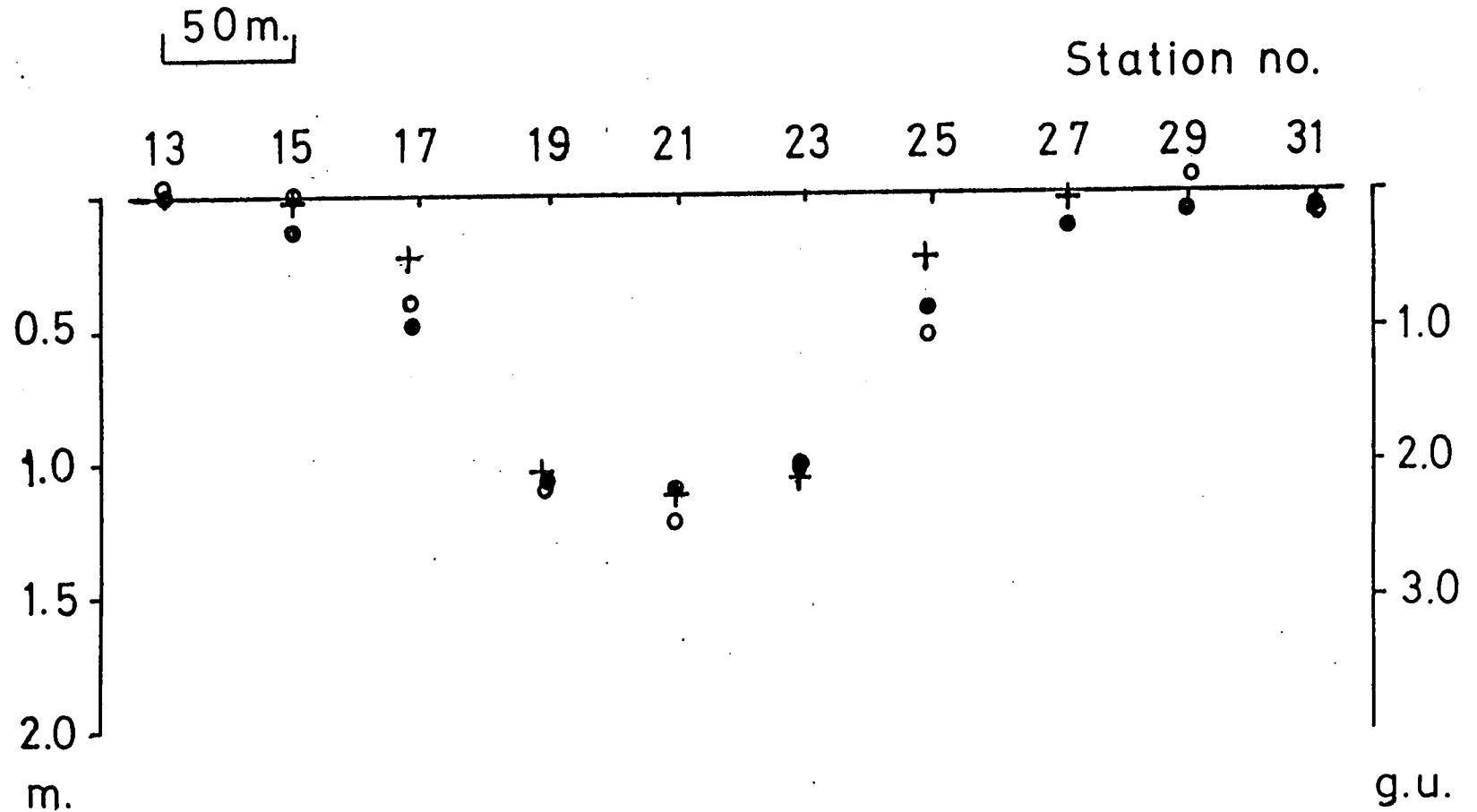
Gravity observations were taken in a ladder sequence. The meter rested on the standard La Coste and Romberg concave dish with one drilled foot seated securely on the masonry pin. One levelling screw of the meter was kept at a constant height by a brass collar. The screw point was kept within a circle scribed on the dish surface and thus the maximum height variation was + 5 mm. and typically much less. Orientation was set by eye with a maximum variation of + 10° .

Examination of Table (10.1) shows that gravity was measured at approximately two week intervals above unit S27 as coal was being extracted. Gravity measurements above unit S29 were made before and after subsidence. All measurements were taken with reference to a stable base approximately one kilometre from station 12; in the case of levelling this meant levelling that distance. The station spacing for unit S27 was 25m. but this was decreased to 12.5 m. for unit S29 because the predicted target area was better defined.

#### 10.4 Field Results

The gravity and level changes are shown together on figure (10.5) for unit S27 and figure (10.6) for unit S29. Also shown is the predicted subsidence as determined from

# Solsgirth Unit S27



- Levelling difference (m.)
- Gravity difference (g.u.)
- + Predicted subsidence (m.)

Figure 10.5 Gravity and level difference caused by extraction of unit S27 (see figure 10.7 and text for gravity-height relationship).

Solsgirth Unit S29

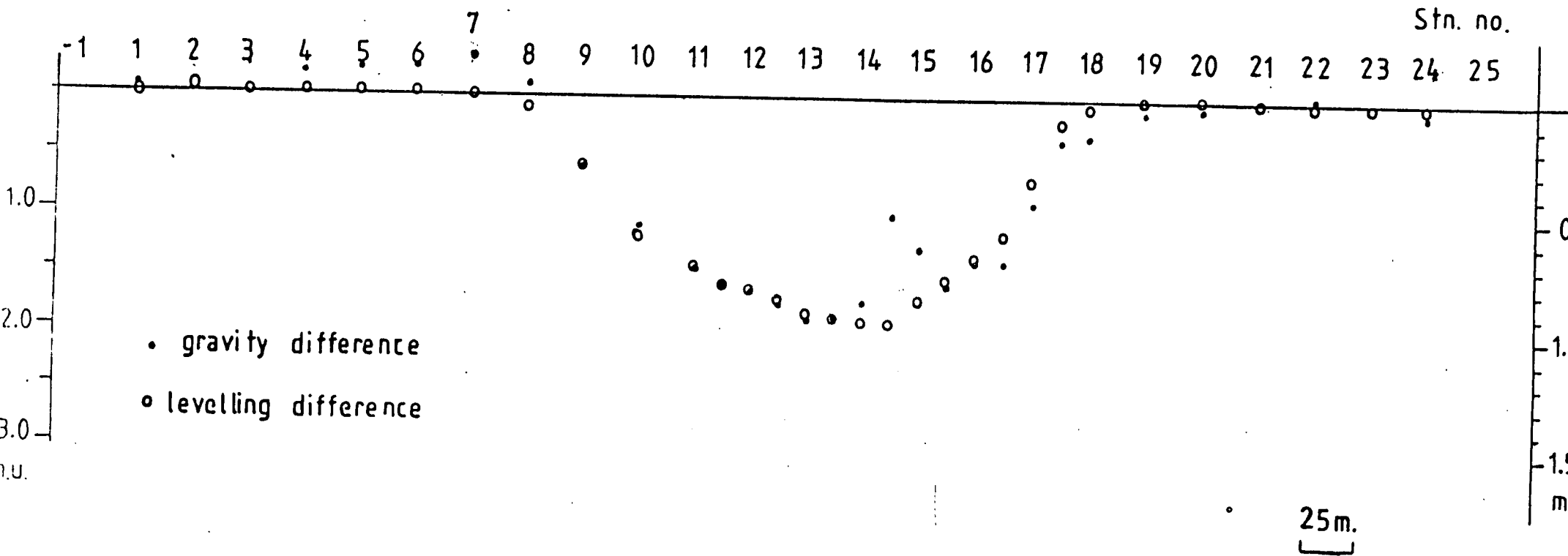


Figure 10.6 Gravity and level difference caused by the extraction of unit S29

the 'Subsidence Engineers Handbook' using the parameters shown. The predicted maximum subsidence (c.67 % of working height) is estimated on the basis of previously levelled subsidence profiles in this area (Robert Longmore, personal communication). It can be seen that the shape of the subsidence curve is in good agreement with the predicted profile . It can be seen that height and gravity are well related with the exception of a positive feature close to station 13 in the case of unit S29. A possible mechanism for this phenomenon is postulated later in this section.

The bedrock consists of cyclic sequences of sandstones, siltstones and mudstones of the Upper Limestone Series. Density measurements on comparable strata have been carried out in Ayrshire (McLean, 1965). McLean suggests a formation density of 2.54 gm/cc. for the Limestone Series. A regression Bouger anomaly against height obtains an identical figure but with a large standard deviation ( 0.45 g.u.). A density of 2.54 gm/c.c. would imply a combined free air and Bouger gradient of 2.10 g.u. per metre. Figure (10.7) is a graph of gravity change versus height change and the best fitting straight line has a gradient of 2.05 g.u./m with a standard deviation of 0.16 g.u./m.; implying a formation density of 2.47gm./c.c.. In this analysis I have not considered the drift density which is possibly less than 2.00gm./c.c. and is of variable depth.



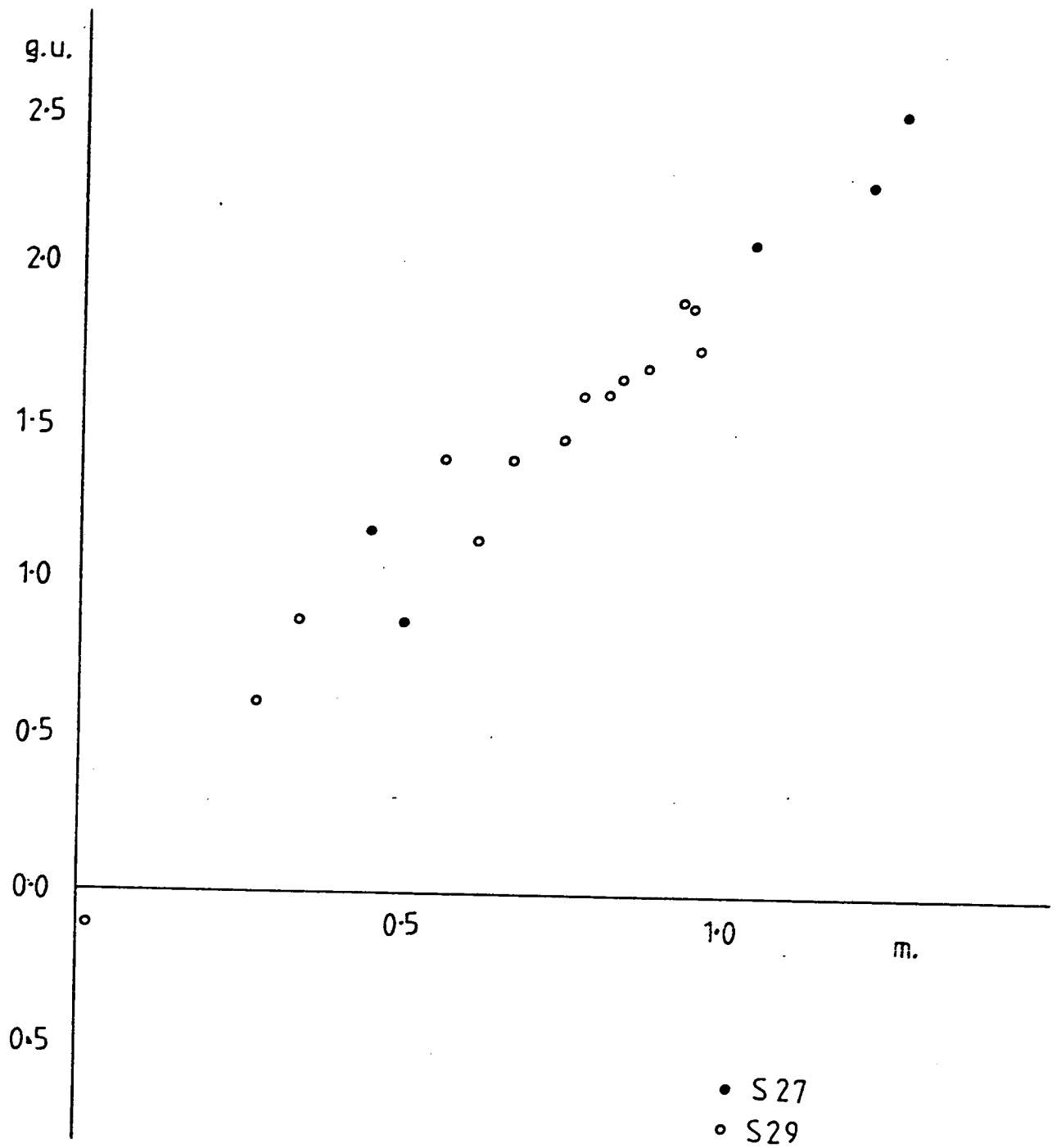


Figure (10.7)

Gravity change versus height change

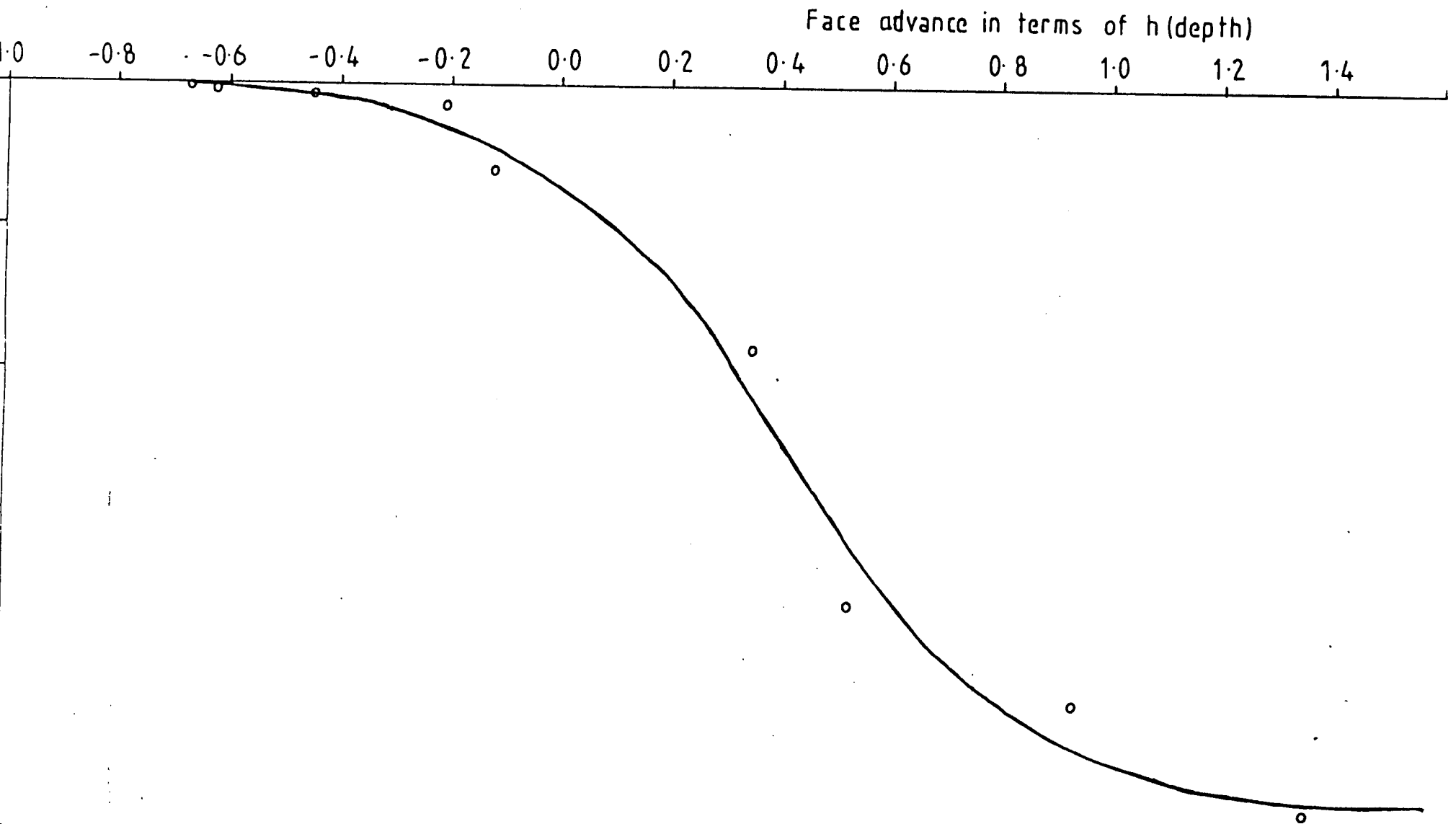
The temporal change of unit S27 was studied in detail by repeated gravity readings over a period of four months. Figure(10.8) illustrates the development of subsidence at a single surface point (station number 17) as unit S27 was extracted beneath it. All but residual subsidence (97.5%)

should cease when the panel face has advanced 0.7 times the seam depth beyond the observation point (National Coal Board, 1975), in this case seventy seven metres. This factor is somewhat variable and in this instance active subsidence terminates at 1.1 times the seam depth but the curve shape is similar to the classic time development curve.

### 10.5 Model Studies

A theoretical gravity profile was calculated in which the seam extraction was numerically modelled in two dimensions following the method of Talwani ( Talwani,M et al., 1959). The two basic models before and after extracion are illustrated in figure (10.9). The coal density of  $1.41 + 0.01$  gm./c.c. is well determined from hand samples by the National Coal Board scientific section (personal communication via R. Longmore). A density contrast of  $1.1$  gm./c.c. was used in the computations. This is consistent with the previous discussion of bedrock density and gave the best fitting model.. The gravity change difference between the two models of figure (10.9) together with the

Figure 10.8  
Subsidence development determined gravimetrically at station no. 17



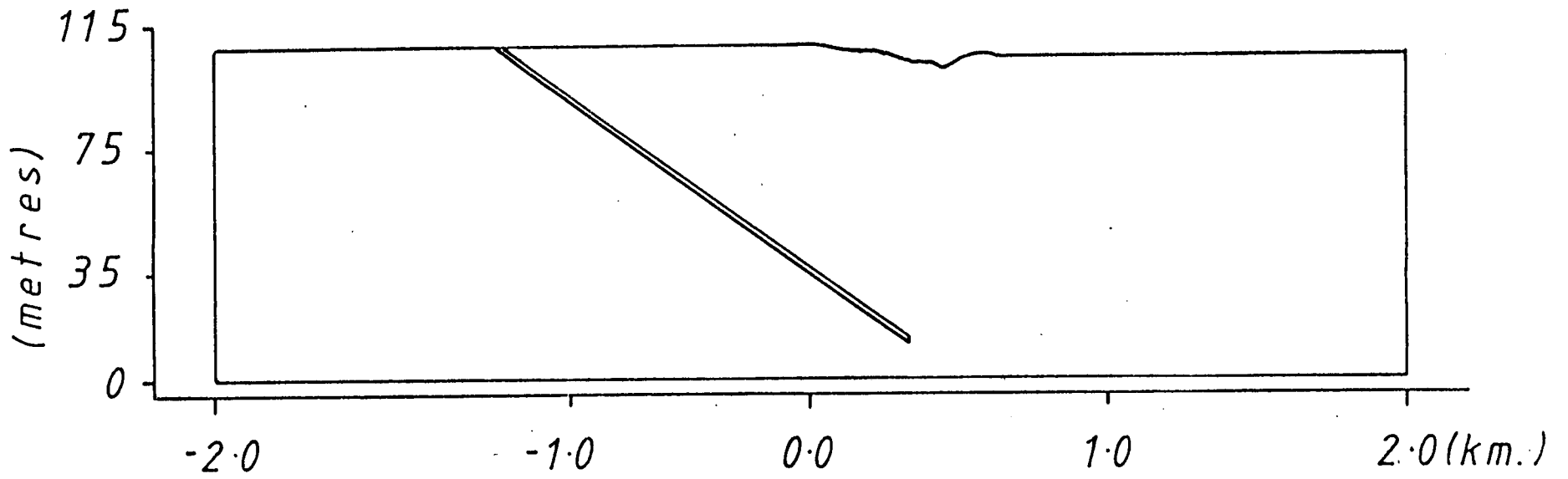
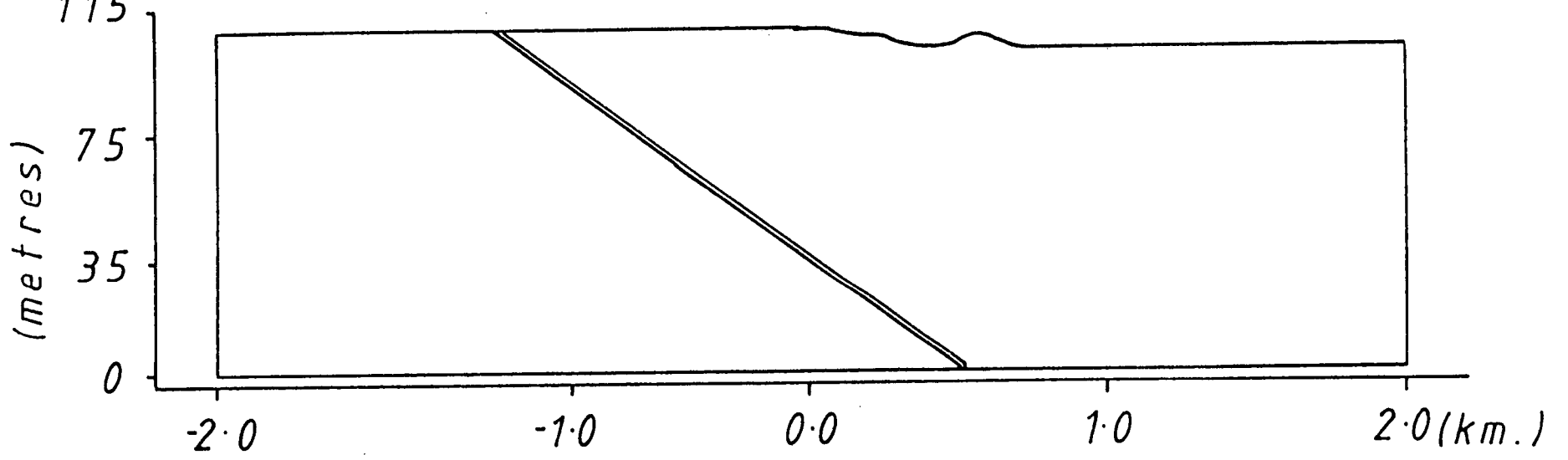


Figure 10.9 Model outline used in two dimensional gravity analysis of seam extraction. (Upper, before extraction; lower, after extraction).

observed profile are shown in figure (10.10). It is possible to estimate the contribution from the removal of the comparatively low density coal seam alone by adjustment of the second model surface.. This is illustrated in figure (10.11) and the effect can be seen to be assymmetric with a maximum amplitude of 0.40 g.u.. If this effect is added to the gravity profile the corrected' gravity height relationship is 2.17 g.u./m with an improved standard deviation of 0.097 g.u./m..

A possible source for the secondary peak in the observed gravity profile of S27 (see figure 10.5) is to be found upon examination the geological sheet for the area ; a simplified diagram is shown in figure (10.12). Detailed examination of the Institute of Geological Sciences sheet number 39E and 'Economic Geology of the Fife Coalfield - Area 1' (Geological Survey Memoirs, Scotland, H.M.S.O.,1930) indicate that the Number 1 Plean Limestone outcrops beneath this point. It is proposed that this local inhomogeneity causes assymmetric slumping of the overburden which can be seen in the level data. Furthermore the higher density limestone may remain protuding as a unit rather than gently subsiding with the adjacent strata possibly causing a small offset fault due to localised stress concentration. Further evidence for this argument is provided by the uncharacteristing cracking of the tarmac road surface directly above this location but not visible elsewhere.

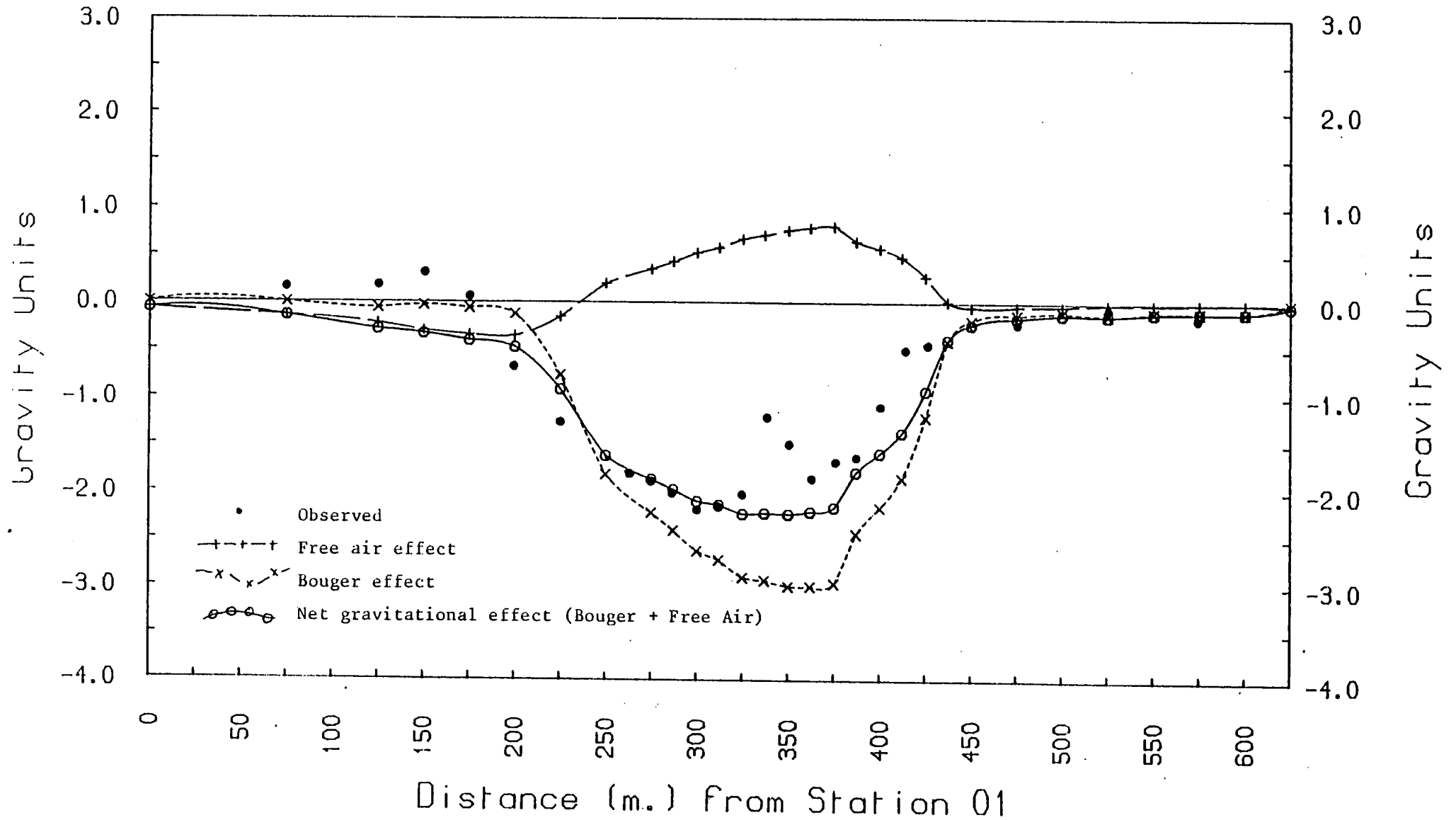


Figure 10.10 Results of two dimensional model studies

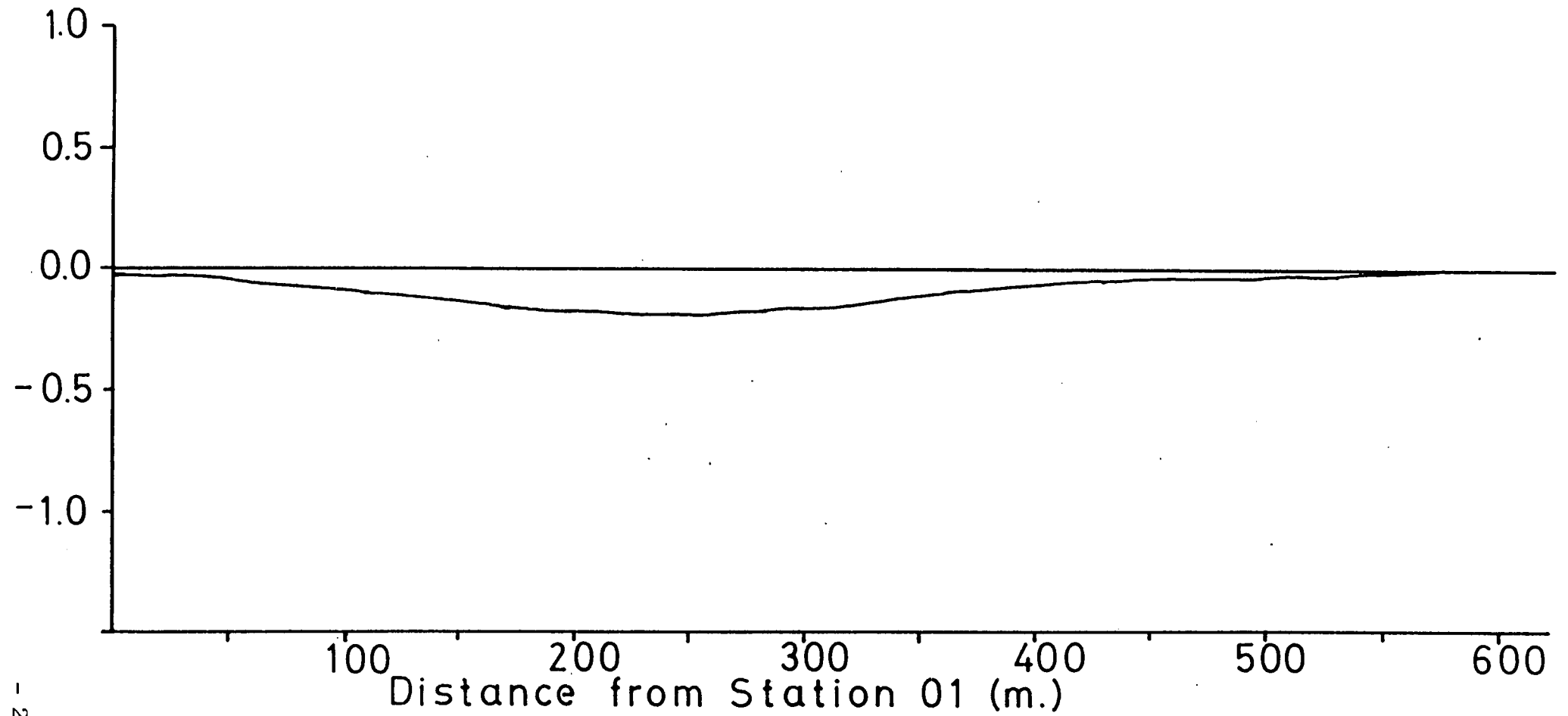


Figure 10.11 Modelled gravitational effect of seam material.

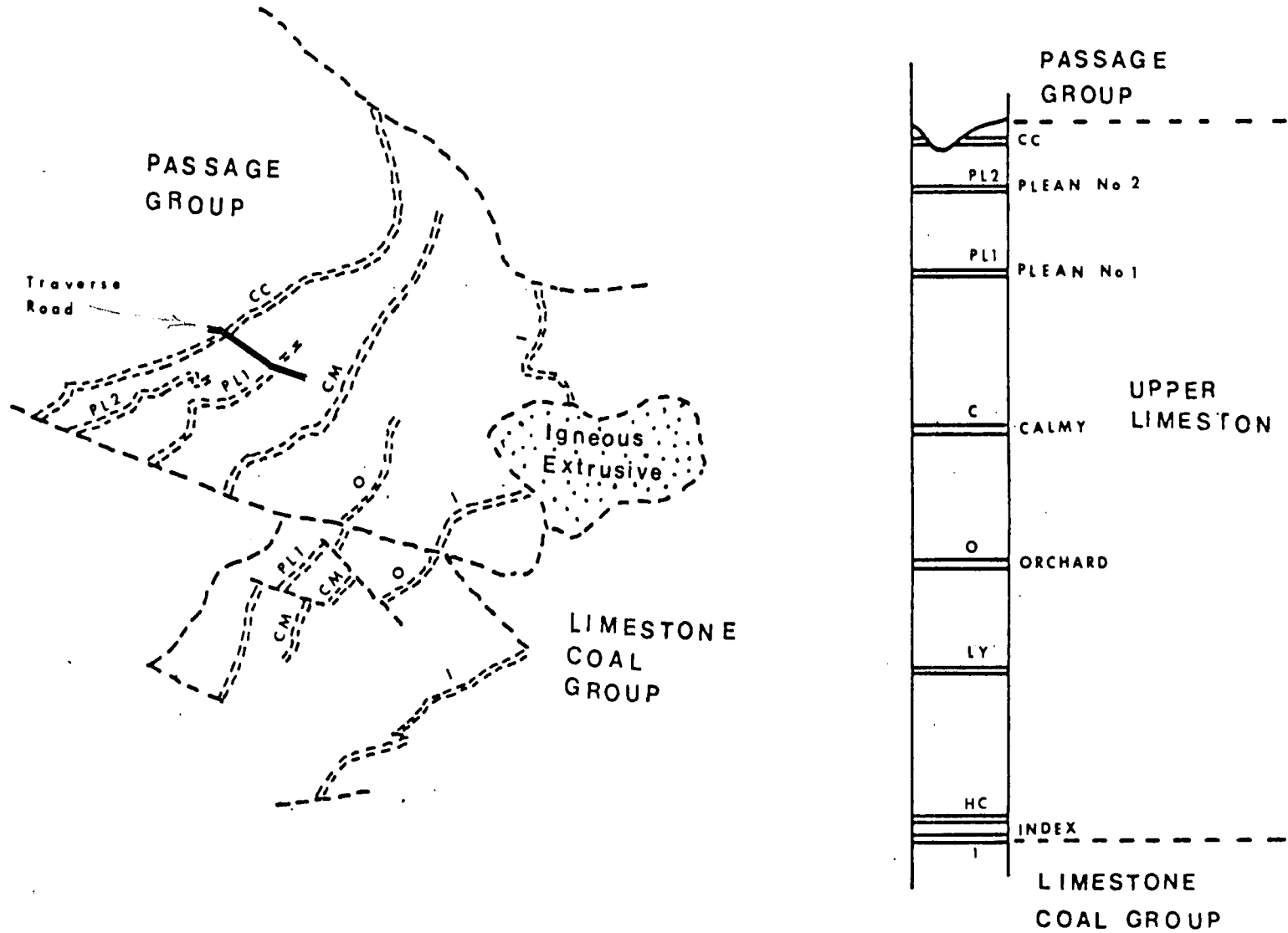


Figure 10.12 Simplified geological map of Solsgirth area.



## 10.6 Conclusions

This small scale study has demonstrated the suitability of gravimetric surveying to the problem of mining subsidence. A gravity survey with a standard deviation of 0.1g.u. can detect elevation changes of 0.05m, which is adequate to assess changes in land drainage - a major source of compensation claims. Levelling in fields, over several kilometres is in fact often less accurate than this figure. The results are sensitive to small scale elevation changes and can be directly related to altitude. This method of inquiry would be particularly suited to subsidence, be it due to mining or say the extraction of water over a large area. The method has the advantage over levelling that observation points may be widely separated and visited in any order in most weather conditions by one person only.

## CHAPTER ELEVEN

### CONCLUSION

#### 11.1 Summary

This work has successfully demonstrated the use of high precision gravimetry in several field studies. The Edinburgh gravity meter has been subject to extensive testing and ancillary equipment manufactured. The instrument testing indicated a low response to environmental effects except magnetic field variations. It also verified the existence of a characteristic drift function after unclamping for this particular instrument. Since such instrumental drift was not linked to any external phenomena it is thought to be associated with clamping induced stress and mechanical hysteresis. The auxillary platform proved useful during Scottish field data collection using the equilibrium technique because of the stable measuring base it provided in conjunction with fundamental bench marks. The attached coincident viewing levels improved the levelling accuracy, but because of the setting up time it is not thought beneficial to use the auxillary platform for other than equilibrium surveys.

Apparatus to tilt the meter, measured by laser interferometry was successfully designed and completed using the secondary plate, but the degree of accuracy is

not presently adequate for the precise calibration of gravity meters. The primary United Kingdom short calibration line appears to be discrepant. Four La Coste and Romberg gravity meters of different ages and usage, independently obtain comparable correction factors, in the range  $8 - 25 \times 10^{-4}$ . These correction factors are unexpectedly large compared to typical values in the literature (less than  $6 \times 10^{-4}$ , Torge, 1971, Nakagawa and Satomura, 1976). They are also inconsistent with observations of the second short calibration line and some stations of the long calibration line undertaken using G-275. A probable correction factor to the short calibration line Hatton Heath - Press is 0.99908, while the earlier Cat and Fiddle - North Rode line is correct.

The data quality of the Eskdalemuir I.D.A. instrument appeared to be of acceptable quality, with slightly lower accuracy than other earth tide stations in Great Britain (see Table 7.3). The standard deviation of unit weight was  $1.4 \times 10^{-8} \text{ m/s}^2$  compared with values of  $0.5 - 0.7 \times 10^{-8} \text{ m/s}^2$  for well maintained La Coste and Romberg Earth Tide meters. But the  $M_2$  load tide is significantly different from a well proven model (Baker, 1980, though this may be attributable to a coarse local model grid), and the  $O_1$  gravimetric factor is unacceptably low for Western Europe (1.083). This apparent lack of accuracy may not be true of other I.D.A. installations, and can only be determined after analysis of the data.

The results of Baker (1980) were used in the reduction of data collected using the equilibrium technique on an expanded Scottish network to study temporal gravity variations. The results of two annual surveys of the expanded network do not achieve the early promise of Hipkin (1978), but attain a level of accuracy similar to the results of conventional high precision surveying (standard deviations between  $5 \times 10^{-8}$  and  $10 \times 10^{-8}$  m/s<sup>2</sup>). The Atalanti network also reveals no significant gravity change over a period over one year. This fact combined with the recent (Jan 1983 - June 1984) lack of seismic activity (I. Main, personal communication)

implies a reduction in the probability of imminent tectonic activity. These gravimetric surveys compare favourably with the work of other investigators.

The mining subsidence survey was initially carried out as an experiment to observe gravity variation in a well controlled setting. The gravity-height correlation was sufficiently well determined to suggest that gravity surveying would be a useful tool in the study of subsidence.

High precision gravity surveying is a neglected area of geophysical investigation. It has been shown to detect precursory tectonic activity (Whitcomb, 1980) and the field measurements acquired by the author are sufficiently

accurate to fulfil that role. Basic field requirements include a familiarity with the individual meter, extreme care during the measuring campaign, a well devised observation and network plan. Tidal corrections (excluding the effects of ocean loading), with an accuracy more than an order of magnitude greater than reading error, can be calculated simply and rapidly by computer. Network adjustment can be similarly calculated.

### Future Work

The results of this study of high precision gravimetry suggest several topics for further work. The Hatton Heath - Prees calibration line adjustment should be examined at the earliest opportunity. Ideally a new survey should be completed using absolute gravimeters and integrated into an accurately determined multiple calibration line. (Similar to the German line with ranges of 2, 20, 200, 2,000, 20,000 g.u.. The 2,000 g.u. range is particularly important as this is just within the range of the model D gravimeter.) This would prove useful to academic and commercial institutions alike. The proposed long calibration line (an extension of the old airport net) is unsatisfactory. Station monumentation is very poor and access is difficult. A laboratory based tilt calibration technique (perhaps based on the laser interferometric arrangement described in Chapter six ) should be developed. A possible improvement to the arrangement described here would be the ability to

determine the direction of movement of the tilt table from the fringe pattern.

The Atalanti network is currently being remeasured on at least an annual basis. It would be desirable to increase the network density and improve the monumentation. The area was carefully selected and will probably be subject to a major seismic event in the near future. Previously published post-earthquake surveys have relied on established low order regional stations subject to large errors (eg. Barnes 1963, Oliver et al., 1976). Frequently observed precise networks will yield new information about tectonic environments. A microgravimetric network is planned for N.W. Turkey; this will benefit from the experience gained in Greece, and is a natural progression in the gravimetric study of seismic risk areas in the E. Mediterranean.

The Scottish network will be remeasured in the future on a long term basis. The existing monumentation involved is so substantial (and legally protected) there is little chance of site eradication. It should prove a valuable control to study gravimeter stability and for the intercomparison of instruments.

## REFERENCES

- Agnew, D., Berger, J., Berglund, R., Farrell, W. and Gilbert, G., (1976). International deployment of accelerometers: a network for very long period seismology, EOS (Trans. A.M. Geophy. Un.), 57, 180-188.
- Airy, G.B., (1856). Phil. Trans. Roy. Soc. London, 146, 297-343.
- Alasia, F., Cannizzo, L., Cerutti, G. and Marson, I., (1981). Absolute measurements with the IMGC transportable gravity meter within 1979 and 1981, Bulletin d'Information B.G.I., 49, 27-37.
- Alsop, L.E. and Kuo, J.T., (1964). The characteristic numbers of semi-diurnal Earth tidal components for various Earth models. Ann. Geophys., 20, 286-300.
- Anderson, D. and Whitcomb, J., (1975). Time dependent seismology, Journal of Geophysical Research, 80, 1497-1503.
- Arzi, A.A., (1975). Microgravimetry for engineering applications, Geophysical Prospecting, 23, 408-425.
- Arzi, A.A., (1977). Discussion on Fajklewicz 1976, Geophysics, 42, 1066-1069.
- Baker, T.F., (1980). Tidal gravity in Britain: tidal loading and the spatial distribution of the marine tide, Geophys. J.R. astr. Soc., 62, 249-267.
- Barnes, D.F., (1966). Gravity changes during the Alaska earthquake, Journal of Geophysical Research, 71, No.2.

- Becker, M., (1981). Results of circular error studies with La Coste and Romberg gravity meters, Bull. D'Inf., Bur. Grav. Int., 49, 72-94.
- Berger, J., Agnew, D.C., Parker, R.L. and Farrell, W., (1979). Seismic system calibration: 2 cross spectral calibration using random binary signals, Bull. Seis. Soc. Amer., 69, No.1, 271-288.
- Blizkovsky, M., (1979). Processing and applications in micro-gravity surveys, Geophys. Pros., 27, 848-861.
- Block, B. and Moore, R.D., (1966). Measurements in the Earth mode frequency range by an electrostatic sensing and feedback gravimeter, Journal of Geophysical Research, 71(3), No.18.
- Blundell, D.J. and Parks, R., (1969). A study of the crustal structure beneath the Irish Sea, Geophys. J.R. astr. Soc., 17, 45-62.
- Boedecker, G., (1981). Instrumental capabilities of La Coste and Romberg gravity meters for detection of small gravity variation with time, Bull. D'Inf. Bur. Grav. Int., 48, 29-47.
- Boedecker, G., (1978). Instrumental investigations and improvements of La Coste and Romberg gravity meters, International Gravity Commission, 8th, Paris.
- Bogdanov, K.T. and Magarik, V.A., (1967). A numerical solution to the problem of the semi-diurnal tidal wave distribution ( $M_2$  and  $S_2$ ) in the world ocean, Proc. (Dokl.) Acad. Sci. USSR, 172, (6), 1315-1317.



- Bogdanov, K.T. and Magarik, V.A., (1969). A numerical solution of the problem of tidal wave propagation in the world ocean, Bull. (Izv.) Acad. Sci. USSR, Atmos. Ocean Phys., 5, (12), 757-761.
- Bomford, G., (1980). Geodesy, 4th Ed., Clarendon Press, Oxford, 855pp.
- Born, M. and Emil, W., (1980). Principles of optics, Pergamon, 1980.
- Boulanger, J.D., (1978). Brief review of research on non-tidal gravity variation, USSR Acad. of Sci. Soviet Geoph. Comm.
- Brien, R., Gerstenecker, C., Kiwiniemi, A. and Petterson, L., (1977). Report on high precision gravimetry, National Land Survey, Sweden.
- Broucke, R.A., Zurn, W. and Schlichter, L.B., (1972). Lunar tidal acceleration on a rigid Earth, Geophysical Mon., 16. Flow and fracture of rocks (The Griggs vol.). A.G.U., 319-324.
- Brown, E.W. (1908). Theory of the motion of the Moon, Mem. R. astron. Soc., 59, 1 - 103.
- Carnizzo, L., Cerutti, G. and Marson, I., (1978). Absolute gravity measurements in Europe, Il Nuovo Cimento, Vol.1C, No.1. International Gravity Commission, 8th, Paris.
- Cartwright, D.E., (1977). Oceanic tides, Rep. Prog. Phys., 40, 665-708.
- Cartwright, D.E. and Edden, A.C., (1973). Corrected tables of tidal harmonics, Geophys. J.R. astr. Soc., 33, 253-264.
- Cartwright, D.E. and Tayler, R.J., (1971). New computations of the tide-generating potential, Geophys. J.R. astr. Soc., 23, 45-74.

- Chen, Yun-Tai, Gu, Hao-ding and Lu, Zao-xun, (1979). Variations of gravity before and after the Haicheng earthquake 1975 and the Tangsham earthquake 1976, *Phys. Earth Planetary Int.*, 18, 330-338.
- Close, C.F., (1965). Textbook on topographic surveying, HMSO, Fourth Ed., 388pp.
- Darwin, Sir G.H., (1879). On the body tides of viscous and semi-elastic spheroids, and the ocean tides on a yielding nucleus, *Phil. Trans. Roy. Soc. London*, 170, 1-35.
- Darwin, Sir G.H., (1880). On the secular changes in the elements of the orbit of a satellite revolving about a tidally distorted planet, *Phil. Trans. Roy. Soc. London*, 171, 713-891.
- Darwin, Sir G.H., (1883). Report of a committee for the harmonic analysis of tidal observations, *Brit. Assoc. Report*, 48-118.
- De Boor, C., (1978). A practical guide to splines, *App. Math Sci.*, 27, Springer Verlag.
- Doodson, A.T., (1921). The harmonic development of the tide-generating potential, *Proc. Roy. Soc.*, V.100, 305-326.
- Dragert, H., Lambert, A. and Liard, J., (1981). Repeated precise gravity measurements on Vancouver Island, British Columbia, *Journal of Geophysical Research*, 86, B7, 6097-6106.
- Draper, N.R. and Smith, H., (1966). Applied regression analysis, John Wiley & Sons, USA, 407pp
- Ducarme, B., Hosoyama, K., Van Ruymbeke, M. and Sato, T., (1976). An attempt to use La Coste and Romberg model G gravimeters at the  $\mu$ -gal levels, *Bull. d'Inf.*, 39.

U.S. Government Printing House , Washington.

Eckert, W.J., Walker, M.J., Eckert, D., Transformations of the lunar co-ordinates and orbital parameters, *Astronomical J.* (1966), 71, 314.

Fajklewicz, Z.J., (1976). Gravity vertical gradient measurements for the detection of small geologic and anthropogenic forms, *Geophysics*, 41.

Farrell, W.E., (1972). Global calculations of tidal loading, *Nature*, 238, 43-44.

Farrell, W.E., (1973). Earth tides, ocean tides and tidal loading, *Phil. Trans. Roy. Soc.*, 274A, 253-259.

Finetti, I., (1976). Mediterranean ridge: a young submerged chain associated with the Hellenic Arc, *Bollet. Geof. Teor. Ed Applic.*, 19, 31-65.

Flather, R.A., (1976). A tidal model of the north-west European continental shelf, *Memoires Soc. Royale des Sciences de Liege*, 10, 6, 141-164.

Galanopoulos, A.G., (1960). A catalogue of shocks with  $I_0 \geq VI$  or  $M \geq 5$  for the years 1801-1958, Athens, 119pp.

Galanopoulos, A.G., (1961). A catalogue of shocks with  $I_0 \geq VI$  or  $M \geq 5$  for the years prior to 1800, Athens, 18pp.

Godin, G., (1972). The analysis of tides, Book, Liverpool University Press.

Goodkind, J.M., (1981). Precision of the superconducting gravimeters determined by simultaneous measurements with two instruments, *Bull. D'Inf. Bur. Grav. Int.*, 49, 128-140.

- Hamilton, A.C. and Brule, B.G., (1967). Vibration induced drift in La Coste and Romberg geodetic gravimeters, *J. Geophys. Res.*, 72.
- Harrison, J.C. and La Coste, L.J.B., (1978). The measurement of surface gravity, *Proc. of Applications of Geodesy to Geodynamics: An International Symposium, Columbus*, (Ed. I. Mueller).
- Heikkinen, M., (1978). On the tide-generating forces, *Pub. of Fin. Geod. Inst.*, No.85.
- Hendershott, M., (1972). The effects of solid earth deformation on global ocean tides, *Geophys. J.R. astr. Soc.*, 29, 389-402.
- Hendershott, M.C. and Munk, W., (1970). Tides, *A Rev. Fluid Mech.*, 2, 205-224.
- Hipkin, R.G., (1978). A microgravimetric network for secular gravity studies in Scotland, *Geophys. J.R. astr. Soc.*, 52, 383-396.
- Holder, A.P. and Bott, M.H.P., (1971). Crustal structure in the vicinity of south-west England, *Geophys. J.R. astr. Soc.*, 23, 465-489.
- Hussain, A. and Walach, G., (1980). Subsurface gravity measurements in a deep intra-alpine tertiary basin, *Geoexploration*, 18, 165-175.
- Institute of Civil Engineers, (1959). Report on mining subsidence, *Inst. of Civil Eng.*, London.
- International Astronomical Union, (1964). System of astronomical constants.
- Jackson, R. and Eaton, G., (1978). Geophysical observations of Kilawa Volcano, Hawaii. Temporal gravity variations related to the 29 November 1975 M = 7.2 Earthquake....., *Journal of Volcanology and*

- Grannell, R. et al., (1982). An assessment on applicability of using precise surface measurements to monitor the response of a geothermal reservoir to exploration, Report submitted on contract 6633802, United States Department of Energy.
- Groten, E., (1971). Measurements of vertical gravity gradient, Bull. Geod., 99, 135-136.
- Groten, E., (1975). Local studies of non-tidal gravity variations in the Rhinegraben zone, Boll. di Geof., Teor. ed Appl., Vol.XX, No.80.
- Groten, (1975). Microgravimetry - high precision observations of small gravity differences, Bull. Geod., 115, 41-56.
- Groten, E., (1981). Introduction to the problems of high precision gravimetry, Bull. D'Inf. Bur. Grav. Int., 49, 15-17.
- Gumbell, E.J., (1966). Statistics of extremes, Columbia University Press, New York, 359pp.
- Hagiwara, Y., (1978). Recent non-tidal gravity changes during earthquake activities in Japan, Boll. di Geof., Vol.XX, No.80.
- Hagiwara, Y., (1980). Gravity changes over the East-Izu Uplift, Japan, J. Phys. Earth, 28, 553-564.
- Hammer, S., (1950). Density determinations by underground gravity measurements, Geophysics,
- Hammer, S., Nettleton, L.L. and Hastings, W.K., (1945). Gravimeter prospecting for chromite in Cuba, Geophysics, 10, (1), 34-49.

- Jolly, H.L.P. and Wolff, A.J., (1922). The second geodetic levelling of England and Wales 1912-1921, HMSO, London.
- Kanngieser, E. and Torge, W., (1981). Calibration of La Coste and Romberg gravity meters model G and D, Bull. D'Inf. Bur. Grav. Int., 49, 50-63.
- Kanngieser, E., Torge, W. and Wenzel, H.G., (1978). Direct comparison of absolute and relative gravity measurements in the Federal Republic of Germany and in N.W. Europe, International Gravity Commission, Paris.
- Karnik, V., (1969). Seismicity of the European area, Part 1, D. Reidel Publishing Co., Dordrecht-Holland, 364pp.
- Karnik, V., (1971). Seismicity of the European Area, Part 2, D. Reidel Publishing Co., Dordrecht-Holland, 218pp.
- Kelsey, J., (1972). Geodetic aspects concerning possible subsidence in S.E. England, Phil. Trans. Roy. Soc., 272, 141-149.
- Kisslinger, C., (1975). Processes during the Matsushiro, Japan Earthquake swarm as revealed by levelling gravity and spring-flow observations, Geology, 3, 57-62.
- Kiviniemi, A., (1974). High precision measurements for studying the secular variation in gravity in Finland, Pub. of the Finnish Geodetic Inst., No.78.
- La Coste, L.J.B., (1934). A new type long period vertical seismograph, Physics, Vol.5, Part 7.

- Lagios, E. and Hipkin, R.G., (1981). Gravity measurements in S.E. Scotland, Geophys. J.R. astr. Soc., 65, 505-506.
- La Coste, L.J.B., (1935). A simplification in the conditions for the zero length spring seismograph, Bull. Seism. Am., 25.
- Lambeck, K., (1980). The earth's variable rotation, Cambridge University Press, 449pp.
- Lambert, A. and Liard, J.O., (1981). Non-linearities in La Coste and Romberg model D gravimeters determined by the "Cloudcroft Junior" method, Bull. D'Inf. Bur. Grav. Int., 49, 95-105.
- Longman, I.M., (1959). Formulas for computing the tidal accelerations due to the Moon and Sun, J. Geophys. Res., 64, 12.
- Longman, I.M., (1963). A Green's function for determining the deformation of the Earth under surface mass loads, J. Geophys. Res., 68, 485-496.
- Love, A.E.H., (1909). The yielding of the Earth to disturbing forces, Proc. Roy. Soc. London, 82, 73-82.
- McConnell, R.K., Hearty, D.B. and Winter, P.J., (1975). An evaluation of the La Coste and Romberg model D microgravimeter, Bull. D'Inf. Bur. Grav. Int., 36, 35-45.
- McKenzie, D.P., (1972). Active tectonics of the Mediterranean region, Geophys. J.R. astr. Soc., 30, 109-185.
- McKenzie, D.P., (1977). Active tectonics of the Alpine-Himalayan belt: The Aegean Sea and surrounding regions, Geophys. J.R. astr. Soc., 217-254.
- McLean, A.C., (1961). Density measurements of rocks in S.W. Scotland, Proc. Roy. Soc. Edin. (B), 68, 103-111.

- Makris, J., (1978). The crust and upper mantle of the Aegean region from deep seismic soundings, *Tectonophysics*, 46, 269-284.
- Makropoulos, K.C., (1978). The statistics of large earthquake magnitude and an evaluation of Greek seismicity, Unpub. Thesis, Edinburgh University, 193pp.
- Makrououlos, K.C. and Burton, P.W., (1981). A catalogue of seismicity in Greece and adjacent areas, *Geophys. J.R. astr. Soc.*, 65, 741-762.
- Masson-Smith, D., Howell, P.M. and Abernethy-Clark, A.B.D.E., (1974). The Nation Gravity Reference Net 1973 (NGRN73), Ordnance Survey Prof. papers No.26, O.S. Southampton.
- Melton, B.S., (1971). The La Coste suspension - principles and practice, *Geophys. J.R. astr. Soc.*, 22, 521-543.
- Melchior, P., Kuo, J.T. and Ducarme, B., (1976). Earth tide gravity maps for western Europe, *Phys. Earth Planet Int.*, 13, 184-196.
- Mercier, J.L., (1977). Principle results of a neotectonic study of the Aegean Arc and its localisation within the Eastern Med., 1281-1290, Athens.
- Morelli, C. et al., (1974). The International Gravity Standardization Net 1971 (IGSN71), International Union of Geodesy and Geophysics, Paris, 194pp.
- Mohammed, I., ( ). Earth tide studies on Mt. Etna, Unpublished Ph.D. Thesis, Imperial College, London.
- Moore, R.D. and Farrell, W.E., (1970). Linearization and calibration of electrostatically feedback gravimeters, *J. Geophys. Res.*, 75, 5, 928-932.



- Nakagawa, I., (1975). On characteristic of La Coste and Romberg gravimeters (Model G). International Union of Geodesists and Geophysicists, 16th Gen. Ass.
- Nakagawa, I. and Satomura, M., (1978). An accuracy of scale constant of La Coste and Romberg gravimeters revealed by International and Domestic gravimetric connections. International Gravity Commission, 8th, Paris.
- National Coal Board, Mining Department, (1975). Subsidence engineer's handbook, National Coal Board, London, 111pp.
- Newcomb, S., (1895). Tables of the rotation of the Earth on its axis and around the Sun, A.P.A.E., 6, Part 1.
- Neumann, R., (1967). La gravimetric de haute precision, Application aux recherches de cartes. Geophysical Prospecting, 15, 167, 116-134.
- Oliver, H.W., Robbins, S.L., Grannell, R.S., Alewine, R.W. and Biehler, S., (1975). Surface and subsurface movements determined by remeasuring gravity, Bull. of Cal. Div. of Mines and Geol., 196, 195-212.
- Orchard, R.I., (1964). Surface subsidence resulting from alternative treatments of colliery goaf, Colliery Engineering, October 1964.
- Parasnis, D.S., (1966). Mining geophysics, Elsevier, Amsterdam.
- Pekeris, C.L. and Accad, Y., (1972). Dynamics of the liquid core of the Earth, Phil. Trans. R. Soc. London, A273, 237-260.
- Pettersson, L., (1978). High precision gravity measurements for studying the secular variation of gravity in Fennoscandia, Presented at the 8th International Gravity Commission, Paris.

- Philippon, A., (1930). Beitrage zur Morphologie Griechenlands, Stuttgart, 47pp.
- Poincare, H., (1910). Sur la precession des corps deformables, Bull. Astron., 27, 321-356.
- Rice, J.R., (1964). The approximation of functions, Vol.1 Linear theory, Addison-Wesley, Massachussetts, 199pp.
- Richter, C.F., (1958). Elementary seismology, Freeman and Co., San Francisco, 766pp.
- Rikitake, T., (1975). Earthquake precursors, Bull. Seis. Soc. Amer., 65, 5, 1133-1162.
- Rossiter, J.R., (1972). Sea level observations and the secular variation, Phil. Trans. Roy. Soc., 272, 131-139.
- Rundle, J.B., (1978). Gravity changes and the poludale bulge, Geophys. Res. Letters, 5, 41-44.
- Sakuma, A., (1971). Observations experimentales de la constance de la pesantaur au BIPM, Bull. Geod., 100, 159-164.
- Sakuma, A., (1983). A industrialized absolute gravimeter: Type GA60. A description of the instrument and its trial use in the French gravity net. Bull. D'Inf. Bur. Grav. Int., 53, 114-118.
- Sanderson, T., (1982). Mount Etna : Direct gravity observation of magma movements, unpub. PhD. thesis, Imperial College, University of London.

- Sato, T., (1977). On an instrumental phase delay of the La Coste and Romberg gravimeter, Bonn. Conf.
- Schleusener, A., (1943). Die gravimetermessungen in niemczyk, (Ed), "Spalten Auf Island", Wittwer, Stuttgart, 124-175.
- Schuller, K., (1977). Tidal analysis by the hybrid least squares frequency domain convolution method, Proc. of the 8th Int. Symp. on earth tides, Bonn, 103-128.
- Schwiderski, E.W., (1980). On charting global ocean tides, Rev. Geophy. and Space, 18, 7, 243-68.
- Shida, T., (1912). Horizontal pendulum observations of the change of plumb line at Kamigano, Kyoto, Mem. of Coll. Sc. and Eng. Kyoto Imp. Univ., IV, 23-174.
- Sissons, J.B., (1967). Evolution of Scotland's scenery, Edinburgh.
- Stacey, F.D., (1977). Physics of the Earth, John Wiley and Sons, New York, 414pp.
- Stacey, F.D., Tuck, G., Holding, S.C., Maher, A.R. and Morris, D., (1981). Constraint on the planetary scale value of the Newtonian gravitational constant from the gravity profile within a mine, Physical Rev. D., 23, 8, 1683-1692.
- Takeuchi, H., (1950). On the earth tide of the compressible earth of variable sensity and elasticity, Trans. Am. Geophys. Union, 31, (5), 651-689.

- Takeuchi, H., Saito, M. and Kobayashi, N., (1962). Statistical deformations and free oscillations of a model Earth, J. Geophys. Res., 67, 1141-1154.
- Talwani, M., Worzel, J.L. and Landisman, M., (1959). Rapid gravity computations for two dimensional bodies, with application to the Mendocino submarine fracture zone, J. Geophys. Res., 64, 49-59.
- Thompson, K.R., (1980). An analysis of British monthly mean sea level, Geophys. J.R. astr. Soc., 63, 57-74.
- Tomaschek, R., (1952). Harmonic analysis of tidal gravity experiments at Peebles and Kirklington, Geophys. Supp. to Mon. Notes Roy. astr. Soc.
- Torge, W., (1971). Determination of the calibration factors of La Coste and Romberg gravity meters and time variation in the calibration, Boll. di Geof. Teor. ed Appl., Vol.XIII, No.51/52, 298-305.
- Torge, W. and Drewes, H., (1977). Gravity variations with time in Northern Iceland 1965-1975, J. Geophys., 43, 771-790.
- Torge, W. and Kanngieser, E., (1980). Gravity and height variations during the present rifting episode in N. Iceland, J. Geophysics, 47, 125-131.
- Vanicek, P., (1980). Tidal corrections to geodetic quantities, NOAA Tech. Report, Nos.83 NGS 14, USA.
- Walsh, J.B., (1975). An analysis of local changes in gravity due to deformation, Pageoph., 113, 98-106.

- Wenzel, H.-G., (1976). Zur Genauigkeit von gravimetrischen erdgezertenbeobachtungen, Hannover, No.67.
- Weir, A., (1969). Principles of ground movement, Paper presented at "Mining Subsidence" Heriot-Watt University, Edinburgh.
- Whitcomb, J.H., (1976). New vertical geodesy, J. Geophys. Res., 81, 26, 4937-4944.
- Whitcomb, J.H., Wolfgang, F.O., Given, J.W., Pechmann, J.C. and Ruff, L.J., (1980). Time dependent gravity in southern California, May 1974 - April 1979, J. Geophys. Res., 85, B8, 4563-4573.
- Williams, J.W., (1983). La Coste and Romberg gravity meters. Laboratory investigations into the effects of changes of air pressure, temperature and meter supply voltage, Bur. of Min. Res. Geol. and Geoph.
- Wold, S., (1974). Spline functions in data analysis, Technometrics, 16, 1-11.
- Yaramanci, U., (1977). The difference between various tidal analysis methods, Proc. 8th Int. Symp. on Earth Tides, Bonn.
- Zschau, J., (1978). Tidal friction in the solid earth: loading versus body tides, In: Tidal Friction and the Earth's Rotation, Ed. by Brosche and Sundermann, Springer Verlag, Berlin, 62-94.

APPENDIX 1

Computer Program: NSPL

Parms set: FIXED

Edinburgh Fortran77 Compiler Release 3.5

```
1
2
3
4          PROGRAM NSPL
5
6
7      C          FITTING CUBIC SPLINES TO SINGLE VALUED
8      C          REAL DATA WITH AN ARBITRARY NUMBER AND DISPOSITION
9      C          OF KNOTS IN A LEAST SQUARES SENSE WITH THE ABILITY TO
10     C          'JOIN' OR 'SUPERIMPOSE' INDEPENDENT DATA SETS
11
12
13
14
15
16
17     C          DECLARATIONS
18
19         DIMENSION RMSM(130),RMSMM(130),NAME(130,4),RMSL(130),RMSLL(130)
20     E         ,DRIFT(600)
21         REAL*8 TIME(600),TSTART(130),GRAV(600),TNODE(130),A(130,130)
22     E         ,OBSERV(600,130),ALPHA(130,130),BETA(130),H(130),AUSED(130,130)
23     E         ,BUSED(130),GRAVO(130),GMAX,GMIN,HSUM,TDIFF,TGAP,TIME1,TIME2
24     E         ,BN(130),TIMEF(600),GDIFF(130),DRIFTF(600),LDIFF(130),C(130)
25     E         ,AL(2,2),BL(2),TSSUM,YSUM,YSSUM,TS(130),TSSQD,DETA,LLEVEL(130)
26     E         ,LEVEL(130),SLOPE(4),B(130,130),AN(130),Y(130),WSPCE(130)
27
28         CHARACTER*16 HEAD
29         INTEGER NUMBM(130),NUMBL(130),SET(600,3),
30     E         PDRIFT,PARTS,J,M,N,MZERO,IFNODE,PPARTS,PM
31         LOGICAL L1,L2,L3
32
33         CHARACTER CONS(2)*15
34         DATA CONS/' UNCONSTRAINED ',' CONSTRAINED '/'
35
36     C          DATA INPUT AND ORGANISATION
37
38     C          READ CONTROL PARAMETERS
39
40
41         CALL EMASFC ('DEFINE',6,'FT01,.IN',8)
42         CALL EMASFC ('DEFINE',6,'FT02,.OUT',9)
43         WRITE (2,('( ' ENDS CONSTRAINED ? (T/F) '))')
44         READ(1,'(L1)') L1
45         IF (L1) CONS(1) = CONS(2)
46         INAME = 0
47
48     C          J =          NUMBER OF OBSERVATIONS: (J<301)
49     C          M =          NUMBER OF DIFFERENT GRAVITY SITES: (M<11)
50     C          N =          NUMBER OF NODAL INTERVALS
51     C          PARTS =      NUMBER OF PARTS OF DATA SET: (PARTS<21)
```

```

52 C           AN ADJUSTED DATUM "LEVEL" IS COMPUTED FOR EACH PART
53 C           PARTS > 1:  PARTS SUPERIMPOSED WITH COINCIDENT INITIAL TIMES
54 C           PARTS < -1:  PARTS JOINED END TO END AFTER GAPS OF TGAP
55 C           WARNING! N+M+PARTS+3 < 51
56 C           MZERO =     NUMBER OF GRAVITY DATUM SITE
57 C           IFNODE = 0  FOR NODES AT EQUAL INTERVALS
58 C           IFNODE > 10 RERUNS PROGRAM WITH DIFFERENT NUMBERS OF NODES
59 C                   BETWEEN IFNODE-10 AND N
60 C           IFNODE = 1  FOR NODES AS SPECIFIED BELOW
61 C           PDRIFT = 0  NO OUTPUT OF DRIFT DATA
62 C           PDRIFT = 1  OUTPUT OF DRIFT DATA TO CHANNAL 6
63 C           PDRIFT = 2  OUTPUT OF DRIFT DATA TO CHANNAL 3
64 1 READ (4, '(7I4)') J,M,N,PARTS,MZERO,IFNODE,PDRIFT
65   PM = M
66   PPARTS = PARTS
67
68   IF (M.GT.0) GO TO 5
69   M= -M
70   INAME = 1
71 5 CONTINUE
72   MDUM = M
73   IF (MZERO.LT.0) THEN
74     INAME = 0
75     MZERO = - MZERO
76     M = 1
77   END IF
78   IF (J.EQ.0) GO TO 10000
79
80
81
82 C           READ TITLE
83
84   READ (4, '(A16)') HEAD
85
86 C           READ SITE NAMES AND THEIR GRAVITY DATUMS
87
88   READ (4, '(4A4,F11.4)') ((NAME(IM,I),I=1,4),GRAVO(IM),IM=1,MDUM)
89   WRITE (50, '( ' ' ',4A4,F11.4)') ((NAME(IM,I),I=1,4),GRAVO(IM),
90   £                               IM=1,MDUM)
91
92   IF (PARTS-1) 9,11,8
93
94 C           OPTIONAL READ FOR PARTS>1
95
96   8 READ(4,5003) (TSTART(IPART),IPART=1,PARTS)
97   5003 FORMAT (F12.5)
98   GO TO 11
99   9 PARTS=-PARTS
100  TDIFF=0.000
101
102 C           OPTIONAL READS FOR PARTS<-1
103
104   READ (4,5003) TGAP
105   DO 10 IPART=1,PARTS
106     READ (4,5003) TIME1,TIME2
107     TSTART(IPART)=TIME1-TDIFF-TGAP*(IPART-1)
108   10 TDIFF=TDIFF+TIME2-TIME1
109
110 C           OPTIONAL READ FOR IFNODE=1
111

```



```

112      11  NPLUS1=N+1
113      IF (IFNODE.NE.1) GO TO 12
114      READ (4,5003) (TNODE(IN),IN=1,NPLUS1)
115      TSCALE=TNODE(NPLUS1)-TNODE(1)
116
117  C          READ TIME, GRAVITY AND SITE NUMBER
118
119      12 DO 650 IJ = 1,J
120          READ (4,5004) (TIME(IJ),GRAV(IJ),SET(IJ,2),SET(IJ,3))
121  5004      FORMAT (2F12.5,2I3)
122          WRITE (7,'(2I3)') SET (IJ,2),SET (IJ,3)
123
124  C          SET(IJ,2) = NUMBER OF GRAVITY STATION SITE
125  C          SET(IJ,3) = NUMBER OF PART OF DATA SET
126
127      650      CONTINUE
128
129          DO 13 IJ=1,J
130      13  GRAV(IJ)=GRAV(IJ)+GRAV0(SET(IJ,2))
131          CALL DMXMIN(J,GRAV,GMAX,IJMAX,GMIN,IJMIN)
132          GSCALE=GMAX-GMIN
133          IF (PARTS.EQ.1) GO TO 20
134          DO 14 IFRED=1,J
135      14  TIME(IFRED)=TIME(IFRED)-TSTART(SET(IFRED,3))
136
137  C          DEFINE NODAL TIMES AND PARAMETERS
138
139      20 IF (IFNODE.EQ.1) GO TO 21
140          CALL DMXMIN(J,TIME,TNODE(NPLUS1),ITMAX,TNODE(1),ITMIN)
141          TSCALE=TNODE(NPLUS1)-TNODE(1)
142          IF (IFNODE.LT.11) GO TO 21
143          NFIRST=IFNODE-10
144          NLAST = N
145          GO TO 49
146      21 NFIRST = 1
147          NLAST = 1
148
149
150      49      DO 20000 N=NFIRST,NLAST
151          N1=N-1
152          MN3=M+N+3
153          NPLUS1=N+1
154          NPLUS2=N+2
155          NPLUS3=N+3
156          NPLUS4=N+4
157          IF (PARTS.GT.1) MN3=MN3+PARTS
158          IF (IFNODE.EQ.1) GO TO 23
159          TINT=TSCALE/N
160          DO 22 IN=1,N
161      22      TNODE(IN+1)=TNODE(1)+TINT*IN
162
163      23 IF (PDRIFT.EQ.1) WRITE(6,'('' NODAL TIMES'',//,F12.5)')
164  E          (TNODE(IN),IN=1,NPLUS1)
165
166          WRITE(6,'(///I4,A15,'''NODAL INTERVAL OF ''',F12.5,
167  E          '' DAYS STARTING AT ''',F12.5)') NPLUS1,CONS(1),TINT,TNODE(1)
168          WRITE(9,'(I4,A15,'''NODAL INTERVAL OF ''',F12.5,
169  E          '' DAYS STARTING AT ''',F12.5)') NPLUS1,CONS(1),TINT,TNODE(1)
170
171  C          NORMALISE TIME AND GRAVITY MEASUREMENTS AND

```

```

172 C                               SET OBSERV EQUAL TO ZERO
173
174 DO 100 IJ=1,J
175 GRAV(IJ)=(GRAV(IJ)-GMIN)/GSCALE
176 DRIFT(IJ)=0.0
177
178 C           ASSIGN SET(IJ,1) = NUMBER OF THE PRECEEDING NODE
179
180 SET(IJ,1)=N
181 IF (N.EQ.1) GO TO 55
182 DO 50 IN=2,N
183 IF (TIME(IJ).GE.TNODE(NPLUS2-IN)) GO TO 55
184 SET(IJ,1)=NPLUS1-IN
185 50 CONTINUE
186 55 CONTINUE
187 TIME(IJ)=(TIME(IJ)-TNODE(SET(IJ,1)))/TSCALE
188 DO 100 I=1,MN3
189 100 OBSERV(IJ,I)=0.0
190
191 C                               NORMALISE NODE TIMES AND SET MATRICES
192 C                               A & B EQUAL TO ZERO
193
194 TNODE(1)=TNODE(1)/TSCALE
195 DO 200 IN=1,N
196 INADD1=IN+1
197 TNODE(INADD1)=TNODE(INADD1)/TSCALE
198 H(IN)=TNODE(INADD1)-TNODE(IN)
199 DO 200 I=1,NPLUS2
200 200 A(IN,I)=0.0
201 B(IN,I)=0.0
202
203
204 C                               SPLINE FITTING
205
206 C           BETWEEN TNODE(N) AND TNODE(N+1),
207 C           DRIFT = A(N) + B(N)*T + C(N)*T*T + D(N)*T*T*T
208 C           WHERE T = TIME - TNODE(N)
209
210 C           THE UNKNOWNNS X(I) (I=1,M+N+PARTS+3) ARE:
211 C           X(1) = A(1)
212 C           X(2) = B(1)
213 C           X(3) = C(1)
214 C           .....
215 C           X(N+3) = C(N+1)
216 C           X(N+4) = G(1)
217 C           .....
218 C           X(N+M+3) = G(M)
219 C           X(N+M+4) = LEVEL(1)
220 C           .....
221 C           X(N+M+PARTS+3) = LEVEL(PARTS)
222
223 C           AFTER THE SOLUTION OF THE NORMALS EQUATIONS
224 C           ALPHA * X = BETA
225 C           THE UNKNOWNNS X ARE RETURNED IN BETA
226
227 C           EVALUATE MATRICES A(N) AND B(N)
228
229 DO 400 IN=1,N
230 IN1=IN-1
231 A(IN,1)=1.0

```

```

232      B(IN,2)=1.0
233      IF (IN.EQ.1) GO TO 400
234      A(IN,2)=TNODE(IN)-TNODE(1)
235      A(IN,3)=2.0*H(1)*H(1)/3.0
236      A(IN,IN+2)=H(IN1)*H(IN1)/3.0
237      B(IN,3)=H(1)
238      B(IN,IN+2)=H(IN1)
239      IF(IN.EQ.2) GO TO 400
240      A(IN,3)=A(IN,3)+H(1)*(TNODE(IN)-TNODE(2))
241      A(IN,IN+1)=(H(IN1)+H(IN-2))*(2.0*H(IN1)+H(IN-2))/3.0
242          DO 300 I=2,IN1
243              B(IN,I+2)=B(IN,I+2)+H(I)+H(I-1)
244              IF (IN.EQ.3) GO TO 300
245              IF (I.EQ.IN1) GO TO 300
246              A(IN,I+2)=A(IN,I+2)+(H(I)+H(I-1))*((2.0*H(I)+H(I-1))/3.0
247          E          +TNODE(IN)-TNODE(I+1))
248      300      CONTINUE
249      400      CONTINUE
250
251      C          SET UP OBSERVATIONAL EQUATIONS
252
253          DO 600 IJ=1,J
254      C          COEFFICIENT OF G(M)
255          OBSERV(IJ,SET(IJ,2)+NPLUS3)=1.0
256          IF (PARTS.LE.1) GO TO 450
257      C          COEFFICIENT OF LEVEL OF PART DATA SET
258          OBSERV(IJ,SET(IJ,3)+NPLUS3+M)=1.0
259      C          COEFFICIENT OF C(N) FROM C(N) AND D(N)
260      450      TIME2=TIME(IJ)*TIME(IJ)
261              TIME3=TIME2*TIME(IJ)/(3.0*H(SET(IJ,1)))
262              OBSERV(IJ,SET(IJ,1)+2)=TIME2-TIME3
263      C          COEFFICIENT OF C(N+1) FROM D(N)
264          OBSERV(IJ,SET(IJ,1)+3)=OBSERV(IJ,SET(IJ,1)+3)+TIME3
265      C          COEFFICIENTS FORM A(N) AND B(N)
266          DO 600 I=1,NPLUS2
267      600      OBSERV(IJ,I)=OBSERV(IJ,I)+A(SET(IJ,1),I)+B(SET(IJ,1),I)*TIME(IJ)
268
269      C          SET UP THE NORMAL EQUATIONS
270
271          DO 800 NORMAL=1,MN3
272          BETA(NORMAL)=0.0
273          DO 700 II=1,MN3
274      700      ALPHA(NORMAL,II)=0.0
275          DO 800 IJ=1,J
276          BETA(NORMAL)=BETA(NORMAL)+GRAV(IJ)*OBSERV(IJ,NORMAL)
277          DO 800 I=1,MN3
278          ALPHA(NORMAL,I)=ALPHA(NORMAL,I)+OBSERV(IJ,NORMAL)*OBSERV(IJ,I)
279      800      CONTINUE
280          DO 801 I=1,MN3
281          ALPHA(NPLUS4+M,I)=0.0
282          ALPHA(NPLUS3+MZERO,I)=0.0
283      801      CONTINUE
284          ALPHA(NPLUS4+M,NPLUS4+M)=1.0
285          BETA(NPLUS4+M)=0.0
286          ALPHA(NPLUS3+MZERO,NPLUS3+MZERO)=1.0
287          BETA(NPLUS3+MZERO)=0.0
288
289      C          SETTING THE SECOND DERIVATIVE EQUAL TO ZERO AT THE ENDS
290
291          IF (.NOT.L1) GO TO 816

```

```

292      DO 802 I=1,MN3
293      ALPHA(3,I)=0.0
294      ALPHA(NPLUS3,I)=0.0
295      802      CONTINUE
296      ALPHA(3,3)=1.0
297      ALPHA(NPLUS3,NPLUS3)=1.0
298      BETA(3)=0.0
299      BETA(NPLUS3)=0.0
300
301      816      IF(INAME.EQ.0) GO TO 815
302      DO 810 IM = 1,M
303      DO 805 I= 1,MN3
304      805      ALPHA(NPLUS3+IM,I)=0.0
305      ALPHA( NPLUS3 + IM, NPLUS3 + IM ) = 1.0
306      810      BETA (NPLUS3+IM) = 0.0
307      815      CONTINUE
308
309      C          SOLVE THE NORMAL EQUATIONS
310
311      CALL NAGSOLVE (AUSED,ALPHA,BETA,MN3,130,WSPCE)
312
313
314      IF (PDRIFT.NE.2) GO TO 880
315
316      C          EVALUATION OF DRIFT AT EQUAL INTERVALS FOR PLOTTING
317
318      HSUM=TNODE(1)
319      DO 870 IN=1,N
320      AN(IN)=0.0
321      BN(IN)=0.0
322      IN2=IN+2
323      IN10=(IN-1)*10.0
324      DO 850 I=2,IN2
325      AN(IN)=AN(IN)+A(IN,I)*BETA(I)
326      850      BN(IN)=BN(IN)+B(IN,I)*BETA(I)
327      DO 860 INT=1,10
328      TINTF=H(IN)*(INT-1)/10.0
329      DRIFTF(IN10+INT)=GSCALE*(AN(IN)+TINTF*(BN(IN)+TINTF*(BETA(IN2)+
330      £          TINTF*(BETA(IN2+1)-BETA(IN2)))/(3.0*H(IN))))
331      860      TIMEF(IN10+INT)=TSCALE*(HSUM+TINTF)
332      870      HSUM=HSUM+H(IN)
333      K=N*10+1
334      IN = IN - 1
335      DRIFTF(K)=GSCALE*(AN(IN)+H(IN)*(BN(IN)+
336      £          H(IN)*(2.0*BETA(IN2)+BETA(IN2+1))/3.0))
337      TIMEF(K)=HSUM*TSCALE
338      C
339      C
340      C          EVALUATE THE RESIDUALS
341      C
342      C
343      880      RMS=0.0
344      YSUM = 0.0
345      YSSUM = 0.0
346      TSSQD = 0.0
347      TSSUM = 0.0
348      C
349      DO 900 IM=1,M
350      NUMBM(IM)=0

```

```

351     900   RMSM(IM)=0.0
352         DO 950 IPART=1,PARTS
353         RMSLL(IPART) = 0.0
354         RMSL(IPART) = 0.0
355         NUMBLL = 0
356         NUMBL(IPART) = 0
357         IF (PARTS.GT.1) TS(IPART) = TSTART(IPART) - TSTART(1)
358         LEVEL(IPART)= BETA(NPLUS3+M+IPART)*GSCALE
359     950   LLEVEL(IPART) = LEVEL(IPART)
360 C
361         DO 1050 IJ=1,J
362         TIME(IJ)=(TIME(IJ)+TNODE(SET(IJ,1)))*TSCALE
363         DO 1000 I=2,NPLUS3
364     1000   DRIFT(IJ)=DRIFT(IJ)+OBSERV(IJ,I)*BETA(I)*GSCALE
365         GRAV(IJ)=(GRAV(IJ)-BETA(1)-BETA(SET(IJ,2)+NPLUS3))*GSCALE
366         IF (PARTS.GT.1) GRAV(IJ)=GRAV(IJ)-LEVEL(SET(IJ,3))
367         ERROR=DRIFT(IJ)-GRAV(IJ)
368         ERROR2=ERROR*ERROR
369         RMS=RMS+ERROR2
370         RMSM(SET(IJ,2))=RMSM(SET(IJ,2))+ERROR2
371         RMSL(SET(IJ,3))=RMSL(SET(IJ,3))+ ERROR2
372         NUMBM(SET(IJ,2))=NUMBM(SET(IJ,2))+1
373         NUMBL(SET(IJ,3)) = NUMBL(SET(IJ,3)) + 1
374     1050   CONTINUE
375         RMS=SQRT(RMS/J)
376         DO 1100 IM=1,M
377         BETA(IM+NPLUS3)=BETA(IM+NPLUS3)*GSCALE
378         RMSM(IM)=SQRT(RMSM(IM)/NUMBM(IM))
379         IF (IM.EQ.1) GO TO 1100
380         GDIFF(IM)=BETA(IM+NPLUS3)-BETA(IM+NPLUS2)
381         RMSMM(IM)=SQRT(RMSM(IM)*RMSM(IM)+RMSM(IM-1)*RMSM(IM-1))
382     1100   CONTINUE
383         TNODE(1)=TNODE(1)*TSCALE
384
385 C           DATA OUTPUT ON CHANNAL 6
386
387         WRITE (6,6002) (HEAD),RMS
388     6002   FORMAT (' ',A16//' LEAST SQUARES FIT OF THE METER DRIFT CURVE '
389           E      , ' CUBIC SPLINE FUNCTIONS'/' ROOT MEAN SQUARE DEVIATION = ',
390           E      F7.4//' SITE NAME & NUMBER',7X,'GRAVITY RMS DEVIATION NUMB'
391           E      , 'BER OF OBSERVATIONS'//)
392         DO 1125 IM=1,M
393         IF (IM.EQ.1) GO TO 1120
394         WRITE (6,6012) GDIFF(IM),RMSMM(IM)
395     6012   FORMAT (' ',20X,F14.4,F10.4)
396     1120   WRITE (6,6013) (NAME(IM,I),I=1,4),IM,BETA(IM+NPLUS3),RMSM(IM)
397           E      ,NUMBM(IM)
398     6013   FORMAT (' ',4A4,I3,F14.4,F10.4,I17)
399     1125   CONTINUE
400
401
402
403         IF (PARTS.GT.1) THEN
404         RMSL(1) = SQRT(RMSL(1)/NUMBL(1))
405         LLEVEL(1) = GRAVO(1) - GRAV(1)
406         WRITE(6,6003) TSTART(1),LLEVEL(1),RMSL(1),NUMBL(1)
407     6003   FORMAT (/ ' DATUM LEVEL FOR DIFFERENT PARTS OF THE DATA SET' /
408           E      / 'PART NO      TSTART      DATUM (GU)      RMS(GU.)'
409           E      , ' NO OF OBS.'/'      1      ',(F12.5,F16.3,F18.3,I12))
410         WRITE (9,('      0'' ,F16.5,F16.3,F18.3,I12)') TSTART(1),

```

```

411     E   LLEVEL(1),RMSL(1),NUMBL(1)
412     YSUM = LLEVEL(1) - AINT(GRAVO(1))
413     YSSUM = TS(1) * YSUM
414
415 C
415     DO 6014 IP = 2, PARTS
416     NUMBLL = NUMBLL + NUMBL (IP-1)
417     RMSL(IP) = SQRT(RMSL(IP) /NUMBL(IP))
418     RMSLL(IP) = SQRT(RMSL(IP)*RMSL(IP) + RMSL(IP-1)
419     * RMSL(IP-1))
420     LLEVEL (IP) = GRAVO (IP) - GRAV (1+NUMBLL )
421     LDIFF(IP) = LLEVEL(IP) - LLEVEL(IP-1)
422     WRITE (6,6005) LDIFF(IP),RMSLL(IP),IP,TSTART(IP),LLEVEL(IP),
423     RMSL(IP),NUMBL(IP)
424     6005   FORMAT (' ',/18X,F19.3,F21.3,//I8,F16.5,F16.3,F18.3,I12)
425     IIP = NINT(REAL(IP/3))
426     WRITE (9,'(I8,F16.5,F16.3,F18.3,I12)') IIP,TSTART(IP),
427     E   LLEVEL(IP),RMSL(IP),NUMBL(IP)
428
429     IF (PARTS.EQ.4) THEN
430     IF(IP.EQ.2.OR.IP.EQ.4) THEN
431     SLOPE(IP) = LDIFF(IP)/(TSTART(IP)-TSTART(IP-1))/2.4D1
432     WRITE (6,6008) SLOPE(IP)
433     6008   FORMAT (/,'SLOPE BETWEEN THE ABOVE TWO = ',F8.3,' G.U./HR,/')
434     END IF
435     IF (IP.EQ.4) THEN
436     SLOPE(IP) = LLEVEL(IP-1) + (TSTART(2)-TSTART(3))* 2.4D1
437     *SLOPE(IP)
438     SLOPE(IP-2) = LLEVEL(IP-3) + (TSTART(3)-TSTART(1))*2.4D1
439     *SLOPE(IP-2)
440     WRITE (6,6009) TSTART(2),SLOPE(IP),TSTART(3),SLOPE(IP-2)
441     6009   FORMAT (/,'EXTRAPOLATED VALUE AT TIME ',F12.5,' IS',F12.3,)
442     SLOPE(IP) = SLOPE(IP) - LLEVEL(2)
443     SLOPE(IP-2) = LLEVEL(3) - SLOPE(IP-2)
444     SLOPE(1) = (SLOPE(IP)+SLOPE(IP-2))/2.D0
445     WRITE (6,6010) SLOPE(IP),SLOPE(IP-2), SLOPE(1)
446     6010   FORMAT(' POSSIBLE VALUE FOR GRAVITY DIFFERENCE ! ',F9.3,' +
447     E   ,F9.3,' /2 = ',F9.3)
448     END IF
449     END IF
450     TSSUM = TSSUM + TS (IP)
451     YSUM = YSUM + LLEVEL(IP) - AINT (GRAVO(1))
452     YSSUM = YSSUM + (TS(IP) * (LLEVEL(IP)-AINT(GRAVO(1))))
453     TSSQD = TSSQD + (TS(IP) * TS(IP))
454     6014   CONTINUE
455     C     CALL DIAG
456     C
457     C     ASSIGN AL & BL VALUES
458     C
459     AL(1,1) = PARTS
460     AL(1,2) = TSSUM
461     AL(2,1) = TSSUM
462     AL(2,2) = TSSQD
463     BL(1) = YSUM
464     BL(2) = YSSUM
465     C     DETA = (AL(1,1)*AL(2,2) - AL(2,1)*AL(1,2))
466     C     BL(1) = (BL(1) * AL(2,2) - BL(2) * AL(2,2)) /DETA
467     C     BL(2) = (BL(2) * AL(1,1) - BL(1) * AL(2,1)) /DETA
468     C
469     CALL F04ARF (AL,2,BL,2,BL,WSPCE,IFAIL)
470     IF (IFAIL.EQ.1) GO TO 999

```

```

471 C
472 C          USE RMSL AND TSSUM AGAIN TO CALC RMS OF OBS TO S. L. FIT
473
474 TSSUM = 0.0
475 DO 6007 IP = 1, PARTS
476 RMSL(IP) = (LLEVEL(IP) - AINT(GRAV0(1)))
477           - (BL(1) + BL(2)*TS(IP))
478           E
478 RMSL(IP) = RMSL(IP) * RMSL(IP)
479 TSSUM = TSSUM + RMSL(IP)
480 6007 CONTINUE
481 TSSUM = SQRT (TSSUM)
482
483 WRITE (6,6006) BL(1),BL(2),TSSUM
484 6006 FORMAT (/ ' STRAIGHT LINE FIT Y = A + B.X'
485           E /' A = ',F12.4,' B = ',F12.4,' RMS = ',F12.4/)
486 END IF
487
488
489 IF (PDRIFT.NE.1) GO TO 1150
490 WRITE (6,6004) (TIME(IJ),DRIFT(IJ),GRAV(IJ),(NAME(SET(IJ,2),I),
491           E I=1,4),SET(IJ,1),IJ=1,J)
492 6004 FORMAT ('1', ' DRIFT CHARACTERISTICS'/// ' TIME DRIFT
493           E OBSERVATION',6X,'SITE NAME SPLINE INTERVAL'///(F12.5,F11.3
494           E ,F13.3,6X,4A4,I6))
495 C
496 1150 IF (PDRIFT.NE.2) GO TO 1200
497 WRITE (3,3000) K,RMS,(TIMEF(IK),DRIFTF(IK),IK=1,K)
498 3000 FORMAT (I3,F7.4/(2F15.5))
499 WRITE (3,3001) J,(TIME(IJ),DRIFT(IJ),GRAV(IJ),SET(IJ,3),IJ=1,J)
500 3001 FORMAT (I3/(3F15.5,I3))
501 WRITE (3,'(4I4,L5)') J,PM,MZERO,PPARTS,L1
502
503 1200 DO 1300 IJ=1,J
504 1300 GRAV(IJ)=GRAV(IJ)+BETA(SET(IJ,2)+NPLUS3)+LEVEL(SET(IJ,3))+GMIN
505 20000 CONTINUE
506
507 GO TO 1
508
509
510 10000 WRITE (2,'('' CREATE PLOT FILE T70 ? (T/F) '')')
511 READ (1,'(L1)') L2
512 IF (L2) CALL EMASFC ('RUN',3,'GPLOTOBJ',8)
513 WRITE (2,'('' LIST TO GP15 ? (T/F) '')')
514 READ (1,'(L1)') L3
515 IF (L3) CALL EMASFC ('GPLIST',6,'T70,.GP15',9)
516 WRITE (2,'('' LIST TO .GP23 ? (T/F) '')')
517 READ (1,'(L1)') L3
518 IF (L3) CALL EMASFC ('LIST',4,'T70,.GP23',9)
519
520
521 STOP
522 999 WRITE (6,'('' SOLUTION IMPOSSIBLE; SINGULAR MATRIX''')')
523 STOP
524 END
525
526 SUBROUTINE NAGSOLVE (AUSED,ALPHA,BETA,MN3,N,WSPCE)

```

```

527     REAL*8 ALPHA(N,N),BETA(N),AUSED(MN3,MN3),WSPCE(N)
528     C      ,C(100),WSPC1(100),WSPC2(100),AA(100,100)

529     INTEGER MN3,N
530     DO 1 IB = 1,MN3
531     DO 1 IA = 1,MN3
532     1     AUSED (IA,IB) = ALPHA (IA,IB)
533     IFAIL = 0
534     CALL F04ARF (AUSED,MN3,BETA,MN3,BETA,WSPCE,IFAIL)
535     C     CALL F04ATF (AUSED,MN3,BETA,MN3,C,AA,MN3,WSPC1,WKSPC2,IFAIL)
536     IF (IFAIL.EQ..1) STOP 'F04ARF ; IFAIL = 1'
537     RETURN
538     END

```

```

CODE    21264 BYTES    PLT + DATA 1217104 BYTES
STACK   3128 BYTES   DIAG TABLES 1252 BYTES    TOTAL 1242748 BYTES
COMPILATION SUCCESSFUL

```



APPENDIX 2

Computer Program: WFIT

Parms set: FIXED

Edinburgh Fortran77 Compiler Release 3.5

```
1      REAL*8 ALPHA(3,3),BETA(3),GSUM,TSUM,GNSUM,WSUM,TNSUM,TGSUM,T2SUM
2      E ,TO,GO,TIME(4),GRAV(4),WEIGHT(4),GRAVADJ(4),ERROR(4),VAR
3      E ,NSUM
4      INTEGER N(4),IREF(4)
5      DATA N/0,0,1,1/
6      10 READ (9,3000,END=999) HEAD,(IREF(I),TIME(I),GRAV(I),WEIGHT(I),I=1
7      E ,4)
8      3000 FORMAT (A4/((I8,F16.5,F16.3,F18.3))
9      GO=GRAV(1)
10     TO=TIME(1)
11     GSUM=0.000
12     TSUM=0.000
13     NSUM=0.000
14     GNSUM=0.000
15     TNSUM=0.000
16     TGSUM=0.000
17     T2SUM=0.000
18     WSUM=0.000
19     VAR=0.000
20     DO 100 I=1,4
21     WEIGHT(I)=1.000/(WEIGHT(I)*WEIGHT(I))
22     GRAV(I)=GRAV(I)-GO
23     GSUM=GSUM+GRAV(I)*WEIGHT(I)
24     TIME(I)=TIME(I)-TO
25     TSUM=TSUM+TIME(I)*WEIGHT(I)
26     WSUM=WSUM+WEIGHT(I)
27     NSUM=NSUM+N(I)*WEIGHT(I)
28     GNSUM=GNSUM+N(I)*GRAV(I)*WEIGHT(I)
29     TNSUM=TNSUM+TIME(I)*N(I)*WEIGHT(I)
30     TGSUM=TGSUM+TIME(I)*GRAV(I)*WEIGHT(I)
31     T2SUM=T2SUM+TIME(I)*TIME(I)*WEIGHT(I)
32     100 CONTINUE
33     BETA(1)=GSUM
34     BETA(2)=GNSUM
35     BETA(3)=TGSUM
36     ALPHA(1,1)=WSUM
37     ALPHA(1,2)=NSUM
38     ALPHA(1,3)=TSUM
39     ALPHA(2,1)=ALPHA(1,2)
40     ALPHA(2,2)=ALPHA(1,2)
41     ALPHA(2,3)=TNSUM
42     ALPHA(3,1)=ALPHA(1,3)
43     ALPHA(3,2)=ALPHA(2,3)
44     ALPHA(3,3)=T2SUM
45     ISING=1
46     CALL GAUSS (ALPHA,BETA,3,9,ISING)
47     DO 200 I=1,4
48     GRAVADJ(I)=BETA(1)+N(I)*BETA(2)+TIME(I)*BETA(3)
49     ERROR(I)=GRAV(I)-GRAVADJ(I)
50     VAR=VAR+ERROR(I)*ERROR(I)*WEIGHT(I)
51     200 CONTINUE
52     SIGMA=DSQRT(VAR/WSUM)
```

```
53          SIGMA=SIGMA*100.000
54          BETA(2)=BETA(2)*100.000
55          WRITE (7,7000) HEAD,BETA(2),SIGMA
56 7000  FORMAT(' ',A4,' NODES'/' GRAVITY DIFFERENCE = ',F15.3,' MICROGALS'
57          1  /' ROOT MEAN SQUARE ERROR = ',F15.3,' MICROGALS')
58          GO TO 10
59 999   STOP
60          END
```

```
CODE      4384 BYTES      PLT + DATA      824 BYTES
STACK     888 BYTES      DIAG TABLES     604 BYTES      TOTAL     6700 BYTES
COMPILATION SUCCESSFUL
```

APPENDIX 3

Computer Program: MULTILINEAR

Parms set: FIXED

Edinburgh Fortran77 Compiler Release 3.5

```
1 C*****
2 C***
3 C*** This program adjusts base station values by fitting an independent qu
4 C*** drift curve to each gravity traverse.
5 C***
6 C***
7 C*** The input data consist of :-
8 C*** Line 1: the total number of observations, N;
9 C*** the number of base stations, M;
10 C*** the number of the base station, MZERO, chosen as datum,
11 C*** and the number of traverses, K.
12 C***
13 C*** Line 2: the value to be assigned to the datum base station, GO.
14 C***
15 C*** Subsequent lines list base station names (up to 8 charecters, 1 per l
16 C***
17 C*** Gravity observations are then listed, one per line, with the format:-
18 C***
19 C*** TIME(I) in any decimal units;
20 C*** GRAV(I), observed gravity;
21 C*** NBASE(I), the base station number.
22 C*** and NTRAV(I), the traverse number.
23 C***
24 C***
25 C*** The dimensions of the normal equation arrays A and B must be set
26 C*** A(M+2*K,M+2*K) and B(M+2*K) before compilation.
27 C***
28 C*****
29 PARAMETER (KX=114,KY=400)
30 DOUBLE PRECISION A(KX,KX),B(KX),GRAV(KY),TIME(KY),GO,CF
31 E ,GRAVO,TIME0,ERROR(KY),SIGMA,DUMPA,Y,D
32
33 DIMENSION RMSG(KX),NBASE(KY),VARG(KX),IHEAD(2,KX),NTRAV(KY)
34 1 ,NUMBER(KX),FREQ(20)
35
36 READ (4,3000) N,M,MZERO,K,GO,((IHEAD(I,J),I=1,2),J=1,M)
37 3000 FORMAT (4I4/F25.0/(2A4))
38 READ (4,3001) (TIME(I),GRAV(I),NBASE(I),NTRAV(I),I=1,N)
39 3001 FORMAT (2F12.5,2I3)
40 M2K=M+2*K
41 DO 90 I=1,M2K
42 B(I)=0.000
43 DO 90 J=1,M2K
44 A(J,I)=0.000
45 90 CONTINUE
46 TIME0=TIME(1)
47 GRAVO=GRAV(1)
48 DO 100 I=1,N
49 MK=M+NTRAV(I)
50 MKK=MK+K
51 TIME(I)=TIME(I)-TIME0
52 GRAV(I)=GRAV(I)-GRAVO
```

```

53      A(NBASE(I),NBASE(I))=A(NBASE(I),NBASE(I))+1.000
54      A(MK,MK)=A(MK,MK)+1.000
55      A(NBASE(I),MKK)=A(NBASE(I),MKK)+TIME(I)
56      A(MKK,MKK)=A(MKK,MKK)+TIME(I)*TIME(I)
57      A(MKK,MK)=A(MKK,MK)+TIME(I)
58      B(NBASE(I))=B(NBASE(I))+GRAV(I)
59      B(MK)=B(MK)+GRAV(I)
60      B(MKK)=B(MKK)+GRAV(I)*TIME(I)
61      100 CONTINUE
62      AMOMO=A(MZERO,MZERO)
63      DO 110 IM=1,M
64      NUMBER(IM)=A(IM,IM)
65      VARG(IM)=0.0
66      A(IM,MZERO)=0.000
67      A(MZERO,IM)=0.000
68      DO 110 IK=1,K
69      MK=M+IK
70      MKK=MK+K
71      A(MK,IM)=A(IM,MK)
72      A(MKK,IM)=A(IM,MKK)
73      110 CONTINUE
74      DO 120 IK=1,K
75      MK=M+IK
76      MKK=MK+K
77      A(MK,MKK)=A(MKK,MK)
78      A(MZERO,MK)=0.000
79      A(MZERO,MKK)=0.000
80      A(MK,MZERO)=0.000
81      A(MKK,MZERO)=0.000
82      120 CONTINUE
83      A(MZERO,MZERO)=1.000
84      B(MZERO)=0.000
85      IFAIL=0
86      CALL SIMQ(A,B,M2K,IFAIL)
87      VAR=0.0
88      DO 200 I=1,N
89      ERROR(I)=GRAV(I)-B(NBASE(I))-B(M+NTRAV(I))-B(M+K+NTRAV(I))*TIME(I)
90      ERROR2=ERROR(I)*ERROR(I)
91      VAR=VAR+ERROR2
92      VARG(NBASE(I))=VARG(NBASE(I))+ERROR2
93      200 CONTINUE
94      RMS=SQRT(VAR/N)
95      A(MZERO,MZERO)=AMOMO
96      DO 130 IM=1,M
97      RMSG(IM)=SQRT(VARG(IM)/NUMBER(IM))
98      130 CONTINUE
99      CF = SQRT(REAL(N)/REAL(N-M2K))
100     SIGMA = CF * RMS
101     WRITE (6,7000) RMS,SIGMA,((IHEAD(I,IM),I=1,2),IM,B(IM),RMSG(IM),
102     E      NUMBER(IM),IM=1,M)
103     7000 FORMAT (' NETWORK ADJUSTMENT USING MULTILINEAR DRIFT'///
104     E      ' ROOT MEAN SQUARE ERROR =',F12.3/
105     E      ' ESTIMATED STANDARD DEVIATION =',F12.3//
106     E      /'      BASE              GRAVITY              STANDARD DEVIATION'
107     E      ', ' NUMBER OF OBSERVATIONS'
108     E      /(2A4,8X,I4,F14.4,F10.4,I17))
109
110     WRITE (7,7001) (GRAV(I),ERROR(I),NBASE(I),NTRAV(I),I=1,N)
111     7001 FORMAT (///'      GRAVITY      ERROR      STATION      TRAVERSE'
112     E      //(2F12.3,2I10))

```

```

113 WRITE (8,'(2F12.5)') (ERROR(I),GRAV(I)-ERROR(I),I=1,N)
114
115 WRITE (9,'(2F12.5)') (ERROR(I),TIME(I),I=1,N)
116
117 C HISTOGRAM
118 WRITE(6,'('' Each class interval is half the estimated standard'',
119 £ '' deviation of'',F7.4)') SIGMA
120
121
122 CALL DAGOST (ERROR,N,CF,D,Y)
123 WRITE (6,'(''Result of Dagostinos test : D ='',F 9.5,
124 £ ''Y = '',F9.5)') D,Y
125
126 DO 71 J=1,20
127 71 FREQ(J) = 0.
128 IC = 0
129
130
131 DO 26 I=1,N
132 IF (ABS(ERROR(I)).GT.(SIGMA*5)) THEN
133 IC = IC + 1
134 GO TO 26
135 END IF
136 DUMPA = ERROR(I)/(SIGMA/2)
137 IF (DUMPA.GT.0.0) THEN
138 J = 11 + AINT (DUMPA)
139 ELSE
140 J = 10 + AINT (DUMPA)
141 END IF
142 FREQ(J)=FREQ(J)+1.
143 26 CONTINUE
144 WRITE (6,'('' The number of residuals greater than 5 std. dev.is''
145 £ ',I2)') IC
146 CALL HIST(1,FREQ,20)
147 STOP
148 END
149

```

```

CODE      5968 BYTES      PLT + DATA 121520 BYTES
STACK    1080 BYTES      DIAG TABLES  412 BYTES      TOTAL 128980 BYTES
COMPILATION SUCCESSFUL

```

APPENDIX 4

Computer Program: PBAS



Source: EGP19.PBAS  
Object: POBJ

Compiled: 11/06/84 09.49.37

Parms set: FIXED

Edinburgh Fortran77 Compiler Release 3.4

```

1      C*****
2      C***
3      C***   THE PROGRAM SUPABASL REDUCES GRAVITY OBSERVATIONS MADE WITH THE
4      C***   LACOSTE & ROMBERG GRAVITY METER G-275 OR ANY OTHER METER
5      C***   WHOSE SCALE FACTOR IS GIVEN, OUTPUTTING THE DRIFT
6      C***   SINCE THE FIRST READING. IT CONVERTS DIAL TURNS TO GRAVITY UNITS
7      C***   USING THE MANUFACTURERS CALIBRATION TABLES. (ONE GRAVITY UNIT =
8      C***   ONE MICROMETRE PER SECOND PER SECOND = ONE HUNDRED MICROGALS)
9      C***   TIDAL CORRECTIONS ARE MADE USING EVERY PARTIAL TIDE GIVEN IN
10     C***   CARTWRIGHT AND TAYLER (1971), AS CORRECTED IN CARTWRIGHT AND
11     C***   EDDEN (1973). STANDARD ATMOSPHERIC PRESSURE IS CALCULATED FOR
12     C***   EACH SITE USING THE I.C.A.O. STANDARD ATMOSPHERE AND THE GRAVITY
13     C***   VALUES ARE CORRECTED USING A COEFFICIENT OF 0.0037 GRAVITY UNITS
14     C***   PER MILLIBAR.
15     C***
16     C*****
17     REAL LONG,LAT,K(6),MBAR(200),MBARO
18     REAL*8 TWOPI,DDAY(200),DCENT,TORAD,DLONG,DLAT,AGRAV,TIME(200),
19     £ DDAY60,DCALIB,GRAV(200),GRAVO,VALUE(200),STND(200),PHI1,PHI2,
20     £ TIME0(20),TIMEF(20)
21
22     INTEGER*2 IIE ,IIN,IE,IN,IW,IS,IIG,IG
23
24     INTEGER SDAY(12),YEAR(200),DAY(200),HOUR(200),SET2(200)
25     DIMENSION MONTH(200),MIN(200),F(7),TID0(200),TID1(200),
26     £ TID2(200),TIDE(200),IREF(200),CIVIL(200),DRIFT(200),TID3(200),
27     £ CELCIUS(200),C(7,484)
28
29     LOGICAL*1 LE(2),L1,L2, LN(2)
30
31     CHARACTER*16 HEAD , STNAME(100)
32     EQUIVALENCE (LE,IIE), (LN,IIN)
33     COMMON NNBAS,ISKIP,N,INBAS,ICOUNT
34     DATA IE/' E'/,IN/' N'/,IW/' W'/,IS/' S'/,IG/' G'/
35
36     DATA LE/2*' '/, LN/2*' '/
37
38     DATA SDAY/0,31,59,90,120,151,181,212,243,273,304,334/
39     DATA SDAY/0,31,59,90,120,151,181,212,243,273,304,334/
40     TWOPI=6.28318530700
41     TORAD=TWOPI/360.DO
42     INBAS = 0
43     ICOUNT = 0
44     NNBAS = 0
45     ISKIP = 0
46     INSTN = 0

```

C INTERACTIVE PROMPTS

```

47      CALL EMASFC ('DEFINE',6,'FT02,.IN',8)
48      CALL EMASFC ('DEFINE',6,'FT04,.OUT',9)
49      WRITE (4,120)
50      120  FORMAT ( '      PRESSURE CORRECTION (T/F)      ' )
51      READ (2,118) L1
52      118  FORMAT (L1)
53      C***
54      C***  READ THE COEFFICIENTS OF THE TIDAL ARGUMENTS AND AMPLITUDES
55      C***  FROM THE FILE CARTRIDE ON CHANNAL 10
56      C***
57      READ (10,171) ((C(I,J),I=1,7),J=1,484)
58      171  FORMAT (6F2.0,F6.0)
59      C***
60      C***  READ SITE NAME
61      C***
62      100  READ (5,60) (HEAD)
63      60  FORMAT (A16)
64      C***
65      C***  READ THE NUMBER OF OBSERVATIONS AT THE SITE, NN, TOGETHER WITH
66      C***  ITS LATITUDE, LONGITUDE AND HEIGHT. NT = 0 GIVES DEFAULT VALUES
67      C***  OF (1.159,0.000) FOR THE GRAVIMETRIC FACTOR AND PHASE LAG.
68      C***  THE ABSOLUTE VALUE OF GRAVITY MAY BE GIVEN IF KNOWN. NN=0 CAUSES
69      C***  THE PROGRAM TO TERMINATE.
70      C***
71      READ (5,260) NN,NT,IIG,SCALE,LE,LOND,LONM,ALONS,LN,LATD,LATM,
72      E  ALATS,HEIGHT,AGRAV,PHI1,PHI2
73      260  FORMAT(2I3,A2,F8.4/2A1,I4,I3,F6.2,2X,2A1,2I3,F6.2,F8.3,F9.2,2F4.1)
74      PHI1 = PHI1 * TORAD
75      PHI2 = PHI2 * TORAD
76      101  IF (NN.EQ.0) GO TO 606
77      IGRAVO=0
78      F(1)=1.159
79      F(2)=1.159
80      F(3)=1.159
81      F(4)=1.069
82      F(5)=1.069
83      F(6)=1.069
84      F(7)=1.069
85      IF (NT.NE.1) GO TO 116
86      C***
87      C***  IF NT=1, READ NF0,NF1,NF2.
88      C***  IF ANY OF NF0,NF1,NF2 IS NON-ZERO, SPECIFIC GRAVIMETRIC FACTORS
89      C***  (F(1)), (F(2)), (F(3)) ARE READ.
90      C***
91      READ (5,110) NF0,NF1,NF2
92      110  FORMAT (3I3)
93      IF (NF0.NE.0) READ (5,113) F(1)
94      IF (NF1.NE.0) READ (5,113) F(2)
95      IF (NF2.NE.0) READ (5,113) F(3)
96      113  FORMAT (F5.3)
97      116  N=NN
98      IF (NN.GE.100) N=100
99      IGRAVO=IGRAVO + 1
100     C***
101     C***  READ REFERENCE NUMBER, TIME, DATE, GRAVITY METER DIAL TURNS,
102     C***  PRESSURE AND TEMPERATURE. CIVIL IS THE DIFFERENCE IN HOURS
103     C***  BETWEEN LOCAL TIME AND GREENWICH MEAN TIME (UNIVERSL TIME).
104     C***
105     READ (5,360) (IREF(I),HOUR(I),MIN(I),DAY(I),MONTH(I),
106     1  YEAR(I),CIVIL(I),GRAV(I),MBAR(I),CELCIUS(I),I=1,N)

```

```

107     360 FORMAT (I5,I3,I3,I3,I3,I5,F4.1,F9.3,F8.2,F5.1)
108     C***
109     C***   CALCULATION OF STANDARD ATMOSPHERIC PRESSURE.
110     C***
111         LONG=(((ALONS/60.0)+LONM)/60.0+LOND)*TORAD
112         IF (IIE.EQ.IW) LONG=-LONG
113         LAT=(((ALATS/60.0)+LATM)/60.0+LATD)*TORAD
114         IF (IIN.EQ.IS) LAT=-LAT
115     1300 DO 501 I=1,N
116     C***
117     C***   THE DAY NUMBER ROUTINE CONVERTS ANY TIME AND DATE OF THE GREGORIAN
118     C***   CALENDAR INTO THE NUMBER OF DAYS AND DECIMALS OF A DAY WHICH HAVE
119     C***   ELAPSED SINCE 24 00 (MIDNIGHT) GREENWICH MEAN TIME DECEMBER 31
120     C***   1899
121     C***
122         DDAY(I)=(YEAR(I)-1)*365-6.93591 D 5-YEAR(I)/100+YEAR(I)/4+SDAY(MON
123     1TH(I))+DAY(I)-1+(HOUR(I)-CIVIL(I))/24.+MIN(I)/1440.
124         IF((YEAR(I)-((YEAR(I))/100)*100).EQ.0) GO TO 301
125         IF(((YEAR(I)-(YEAR(I)/4)*4)*365+SDAY(MONTH(I))+DAY(I)).GE.60) GO T
126     10 301
127         DDAY(I)=DDAY(I)-1
128     301 IF(DAY(I)*MONTH(I).EQ.58)DDAY(I) = DDAY(I) - 1
129         CALL TIDAL(DDAY(I),LAT,LONG,STATIC,TID0(I),TID1(I),TID2(I),TIDE30,
130     E TIDE31,TIDE32,TIDE33,F,C,HEIGHT,PHI1,PHI2)
131         TID3(I)=TIDE30+TIDE31+TIDE32+TIDE33
132         TIDE(I)=TID0(I)+TID1(I)+TID2(I)+TID3(I)
133
134         MBARO = 1013.2 * ((1.0-HEIGHT*2.2557D-5)**5.2613)
135
136         IF (MBAR(I).EQ.0..AND.L1) THEN
137             L1 = .FALSE.
138             WRITE (4,('( ' WARNING CHECK PRESSURE OF ',I4)')I
139             END IF
140
141         IF (SCALE.GT.1.0E-4) THEN
142             IF (L1) THEN
143                 GRAV(I)=GRAV(I)*SCALE+TIDE(I)+(MBAR(I)-MBARO)*0.0037
144             ELSE
145                 GRAV(I) = GRAV(I) * SCALE + TIDE (I)
146             END IF
147         END IF
148         IF (SCALE .EQ. 0.000) THEN
149             IF (.NOT.L1) THEN
150                 GRAV(I)=DCALIB(GRAV(I))+TIDE(I)
151             ELSE
152                 GRAV(I)=DCALIB(GRAV(I))+TIDE(I)+(MBAR(I)-MBARO)*0.0037
153             END IF
154         END IF
155     501 CONTINUE
156
157         GRAVO = GRAV(1)
158
159         DO 502 I=1,N
160             INEW1 = I + INSTN
161             TIME (INEW1) = DDAY (I)
162             DRIFT (I) = GRAV(I) - GRAVO
163     502 VALUE (INEW1)= DRIFT(I)
164             INSTN = INSTN + N
165
166         CALL SBAS (HEAD,STNAME,STND,GRAVO,SET2)

```

```

167
168         TIMEO (INBAS) = DDAY (1)
169         TIMEF (INBAS) = DDAY (N)
170
171     600 IF (IGRAVO.NE.1) GO TO 607
172 C***
173 C***   DATA OUTPUT
174 C***
175     WRITE (6,160) (HEAD)
176     160 FORMAT (' ',A16)
177     WRITE (6,460) LOND,LONM,ALONS,LE(2),LATD,LATM,ALATS,LN(2),
178     1   HOUR(1),MIN(1),DAY(1),MONTH(1),YEAR(1),DDAY(1),AGRAV,GRAV(1),
179     2   HEIGHT,MBARO
180     460 FORMAT ('0',29X,'LONGITUDE',I8,I3,F6.2,1X,A1,14X,'LATITUDE',
181     2   I9,I3,F6.2,1X,A1/30X,'EPOCH',I11,'H',I3,'M',I5,I3,I5,5X,
182     3   'DAY NUMBER',F16.5/30X,'GRAVITY',F17.2,' GU',12X,'METER READING'
183     4   ,F11.3,' GU'/30X,'STATION HEIGHT',F8.3,' METRES '/30X,'STANDARD
184     5   ATMOSPHERIC PRESSURE ',F8.2,' MILLIBARS')
185     WRITE (6,470) STATIC,F(1),F(2),F(3),F(4)
186     470 FORMAT('0',4X,'THE HONKASALO TERM OF ',F6.3,' GU HAS BEEN ADDED
187     1   IN ORDER TO MAKE THE TIDAL CORRECTIONS EQUIVALENT TO THOSE OF
188     2   LONGMAN'//4X,'THE GRAVIMETRIC FACTOR IS '//10X,F5.3,
189     3   ' FOR LONG-PERIOD TIDES'//10X,F5.3,' FOR DIURNAL TIDES'//
190     4   10X,F5.3,' FOR SEMI-DIURNAL TIDES'//10X,F5.3,' FOR THIRD DEGREE
191     5   TIDES')
192     IF (.NOT.L1.OR.MBAR(I-1).EQ.0) WRITE (6,(''          ***'',
193     E          ' NO PRESSURE CORRECTION      ***',/))
194 C     IF (NN.EQ.1) GO TO 100
195     607 IF (N-50) 601,601,602
196     601 N1=1
197     601 N2=N
198     601 GO TO 603
199     602 N1=1
200     602 N2=50
201     603 WRITE (6,480) (IREF(I),DDAY(I),HOUR(I),MIN(I),DAY(I),MONTH(I),YEAR
202     1(I),DRIFT(I),TIDE(I),TID0(I),TID1(I),TID2(I),TID3(I),IREF(I),I=N1,
203     2N2)
204     480 FORMAT(' ',4X,'REFERENCE',5X,'DAY NUMBER',5X,'TIME',7X,'DATE',8X,
205     1'DRIFT',6X,'TIDE',4X,'SPECIES 0',2X,'SPECIES 1',2X,'SPECIES 2',2X,
206     2'DEGREE 3',2X,'REFERENCE'/(5X,I7,F18.5,I5,'H',I3,'M',I5,I3,I5,F9.3
207     3,' GU',F8.3,' GU',F8.3,' GU',F8.3,' GU',F8.3,' GU',F8.3,' GU',I9))
208     WRITE (7,111) (DDAY(I),DRIFT(I),I=N1,N2)
209     111 FORMAT (F12.5,3X,F7.3)
210     IF ((N-N2).EQ.0) GO TO 604
211     N1=51
212     N2=N
213     GO TO 603
214     604 CONTINUE
215     NN=NN-N
216     IF (NN.EQ.0) GOTO 605
217     GO TO 116
218     605 CONTINUE
219     GO TO 100
220     606 WRITE (6,550)
221     550 FORMAT ('1      END OF DATA')
222
223 C     OUTPUT TO CHANNEL 08 SUITABLE FOR PROGRAM SPLINEX
224
225
226     WRITE (8,('2I4,' ' 4 4 -1 11 2''')) INSTN,0-INBAS

```

```

227     WRITE (8,(' ' ' ',A16,I5,I3,I5,' ' G-275'))
228     £ STNAME(1),DAY(1),MONTH(1),YEAR(1)
229     WRITE (8,'(A16,F11.3)') (STNAME(J),STND(J),J=1,INBAS)
230     WRITE (8,(' ' ' ',F12.5)) (TIMEO(J),J=1,INBAS)
231     WRITE(8,'(F12.5,F12.3,' ' 1','I3)') (TIME(J),VALUE(J)
232     £ ,SET2(J), J = 1 , INSTN)
233     WRITE (8,'(////)')
234
235     CLOSE (55)
236     STOP
237     END
238
239

```

```

240 C*****
241 C***
242 C***   CONVERSION FROM DIAL TURNS TO GRAVITY UNITS FOR THE LACOSTE
243 C***   & ROMBERG GRAVITY METER G-275 USING THE MANUFACTURES CALIBRATION
244 C***   TABLES.
245 C***
246     DOUBLE PRECISION FUNCTION DCALIB(SGRAV)
247     REAL*8 TG(71), CG(70), SGRAV

```

```

248     DATA TG/0.,105.12,210.22,315.33,420.43,525.52,630.62,725.71,840.8,
249     1945.89,1050.98,1156.07,1261.17,1366.27,1471.38,1576.49,1681.62,178
250     26.75,1891.89,1997.04,2102.20,2207.37,2312.55,2417.74,2522.93,2628.
251     314,2733.36,2838.58,2943.82,3049.07,3154.33,3259.60,3364.88,3470.18
252     4,3575.48,3680.80,3786.12,3891.46,3996.81,4102.16,4207.53,4312.90,4
253     5418.28,4523.67,4629.06,4734.46,4839.86,4945.27,5050.69,5156.11,526
254     61.52,5366.94,5472.35,5577.76,5683.16,5788.55,5893.94,5999.32,6104.
255     769,6210.06,6315.41,6420.76,6526.09,6631.40,6736.70,6841.97,6947.23
256     8,7052.45,7157.65,7262.82,7367.93/
257     DATA CG/1.05115,1.05108,1.05104,1.05100,1.05095,1.05093,1.05090,1.
258     105090,1.05090,1.05090,1.05094,1.05097,1.05103,1.05107,1.05115,1.05
259     2124,1.05133,1.05140,1.05150,1.05160,1.05170,1.05180,1.05187,1.0519
260     38,1.05207,1.05216,1.05226,1.05237,1.05248,1.05260,1.05270,1.05283,
261     41.05295,1.05305,1.05316,1.05326,1.05337,1.05347,1.05356,1.05365,1.
262     505374,1.05380,1.05385,1.05392,1.05399,1.05405,1.05411,1.05415,1.05
263     6417,1.05416,1.05415,1.05412,1.05407,1.05402,1.05395,1.05388,1.0538
264     70,1.05372,1.05364,1.05355,1.05344,1.05330,1.05315,1.05297,1.05275,
265     81.05253,1.05227,1.05200,1.05163,1.05115/
266     IG=SGRAV/100+1
267     DCALIB=TG(IG)+(SGRAV+100-IG*100)*CG(IG)
268     DCALIB=DCALIB*10.0
269     RETURN
270     END

```

```

271 C*****
272 C***
273 C***   THE SUBROUTINE TIDAL COMPUTES THE VERTICAL COMPONENT OF
274 C***   GRAVITATIONAL ATTRACTION DUE TO THE SUN AND MOON FOLLOWING
275 C***   THE EXPANSION OF CARTWRIGHT & TAYLOR AND CARTWRIGHT & EDDEN
276 C***
277 C*****
278     SUBROUTINE TIDAL(DDAY,LAT,LONG,STATIC,TIDE20,TIDE21,TIDE22,TIDE30,
279     £ TIDE31,TIDE32,TIDE33,F,C,HEIGHT,PHI1,PHI2)

```

```

280 REAL LONG, LAT, LATC
281 REAL*8 TWOPI,DDAY,DDAY60,DCENT,K(6),PHI1,PHI2

282 DIMENSION C(7,484), F(7)
283 TWOPI = 6.28318530700
284 DDAY60=(DDAY-22056.5)*TWOPI
285 TIDE20=0.0
286 TIDE21=0.0
287 TIDE22=0.0
288 TIDE22=0.0
289 TIDE30=0.0
290 TIDE31=0.0
291 TIDE32=0.0
292 TIDE33=0.0
293 C***
294 C*** EVALUATION OF THE FUNDAMENTAL ARGUMENTS
295 C***
296 K(2)=DMOD((DDAY60*0.036601101300+0.3878297800),TWOPI)
297 K(3)=DMOD((DDAY60*0.002737909200+1.0492785000),TWOPI)
298 K(4)=DMOD((DDAY60*0.000309454800+4.7397039000),TWOPI)
299 K(5)=DMOD((DDAY60*0.000147094000+3.2955390700),TWOPI)
300 K(6)=DMOD((DDAY60*0.000000130800+4.9263522000),TWOPI)
301 K(1)=DMOD((DDAY60-K(2)+K(3)+TWOPI/2.0+LONG),TWOPI)
302 C***
303 C*** SECOND DEGREE TIDES - LONG PERIOD COMPONENTS
304 C***
305 DO 201 I=1,104
306 201 TIDE20=TIDE20+COS(C(1,I)*K(1)+C(2,I)*K(2)+C(3,I)*K(3)
307 1 +C(4,I)*K(4)+C(5,I)*K(5)+C(6,I)*K(6))*C(7,I)
308 C***
309 C*** SECOND DEGREE TIDES - DIURNAL COMPONENTS
310 C***
311 DO 202 I=105,266
312 202 TIDE21=TIDE21+SIN(C(1,I)*K(1)+C(2,I)*K(2)+C(3,I)*K(3)
313 1 +C(4,I)*K(4)+C(5,I)*K(5)+C(6,I)*K(6)+PHI1)*C(7,I)
314 C***
315 C*** SECOND DEGREE TIDES - SEMI-DIURNAL COMPONENTS
316 C***
317 DO 203 I=267,385
318 203 TIDE22=TIDE22+COS(C(1,I)*K(1)+C(2,I)*K(2)+C(3,I)*K(3)
319 1 +C(4,I)*K(4)+C(5,I)*K(5)+C(6,I)*K(6)+PHI2)*C(7,I)
320 C***
321 C*** THRID DEGREE TIDES - LONG PERIOD COMPONENTS
322 C***
323 DO 204 I=386,402
324 204 TIDE30=TIDE30+SIN(C(1,I)*K(1)+C(2,I)*K(2)+C(3,I)*K(3)
325 1 +C(4,I)*K(4)+C(5,I)*K(5)+C(6,I)*K(6))*C(7,I)
326 C***
327 C*** THRID DEGREE TIDES - DIURNAL COMPONENTS
328 C***
329 DO 205 I=403,437
330 205 TIDE31=TIDE31+COS(C(1,I)*K(1)+C(2,I)*K(2)+C(3,I)*K(3)
331 1 +C(4,I)*K(4)+C(5,I)*K(5)+C(6,I)*K(6))*C(7,I)
332 C***
333 C*** THIRD DEGREE TIDES - SEMI-DIURNAL COMPONENTS
334 C***
335 DO 206 I=438,468
336 206 TIDE32=TIDE32+SIN(C(1,I)*K(1)+C(2,I)*K(2)+C(3,I)*K(3)
337 1 +C(4,I)*K(4)+C(5,I)*K(5)+C(6,I)*K(6))*C(7,I)
338 C***

```

```

339 C*** THRID DEGREE TIDES - TER-DIURNAL COMPONENTS
340 C***
341 DO 207 I=469,484
342 207 TIDE33=TIDE33+COS(C(1,I)*K(1)+C(2,I)*K(2)+C(3,I)*K(3)
343 1 +C(4,I)*K(4)+C(5,I)*K(5)+C(6,I)*K(6))*C(7,I)
344 C***
345 C*** CORRECTIONS FOR THE ELLIPTICTY OF THE EARTH.
346 C*** GEODETIC LATITUDE IS CONVERTED TO GEOCENTRIC LATITUDE AND THE
347 C*** RADIUS IS REDUCED TO THAT OF THE INTERNATIONAL SPHEROID OF 1967.
348 C***
349 ECCEN2 = 6.694605 E -3
350 LATC = ATAN((1.0-ECCEN2)*TAN(LAT))
351 SINLAT = SIN(LATC)
352 COSLAT = COS(LATC)
353 RADIUS = 1.0/SQRT(1.0+ECCEN2*SINLAT*SINLAT/(1.0-ECCEN2)
354 E +HEIGHT/6378160.000)
355 RAD2 = RADIUS*RADIUS
356 C***
357 C*** CALCULATION OF THE LATITUDE FUNCTIONS
358 C***
359 TOGRAV = 3.0725E-5*RAD2
360 TEMP20=(1.5*SINLAT*SINLAT-0.5)*0.6307831*TOGRAV*(1)
361 TEMP21= -3.0*SINLAT*COSLAT*0.2575161*TOGRAV*(2)
362 TEMP22=3.0*COSLAT*COSLAT*0.1287580*TOGRAV*(3)
363 TOGRAV=TOGRAV*RADIUS*1.5
364 TEMP30=SINLAT*(2.5*SINLAT*SINLAT-1.5)*0.7463527*TOGRAV*(4)
365 TEMP31=-1.5*COSLAT*(5*SINLAT*SINLAT-1)*0.2154534*TOGRAV*(5)
366 TEMP32=15.0*COSLAT*COSLAT*SINLAT*0.06813236*TOGRAV*(6)
367 TEMP33=-15.0*COSLAT*COSLAT*COSLAT*0.02781492*TOGRAV*(7)
368 C***
369 C*** EVALUATION OF THE STATIC TIDE
370 C***
371 STATIC=C(7,1)*TEMP20
372 C***
373 C*** WEIGHTING TIDAL FAMILIES WITH THEIR LATITUDE FUNCTION
374 C***
375 TIDE20=TIDE20*TEMP20
376 TIDE21=TIDE21*TEMP21
377 TIDE22=TIDE22*TEMP22
378 TIDE30=TIDE30*TEMP30
379 TIDE31=TIDE31*TEMP31
380 TIDE32=TIDE32*TEMP32
381 TIDE33=TIDE33*TEMP33
382 RETURN
383 END

384 SUBROUTINE SBAS (HEAD,STNAME,STND,GRAVO,SET2)
385 CHARACTER*16 HEAD,STNAME(*)
386 INTEGER SET2(*),INBAS
387 REAL*8 STND(*),GRAVO

388 COMMON NNBAS,ISKIP,N,INBAS,ICOUNT
389 INBAS = INBAS + 1
390 ICOUNT = ICOUNT + 1
391
392 IF (INBAS.EQ.1) THEN
393 STND(1) = GRAVO
394 STNAME (1) = HEAD

```

```

395             DO 1 J = 1,N
396   1          SET2 (J) = 1
397             NNBAS = NNBAS + N
398             RETURN
399             END IF
400
401   C          DO 3 I = 1,INBAS-1
402   C          IF (STNAME(I).EQ.HEAD.AND.ICOUNT.GT.ISKIP) THEN
403   C                                 DO 2 J = NNBAS+1 , NNBAS+N
404   C                                 SET2(J) = I
405   C                                 CONTINUE
406   C                                 NNBAS = NNBAS + N
407   C                                 ISKIP = ICOUNT
408   C                                 END IF
409   C3         CONTINUE
410
411             STND(INBAS) = GRAVO
412             STNAME(INBAS) = HEAD
413             DO 4 I = NNBAS+1 , NNBAS+N
414   4          SET2(I) = INBAS
415             NNBAS = NNBAS+N
416             RETURN
417
418             END

```

```

CODE      13664 BYTES      PLT + DATA  41408 BYTES
STACK     2016 BYTES      DIAG TABLES  1604 BYTES      TOTAL  58692 BYTES
COMPILATION SUCCESSFUL

```



APPENDIX 5

Computer Program: LSQTILT

C Simple multivariate polynomial regression for data  
C obtained due tilting experiments .  
C David , Geophysics , Edinburgh University

PARAMETER ( IUNK=20, NOBS=200 )  
REAL\*8 A( IUNK, IUNK ), B( IUNK ), AINV( IUNK, IUNK ), TEMP( IUNK ), W( IUNK,  
ENOBS ), N( NOBS ), X, Y, RESULT( NOBS, 3 ), ERROR( NOBS ), WEIGHT, ERROR2  
E, YHAT( NOBS ), YMEAN, YHATM, SDR, SSAM, RSQD, R, CCORRN, LAMBDA, CTHEO

NING 242 Specification of item length in bytes is not standard FORTRAN

NING 201 Identifier CTHEORY contains >6 characters - not standard FORT

INTEGER EXP, ICOUNT, REXP( NOBS )  
LOGICAL LWEIGH, LLONG, LEXPT  
DATA LAMBDA/632. BD-9/, GRAV/9. B15BD0/  
ICOUNT=0

WRITE( 6, '( " DO YOU WISH TO WEIGHT? (T/F) ' ) )

READ( 5, \* ) LWEIGH

READ( 3, \* ) NEXP

N2EXP = 2 \* NEXP

N2EXP1 = N2EXP + 1

DO 3 I=1, N2EXP1

B( I ) = 0. DO

DO 3 J=1, N2EXP1

3 A( J, I ) = 0. DO

SSDR = 0. DO

SSAM = 0. DO

YHATM = 0. DO

YMEAN = 0. DO

WEIGHT=1. DO

1 READ( 3, \*, END=2 ) X, Y, EXP

ICOUNT = ICOUNT+1

RESULT( ICOUNT, 1 ) = X

RESULT( ICOUNT, 2 ) = Y

RESULT( ICOUNT, 3 ) = EXP

REXP( ICOUNT ) = EXP

YMEAN = Y + YMEAN

IF ( LWEIGH ) WEIGHT = 1. DO / ( RESULT( ICOUNT, 1 ) \* RESULT( ICOUNT, 1 ) )

A( EXP, EXP ) = A( EXP, EXP ) + 1 \* WEIGHT

A( NEXP+EXP, NEXP+EXP ) = A( NEXP+EXP, NEXP+EXP ) + X \* X \* WEIGHT

A( NEXP+EXP, EXP ) = A( NEXP+EXP, EXP ) + X \* WEIGHT

A( N2EXP+1, EXP ) = A( N2EXP+1, EXP ) + X \* X \* WEIGHT

A( N2EXP+1, NEXP+EXP ) = A( N2EXP+1, NEXP+EXP ) + X \* X \* X \* WEIGHT

A( N2EXP+1, N2EXP+1 ) = A( N2EXP+1, N2EXP+1 ) + X \* X \* X \* X \* WEIGHT

B( EXP ) = B( EXP ) + Y \* WEIGHT

B( NEXP+EXP ) = B( NEXP+EXP ) + X \* Y \* WEIGHT

B( N2EXP+1 ) = B( N2EXP+1 ) + X \* X \* Y \* WEIGHT

GO TO 1

2 CONTINUE

DO 4 EXP=1, NEXP

A( EXP, NEXP+EXP ) = A( NEXP+EXP, EXP )

A( EXP, N2EXP+1 ) = A( N2EXP+1, EXP )

A( NEXP+EXP, N2EXP+1 ) = A( N2EXP+1, NEXP+EXP )

4 CONTINUE

C CALL SIMQ ( A, B, 9, IFAIL )

IFAIL = 1

CALL FO1AAF ( A, IUNK, N2EXP1, AINV, IUNK, TEMP, IFAIL )

IF ( IFAIL .NE. 0 ) STOP ( 'FAIL' )

```

4 CONTINUE
58
59
60 C CALL SIMQ (A,B,9,IFAIL)
61
62 IFAIL = 1
63 CALL F01AAF(A,IUNK,N2EXP1,AINV,IUNK,TEMP,IFAIL)
64 IF (IFAIL.NE.0) STOP 'IFAIL.NE.0'
65
66 DO 5 I=1,N2EXP1
67 5 TEMP(I) = 0.D0
68
69 DO 6 I=1,N2EXP1
70 DO 6 J=1,N2EXP1
71 6 TEMP(I) = AINV(J,I) * B(J) + TEMP(I)
72
73 ERROR2 = 0.D0
74 YMEAN = YMEAN/ICOUNT
75
76 DO 8 I=1,ICOUNT
77 YHAT(I) = TEMP(REXP(I)) + TEMP(NEXP+REXP(I)) * RESULT(I,1) + TEMP
78 £ (N2EXP1) * RESULT(I,1) * RESULT(I,1)
79 YHATM = YHATM + YHAT(I)
80 ERROR(I) = YHAT(I) - RESULT(I,2)
81 ERROR2 = ERROR(I) * ERROR(I) +ERROR2
82 SSSDR = (YHAT(I) - YMEAN) * (YHAT(I) - YMEAN) + SSSDR
83 SSAM = (RESULT(I,2) - YMEAN) * (RESULT(I,2) - YMEAN) + SSAM
84
85 C Output to ft08 for plotting routines
86
87 WRITE (8,*) RESULT(I,1),RESULT(I,2)
88
89 8 CONTINUE
90 WRITE (8,(''PLOT'',/, ''OVERLAY'',/, ''LINE CURVE'',/, ''DATA''))
91 WRITE (8,('2E12.5'))( RESULT(I,1),YHAT(I),I=1,ICOUNT)
92
93 RSQD = SSSDR/SSAM
94 SIGMA = ERROR2/(ICOUNT-N2EXP1)
95 WRITE (7,('8X, ''Results of analysis of tilting experiment'',/))
96 WRITE (7,('' The number of observations is'',I4, '' with'',I4
97 £ , '' constraints'')) ICOUNT,N2EXP1
98 WRITE (7,('' The estimated standard deviation of the fit is'',F1
99 £2.4)) SQRT(SIGMA)
100 WRITE (7,('' R squared for fit:'',F12.5)) RSQD
101 WRITE (7,('' The Regression Coefficients with their variances'',
102 £ '' (std. err. squared) are:''))
103 WRITE (7,('I6,2E15.5')) ( (I,TEMP(I),AINV(I,I)*SIGMA),I=1,N2EXP1)
104
105 WRITE (6,('' Is this a laser experiment? (T/F)''))
106 READ (5,*) LEXPT
107 WRITE (6,('' Is this the long level? (T/F)''))
108 READ(5,*) LLONG
109 IF (LEXPT) THEN
110 R = 3.5747D-1
111 IF (.NOT.LLONG) R = 3.4334D-1
112 CTHEORY = (GRAV*LAMBDA*LAMBDA)/(8.DO*R*R)
113 CCORRN = 0.D0 - CTHEORY/TEMP(N2EXP+1) * 1.0D6
114 WRITE (7,('' CCORRN is :'',F12.9)) CCORRN
115 ELSE
116 R = 0.365D0
117 IF (.NOT.LLONG) R = 0.3275D0
118 CTHEORY = GRAV*2.54D-2*2.54D-2 / (4.92D3 * 4.92D3 * R * R * 4.DO)
119 CCORRN = 0.D0 - CTHEORY / TEMP(N2EXP1) * 1.0D6
120 WRITE (7,('' CCORRN is :'',F12.9)) CCORRN
121 END IF
122
123 STOP

```

APPENDIX 6

Computer Program: NEWSM9

Source: EGP19.NEWSM9  
Object: NEW9OBJ

Compiled: 12/06/84 21.50.13

Parms set: FIXED

Edinburgh Fortran77 Compiler Release 3.5

```

1      CCCCCCCCCCCCCCCCCCCCCCCCCCCCCCCCCCCCCCCCCCCCCCCCCCCCCCCCCCCCCCCCCCCCCC
2      C
3      C           IDA TAPE READING PROGRAM
4      C           INTERACTIVE CORRECTIONS
5      C
6      C
7      C
8      CCCCCCCCCCCCCCCCCCCCCCCCCCCCCCCCCCCCCCCCCCCCCCCCCCCCCCCCCCCCCCCCCCCCCC
9
10     C           DECLARATIONS
11
12     INTEGER*2 IA2(500),IFRED(20)
13     LOGICAL LSHIFT,LSUBS,LVIEW,LJOIN,LTRY,LSKIP,LOK,LBAD
14     INTEGER BUFF1(500),OARRAY(1000),BUFF2,SAVE(500)
15     E      ,BUFF3(2500),DSHIFT
16     REAL*8 X(2500),Y(2500),W(2500),WORK1(3,2500)
17     REAL SMOOTH(50000),OPUT
18     COMMON BUFF2(50000)
19     CHARACTER CHAR(3)*4,NUM(27)*4,FILE(2)*4
20
21     C           INTIAL VALUES AND DATA STATEMENTS
22
23     DATA NUM /'1001','1003','1005','1007','1009'
24     E      , '1011','1013','1015','1017','1019'
25     E      , '0001','0003','0005','0007','0009'
26     E      , '0011','0013','0015','0017','0019','0021'
27     E      , '0023','0025','0027','0029','0031','0033' /
28     C      E      , '0035','0037','0039','0041','0043','0045'
29     C      E      , '0047','0049','0051','0053','0055','0057' /
30     DATA CHAR(1) /'007,' /
31     DATA CHAR(2) /'PART' /
32     DATA FILE(1) /'PART' /
33     LBAD = .FALSE.
34     IBAD = 0
35     ISMCT2 = 1
36     I180 = 0
37     I180TOT = 0
38     IPT = 0
39     DSHIFT = 0
40     IDIFF = 0
41     IDIFF2 = 0
42     J = 1
43     IDATUM = 0
44     ISMCT = 0
45     IEND2 = 0
46
47     C           OPEN LOGICAL UNIT NO 7
48     C           PROGRAM REQUIRES SOME ALTERATIONS HERE IF
49     C           RUN AT INSTALLATIONS OTHER THAN EMAS
50
51     C1000 OPEN (7,FILE=FILE(J),ACCESS='SEQUENTIAL',FORM='UNFORMATTED')
52
53     1000 CHAR(3) = NUM(J)
54     CLOSE (7)
```

```

55     CALL EMASFC ('DEFINE',6,CHAR,12)
56     CALL EMASFC ('DEFINE',6,'FT05,.IN',8)
57     CALL EMASFC ('DEFINE',6,'FT06,.OUT',9)
58
59     C           READ FIRST BLOCK WHICH CONTAINS HEADER INFORMATION
60
61     READ (7,END=999) IA2
62
63     C           DECODE BINARY DATA BY SPLITTING UP HEX
64     C           AND CALL EBCDIC TO OBTAIN INTEGER
65     C           VALUE OF HEADER VARIABLES
66
67     DO 1002 I = 1,500
68     1002  BUFF1(I) = IA2(I)
69     CANCEL      PRINT*, ' THE FIRST 100 INTEGERS ARE '
70     CANCEL      WRITE (6,('( ' ',20I6,/)) (IA2(I),I=1,100)
71
72     CALL DECODE (BUFF1,OARRAY,500,1000)
73     CALL EBCDIC (OARRAY,1000,IYO,IDO,IHO,IMO,ISO,IY1,ID1
74     E,IH1,IM1,IS1,ISCANS)
75     CANCEL      WRITE (6,('( ' START TIME ' ',6I8)') IYO,IDO,IHO,IMO,ISO,ISCANS
76     IF (J.EQ.1) THEN
77         IYORIG = IYO
78         IDORIG = IDO
79         IHORIG = IHO + 1
80         IMORIG = IMO
81         ISORIG = ISO
82         IFIRST = ITDIFF (IYO,IYO,IDO,IDO,IHO+1,IHO,0,IMO,0,ISO,ISCANS)+90
83         IPIRST = IFIRST
84     ELSE
85         IPIRST = 0
86     END IF
87     CANCEL      PRINT*, ' START TIME ',IYO,IDO,IHO,IMO,ISO,ISCANS
88     PRINT*, 'IFIRST IS', IFIRST
89
90
91
92     ICOUNT = 0
93     IBLOCK = 1
94     IF (J.NE.1) IDIFF = ITDIFF(IYO,IY2,IDO,ID2,IHO,IH2,IMO,IM2
95     E           ,ISO,IS2,ISCANS2)
96
97
98     C           READ IN TWO'S COMPLIMENT INTEGER DATA A BLOCK AT A TIME
99
100
101     WRITE (10,('( ' IFIRST IS'' ,I10,' 'IPIRST IS'' ,I10)') IFIRST,IPIRST
102     CANCEL      WRITE (10,('( ' ICOUNT IEND2 IDIFF IX IY
103     CANCEL      E BUFF2(IX) ''))
104     1001 READ(7,END=999) IA2
105     IFLAG = 0
106
107     C           INTERACTIVE TEST PROCEDURE
108     C           NOTE: PROMPTS PREFIXED 'L' REQUIRE A LOGICAL
109     C           RESPONSE ; E.G. .TRUE. , F ,T
110
111     1015 DO 1003 I = 3 + IFIRST,502
112     IF (IFLAG.GT.I) GO TO 1012
113     IF (I.EQ.502) GO TO 1012
114

```

```

115     QUERY = IA2(I-1) - IA2 (I-2)
116
117     IF (ABS(QUERY).GT.25.000.OR.IBAD.GT.0) THEN
118     IF (IBAD.GT.0) GO TO 1013
119     IQUERY = ABS(QUERY)
120
121     C           BAD BITS
122
123     IF ((IA2(I-1).EQ.1286) .OR.
124     E     IA2(I-1).EQ.1287 .OR.
125     E     IA2(I-1).EQ.817) THEN
126     1024     CALL ROUTE1286 (IA2,I,IFLAG)
127     GO TO 1012
128     END IF
129
130     C           DESPIKING
131
132     IF (ABS (ABS(IA2(I)-IA2(I-1))-IQUERY).LT.2) THEN
133     IFLAG = I + 1
134     IA2(I-1) = IA2 (I)
135     GO TO 1012
136     END IF
137
138     C           INTERACTIVE PROMPTS
139
140     WRITE (6,('( DIFFERENCE .GT. 25.00 DETECTED AT',I5)')
141     E     ICOUNT + 2 + IPIRST
142     WRITE (6,'(2015)') (IA2(K),K=(I/20-1)*20+1,(I/20+2)*20)
143
144     IF (IA2(I+1).EQ.0) THEN
145     CALL FPRMPT ('LSKIP?:',7)
146     READ (5,*,ERR=1013) LSKIP
147     IF (LSKIP) GO TO 1012
148     END IF
149
150     1013     CALL FPRMPT ('VIEW BLOCK?:',12)
151     READ(5,*,ERR=1013) LVIEW
152
153     IF (LVIEW) THEN
154     WRITE (6,'(2015)') IA2
155     1019     CALL FPRMPT ('BAD BLOCK?:',11)
156     READ(5,*,ERR=1013) LBAD
157     IF (LBAD) THEN
158     IFLAG = 502
159     IBAD = IBAD + 1
160     GO TO 1012
161     END IF
162     IF (IBAD.GT.0) GO TO 1020
163     END IF
164     CALL FPRMPT ('LSHIFT?:',8)
165     READ(5,*,ERR=1013) LSHIFT
166
167     IF (LSHIFT) THEN
168     DSHIFT = 0
169     CALL FPRMPT ('DSHIFT?:',8)
170     READ(5,*,ERR=1013) DSHIFT
171     PRINT*, DSHIFT,IDATUM
172     CALL FPRMPT ('STARTING AT?:',13)
173     READ(5,*,ERR=1013) IPT
174     CALL FPRMPT ('IMAX?:',7)

```

```

175 READ(5,*,ERR=1013) IMAX
176 PRINT*, IPT,IMAX
177 CALL FPRMPT ('LOK?:',5)
178 READ(5,*,ERR=1013) LOK
179 IF (.NOT.LOK) GO TO 1013
180 DO 1010 IM = 1,IMAX
181     IF (IM.LT.IPT) THEN
182         BUFF1(IM) = IA2(IM)
183     ELSE
184         BUFF1(IM) = IA2(IM) - DSHIFT
185     END IF
186 1010 CONTINUE
187 CALL JOIN (BUFF1,IMAX+1,I-3,IPT-I+2,IMAX,X,Y,W,WORK1)
188 WRITE (6,'(20I5)') (BUFF1(K),K= (I/20)*20+1,(I/20+4)*20)
189 DO 1011 IM = I-2,IPT
190 1011 IA2(IM) = BUFF1(IM) +DSHIFT
191     IFLAG = IPT + 1
192     CALL FPRMPT ('TRY AGAIN?:',11)
193     READ(5,*,ERR=1013) LTRY
194     IF (LTRY) GO TO 1013
195     IDATUM = IDATUM + DSHIFT
196     GO TO 1012
197     END IF
198
199 CALL FPRMPT ('LSUBS?:',7)
200 READ(5,*,ERR=1013) LSUBS
201
202     IF (LSUBS) THEN
203         CALL FPRMPT ('HOW MANY?:',10)
204         READ(5,*,ERR=1013) IHM
205         CALL FPRMPT ('STARTING AT?:',13)
206         READ(5,*,ERR=1013) ISTART
207         CALL FPRMPT ('LOK?:',5)
208         READ(5,*,ERR=1013) LOK
209         IF (.NOT.LOK) GO TO 1013
210         DO 1006 IK = ISTART,ISTART + IHM-1
211             PRINT*, IA2(IK)
212             CALL FPRMPT ('SUBSTITUTE?:',12)
213             READ(5,*,ERR=1013) IX
214             PRINT *, IX
215             IA2 (IK) = IX
216 1006 CONTINUE
217             IFLAG = ISTART + IHM
218             GO TO 1007
219
220         END IF
221     CALL FPRMPT ('LJOIN?:',7)
222     READ(5,*,ERR=1013) LJOIN
223
224     IF (LJOIN) THEN
225         CALL FPRMPT('START & END?:',13)
226         READ(5,*,ERR=1013) IBOT,ITOP
227         PRINT*, IBOT,ITOP
228         CALL FPRMPT ('LOK?:',5)
229         READ(5,*,ERR=1013) LOK
230         IF (.NOT.LOK) GO TO 1013
231         DO 1008 IL = 1,500
232 1008 BUFF1(IL) = IA2 (IL)
233         CALL JOIN (BUFF1,501,IBOT-2,ITOP-IBOT,500,X,Y,W,WORK1)
234         DO 1009 IL = 1,500

```



```

235      1009      IA2(IL) = BUFF1(IL)
236              IFLAG = ITOP
237              END IF
238
239      1007      WRITE (6, '(2015)') (IA2(K), K=(I/20-1)*20+1, (I/20+2)*20)
240      1014      CALL FPRMPT ('TRY AGAIN?:', 11)
241              READ(5, *, ERR=1013) LTRY
242              IF (LTRY) GO TO 1013
243              END IF
244
245      1012      ICOUNT = (IBLOCK-1)*500 + I - 2 - IPIRST
246              IF (ICOUNT.LT.1) GO TO 1003
247              BUFF2 (ICOUNT+IEND2+IDIFF) = IA2(I - 2) - IDATUM
248              IF (ICOUNT.LT.I180TOT+700) THEN
249                  IX = ICOUNT + IEND2 + IDIFF
250                  IY = I - 2
251      CANCEL      WRITE (10, '(6I10)') ICOUNT, IEND2, IDIFF, IX, IY, BUFF2(IX)
252                  END IF
253      1003      CONTINUE
254
255      1020      IF ( IFLAG.EQ.IPT + 1)
256      E      WRITE (6, '(2015)') (BUFF2(K), K=(IBLOCK-1)*500+IEND2+IDIFF+1
257      E      -IPIRST, IBLOCK*500+IEND2+IDIFF-IPIRST)
258
259              IF (IBAD.GT.0) THEN
260                  IF (IBAD.EQ.1) THEN
261                      DO 1022 K = ICOUNT - 999 , ICOUNT-500
262      1022          BUFF3 (K-ICOUNT+1000) = BUFF2 (K)
263                      END IF
264                  IF (.NOT.LBAD) THEN
265                      DO 1017 K = (IBAD)*500 + 1 , IBAD*500 + 500
266      1017          BUFF3( K ) = IA2 (K-(IBAD)*500) - IDATUM
267
268                  ELSE
269                      IF (IBAD.GT.3) STOP 'BUFF3 TOO SMALL'
270                      DO 1023 K = (IBAD+1) * 500 + 1, (IBAD+1) * 500 + 500
271      1023          BUFF3 (K) = IA2 (K-(IBAD+1)*500) - IDATUM
272      C      WRITE (6, '(2016)')(BUFF3(K), K=1, (IBAD+2)*500)
273      C      DO 1021 K = 501 + IBAD*500, 1000 + IBAD*500
274      C 1021          BUFF3(K) = IA2 (K-500)
275                      IMAX = (IBAD+2) * 500
276                      CALL JOIN (BUFF3, IMAX+1, 499, IBAD*500,
277      E                      IMAX, X, Y, W, WORK1)-----
278                      DO 1018 K = 501, (IBAD*500) + 500
279      1018          BUFF2(ICOUNT-(IBAD+1)*500+K) = BUFF3(K)
280      C      DO 1018 K = 501, 501, IBAD*500+499
281      C 1018          BUFF2(IMEM+K) = BUFF3(K)
282                      IBAD = 0
283                      GO TO 1015
284                  END IF
285              END IF
286
287              IBLOCK = IBLOCK + 1
288              IFIRST = 0
289              GO TO 1001
290      999      CONTINUE
291
292
293
294      I180 = ((ISCANS-IPIRST+IEND2+IDIFF)/180)*180

```

```

295         IEND = ISCANS - I180 - IPIRST + IEND2 + IDIFF
296
297         IF (J.NE.1) THEN
298             CALL SAVER (BUFF2,SAVE,IDIFF,IEND2)
299     CANCEL      WRITE (10,('( ' PARAMETERS ENTERING JOIN  IEND2,IDIFF,SAVE' ',
300     CANCEL      E           /,2I10,/,50(10I8/),/))' ) IEND2,IDIFF,SAVE
301             CALL JOIN (SAVE,IEND2,250,IDIFF,500,X,Y,W,WORK1)
302             WRITE (10,('( ' PARAMETERS LEAVING JOIN  IEND2,IDIFF,SAVE' ',
303     E           /,2I10,/,50(10I8/),/))' ) IEND2,IDIFF,SAVE
304             END IF
305
306             DO 1005 I = ISCANS - 249 , ISCANS
307                 SAVE ( I-ISCANS+250 ) = BUFF2 ( I - IPIRST )
308     1005      CONTINUE
309
310
311             IY2 = IY1
312             ID2 = ID1
313             IH2 = IH1
314             IM2 = IM1
315             IS2 = IS1
316             ISCANS2 = ISCANS
317             IEND2 = IEND
318
319             ISTART = 1
320             ISTOP = 180
321
322     4000      DO 4001 I= ISTART,ISTOP
323     4001      BUFF1(I-ISTART+1) = BUFF2(I)
324
325             ISMCT = ISMCT + 1
326             IF (ISTOP.LT.400) THEN
327                 WRITE (10,('( ' PARAMETERS ON ENTERING FIT  ISTART,ISTOP,ISMCT,
328     EISMCT2,BUFF1  ''/4I10,/,18(10I8/),/,18(10I8/))' )ISTART,ISTOP,ISMCT
329     ET,ISMCT2,(BUFF1(K),K=1,180),(BUFF1(K)+IDATUM,K=1,180)
330             END IF
331
332             IF (ISTART.EQ.1) WRITE (10,('( '          I180          ISMCT          ISTART
333     E ISTOP          I180TOT          OPUT' ',/))' )
334             CALL FIT (BUFF1,180,OPUT)
335             WRITE (10,('(5I10,F10.3)') I180,ISMCT,ISTART,ISTOP,I180TOT,OPUT
336             SMOOTH(ISMCT) = OPUT
337     CANCEL      ITIM = (IYORIG - 1900) * 100000
338     CANCEL      WRITE (10,('(4I10,4X,F10.3)') I180,ISMCT,ISTART,ISTOP,OPUT
339     CANCEL      E           + (IDORIG + INT ((IHORIG+ISMCT - 1)/24)) * 100
340     CANCEL      E           + IHORIG + ISMCT -INT ((ISMCT+IHORIG)/24) * 24
341             BTIM = IDORIG + (IHORIG + ISMCT)/2.401
342             WRITE (8, '( ' ' ',F10.3,3X,F10.3)' ) BTIM,OPUT/2.
343             ISTART = ISTART + 180
344             ISTOP = ISTOP +180
345             IF (ISTOP.LE.I180) GO TO 4000
346     C          DO 1025 K = ISMCT2,ISMCT
347     C          ITIM = ITIM + 1
348     C 1025      WRITE (8 , '( ' ' ', I8,3X,F10.3)' ) ITIM , SMOOTH (K)
349             ISMCT2 = ISMCT
350
351
352     C          INSTALLATION SPECIFIC CALL TO
353     C          CLEAR VIRTUAL MEMORY OF READ FILES
354

```

```

355     IF (J.GT.3) THEN
356     FILE (2) = NUM (J-3)
357     CALL EMASFC ('DISCONNECT',10,FILE,8)
358     END IF
359
360     I180TOT = I180TOT+ I180TOT
361     J = J + 1
362     IF (J.LT.28)      GO TO 1000
363
364     C225  FORMAT (' RUN EBMO07.GRAPH'/'LINETYPE 5'/'FILE IDAPLOT01'/
365     C      E'IDENTIFICATION DAVID LYNNESS GEOPHYSICS'/'SYMBOL 11'
366     C      E/'XSCALE DAYS'/'DATA'   )
367
368     CANCEL      DO 1004  I = 1,ISMCT
369     CANCEL      DY = IDORIG +(((ISORIG/60.DO)+IMORIG)/60.DO+IHORIG+(I-1))/24.DO
370     CANCEL      WRITE (9,226) (DY,SMOOTH(I))
371     CANCEL226   FORMAT (' ',F8.3,2X,F10.3)
372     CANCEL1004  CONTINUE
373
374     STOP ' HOPEFULLY SUCCESSFUL '
375     9999  STOP ' ERROR IN OPEN '
376     END

```

```

377     SUBROUTINE DECODE (JARRAY,OARRAY,IRLTH,IRLTH2)
378     INTEGER JARRAY(IRLTH),OARRAY(IRLTH2)
379     DO 105 I=1,IRLTH
380     IF (JARRAY(I)) 100,101,102
381     101  STOP 'ZERO VALUE PASSED TO DECODE'
382     100  JARRAY(I) = 256*256 + JARRAY(I)
383     102  ITEMP1 = JARRAY(I)/256
384     ITEMP2 = JARRAY(I) -( ITEMP1 *256) -240
385     OARRAY(I*2-1) = ITEMP1 - 240
386     OARRAY(I*2) = ITEMP2
387     CANCEL      IF (I.LT.25) THEN
388     CANCEL      PRINT*, ' DECODE - OARRAY(I*2-1) ', OARRAY(I*2-1)
389     CANCEL      PRINT*, ' DECODE - OARRAY(I*2) ', OARRAY(I*2)
390     CANCEL      END IF
391     105  CONTINUE
392     RETURN
393     END

```

```

394     SUBROUTINE EBCDIC (OARRAY,IRLTH2,IY0,IDO,IHO,IMO,ISO,
395     E      IY1,ID1,IH1,IM1,IS1,ISCANS)
396     INTEGER OARRAY (IRLTH2)
397     IY0 = I4(OARRAY,20,IRLTH2)
398     IDO = I4(OARRAY,24,IRLTH2)
399     IHO = I4(OARRAY,28,IRLTH2)
400     IMO = I4(OARRAY,32,IRLTH2)
401     ISO = I4(OARRAY,36,IRLTH2)
402     IY1 = I4(OARRAY,42,IRLTH2)
403     ID1 = I4(OARRAY,46,IRLTH2)
404     IH1 = I4(OARRAY,50,IRLTH2)
405     IM1 = I4(OARRAY,54,IRLTH2)
406     IS1 = I4(OARRAY,58,IRLTH2)
407     ISCANS = OARRAY(63)*10000 + I4(OARRAY,64,IRLTH2)
408     RETURN

```

```

409          END

410          INTEGER FUNCTION I4 (OARRAY,I,IRLTH2)
411          INTEGER OARRAY (IRLTH2)
412          I4 = 0
413          DO 200 J = 0,3
414          IF (OARRAY(I+J).LT.0.OR.OARRAY(I+J).GT.9) THEN
415          OARRAY(I+J) = 0
416          GO TO 200
417          ELSE
418          I4 = OARRAY(I+J) * (10**(3-J))+I4
419          END IF
420          200 CONTINUE
421          RETURN
422          CANCEL PRINT*, ' I4 ',I4
423          END
424

```

```

425          INTEGER FUNCTION ITDIFF (IY2,IY1,ID2,ID1,IH2,
426          £          IH1,IM2,IM1,IS2,IS1,ISCAN2)
427          IMINC = 0
428          IF(IY2.NE.IY1 ) WRITE (6,('( ' ***** WARNING - IY2.NE.IY1 ' '))')
429          IF (ID2.NE.ID1) WRITE (6,('( ' ***** WARNING - ID2.NE.ID1 ' '))')
430          C          ID1 = ID1 + ISCAN2/3.D0/6.D1/2.4D1
431          C          HR1 = ISCAN2/3.D0/6.D1 - ID1 * 2.4D1
432          C          £          + IH1 + (IS1/6.D1 + IM1)/6.D1
433          C          IH1 = INT (HR1)
434          C          IM1 = INT ((HR1-IH1)*6.D1)
435          C          IS1 = INT (((HR1-IH1)*6.D1 - IM1) * 6.D1)
436          IF (IH2.LT.IH1) PRINT*, ' FUNCTION ITDIFF HI2.LT.IH1 '
437          IF (IH2.GT.IH1) THEN
438          IM1 = 60.0 - IM1 - 1
439          IS1 = 60.0 - IS1
440          ITDIFF = ((IM2+IM1)*60.0 + IS2 +IS1 )/20
441          RETURN
442          END IF
443          ITDIFF = ((IM2-IM1)*60.0 + (IS2 - IS1))/20
444          CANCEL WRITE (10, '( ' END TIME ' ',3I10)')IH1,IM1,IS1
445          CANCEL WRITE (10, '( ' START TIME ' ',3I10)') IH2,IM2,IS2
446          PRINT*, ' ITDIFF ' ,ITDIFF
447          RETURN
448          END

```

```

449          SUBROUTINE SAVER (BUFF2,SAVE,IDIFF,IEND)
450          INTEGER SAVE (500)
451          INTEGER BUFF2(50000)
452          DO 400 I = 251,250 + IDIFF
453          SAVE (I) = 9999
454          400 CONTINUE
455          DO 401 I = 251 + IDIFF , 500
456          SAVE (I) = BUFF2 (I - 250 + IEND )
457          401 CONTINUE
458          RETURN
459          END

```

```

460     SUBROUTINE JOIN (SAVE,IEND2,IBOT,IDIFF,IMAX,X,Y,W,WORK1)
461     REAL *8   Y(IMAX), X(IMAX), W(IMAX), WORK1(3,IMAX)
462     E         ,WORK2(2,3), A(3,3), S(3), AK(3), XM, MPUT
463     INTEGER SAVE(IMAX),BUFF2,M,IFAIL,NROWS,K1,IMAX
464     COMMON BUFF2(50000)
465     M = IMAX - IDIFF
466     NROWS = 3
467     K1 = 2 + 1
468     DO 501 I = 1, IBOT
469     Y (I) = SAVE(I)
470     X(I) = I
471     501   W(I) = 1.0
472     DO 502 I = IBOT + 1 , IMAX - IDIFF
473     Y(I) = SAVE (I + IDIFF)
474     W(I) = 1.00
475     502   X(I) = I + IDIFF
476     IFAIL = 0
477
478     C         TEMPORARY OUTPUT CHANNEL FOR EXAMINING INPUT TO E02ADF
479     CANCEL   WRITE (10,'(4I6)') IEND2,IBOT,IDIFF,IMAX
480     CANCEL   WRITE (10,'(12F8.2)') (X(K),K=1,M)
481     CANCEL   WRITE (10,'(12F8.2)') (Y(K),K=1,M)
482     CANCEL   WRITE (10,'(12F8.2)') (W(K),K=1,M)
483
484     CALL E02ADF (M,K1,NROWS,X,Y,W,WORK1,WORK2,A,S,IFAIL)
485     IF (IFAIL.NE.0) GO TO 598
486     DO 504 I = 1,K1
487     504   AK(I) = A(K1,I)
488     K1 = 3
489     DO 503 I = IBOT + 1 , IBOT + IDIFF
490     XM = ((I-1) - (IMAX-I)) / (IMAX - 1.0)
491     IF (DABS(XM).GT.1) GO TO 599
492     IFAIL = 0
493     CALL E02AEF (K1,AK,XM,MPUT,IFAIL)
494     SAVE(I) = NINT(MPUT)
495     503   CONTINUE
496     IF (IEND2.GT.IMAX) RETURN
497     DO 500 I = 1 , IDIFF + IEND2
498     BUFF2 (I) = SAVE (IBOT-IEND2+I)
499     500   CONTINUE
500     RETURN
501     598   STOP ' JOIN E02ADF - IFAIL '
502     599   STOP ' JOIN DABS (XM) '
503     END

```

```

504     SUBROUTINE FIT (BUFF1,M,OPUT)
505     INTEGER BUFF1 (M),M,IFAIL,NROWS,K1
506     REAL*8 X(360),Y(360),W(360),A(3,3), MPUT,
507     EWORK1(3,360),WORK2(2,3),S(4),AK(4)
508     NROWS = 3
509     K1 = 2 + 1
510     DO 600 I = 1,M
511     Y(I) = REAL (BUFF1(I))
512     X(I) = I
513     600   W(I) = 1.00

```

```

514         IFAIL = 0
515         CALL E02ADF (M,K1,NROWS,X,Y,W,WORK1,WORK2,A,S,IFAIL)
516         IF(IFAIL.NE.0) GO TO 699
517         DO 601 I = 1 , 3
518     601     AK (I) = A (K1,I)
519         CALL E02AEF (K1,AK,0,MPUT,IFAIL)
520         IF (IFAIL.NE.0) GO TO 699
521         OPUT = SNGL(MPUT)
522         RETURN
523     699     WRITE (6,('( 'IFAIL.NE.0' '))
524         END

```

```

525         INTEGER FUNCTION ISHIFT (IA2,IP,ISIZE)
526         INTEGER*2 IA2(ISIZE)
527         INTEGER IP, ISIZE
528         IF ((IP+10).GT.500) STOP ' IP.GT.490 SHIFT '
529         DO 700 I = IP, IP+20
530         PRINT*, IA2(I),I
531         IF (IA2(I)-IA2(I-1).EQ.0.AND.I.NE.IP) GO TO 703
532     700     CONTINUE
533         703     IB = IA2(I)
534         DO 701 I = IP, IP-20,-1
535         PRINT*, IA2(I),I
536         IF (IA2(I) - IA2(I+1).EQ.0.AND.I.NE.IP) GO TO 704
537     701     CONTINUE
538         704     IA = IA2(I)
539         ISHIFT = IB - IA
540         PRINT*, ISHIFT
541         RETURN
542         END

```

```

543         SUBROUTINE ROUTE1286 (IA2,I,IFLAG)
544         INTEGER*2 IA2(500)
545         DO 801 K = I-1,I+1
546     801     IA2(K) = IA2 (I-2)
547         IFLAG = I + 4
548         RETURN
549         END

```

```

CODE      16080 BYTES      PLT + DATA  361888 BYTES
STACK     3592 BYTES      DIAG TABLES  2152 BYTES      TOTAL  383712 BYTES
COMPILATION SUCCESSFUL

```

probable annual magnitude of 5.3 (Makropoulos 1978, fig. 7.3). The earthquakes of 1894 were the last major events in this locality and the elapsed time, 88 yr exceeds the determined return period (82 yr) of a magnitude 6.5 event. After the 1981 February/March earthquakes in the Gulf of Corinth ( $M_S = 6.7, 6.4, 6.4$ , USGS) seismic activity increased in the area north of Thibes consistent with the hypothesis of eastward migration (Båth 1979). In 1981 July the Seismological Laboratory of the University of Athens established a local network of six 'Sprengnether' instruments. These were withdrawn in 1982 July with the introduction of a telemetred network of Willmore MK III seismometers operated jointly with the Institute of Geological Sciences, UK. The positions of four of these seismic stations are shown in Fig. 1, five further stations are located approximately radially about station VSI (average distance, 70 km).

### Data collection

A network of 68 stations (with a total of 370 observations) was established during each survey period. The instruments used were La Coste and Romberg model G gravimeters with optical read out only (1981, G-496 and G-275; 1982, G-496 and G-478). La Coste and Romberg gravimeters have been shown to be capable of measuring single gravity differences with a standard error of 0.018 gu when rigorous measuring procedures are followed (Hipkin 1978). Many high precision surveys quote standard deviations in the range 0.10–0.20 gu (e.g. Kinviemi 1974; Torge & Drewes 1977).

All measurements were made in a ladder sequence of the form ABCDEEDCBA which controls a wide spectrum of drift. The station locations are shown in Fig. 1. Base stations (●, Fig. 1) were measured on more than one sequence and were also tied independently to the master base in Athens in a separate ladder sequence. The Greek National Calibration Line, consisting of five monumented stations on Mount Parnis, near Athens, was measured before and after any field campaign. The calibration line overlaps only part of the gravity range of the network. It serves to demonstrate possible variations in the scale factor before and after a campaign and to relate different field campaigns.

Station locations were photographed and positions marked with a masonry pin and a circle of paint. Wherever possible, sites, particularly base stations, are located on bedrock. One foot of a hemispherical plate sits on the masonry pin and the meter, which has one foot fixed, is placed within a confined location on the plate. In this manner height variations upon return to a station are in the range 0–2 mm and never exceed 5 mm. Pressure and temperature are read simultaneously with gravity to 0.01 mbar and 0.1 K respectively. The resurvey of 1982 failed to locate only one station, S7.

The stations are located on both sides of the main fault with a predominance of stations on the downthrown side in the area of complex secondary faulting. A group of 10 stations is located a few kilometres north of Thibes where local activity increased ( $M_L 4.0$ – $4.4$ ) immediately following the 1981 Gulf of Corinth earthquakes ( $M_S 6.7, 6.4, 6.4$ , USGS). Some poorly built rough-hewn stone outhouses collapsed in this area during these major shocks.

### Data processing

The data were first corrected for earth tides using the harmonic expansion of Cartwright & Tayler (1971) as amended in Cartwright & Edden (1973). Tests on the program show it to be in good agreement with Broucke, Zurn & Schlichter (1972) and also Heikkanen (1978) with maximum differences at the hundredth of a gravity unit level. No pressure correction was applied ( $0.004 \text{ gu mb}^{-1}$ , Brien *et al.* 1977) as the pressure was not measured sufficiently

G-496 data, 19-09-81

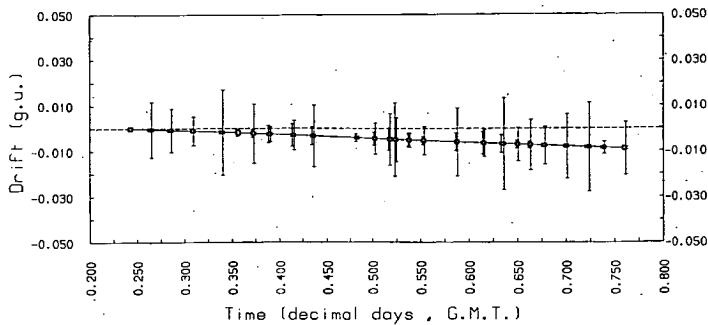


Figure 2. Typical daily linear fit.

accurately in 1982. It should be noted that pressure systems over Greece during the summer months are very stable and frequently the pressure difference upon return to a site during a ladder sequence was less than 1 mb, during the 1981 survey.

The advantage of using a harmonic expansion to evaluate the tidal potential rather than the computationally more rapid closed expression is that it enables one to apply different gravimetric factors at different frequencies. In the case of the eastern Mediterranean the ocean loading signal is not well determined but may be assumed to be small because of the limited tidal range of the Mediterranean and the distance from large oceans.

Daily drift curves were constructed for each instrument using a simple linear fit to isolate misreadings and abnormally high drift rates. Fig. 2 illustrates such a fit for the 1981 September 19 using G-275. These daily drift curves exhibit very low root mean square values and illustrate the consistency of the measured gravity differences during one day. No readings from instrument G-496 have been excluded from the final adjustment but it was necessary to exclude station S25 from the G-275 data set. Furthermore it was noted that G-275 exhibited a large scatter on the 1981 September 15 when a battery failure occurred. The results from instrument G-478 are not discussed here as this instrument possesses significantly higher root mean square errors than G-275 and G-496. This instrument had presented problems in the field, the beam sticking firmly in the mid-range.

A network adjustment computer program (a modified version of Lagios & Hipkin 1980) was now applied to the culled data set as corrected for earth tides. This program performs a least squares adjustment to all the data and also incorporates an independent first, or optionally second-order drift curve to each observation sequence; only linear solutions were used in the final analysis. More than half the total observations are repeat readings at a base station (i.e. stations occupied on more than one day) and every third day includes a remeasurement of base stations only. These repeat measurements in addition to the calibration line observations control the long-term drift and strengthen the network adjustment.

### Results of observations

Table 1 lists the gravity differences obtained in 1981 from a combined network adjustment of both instruments. (Values shown are relative to the Mount Parnis Summit Station, an arbitrary choice of the lowest valued station.) Fig. 3 is the histogram of the network residuals compared with the best fitting normal curve.

The standard deviation is 0.083 gravity units and  $P(\chi^2_9 < 5.02)$  equals 0.84 implying a normal distribution of the sample with that standard deviation (class intervals with fewer



Table 1. Gravity values with respect to Mount Parnis, summit, 1981.

## NETWORK ADJUSTMENT USING MULTILINEAR DRIFT

| BASE  |    | GRAVITY  | STD. DEV. | NO. OF OBS. |
|-------|----|----------|-----------|-------------|
| B0    | 1  | 2217.705 | 0.095     | 9           |
| B1    | 2  | 2027.146 | 0.048     | 12          |
| B1A   | 3  | 2025.812 | 0.098     | 5           |
| B2    | 4  | 2508.173 | 0.118     | 6           |
| B3    | 5  | 2462.735 | 0.074     | 6           |
| B4    | 6  | 2443.064 | 0.066     | 6           |
| B5    | 7  | 1884.791 | 0.099     | 12          |
| B6    | 8  | 2189.887 | 0.085     | 4           |
| B7    | 9  | 2070.269 | 0.142     | 14          |
| B8    | 10 | 2659.036 | 0.086     | 8           |
| B9    | 11 | 2592.061 | 0.096     | 12          |
| B10   | 12 | 2383.158 | 0.080     | 20          |
| B11   | 13 | 1405.987 | 0.096     | 8           |
| B12   | 14 | 2249.939 | 0.095     | 12          |
| B13   | 15 | 2057.332 | 0.039     | 8           |
| B14   | 16 | 2441.320 | 0.059     | 8           |
| B15   | 17 | 2158.449 | 0.268     | 8           |
| GNCL1 | 18 | 1819.474 | 0.140     | 6           |
| GNCL2 | 19 | 1249.472 | 0.153     | 6           |
| GNCL3 | 20 | 846.135  | 0.113     | 6           |
| GNCL4 | 21 | 379.121  | 0.119     | 6           |
| GNCL5 | 22 | 0.000    | 0.116     | 6           |
| S1    | 23 | 1536.709 | 0.115     | 2           |
| S2    | 24 | 2462.167 | 0.011     | 4           |
| S3    | 25 | 2532.478 | 0.027     | 4           |
| S4    | 26 | 2529.381 | 0.074     | 4           |
| S5    | 27 | 2542.742 | 0.036     | 4           |
| S6    | 28 | 2164.528 | 0.034     | 4           |
| S7    | 29 | 2482.211 | 0.074     | 4           |
| S8    | 30 | 2508.927 | 0.047     | 4           |
| S9    | 31 | 2129.428 | 0.111     | 4           |
| S10   | 32 | 2110.166 | 0.085     | 4           |
| S11   | 33 | 2428.242 | 0.060     | 4           |
| S12   | 34 | 2558.103 | 0.031     | 4           |
| S13   | 35 | 2546.457 | 0.067     | 4           |
| S14   | 36 | 2554.550 | 0.084     | 4           |
| S15   | 37 | 2530.514 | 0.088     | 4           |
| S16   | 38 | 2464.732 | 0.034     | 4           |
| S17   | 39 | 2450.075 | 0.060     | 4           |
| S18   | 40 | 2221.558 | 0.043     | 4           |
| S19   | 41 | 2044.108 | 0.051     | 4           |
| S20   | 42 | 1955.573 | 0.062     | 4           |
| S21   | 43 | 1901.396 | 0.105     | 4           |
| S22   | 44 | 1709.467 | 0.077     | 4           |
| S23   | 45 | 2285.937 | 0.088     | 4           |
| S24   | 46 | 2283.740 | 0.058     | 4           |
| S25   | 47 | 2386.083 | 0.060     | 2           |
| S26   | 48 | 2411.504 | 0.079     | 4           |
| S27   | 49 | 2448.345 | 0.061     | 4           |
| S28   | 50 | 2483.059 | 0.086     | 4           |
| S29   | 51 | 2503.796 | 0.033     | 4           |
| S30   | 52 | 2479.436 | 0.054     | 5           |
| S31   | 53 | 2258.368 | 0.094     | 4           |
| S32   | 54 | 2210.567 | 0.061     | 4           |
| S33   | 55 | 2228.518 | 0.006     | 4           |
| S34   | 56 | 2233.458 | 0.061     | 4           |
| S35   | 57 | 2032.695 | 0.079     | 4           |
| S36   | 58 | 1909.074 | 0.116     | 4           |
| S37   | 59 | 2638.612 | 0.135     | 4           |
| S38   | 60 | 2002.174 | 0.072     | 4           |
| S39   | 61 | 1998.661 | 0.027     | 4           |
| S40   | 62 | 2116.910 | 0.091     | 4           |
| S41   | 63 | 1934.386 | 0.050     | 4           |
| S42   | 64 | 2025.181 | 0.069     | 4           |
| S43   | 65 | 2143.646 | 0.019     | 4           |
| S44   | 66 | 2192.978 | 0.008     | 4           |
| S45   | 67 | 2220.827 | 0.038     | 4           |
| S46   | 68 | 2176.563 | 0.058     | 4           |

than five members are excluded). The individual single instrument adjustments yield standard deviations of 0.046, 0.066 and 0.077 gravity units for G496 (1981), G275 (1981) and G496 (1982) respectively.

Fig. 4 illustrates the difference between the readings before and after 10 days of field observations as measured on the calibration line during the 1981 survey. The gravity values used to obtain the differences were derived from independent daily straight line fits. The standard deviation of the differences is 0.09 gravity units, and the curve exhibits no discernible trend. The manufacturer's calibration tables were used throughout since it was not possible to observe on well-defined gravity differences in Greece.

TOTAL NUMBER OF OBS. = 368  
 STANDARD DEVIATION OF BEST FITTING NORMAL DISTRIBUTION IS 0.083 G.U.  
 EACH CLASS INTERVAL IS HALF THE STANDARD DEVIATION  
 NUMBER OF DEGREES OF FREEDOM = 9  
 CHI SQUARED IS 5.02

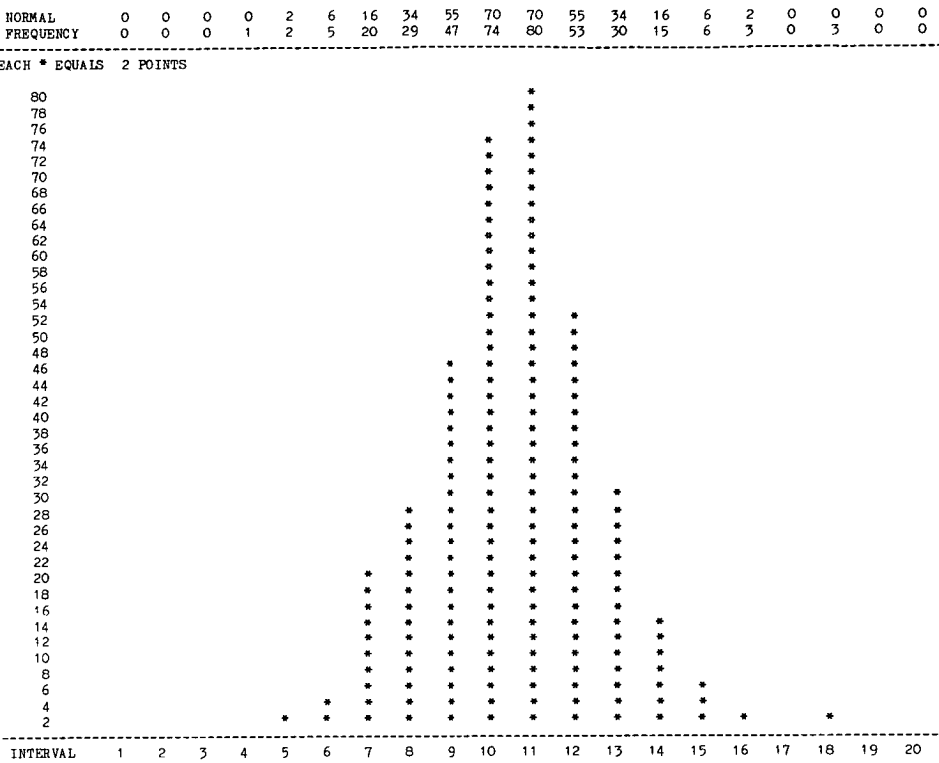


Figure 3. Histogram of residuals; least squares network adjustment, 1981.

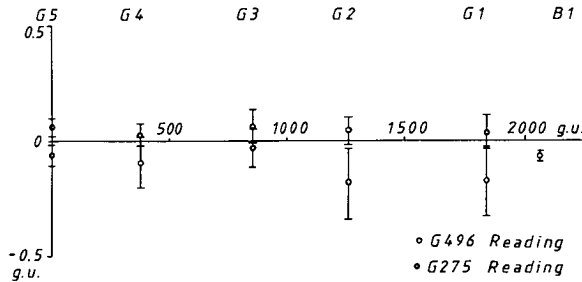


Figure 4. Differences between initial and final readings on Mount Parnis calibration line. Gravity values are relative to GNCL5, linear least squares adjustment.

Fig. 5 is a graph of the temporal variation of observed gravity between 1981 and 1982, adjusted such that there is zero change of the mean. The error bars shown are the combined root mean square errors of that individual station's adjustment. A histogram of the distribution (Fig. 6) indicates a high probability of normality ( $P(\chi^2 < 0.21) = 0.97$ ). The difference distribution's standard deviation of 0.11 gu is in agreement with the combination of sigmas of the component data sets 0.077 and 0.083 gu ( $(0.077^2 + 0.083^2)^{1/2} = 0.113$ ). Therefore the residual differences are consistent with the hypothesis of no gravity change at the 0.11 gu level.

### Acknowledgments

We should like to acknowledge the assistance of members of the Department of Geophysics, Edinburgh, and the Geophysics – Geothermics Division Athens, in particular Professor J. Dakropoulos. Also Professor N. Delibasis of Athens who assisted with the data collection and Dr R. Hipkin of Edinburgh who assisted with the data processing. This work was funded by the Bodossakis Foundation and Mr Lyness was in receipt of a studentship from the Northern Ireland Department for Education.

### References

- Anderson, D. & Whitcomb, J., 1975. Time dependent seismology, *J. geophys. Res.*, **80**, 1497–1503.
- Barnes, D. F., 1966. Gravity changes during the Alaska Earthquake, *J. geophys. Res.*, **71**, No. 2.
- Báth, M., 1979. A Mediterranean earthquake project, *Tectonophys.*, **58**, T17–T21.
- Bomford, G., 1980. *Geodesy*, 4th edn, Clarendon Press, Oxford, 855 pp.
- Brein, R., Gerstenecker, C., Kinviemi, A. & Pettersson, L., 1977. *Report on high precision gravimetry*, No. 1, National Land Survey, Sweden.
- Broucke, R. A., Zurn, W. & Schlichter, L. B., 1972. Lunar tidal acceleration on a rigid Earth, in *Flow and Fracture of Rocks* (The Griggs volume), *Geophys. Monogr. Am. Geophys. Un.*, **16**, 319–324.
- Cartwright, D. E. & Edden, A. C., 1973. Corrected tables of tidal harmonics, *Geophys. J. R. astr. Soc.*, **33**, 253–264.
- Cartwright, D. E. & Tayler, R. J., 1971. New computations of the tide-generating potential, *Geophys. J. R. astr. Soc.*, **23**, 45–74.
- Chen, Yun-Tai, Hao-Ding, G. U. & Lu, Zao-Xun, 1979. Variations of gravity before and after the Haicheng Earthquake 1975 and the Tangsham Earthquake 1976, *Phys. Earth planet. Int.*, **18**, 330–338.
- Gumbell, E. J., 1966. *Statistics of Extremes*, Columbia University Press.
- Heikkänen, M., 1978. On the tides generating forces, *Publs Finnish Geod. Inst. No. 85*, Helsinki.
- Hipkin, R. G., 1978. A microgravimetric network for secular gravity studies in Scotland, *Geophys. J. R. astr. Soc.*, **52**, 383–396.
- Karnik, 1969–1971. *Seismicity of the European Areas. Part I 1969, Part II 1971*, Academia, Praha.
- Kinviemi, A., 1974. High precision measurements for studying the secular variation in gravity in Finland, *Publs Finnish Geod. Inst. No. 78*.
- Lagios, E. & Hipkin, R., 1980. Least squares network analysis, *Int. Rep. 80.1*, Department of Geophysics, University of Edinburgh.
- Mackenzie, D., 1977. Active tectonics of the Alpine-Himalayan belt: the Aegean Sea and surrounding regions, *Geophys. J. R. astr. Soc.*, **55**, 217–254.
- Makropoulos, K. C., 1978. The statistics of large earthquake magnitude and an evaluation of Greek seismicity, *unpublished thesis*, University of Edinburgh, 193 pp.
- Mercier, J. L., 1975. Rapport d'activité scientifique de l'équipe du labor de Géologie Dynamique de l'université Paris-Sud pour 1975 sur le resultat des études de méotectonique en Grèce.
- Oliver, H. W., Robbins, S. L., Grannell, R. S., Alewine, R. W. & Beihler, S., 1975. Surface and sub-surface movements determined by remeasuring gravity, *Bull. Calif. Div. Mines Geol.*, **196**, 195–212.
- Philippson, A., 1930. *Beiträge zur Morphologie Griechenlands*, Stuttgart, 47 pp.
- Rundle, J. B., 1978. Gravity changes and the Palmdale Bulge, *Geophys. Res. Lett.*, **5**, 41–44.
- Torge, W. & Drewes, H., 1977. Gravity variations with time in Northern Iceland, *J. Geophys.*, **43**, 771–790.
- Tsubokawa, I., 1973. On relation between duration of precursory geophysical phenomena and duration of crustal movement before earthquakes, *J. geol. Soc. Japan*, **10**, 165–171.
- Whitcomb, J. H., 1976. New vertical geodesy, *J. geophys. Res.*, **81**, 4937–4944.
- Whitcomb, J. H., Wolfgang, F. O., Given, J. W., Pechmann, J. C. & Ruff, L. J., 1980. Time dependent gravity in Southern California May 1974–April 1979, *J. geophys. Res.*, **85**, B8, 4563–4573.

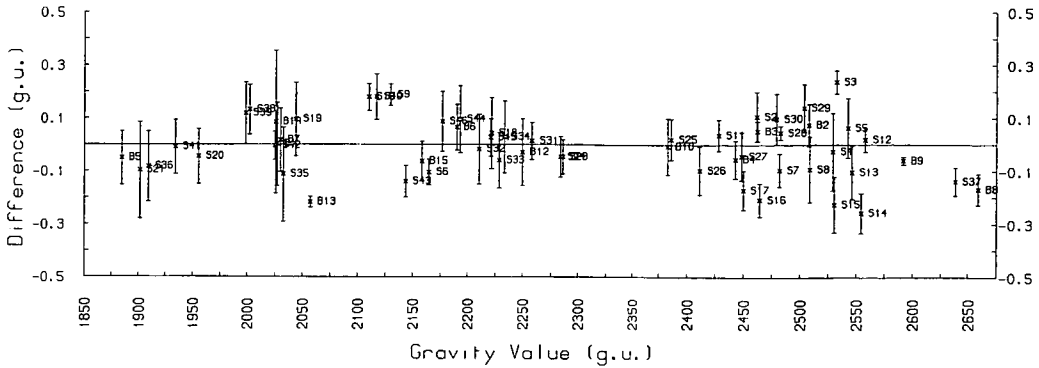


**Figure 5.** Gravity difference 1981–1982. Values are with respect to station GNCL5 (Mount Parnis summit). Six stations with values between 0 and 1850 gu are not shown.

TOTAL NUMBER OF OBS. = 64  
 DISTRIBUTION STANDARD DEVIATION OF 0.11 G.U.  
 EACH CLASS INTERVAL IS HALF THE STANDARD DEVIATION  
 NUMBER OF DEGREES OF FREEDOM = 4  
 CHI SQUARED IS 0.21

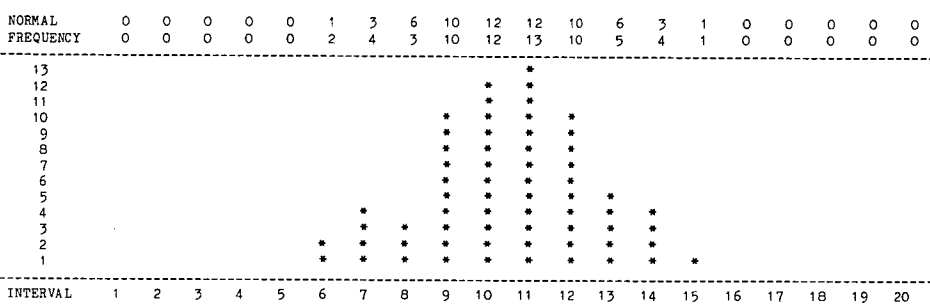


**Figure 6.** Histogram of gravity differences 1981–1982.

Future measurements, collected in an identical fashion, will be included in a common adjustment procedure to detect sites with a ‘non-normal’ behaviour possibly caused by tectonic activity.

**Conclusion**

A high precision gravity network has been established in the Atalanti area involving a comparatively short measuring period (10 day). This network has obtained a normally distributed set of residual differences between the years 1981 and 1982 with a standard deviation of 0.11 gu. Should the difference distribution have been non-normally distributed or possessed a higher standard deviation (> 0.11 gu) there would be grounds for an immediate gravity remeasurement and possibly other geodetic observations. Hence it has been shown that no tectonic movements have occurred in the period 1981–1982, in the Atalanti region, within the limits of accuracy of the survey.

Anderson & Whitcomb (1975) present a relationship between earthquake magnitude and a precursory anomalous area of the form:

$$\log L \text{ (km)} = 0.26 M + 0.46$$

$L$  = horizontal extent,  $M$  = earthquake magnitude

for some events. Thus for a magnitude 6.5 event the horizontal extent of the anomalous area is 141 km. The duration of preseismic crustal deformation of a magnitude 6.5 event is five years when calculated using the formulation of Tsubokawa (1973). The network established by the authors in the Atalanti area of Eastern Greece is situated on an active fault zone with a station spacing of approximately 2 km traversing the anticipated anomalous area. Rundle (1978) has modelled the gravitational effect of a thrust fault at a depth of 10 km, and obtains a maximum gravity change of 0.5 gu, well within the precision limits of the network (see 'Results of observations').

### Background

The Atalanti region (Fig. 1), is one area of high seismic potential in the Hellenides (Makropoulos 1978). One large fault, trending WNW–ESE, extends from the town of Molos, passing through the southern outskirts of Atalanti, and terminates in Western Evia. The region to the east, on the downthrow side of the main fault, is dissected by minor faulting as shown in Fig. 1 (based on Mercier 1975; Philippson 1930). The most recent large magnitude events last occurred in 1894 April ( $M > 6.7$ ,  $M > 6.9$ , Karnik 1970) and resulted in large surface ruptures (maximum 2 m, Karnik 1970) visible on *Landsat* images (Mackenzie 1977, fig. 17).

Statistical analysis using the Extreme Value Method (Gumbell 1966) of a reconstructed earthquake catalogue for the Hellenic Area shows a pronounced high in this area with a most

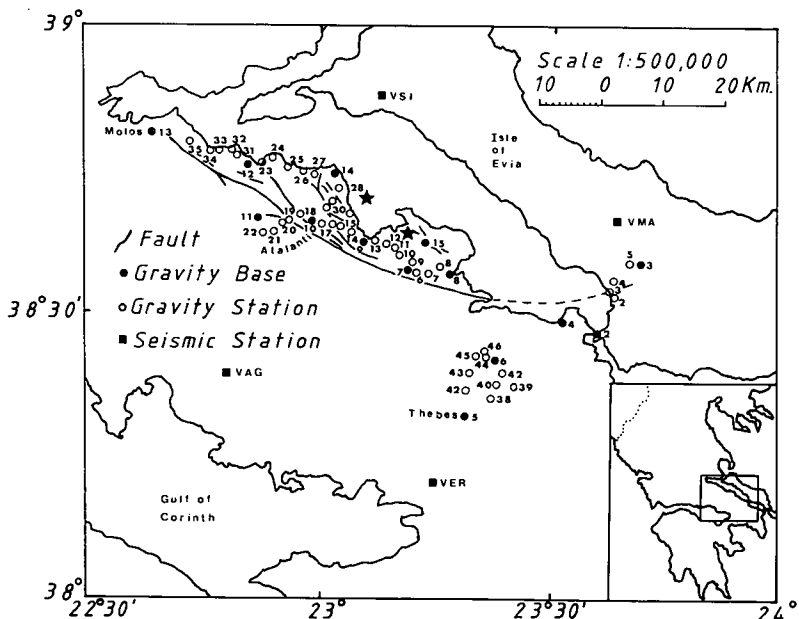


Figure 1. Map and station plan of the survey area (\* shows the epicentres of the seismic events of 1894 April).

## **A microgravimetric network in East Central Greece — an area of potential seismic hazard**

**D. Lyness** *Department of Geophysics, University of Edinburgh,  
James Clerk Maxwell Building, Mayfield Road, Edinburgh EH9 3JZ*

**E. Lagios** *Department of Geology, Geophysics – Geothermics Division,  
Athens University, Panipistimiopolis, Athens 15771, Greece*

Received 1983 October 24; in original form 1983 July 15

**Summary.** The eastern Mediterranean is a region of complex tectonic processes and associated horizontal and vertical displacements. A high precision gravity network has been established in the Atalanti area of central Greece to monitor temporal gravity changes on an annual or more frequent basis. A total of 68 sites have been measured in 1981 and 1982 with a maximum single instrument standard deviation of 0.08 gravity units after a least squares network adjustment. Analysis of the gravity differences between the two measuring epochs exhibits no change of gravity over the network with a precision of 0.11 gravity units. It is proposed that the gravity values given form a stable base for continued observations which will enable the authors to resurvey the region in the event of precursory foreshocks. Observation of the Atlantic network will continue on an annual basis preserving the same observation sequence for reasons of symmetry.

### **Introduction**

It has been shown that conventional gravity surveys can register gravity changes before and after earthquakes (e.g. Barnes 1966; Chen, Hao-Ding & Zao-Xun 1979; Oliver *et al.* 1975). Gravity surveying is inexpensive and extremely rapid when compared with geodetic levelling. Though not capable of detecting as small a deformation, gravity surveying has the advantage that errors are not significantly distance dependent (levelling precision is related to the square root of the distance traversed, typically 1.5 mm  $\sqrt{\text{km}}$ , Bomford 1980). High precision gravity surveying to assist in the assessment of earthquake deformation parameters is currently taking place in several seismic risk areas on the globe. Networks have been established in southern California (Whitcomb *et al.* 1980), Japan (National Report IUGG 1975) and also in Iceland (Torge & Drewes 1977).

Gravity data alone can provide important diagnostic information and perhaps precursory data but Whitcomb (1976) emphasizes the need for combined levelling and gravity measurements and presents analytic relationships between the measured quantities. It is proposed that should a large seismic event take place, new first-order levelling will be undertaken.